Order Number 9315516

Contributions to the theory of machine dynamics

Xu, Tao, Ph.D.

City University of New York, 1993

U·M·I
300 N. Zeeb Rd.
Ann Arbor, MI 48106

CONTRIBUTIONS TO THE THEORY OF MACHINE DYNAMICS

by

TAO XU

A dissertation submitted to the Graduate Faculty in Engineering
in partial fulfillment of the requirements for the degree of
Doctor of Philosophy, The City University of New York

1993

This manuscript has been read and accepted for the Graduate Faculty in Engineering in satisfaction of the dissertation requirement for the degree of Doctor of Philosophy.

1/13/93 — Gerard G. Lowen

Date — Chair of Examining Committee

1/13/93 — Gerard G. Lowen

Date — Executive Officer

Prof. G. G. Lowen (Chair)

Prof. C. N. Bapat

Prof. S. Cowin

Prof. F. R. E. Crossley (Emeritus)

Prof. S. B. Menkes

Prof. M. L. Pei (Emeritus)

Supervisory Committee

The City University of New York

Abstract

CONTRIBUTIONS TO THE THEORY OF MACHINE DYNAMICS

By

Tao Xu

Adviser: Professor Gerard G. Lowen

Certain contributions to the theory of machine dynamics, which were inspired by a previous investigation into the dynamic behavior of a press feed mechanism, were made:

(1) A new, simplified, mathematical model of the complete multi-regime per cycle machine was developed. The ability to obtain a fully analytical solution allowed the exploration of the all-important transient components of the responses during the feeding stroke. Further, the solution clarified the relationship between the resulting system frequencies and the individual stand-alone frequencies of the elastic components of the mechanism.

(2) Based on an energy dissipation study as well as comparison with experimentally obtained responses of the sprag clutch of the mechanism, it was shown that a non-linear damping force, which is a function of both velocity and displacement, is superior to a linear one when dealing with non-linear stiffness systems.

(3) A new and complete mathematical model for a sprag clutch was devised. By postulating a two point Hertzian contact at each sprag-race interface, the experimentally obtained torque-displacement relationship could be theoretically duplicated.

(4) A practical analytical approach for the determination of the transient responses in elastic mechanisms was given. Based on mathematical work by E.T. Whittaker, they were obtained by the determination of the characteristic exponent in the stable regions of the Floquet solution to the Hill's equations involved. Several sample computations showed that the transient responses may very from near-periodic to totally aperiodic.

ACKNOWLEDGEMENTS

First and foremost, I wish to express my sincere and deep appreciation to my mentor, Professor Gerard G. Lowen. It has been a great privilege for me to be able to study under his distinguished scholarship, ample knowledge and boundless inspiration. I am truly indebted to him for his constant guidance, encouragement and assistance.

The technical help of Dr. C. Chassapis and Dr. Q.Y. Jiang in the work of experimentation is specially acknowledged.

I would like to thank the members of my supervisory committee, as well as Professor F.R.E. Crossley, who served as examiner, for their interest.

The financial support received from the National Science Foundation under Grant No. MSM-8502112 and the University Fellowship is gratefully appreciated.

Finally, I owe a very special debt of gratitude to my wife Yi, my parents and my son Jack, whose unique love, support and encouragement made this work possible.

TABLE OF CONTENTS

		Page
GENERAL INTRODUCTION		1
	PART I	
	A SIMPLIFIED MATHEMATICAL MODELFOR	
	A PRESS FEED MECHANISM	
1.	INTRODUCTION	8
2.	DESCRIPTION OF MECHANISM	10
3.	FORMULATION OF MATHEMATICAL MODEL	12
	a. Replacement Mechanism	12
	b. Coordinate Systems and Angles	12
	c. Treatment of the Sprag Clutch	13
	d. Rigid and Elastic Links	13
	e. Damping and Friction	13
	f. Description of Motion Regimes	14
4.	INVERTED CANTILEVER MODEL OF COUPLER	15
5.	DERIVATION OF EQUATIONS OF MOTION FOR REGIME NO.2	19
	a. Hamilton's Integral	19
	b. Equations of Motion for Regime No.2	20
	c. Reduction of Equations of Motion to Linear Form with Constant Coefficients	21
6.	SOLUTION OF LINEARIZED SYSTEM EQUATIONS FOR REGIME NO.2	24
	a. System Characteristic Equation	24
	b. Solution of the Homogeneous System of Equations	25

		Page
	c. Approximation of Particular Solutions of the System Equations	26
	d. Complete Solutions of System Equations	27
	e. Clutch Windup Angle $\phi_{5/4}$	29
7.	COMPARISON BETWEEN COMPUTED AND EXPERIMENTAL RESULTS	31
	a. Method of Computation	31
	b. Determination of coupler strain	32
	c. Experimental Setup	32
	d. Physical Parameters	35
	e. Model Verification	37
8.	INSIGHTS TO BE GAINED FROM NEW ANALYTICAL SOLUTION	47
	a. Responses During Forward Motion	47
	b. Relationship between Component Frequencies and System Frequencies	47
	c. Maximum Coupler and Clutch Deflections	57
9.	ESTIMATE OF MINIMUM BRAKE TORQUE	60
10.	CONCLUSIONS	62

PART II

A NEW DAMPING MODEL FOR NON-LINEAR STIFFNESS SYSTEMS WITH VARIABLE PRELOAD DISPLACEMENTS AND CONSTANT AMPLITUDE DECAY RATIO

1.	INTRODUCTION	65
2.	LINEAR DAMPING MODEL FOR SYSTEMS WITH LINEAR SPRINGS	67
3.	POSSIBLE DAMPING MODELS FOR SYSTEMS WITH NON-LINEAR SPRINGS	70
	a. Linear (Viscous) Damping Model	71

		Page
	b. Non-linear Damping Model	72
4.	APPLICATION OF THE NON-LINEAR DAMPING MODEL TO A SPRAG CLUTCH	75
	a. System Description	75
	b. Mathematical Model of Sprag Clutch with Non-linear Damping	77
	c. Determination of Damping Parameters	78
	d. Experimental Setup	79
	e. Experimental Determination of Amplitude Decay Ratio	80
	f. Determination of Damping Constant	83
	g. Comparison between Computed and Experimental Results	83
5.	LACK OF GENERALITY OF LINEAR DAMPING MODEL FOR SPRAG CLUTCH	88
6.	CONCLUSIONS	89

PART III

A MATHEMATICAL MODEL OF AN OVER-RUNNING SPRAG CLUTCH

1.	INTRODUCTION	91
	a. Background and Outline of Present Work	91
	b. Previous Work	92
2.	CLUTCH DESCRIPTION	94
3.	DETERMINATION OF NORMAL CONTACT FORCES	98
	a. Hertzian Contact Force N_h	98
	b. Contact Damping Forces N_{id} and N_{od}	100
4.	EQUATION OF MOTION	102
	a. Derivation of Equation of Motion	102

Page

b. Influence of Sprags in Differential Equations 104

5. CONCLUSIONS 107

PART IV

A PRACTICAL ANALYTICAL APPROACH FOR THE DETERMINATION OF THE TRANSIENT RESPONSE IN ELASTIC MECHANISMS

1. INTRODUCTION 109

2. BACKGROUND 111

3. DETERMINATION OF CHARACTERISTIC EXPONENT IN STABLE REGIONS 116

4. APPLICATION TO MECHANISM EXAMPLE 120

5. DISCUSSION AND CONCLUSIONS 131

APPENDICES

	Page
APPENDIX A. KINEMATICS OF THE LINKAGE	134
a. Elastic Constraint Equations and Various Angles	134
b. Additional Component of Rotation and Virtual Rotation of the Elastic Angles	135
c. Elastic Angular Velocity and Acceleration of the Coupler	137
d. Kinematics of Points on Elastic Coupler	138
e. Virtual Displacement of Points on Elastic Coupler	141
APPENDIX B. DERIVATION OF EQUATIONS OF MOTION FOR REGIME NO.2	142
a. Kinetic Energy of System and Its Variation	142
b. Potential Energy of System and Its Variation	142
c. Virtual Work Done by Non-Conservative Forces	143
d. Working Form of Hamilton's Integral	144
e. Final Form of Equations of Motion for Regime No.2	145
APPENDIX C. SIMPLIFICATION OF EQUATIONS OF MOTION	150
a. Linearization of the Clutch Spring For Various Regimes	150
b. Simplification of Functions P_1 , P_2 , P_3 and F_2 (See equations (B.18), (19), (20) and (22))	152
c. Fourier Series Representation of Forcing terms R_1 and R_2	155
APPENDIX D. SOLUTION FOR REGIME NO.1	158
a. Equation of Motion	158
b. Complete Solution of Equation of Motion	158
APPENDIX E. SOLUTION FOR REGIME NO.3	160
a. Equation of Motion	160
b. Complete Solution of Equation of Motion	160

	Page
APPENDIX F. SOLUTION FOR REGIME NO.4	162
a. Equation of Motion	162
b. Complete Solution of Equation of Motion	162
APPENDIX G. EFFECT OF ADDITION OF MASS TO COUPLER AT POINT B	164
a. Experimental Setup	164
b. Derivation of Equation of Motion	164
APPENDIX H. SAMPLE COMPUTATIONS FOR RUN NO.1	168
a. Constants Common to All Regimes	168
b. Computations for Cycle No.1 (Start-up)	169
c. Computations for Cycle No.2 (Normal)	174
APPENDIX I. COMPUTER ALGORITHMS FOR THE DETERMINATION OF THE WINDUP ANGLE AND SAMPLE OUTPUT	178
a. Data Transfer from the Data Acquisition System to the Computer	178
b. Determination of Windup Angle $\phi_{5/4}$	195
APPENDIX J. APPROXIMATION OF FUNCTION A(δ)	228
APPENDIX K. PROCEDURE FOR OBTAINING THE AMPLITUDE DECAY RATIO	231
APPENDIX L. DETERMINATION OF RELATIVE ROTATION $\phi_{5/4}$ DUE TO CONTACT DEFORMATIONS	233
a. Windup Angle Due to δ_o	235
b. Windup Angle Due to δ_i	236
c. Total Windup Angle due to δ_o and δ_i	237
APPENDIX M. DETERMINATION OF REALISTIC CONTACT MODE BETWEEN SPRAGS AND RACES	239
a. Line Contact	239
b. Single Point Contact	241

Page

c. Two Point Contact 241

d. Comparison of Torque Curves 242

APPENDIX N. FORTRAN PROGRAM FOR THE DETERMINATION OF Δ(0) 245

APPENDIX O. REVIEW OF REFERENCES ON LINKAGE ELASTICITY 250

REFERENCES 258

LIST OF TABLES

		Page
Table 1:	Parameters of the Standard Feed Mechanism	36
Table 2:	Determination of Amplitude Decay Ratio	82
Table 3:	RSSR Linkage Dimensions	84
Table 4:	Clutch Data for Formsprag Indexing Clutch Model HPI-500	105
Table 5:	Component Magnitudes of Coefficients	105
Table 6:	Instability Boundaries of Mechanism Example (*These six boundaries have no physical meaning for the present example, but are needed for the counting of the k's.)	124
Table 7:	Coefficients of Solution Series	126
Table H-1:	Constants Common to All Regimes	169
Table H-2:	Initial Conditions for Regime No.1 of Start-up Cycle	170
Table H-3:	End Values of Regime No.1 of Start-up Cycle	170
Table H-4:	Basic Constants for Regime No.2 of Start-up and Normal Cycles	172
Table H-5:	Solution Related Constants for Regime No.2 of Start-up and Normal Cycles	172
Table H-6:	End Values of Regime No.2 for Start-up Cycle	173
Table H-7:	End Values of Regime No.3 for Start-up Cycle	174
Table H-8:	End Values of Regime No.4 for Start-up Cycle	174
Table H-9:	End Values of Regime No.1 of Normal Cycle	175
Table H-10:	End Values of Regime No.2 for Normal Cycle	176
Table H-11:	End Values of Regime No.3 for Normal Cycle	177
Table H-12:	End Values of Regime No.4 for Start-up Cycle	177

LIST OF FIGURES

		Page
Figure 1:	Schematic Drawing of Feed Mechanism with Replacement Linkage	11
Figure 2:	Coupler Coordinates and Deflections	16
Figure 3:	Inverted Cantilever Beam	17
Figure 4:	Experimental Setup of the Feed Mechanism with Lumped Mass	33
Figure 5:	Schematic of Instrumentation	34
Figure 6:	Run No.1: Oscillogram of Coupler Strain Horizontal Scale: .1 sec/div Vertical Scale: 40 microstrain/div Input Speed: 200 RPM Strip Size: 4.0x.125x130.0 in Brake Torque: 160 lb-in	38
Figure 7:	Comparison between Computed and Experimental Results for Run No.1 Input Speed: 200 RPM Strip Size: 4.0x.125x130.0 in Brake Torque: 160 lb-in Coupler: Standard (without lumped mass)	
	a) Coupler Strain vs. Input Angle	39
	b) Clutch Windup Angle vs. Input Angle	40
Figure 8:	Comparison between Computed and Experimental Results for Run No.2 Input Speed: 300 RPM Strip Size: 4.0x.25x153.5 in Brake Torque: 300 lb-in Coupler: Standard (without lumped mass)	
	a) Coupler Strain vs. Input Angle	41
	b) Clutch Windup Angle vs. Input Angle	42

		Page
Figure 9:	Comparison between Computed and Experimental Results for Run No.3 Input Speed: 200 RPM Strip Size: 4.0x.125x130.0 in Brake Torque: 260 lb-in Coupler: Modified (with lumped mass)	
	a) Coupler Strain vs. Input Angle	43
	b) Clutch Windup Angle vs. Input Angle	44
Figure 10:	Components of Coupler and Clutch Responses for Run No.1	
	a) Coupler Strain	48
	b) Clutch Windup Angle	49
Figure 11:	Components of Coupler and Clutch Responses for Run No.2	
	a) Coupler Strain	50
	b) Clutch Windup Angle	51
Figure 12:	Components of Coupler and Clutch Responses for Run No.3	
	a) Coupler Strain	52
	b) Clutch Windup Angle	53
Figure 13:	Relationship between System and Component Frequencies as function of Coupler Diameter	55
Figure 14:	Relationship between System and Component Frequencies as function of Coupler Density	56
Figure 15:	Maximum Coupler Deflection as Function of Coupler Diameter for Various Parameter Combinations and 200 RPM	58
Figure 16:	Maximum Clutch Windup Angle as Function of Clutch Stiffness for Various Parameter Combinations and 200 RPM	59
Figure 17:	Estimated Minimum Brake Torque Requirement as a Function of Input Speed for Various Strip Sizes.	61
Figure 18:	Damped Spring-Mass System Oscillating about Non-Zero Preload Displacement δ	68
Figure 19:	Schematic Diagram of Feed Mechanism with Sprag Clutch	76
Figure 20:	Typical Experimental Curves of Windup Angle vs. Input Crank Angle	81

		Page
Figure 21:	Comparison between Experimental and Computed Results of Windup Angle vs. Input Crank Angle at 72 RPM	85
Figure 22:	Comparison between Experimental and Computed Results of Windup Angle vs. Input Crank Angle at 197 RPM	86
Figure 23:	Formsprag Indexing Clutch Model HPI-500	95
Figure 24:	Schematic of Sprag Clutch (All Forces Shown to Act on Sprag)	96
Figure 25:	Free Body Diagrams of Sprag and Inner Race in Locking Mode	99
Figure 26:	Typical Stability Line	115
Figure 27:	Slider-Crank Mechanism	121
Figure 28:	Stability Line of Mechanism Example	125
Figure 29:	Homogeneous Solution with $\lambda = 12.7066$ (590 RPM) and $\gamma = 11.742$	128
Figure 30:	Homogeneous Solution with $\lambda = 23.9219$ (430 RPM) and $\gamma = 11.742$	129
Figure 31:	Homogeneous Solution with $\lambda = 105.2507$ (205 RPM) and $\gamma = 11.742$	130
Figure 32:	Values of the Parameter A and the Characteristic Exponent μ in Stable Region where $11.7811 \leq \lambda \leq 13.6074$	133
Figure C-1:	Linearization of the Clutch Spring for Regimes No.1 and No.2	151
Figure C-2:	Magnitudes of Functions P_1, P_2, P_3 and F_2 vs. Input Angle ϕ_1	154
Figure G-1:	Addition of Mass to the Coupler at Point B	165
Figure J-1:	Error Ratio A_{approx}/A	230
Figure L-1:	Determination of Relative Rotation due to Contact Deformation a. Deformation at Outer Interface with Inner Race Stationary b. Deformation at Inner Interface with Outer Race Stationary	234

Page

Figure M-1: Examination of Contact Modes at Sprag/Race Interfaces 240
a. Line Contact b. Single Point Contact c. Two Point Contact

Figure M-2: Comparison of Theoretical Torque Curves with Experimental One 244

GENERAL INTRODUCTION

The present dissertation provides answers to certain questions that arose as a consequence of a previous investigation of the dynamic behavior of a press feed mechanism (Chassapis and Lowen, 1990). That work provided both a non-linear mathematical model as the basis for a numerical simulation of the machine and an experimental confirmation.

Figures 1 and 4 show the lever type roll feed mechanism to consist of a RSSR spatial linkage with a bent coupler, an indexing sprag clutch, a disk type friction brake and a set of feed and pressure rollers, which advance strip stock under a power press. One cycle of the mechanism contains four distinct regimes. During the forward stroke of the rocker link, the clutch is first wound up against the constant torque brake which assure that the strip does not overshoot. Subsequently, the stock is moved forward while the clutch oscillates between its input and output (windup angle). At the beginning of the return motion of the rocker one finds that the clutch must unwind before the over-running regime begins (for detail see also sections 2 and 3 of Part I).

The following briefly describes the nature of these questions and the manner in which they were resolved by the four parts of this work.

(1) A Simplified Mathematical Model for a Press Feed Mechanism

The previous work on the press feed mechanism could not explain the observation that the primarily transient responses of both the coupler strain and the clutch windup angle, regardless of the loading conditions of the mechanism, always oscillated close to the component frequency of the free standing clutch-strip system during the feeding stroke. Further, clarification was needed concerning the composition of these transient responses

and the contribution of the forced ones. Finally, it is of interest to determine the circumstances under which the component frequency of the free standing coupler plays a larger role in the responses, both in terms of frequency and amplitude.

To be able to answer the above questions, an analytical solution, which can separate the transient responses from the steady state ones and give the system natural frequencies became essential. This led to the development of a simplified two-degree of freedom model of the mechanism, in which an "inverted cantilever" type space function was used to approximate the shape of the coupler deflection and the non-linear sprag clutch replaced by a linear torsional spring. Further, the time dependent coefficients were averaged.

Hamilton's Integral serves for the derivation of the system equations of motion and classical methods were employed to obtain the analytical solutions both for the coupler strain as well as the clutch windup angle. Experiments, which utilized newly developed PC-based algorithms for obtaining the windup angle, showed that this simplified model provides a good approximation of the dynamic behavior of the multi-regime per cycle mechanism[1]

The analytical results for the all-important feeding stroke clearly showed that the principal parts of the responses are transient in nature and contain two system frequencies (natural frequencies of the mechanism system). It was further found that the lower system frequency of the transient response is always near to and smaller than the lower of the two component frequencies, while the higher system frequency is always near to and larger than the higher component frequency. Specifically, for the standard configuration of the mechanism, where the component frequency of the clutch is considerably lower than the component frequency of the coupler, the lower system frequency is near that of the clutch, while

---

1 A multi-regime per cycle machine is defined as one, where due to the abrupt application and removal of the work load during each revolution, the governing equations change accordingly.

higher system frequency is near that of the coupler. When the coupler component frequency was made lower than that of the clutch, the lower system frequency was nearer to that of the coupler.

While no general rule concerning the amplitudes associated with the two transient system frequencies could be discerned, it was found in the analysis of the standard configuration, that the amplitude associated with the lower system frequency was always considerably greater, both for the coupler strain and the clutch windup angle, than that associated with the higher system frequency. Since all the cases considered by Chassapis and Lowen (1990) dealt with the standard configuration of the mechanism, their observation of the predominance of the component frequency of the clutch in the coupler strain and the clutch windup angle is not surprising.

When the coupler component frequency was made lower than the clutch component frequency, the amplitude associated with the lower system frequency (i.e. near that of the coupler component frequency) lost some of its importance. While for the strain response the higher frequency amplitude was approximately one third of that of the lower frequency one, it became somewhat larger than the latter for the windup angle response.

Finally, the parametric study demonstrated that the maximum deflections of the coupler and the clutch windup angle are essentially independent of each other over a wide range of parameters at a speed of 200 RPM, and that reductions of these deflections may be achieved by a modest increase of the coupler stiffness and the clutch spring constant, respectively.

(2) A New Damping Model For Non-Linear Stiffness System with Variable Preload Displacements and Constant Amplitude Decay Ratio[2]

---

2 The relevant part of the dissertation has been published verbatim in Proceedings of 1992 ASME Mechanisms Conference, DE-Vol.46, pp.27-33. Also accepted for publication in Trans. ASME, *Journal of Mechanical Design.*

This part of the investigation was stimulated by the observation of the special nature of the vibrations of the non-linear sprag clutch (Chassapis and Lowen, 1990). These oscillations of the clutch windup angle are always about a preload displacement and never in the direction of unloading. In addition, it was found experimentally that the amplitude decay ratio is essentially constant, regardless of the level of the preload. This led to the question of the influence of such preloads on the energy dissipation in non-linear stiffness systems and with that to the question of what represents the best damping model for such systems, including the sprag clutch.

In order to clarify the approach taken by the author in the determination of an appropriate damping model for a non-linear stiffness system with a preload, a linear mass-spring system is first considered. By introducing the concept of interchangeable potential energy, it could be shown that the energy loss per cycle of such systems is independent of the preload displacement and therefore a linear (viscous) damping model is adequate for them.

The extension of these ideas to a non-linear stiffness system has shown that the energy dissipation per cycle and the damping coefficient associated with a linear damping model depend very much on the momentary preload displacement. Thus, such a linear damping model cannot satisfy all preloading conditions.

To solve this problem, a new non-linear damping model, which takes displacement in addition to velocity into account, is introduced. Such a model has the desired generality, since the influence of the preload displacement on the associated damping coefficient can be minimized. Subsequently, this new damping model was incorporated into the "non-linear lumped spring-mass" mathematical description of the sprag clutch. Very good agreement between computed and experimental results was found.

(3) A Mathematical Model of a Over-Running Sprag Clutch[3]

The previous work by Chassapis and Lowen (1990) used a "lumped" spring-mass model for an over-running sprag clutch, in which the presence of the sprags is disregarded. The torque of the clutch was experimentally found to be proportional to the 3/2 power of the windup angle.

To be able to understand the influence of the sprags and explain the non-linear nature of the clutch stiffness, a complete mathematical model for such a sprag clutch was developed. It considers the Hertzian contact forces between the sprags and the races, the inertias of the sprags and the output race, and the newly developed non-linear damping model shown in Part II. The work of Stoelzle and Hart (1961) is adapted to relate the Hertzian contact deformations to the windup angle.

Comparison with experiment showed that a line contact assumption between the races and the sprags, which one would normally postulate, is not valid and that a two point contact assumption gives a better description of the existing Hertzian contact.

The resulting clutch model showed that the influence of the sprags cannot be neglected when the moment of inertia of the clutch output side is relatively small. The earlier developed "lumped" model of the clutch yields satisfactory results for the feed mechanism, because of the presence of very large referred moment of inertia due to the roller shaft and feed strip.

(4) A Practical Analytical Approach for the Determination of the Transient Response in Elastic Mechanisms[4]

---

3 The relevant part of the dissertation has been accepted verbatim for publication in *Mechanism and Machine Theory.*

4 The relevant part of the dissertation has been published verbatim in Proceedings of 1992 ASME Mechanisms Conference, DE-Vol.47, pp.347-352. Also accepted for publication in Trans. ASME, *Journal of Mechanical Design.*

Previous work on multi-regime per cycle machinery containing elastic links (Chassapis and Lowen, 1990) has made it clear that the contribution of the transient response of the link deflections cannot be neglected. This pointed out the need to develop an analytical solution for the response of Hill's equation in the stable regions, where such mechanisms operate.

Based on mathematical work by Whittaker (1944), this dissertation shows a practical analytical approach for obtaining such transient responses by way of the determination of the characteristic exponent in the stable regions of the Floquet solution to Hill's equation. This technique, together with the known analytical solution of the steady state response, due to Kotowski (1943) and applied to mechanism by Jandrasits and Lowen (1979), makes it possible to get a complete analytical solution for forced Hill-type differential equations.

An application to a specific slider- crank mechanism with an elastic connecting rod using only a first mode description has shown that the nature of the transient response depends on the location of the stable region, which is a function of the mechanism speed, the mechanism parameters and the loading conditions of the slider. It may vary from being almost periodic, with a frequency near the natural one of the lateral deflection of the connecting rod, to being fully non-periodic with vastly changing amplitudes. Thus, it should not be surprising when a non-periodic response trace appears on an oscilloscope.

PART I

A SIMPLIFIED MATHEMATICAL MODEL FOR A PRESS FEED MECHANISM

1. INTRODUCTION

Previous numerical and experimental work on the press feed mechanism system left some unresolved questions. To begin with, it was not clear to what extent the transient portions of the coupler strain and the clutch windup angle responses were dominant during the forward stroke of the mechanism. Secondly, an explanation was needed for the observation that the aforementioned responses had, for all loading conditions of the standard configuration, the approximate the component frequency of the clutch-strip system.

To be able to explain the question of the transients and to obtain some general conclusions concerning the relationship between the frequencies of the transient system responses and of the component frequencies of the coupler and the clutch-strip system, it was decided to develop a simplified model of the mechanism, which is amenable to an analytic solution that approximates the dynamic behavior of the mechanism.

The following reports on the development of such a linearized two degree of freedom system where the time dependent coefficients have been averaged and where the non-linear sprag clutch has been replaced by a linear torsional spring. To account for the coupler deflection an "inverted cantilever type" space function is introduced. Hamilton's Integral serves for the derivation of the system equations for the forward stroke of this multi-regime per cycle machine. The windup, release and return portions of the complete cycle represent reduced cases of this motion regime. Classical methods are used to obtain both transient and steady state solutions, which are subsequently shown to agree well with experimental results. The newly developed PC-based algorithms made it possible to automate the processing of the angular encoder data. A number of parametric investigations provided valuable insight concerning the role of the transients and the relationship between component and system frequencies.

While the literature search on linkage elasticity, associated with this research and given in Appendix O, furnished much valuable background material, it revealed no specific work that considered multi-regime per cycle machinery.

To set the stage for this new investigation, which begins with the introduction of the "inverted cantilever" type space function of the coupler, certain needed background, given previously by Chassapis and Lowen (1990), is repeated in sections 2 and 3.

2. DESCRIPTION OF MECHANISM

The lever-type roll feed mechanism, as shown in Figure 1, is composed of an RSSR spatial linkage, an indexing sprag clutch, a disk-type adjustable friction brake and a set of feed and pressure rollers.

The input shaft of the spatial linkage is directly connected to the crank shaft of the power press and drives the throw block whose angular relationship with respect to the press crank shaft may be varied to adjust the feed cycle with respect to the press cycle. The distance between the centers of the throw block and the sliding block forms the input crank of the linkage, whose length is adjustable to obtain different feed lengths for the stock. The spatial coupler, which is bent in order to clear the feed roller shaft support assembly as well as the OSHA-mandated safety cover, connects the sliding block and the rocker by way of two ball joints. The shaft of the rocker is attached to the outer race of the sprag clutch. This sprag clutch, which only transfers the motion in one direction, drives the feed roller shaft and with that moves the strip forward when the sprags are engaged. Once the rocker is in its return motion, the sprags are unlocked and no motion is conveyed to the feed roller shaft. To prevent the over-shooting of the strip at the end of feeding, a friction brake is attached to the feed roller shaft. Possible slip between the feed rollers and the strip is minimized with the help of a set of spring activated pressure rollers.

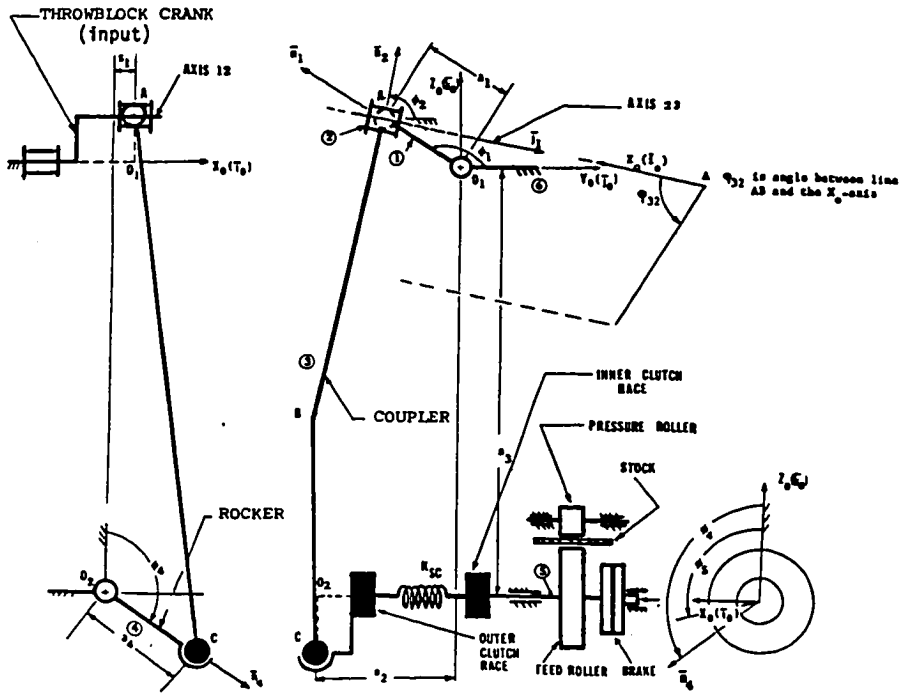

Figure 1 Schematic Drawing of Feed Mechanism with Replacement Linkage

3. FORMULATION OF MATHEMATICAL MODEL

a. Replacement Mechanism

In order to avoid the extra variable which is needed to express the free, though limited, rotation of the coupler about the axis connecting its two ball joints, as well as to obtain a fully defined reference plane for the elastic deflection of the coupler, it is assumed, for purposes of kinematics only, that the RSSR linkage is replaced by an equivalent RRRSR one, which has the same basic dimensions. This is accomplished by substituting the cross link and coupler clevis for the upper ball joint A. This replacement does not change the motion of the pivot-to-pivot line AC of the coupler.

b. Coordinate Systems and Angles

The X_0 axis of the space fixed $O_1X_0Y_0Z_0$ coordinate system coincides with the axis of rotation of the input crank. The length $O_1A = a_1$ of this crank lies in the Y_0Z_0 plane and forms the angle ϕ_1 with respect to Y_0 axis. The rocker of length a_4 is pivoted at point O_2, which lies on an axis parallel to the Y_0 axis and is located by the ground dimensions S_1, S_2 and S_3. The rocker position is defined by angle ϕ_4 with respect to the Z_0 axis in the X_0Z_0 plane. Link 2 is the cross link connecting the revolutes of links 1 and 3, with axes 12 and 23 normal to each other and intersecting at point A. Its position is defined by angle ϕ_2 with the help of unit vector $\overline{n}_2$, which is normal to axis 23 and lies in the Y_0Z_0 plane. Link 3 of length $AC = a_3$ represents the bent spatial coupler with its reference plane defined by points A, B and C. Three body-fixed coordinate systems xyz, $x_1y_1z_1$ and $x_2y_2z_2$, as shown in Figure 2, are

attached to the coupler. To define the relative position of the coupler with respect to link 2, the angle ϕ_{32} between the X_o and x_1 axes is introduced. Link 5 is a rigid body consisting of the inner race of the clutch, the feed roller shaft, the feed rollers and part of disk brake. Its position is measured by angle ϕ_5 which has the same reference position as angle ϕ_4.

c. Treatment of the Sprag Clutch

To simplify matters, the clutch elasticity, caused by the Hertzian deformation at the contact interfaces of races and sprags, is represented by way of a massless torsional spring. This spring, which is assumed to connect the inner and outer races of the clutch, has a non-linear character as shown experimentally by Chassapis and Lowen (1990). When this non-linearity is expressed in terms of the relationship between the relative rotation of the races and the torque T being transferred, one obtains:

$$T = K_{sp}(\phi_5 - \phi_4)^{3/2} \tag{1}$$

d. Rigid and Elastic Links

Because of their massive construction, the input crank assembly, the rocker and clutch input assembly, the clutch output and feed roller shaft assembly as well as the frame of the machine are assumed to be rigid. The bent spatial coupler is considered to be an elastic member.

e. Damping and Friction

Both the elastic coupler and the torsional clutch spring are assumed to be subject to linear velocity dependent damping. The frictional effects in the various bearings as well as in the clutch are neglected. The friction torque from the brake and the friction force from the sliding of the metal strips over the feed table are combined in the resisting torque T_b, exerted on the feed roller shaft.

f. Description of Motion Regimes

Because of the discontinuous nature of the clutch operation, it is necessary to define the motion of the feed mechanism in terms of the following four regimes:

Regime No.1, Clutch Windup: The initial forward motion of the rocker winds the clutch spring while the feed roller shaft is held stationary by the resisting torque. This phase ends when the torque transmitted by the clutch is equal to the resisting torque.

Regime No.2, Forward Motion of Strip: The rocker drives the feed roller shaft and with that the metal strip by way of the clutch. This phase ends when the rocker reaches its final extreme position.

Regime No.3, Unwinding of the Clutch: The clutch spring unwinds during the initial return motion of the rocker until the clutch is completely disengaged.

Regime No.4, Return Motion: The return motion of the rocker continues, while the clutch undergoes its overrunning mode, until the initial extreme position of the rocker is reached.

4. INVERTED CANTILEVER MODEL OF COUPLER

Figures 2a and 2b show the coupler in its reference plane under tension as well as compression. It represents a simply supported beam that is fixed at point A and free to move at point C along the original line AC, which defines the x axis. The x_1y_1 and x_2y_2 coordinate systems are defined by the undeformed positions of sections 1 and 2, respectively.

The overall boundary conditions are maintained if one assumes that each individual section of the coupler moves like an inverted cantilever beam as shown in Figure 3. Thus, when a general load is applied, point B, a common point in the rigidly connected sections, moves to point B', in the direction of the y_1 axis only. This neglects axial foreshortening due to bending as well as due to tension or compression. Therefore,

$$\overline{BB'} = q(t)\bar{j}_1 \tag{2}$$

The elastic deflections v_1 and v_2 of arbitrary points on beam sections 1 and 2, respectively, are expressed with respect to the reference lines x_1' and x_2', which are at all times parallel to the original body fixed x_1 and x_2 axes. It is now further assumed that the first mode deflections of both inverted cantilever beams can be expressed in terms of quarter-wave harmonics. Then, for section 1:

$$\bar{v}_1 = -q(t)\left(1 - \sin\frac{\pi}{2L}x_1\right)\bar{j}_1 \tag{3}$$

Similarly, for section 2:

$$\bar{v}_2 = -q(t)\left(1 - \cos\frac{\pi}{2L}x_2\right)\bar{j}_2 \tag{4}$$

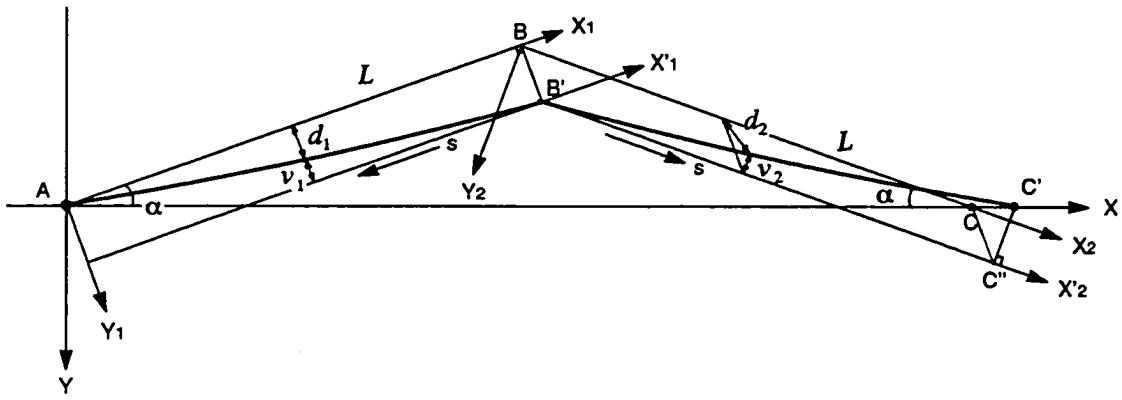

a. Tension

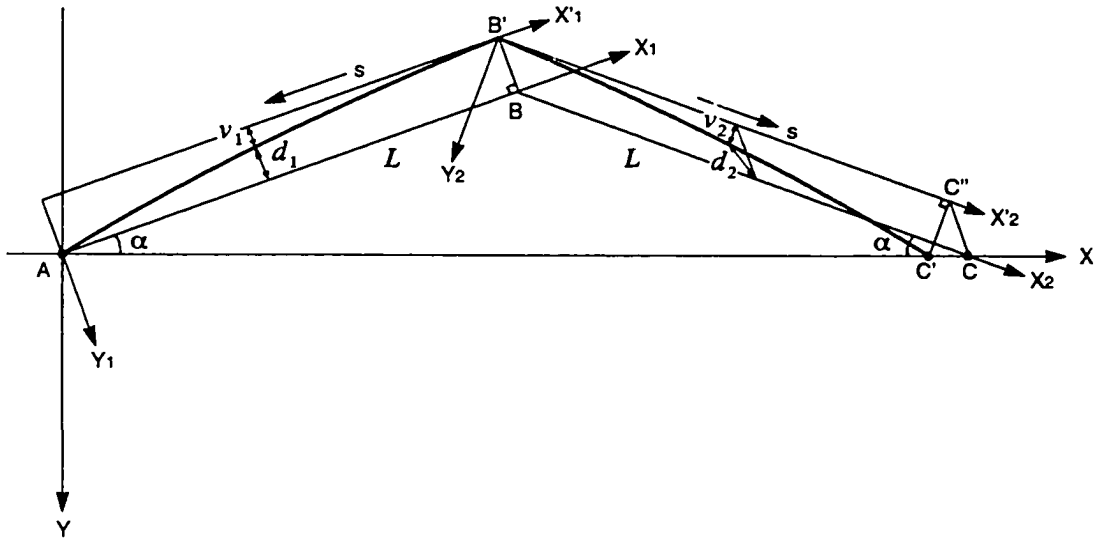

b. Compression

Figure 2 Coupler Coordinates and Deflections

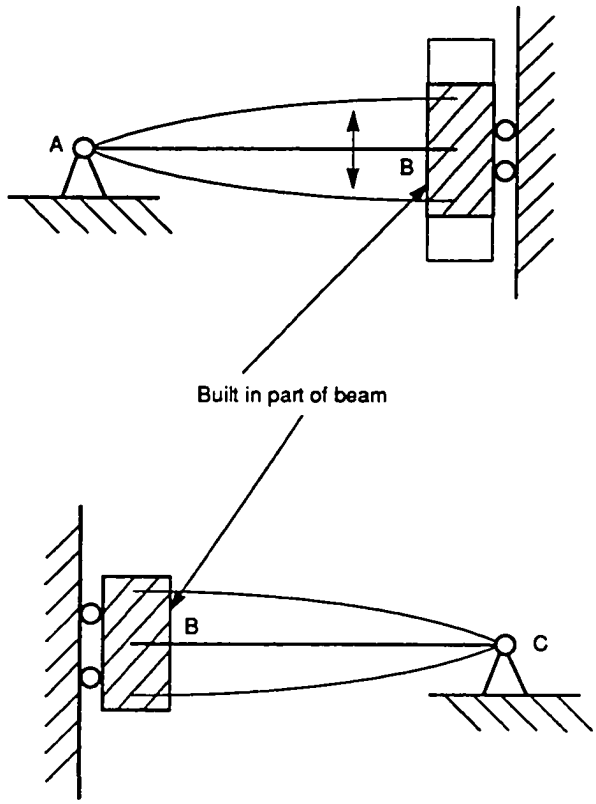

Figure 3 Inverted Cantilever Beams

The resulting displacements d_1 and d_2 of arbitrary points on sections 1 and 2 with respect to coordinates x_1y_1 and x_2y_2 are given by:

$$\bar{d}_1 = \overline{BB'} + \bar{v}_1 = q(t)V_1(x_1)\bar{j}_1 \tag{5}$$

where

$$V_1(x_1) = \sin\frac{\pi}{2L}x_1 \tag{6}$$

and

$$\bar{d}_2 = \overline{BB'} + \bar{v}_2 = q(t)\sin 2\alpha\bar{i}_2 + q(t)V_2(x_2)\bar{j}_2 \tag{7}$$

where

$$V_2(x_2) = \cos 2\alpha - 1 + \cos\frac{\pi}{2L}x_2 \tag{8}$$

The elongation of the coupler is now obtained from inspection of Figure 2:

$$CC' = \Delta AC = 2q\sin\alpha \tag{9}$$

which is positive when the coupler is in tension.

5. DERIVATION OF EQUATIONS OF MOTION FOR REGIME NO.2

Since the physical conditions of all other regimes represent reduced cases of Regime No.2, only the derivation of the latter will presently be discussed. The generalized coordinates are the time function $q(t)$ of the elastic deflection of the coupler in its reference plane (see equation (3)), as well as the clutch output rotation $\phi_5(t)$. The equations of motion for Regimes 1, 3 and 4, which are needed for the determination of the initial conditions of Regime No.2, are given in Appendixes D, E and F, respectively.

a. Hamilton's Integral

Hamilton's principle states that the variation of the integral of the sum of the kinetic and the potential energies as well as the work done by non-conservative forces in a system between two instants t_0 and t_1 must vanish, i.e.:

$$\delta \int_{t_0}^{t_1} (T - V + W)dt = 0 \tag{10}$$

The substitution of the variations of the integrals of T, V and W, according to equations (B.2), (B.5) and (B.7) of Appendix B, into the above leads to the following:

$$\int_{t_0}^{t_1} \Bigg\{ \left[J_{o4}\bar{\ddot{\phi}}_{4c} \cdot \delta\bar{\phi}_{4c} + J_{o5}\bar{\ddot{\phi}}_5 \cdot \delta\bar{\phi}_5 + \int_0^L \rho A \bar{\ddot{r}}_{P_1} \cdot \delta\bar{r}_{P_1} dx_1 + \int_0^L \rho A \bar{\ddot{r}}_{P_2} \cdot \delta\bar{r}_{P_2} dx_2 \right] +$$

$$+ \left[\frac{EI}{L^3}\left(\frac{\pi}{2}\right)^4 q\,\delta q + K_{sp}(\phi_5 - \phi_{4c})^{3/2}\delta\phi_5 - K_{sp}(\phi_5 - \phi_{4c})^{3/2}\delta\phi_{4c} \right] +$$

$$\Bigg\{ + \left[\left(3 - \frac{8}{\pi}\right) LC_{co}\dot{q}\,\delta q - T_b\delta\phi_5 + C_{sp}(\dot{\phi}_5 - \dot{\phi}_{4c})\delta(\phi_5 - \phi_{4c}) \right] \Bigg\} \; dt = 0 \tag{11}$$

The kinetic energy terms consider the contributions of the coupler link, the rocker-clutch assembly and the clutch-feed roller shaft assembly. It must be noted that these kinetic energies are not only functions of the total motions of the rigid body and the local deflection of the coupler but also of the elastic rotation due to the length change of the coupler. The potential energy terms deal with the strain energy due to the coupler deflection, as well as the torsional spring energy of the clutch. The remaining terms account for the work done by the non-conservative friction and damping forces, which include the constant dry friction of the brake and the sliding of the strip over the feeding table, as well as the viscous type of damping in both the coupler and the clutch. (For details see Appendix B.)

b. Equations of Motion for Regime No.2

Appendix B gives detailed derivations of all substitutions into equation (11) and the subsequent operations. When the non-linear terms in q and its derivatives are neglected because of the small deflection assumption, one obtains the system equations of motion (B.15) and (B.16) in terms of the generalized coordinates $q(t)$ and $\phi_5(t)$. If these resulting differential equations are expressed in terms of input angle ϕ_1, i.e. $q(\phi_1)$ and $\phi_5(\phi_1)$, and all terms are divided by $\dot{\phi}_1^2$, they take the following form:

$$\rho A[(V_{2s1}+V_{2s2}+\sin^2 2\alpha)L+P_1(\phi_1)]\ \frac{d^2q}{d\phi_1^2}+\frac{1}{\dot{\phi}_1}[0.45LC_{co}+\rho AP_2(\phi_1)]\ \frac{dq}{d\phi_1}+\frac{1}{\dot{\phi}_1^2}[\left(\frac{\pi}{2}\right)^4\frac{EI}{L^3}+$$

$$+\rho AP_3(\phi_1)]\ q=\rho A\frac{F_1(\phi_1)}{\dot{\phi}_1^2}+[\frac{1}{\dot{\phi}_1^2}K_{sp}(\phi_5-\phi_{4c})^{3/2}+\frac{1}{\dot{\phi}_1}C_{sp}(\frac{d\phi_5}{d\phi_1}-\frac{d\phi_{4c}}{d\phi_1})-J_{o4}\frac{d^2\phi_{4c}}{d\phi_1^2}]F_2(\phi_1) \quad (12)$$

and

$$J_{o5}\frac{d^2\phi_5}{d\phi_1^2}+\frac{1}{\dot{\phi}_1}C_{sp}(\frac{d\phi_5}{d\phi_1}-\frac{d\phi_{4c}}{d\phi_1})+\frac{1}{\dot{\phi}_1^2}K_{sp}(\phi_5-\phi_{4c})^{3/2}=\frac{1}{\dot{\phi}_1^2}T_b \quad (13)$$

where the elastic angle ϕ_{4e} may be expressed, with the help of equations (9), (A.7) and (A.13) of Appendix A, as a function of q:

$$\phi_{4e} = \phi_{4r} + \Delta\phi_4 = \phi_{4r} + F_2(\phi_1)q \tag{14}$$

The expressions of the input angle dependent functions $P_1(\phi_1)$, $P_2(\phi_1)$, $P_3(\phi_1)$, $F_1(\phi_1)$ and $F_2(\phi_1)$ as well as V_{2s1} and V_{2s2} in the above equations of motion are listed in detail in Appendix B.

It is useful at this point to consider the nature of some of the input angle dependent functions in the equations of motion. Both functions $P_1(\phi_1)$ and $P_2(\phi_1)$ originate from the consideration of the additional component of the rotation of the coupler caused by the change of length of AC. The function $P_3(\phi_1)$ is due to the inclusion of both the inertia force introduced by the elastic deformation of the coupler and the aforementioned additional rotation.

c. Reduction of Equations of Motion to Linear Form with Constant Coefficients

Since the purpose of this investigation is to find an analytical solution of the equations of motion, it is necessary to obtain a linearized system of differential equations with constant coefficients.

An analysis of the coefficient terms in Section b of Appendix C, which uses the general geometric dimensions of this feed mechanism, has shown the following:

(1) The maximum values of the functions $P_2(\phi_1)$ and $P_3(\phi_1)$ are both very small when compared with the terms of $0.45LC_{co}/(\rho A)$ and $(EI\pi^4)/(2^4L^3\rho A)$, respectively. Thus, they may be neglected.

(2) The function $P_1(\phi_1)$, which is part of the equivalent mass of the coupler, varies little

during Regime No.2 and therefore can be treated as a constant, i.e. $P_1 = 2.65$.

(3) The coupling function $F_2(\phi_1)$, which changes its value very little during Regime No.2, is also assumed to be constant with a value of 0.098.

Equation (C.5) of Appendix C gives the result of the linearization of the non-linear clutch spring for Regime No.2, i.e.:

$$T = K_{sp}(\phi_5 - \phi_{4e})^{3/2} \approx K_{l2}(\phi_5 - \phi_{4e}) - T_b/2 \tag{15}$$

where the linearized spring constant K_{l2} at an arbitrary load point T_b, according to equation (C.3), has the form:

$$K_{l2} = \frac{3}{2} K_{sp}^{2/3} T_b^{1/3} \tag{16}$$

Further, the term $C_{sp}(\dot{\phi}_5 - \dot{\phi}_{4e})$ in equation (12) is neglected since it is small when compared to the term $K_{sp}(\phi_5 - \phi_{4e})^{3/2}$, which is in the same bracket.

With all the above, one can now write the linearized equations of motion in the following matrix form:

$$\begin{bmatrix} 1 & 0 \\ 0 & 1 \end{bmatrix} \begin{Bmatrix} q'' \\ \phi_5'' \end{Bmatrix} + \begin{bmatrix} 2\zeta_{co}\lambda_{co} & 0 \\ -2\zeta_{sp}\lambda_{sp}F_2 & 2\zeta_{sp}\lambda_{sp} \end{bmatrix} \begin{Bmatrix} q' \\ \phi_5' \end{Bmatrix} + \begin{bmatrix} \lambda_{co}^2 + K_r F_2^2 \lambda_{co}^2 & -K_r F_2 \lambda_{co}^2 \\ -\lambda_{sp}^2 F_2 & \lambda_{sp}^2 \end{bmatrix} \begin{Bmatrix} q \\ \phi_5 \end{Bmatrix} = \begin{Bmatrix} R_1(\phi_1, \dot{\phi}_1) \\ R_2(\phi_1, \dot{\phi}_1) \end{Bmatrix} \tag{17}$$

where

$$\lambda_{co} = \frac{\omega_{co}}{\dot{\phi}_1} \quad \text{frequency ratio for coupler} \tag{18.a}$$

$$\lambda_{sp} = \frac{\omega_{sp}}{\dot{\phi}_1} \quad \text{frequency ratio for clutch} \tag{18.b}$$

$$\omega_{co} = \sqrt{K_c/M_e} \quad \text{component frequency of coupler} \tag{18.c}$$

$\omega_{sp} = \sqrt{K_{l2}/J_{o5}}$ component frequency of clutch-strip system (18.*d*)

$\zeta_{co} = \dfrac{0.45LC_{co}}{2\sqrt{K_e M_e}}$ damping ratio for coupler (18.*e*)

$\zeta_{sp} = \dfrac{C_{sr}}{2\sqrt{K_{l2}J_{o5}}}$ damping ratio for clutch (18.*f*)

$K_r = K_{l2}/K_e$ ratio of the stiffness (18.*g*)

Both the equivalent mass and stiffness of the coupler M_e and K_e are defined by

$$M_e = \rho A[(V_{2s1} + V_{2s2} + \sin^2 2\alpha)L + P_1] + J_{o4}F_2^2 \tag{19}$$

$$K_e = \left(\frac{\pi}{2}\right)^4 \frac{EI}{L^3} \tag{20}$$

The forcing terms on the right hand side of the system equation are found to be:

$$R_1(\phi_1, \dot{\phi}_1) = \frac{\rho A}{M_e}\frac{F_1(\phi_1)}{\dot{\phi}_1^2} - F_2\frac{J_{o4}}{M_e}\frac{d^2\phi_{4r}(\phi_1)}{d\phi_1^2} - F_2K_r\lambda_{co}^2\phi_{4r}(\phi_1) - \frac{F_2T_b}{2\dot{\phi}_1^2M_e} \tag{21}$$

and

$$R_2(\phi_1, \dot{\phi}_1) = \frac{1.5T_b}{J_{o5}\dot{\phi}_1^2} + 2\zeta_{sp}\lambda_{sp}\frac{d\phi_{4r}(\phi_1)}{d\phi_1} + \lambda_{sp}^2\phi_{4r}(\phi_1) \tag{22}$$

The initial conditions for angle ϕ_5 and its derivative ϕ_5' for this regime are:

$$\phi_5 = \phi_{4e\ max} \quad \text{and} \quad \phi_5' = 0 \tag{23}$$

($\phi_{4e\ max}$ the starting position of the rocker for the forward motion),

while the starting values of q and q' depend on their end values of Regime No.1.

6. SOLUTION OF LINEARIZED SYSTEM EQUATIONS FOR REGIME NO.2

The analytical solutions of the linearized system equations with constant coefficients can be obtained by the sum of their homogeneous as well as their particular solutions, as described in the following.

a. System Characteristic Equation

With the form of the homogeneous solution given by:

$$q = C_{1i} e^{(S_i/\dot{\phi}_1)\phi_1} \qquad (i = 1,2,3,4) \tag{24}$$

and

$$\phi_5 = C_{2i} e^{(S_i/\dot{\phi}_1)\phi_1} \qquad (i = 1,2,3,4) \tag{25}$$

one arrives at the following expression by substitution into equation (17):

$$\begin{bmatrix} (S_i/\dot{\phi}_1)^2 + 2\zeta_{co}\lambda_{co}(S_i/\dot{\phi}_1) + (1 + K_r F_2^2)\lambda_{co}^2 & -K_r F_2 \lambda_{co}^2 \\ -2\zeta_{sp}\lambda_{sp} F_2 (S_i/\dot{\phi}_1) - F_2 \lambda_{sp}^2 & (S_i/\dot{\phi}_1)^2 + 2\zeta_{sp}\lambda_{sp}(S_i/\dot{\phi}_1) + \lambda_{sp}^2 \end{bmatrix} \begin{Bmatrix} C_{1i} \\ C_{2i} \end{Bmatrix} = 0 \tag{26}$$

To obtain a non-trivial solution for C_{1i} and C_{2i} the above determinant must vanish. This leads to the following characteristic equation:

$$S_i^4 + (2\zeta_{sp}\omega_{sp} + 2\zeta_{co}\omega_{co})S_i^3 + [\omega_{sp}^2 + (1 + K_r F_2^2)\omega_{co}^2 + 4\zeta_{co}\zeta_{sp}\omega_{co}\omega_{sp}]S_i^2 + (2\zeta_{co}\omega_{co}\omega_{sp}^2 + 2\zeta_{sp}\omega_{sp}\omega_{co}^2)S_i + \omega_{co}^2\omega_{sp}^2 = 0 \tag{27}$$

The four complex roots of the above have the from:

$$S_1 = -\alpha_1 + j\omega_1 , \quad S_2 = -\alpha_1 - j\omega_1$$
$$S_3 = -\alpha_2 + j\omega_2 , \quad S_4 = -\alpha_2 - j\omega_2 \tag{28}$$

where α_1 and α_2 are damping related constants, and ω_1 and ω_2 are the two natural frequencies of the system.

b. Solution of the Homogeneous System of Equations

With the four roots S_i, the solution of the homoqeneous system of equations becomes:

$$q = C_{11}e^{(-\alpha_1 + j\omega_1)\phi_1/\dot{\phi}_1} + C_{12}e^{(-\alpha_1 - j\omega_1)\phi_1/\dot{\phi}_1} + C_{13}e^{(-\alpha_2 + j\omega_2)\phi_1/\dot{\phi}_1} + C_{14}e^{(-\alpha_2 - j\omega_2)\phi_1/\dot{\phi}_1} \tag{29}$$

and

$$\dot{\phi}_5 = C_{21}e^{(-\alpha_1 + j\omega_1)\phi_1/\dot{\phi}_1} + C_{22}e^{(-\alpha_1 - j\omega_1)\phi_1/\dot{\phi}_1} + C_{23}e^{(-\alpha_2 + j\omega_2)\phi_1/\dot{\phi}_1} + C_{24}e^{(-\alpha_2 - j\omega_2)\phi_1/\dot{\phi}_1} \tag{30}$$

The relationships between the above constant coefficients C_{1i} and C_{2i}, respectively, are obtained from either of the two expressions in equation (26) and with the help of equation (18a), i.e.:

$$C_{2i} = \frac{1}{K_r F_2 \omega_{co}^2}[S_i^2 + 2\zeta_{co}\omega_{co}S_i + (1 + K_r F_2^2)\omega_{co}^2]C_{1i} \tag{31}$$

With the above and expressing the solutions in terms of trigonometric fuctions, one obtains:

$$q = e^{-\alpha_1\phi_1/\dot{\phi}_1}\left[L_{11}\cos\frac{\omega_1}{\dot{\phi}_1}\phi_1 + L_{12}\sin\frac{\omega_1}{\dot{\phi}_1}\phi_1\right] + e^{-\alpha_2\phi_1/\dot{\phi}_1}\left[L_{13}\cos\frac{\omega_2}{\dot{\phi}_1}\phi_1 + L_{14}\sin\frac{\omega_2}{\dot{\phi}_1}\phi_1\right] \tag{32}$$

and

$$\phi_5 = e^{-\alpha_1\phi_1/\dot{\phi}_1}\left[L_{11}\left(n_1\cos\frac{\omega_1}{\dot{\phi}_1}\phi_1 - m_1\sin\frac{\omega_1}{\dot{\phi}_1}\phi_1\right) + L_{12}\left(m_1\cos\frac{\omega_1}{\dot{\phi}_1}\phi_1 + n_1\sin\frac{\omega_1}{\dot{\phi}_1}\phi_1\right)\right] +$$

$$+ e^{-\alpha_2\phi_1/\dot{\phi}_1}\left[L_{13}\left(n_2\cos\frac{\omega_2}{\dot{\phi}_1}\phi_1 - m_2\sin\frac{\omega_2}{\dot{\phi}_1}\phi_1\right) + L_{14}\left(m_2\cos\frac{\omega_2}{\dot{\phi}_1}\phi_1 + n_2\sin\frac{\omega_2}{\dot{\phi}_1}\phi_1\right)\right] \quad (33)$$

where the L's are arbitrary constants and

$$n_1 = \frac{1}{K_r F_2 \omega_{co}^2}[\alpha_1^2 - \omega_1^2 - 2\zeta_{co}\omega_{co}\alpha_1 + (1 + K_r F_2^2)\omega_{co}^2] \quad (34)$$

$$m_1 = \frac{2}{K_r F_2 \omega_{co}^2}(\zeta_{co}\omega_{co}\omega_1 - \alpha_1\omega_1) \quad (35)$$

$$n_2 = \frac{1}{K_r F_2 \omega_{co}^2}[\alpha_2^2 - \omega_2^2 - 2\zeta_{co}\omega_{co}\alpha_2 + (1 + K_r F_2^2)\omega_{co}^2] \quad (36)$$

$$m_2 = \frac{2}{K_r F_2 \omega_{co}^2}(\zeta_{co}\omega_{co}\omega_2 - \alpha_2\omega_2) \quad (37)$$

c. Approximation of Particular Solutions of the System Equations

To obtain the particular solutions of the system equations, it is necessary to express the forcing terms $R_1(\phi_1, \dot{\phi}_1)$ and $R_2(\phi_1, \dot{\phi}_1)$ of equations (21) and (22) in terms of Fourier series. If only the constant and first harmonic terms are kept, the forcing terms are approximated by[5]:

$$R_1(\phi_1, \dot{\phi}_1) = A_{10} + A_{11}\cos\phi_1 + B_{11}\sin\phi_1 \quad (38)$$

$$R_2(\phi_1, \dot{\phi}_1) = A_{20} + A_{21}\cos\phi_1 + B_{21}\sin\phi_1 \quad (39)$$

---

5 The numerical computations for the coefficients, associated with the standard feed mechanism, have shown that the magnitudes of the coefficients of the higher terms decrease rapidly.

The expressions for the above coefficients are given by equations (C.17) and (C.22) in Appendix C.

Thus, the particular solutions of the system equation are obtained by assuming that

$$q = C_0 + C_{s1}\sin\phi_1 + C_{c1}\cos\phi_1 \tag{40}$$

and

$$\phi_5 = D_0 + D_{s1}\sin\phi_1 + D_{c1}\cos\phi_1 \tag{41}$$

Substituting the above into the system equation (17) and equating like terms furnishes all constants. Thus,

$$C_0 = \frac{A_{10}}{\lambda_{co}^2} + K_r F_2 \frac{A_{20}}{\lambda_{sp}^2} \tag{42}$$

$$D_0 = \frac{A_{20}}{\lambda_{sp}^2} + F_2 C_0 \tag{43}$$

and C_{s1}, C_{c1}, D_{s1} and D_{c1} are obtained from:

$$\begin{bmatrix} (1+K_r F_2^2)\lambda_{co}^2 - 1 & -2\zeta_{co}\lambda_{co} & -K_r F_r \lambda_{co}^2 & 0 \\ 2\zeta_{co}\lambda_{co} & (1+K_r F_2^2)\lambda_{co}^2 - 1 & 0 & -K_r F_2 \lambda_{co}^2 \\ -F_2\lambda_{sp}^2 & 2\zeta_{sp}\lambda_{sp}F_2 & \lambda_{sp}^2 - 1 & -2\zeta_{sp}\lambda_{sp} \\ -2\zeta_{sp}\lambda_{sp}F_2 & -F_2\lambda_{sp}^2 & 2\zeta_{sp}\lambda_{sp} & \lambda_{sp}^2 - 1 \end{bmatrix} \begin{Bmatrix} C_{s1} \\ C_{c1} \\ D_{s1} \\ D_{c1} \end{Bmatrix} = \begin{Bmatrix} B_{11} \\ A_{11} \\ B_{21} \\ A_{21} \end{Bmatrix} \tag{44}$$

d. Complete Solutions of System Equations

By combining the respective homogeneous and particular solutions, the complete solutions of the system equations for Regime No.2 become:

$$q = e^{-\alpha_1\phi_1/\dot{\phi}_1}\left[L_{11}\cos\frac{\omega_1}{\dot{\phi}_1}\phi_1 + L_{12}\sin\frac{\omega_1}{\dot{\phi}_1}\phi_1\right] + e^{-\alpha_2\phi_1/\dot{\phi}_1}\left[L_{13}\cos\frac{\omega_2}{\dot{\phi}_1}\phi_1 + L_{14}\sin\frac{\omega_2}{\dot{\phi}_1}\phi_1\right] +$$

$$+ C_0 + C_{s1}\sin\phi_1 + C_{c1}\cos\phi_1 \tag{45}$$

$$\phi_5 = e^{-\alpha_1\phi_1/\dot{\phi}_1}\left[L_{11}\left(n_1\cos\frac{\omega_1}{\dot{\phi}_1}\phi_1 - m_1\sin\frac{\omega_1}{\dot{\phi}_1}\phi_1\right) + L_{12}\left(m_1\cos\frac{\omega_1}{\dot{\phi}_1}\phi_1 + n_1\sin\frac{\omega_1}{\dot{\phi}_1}\phi_1\right)\right] +$$

$$+ e^{-\alpha_2\phi_1/\dot{\phi}_1}\left[L_{13}\left(n_2\cos\frac{\omega_2}{\dot{\phi}_1}\phi_1 - m_2\sin\frac{\omega_2}{\dot{\phi}_1}\phi_1\right) + L_{14}\left(m_2\cos\frac{\omega_2}{\dot{\phi}_1}\phi_1 + n_2\sin\frac{\omega_2}{\dot{\phi}_1}\phi_1\right)\right] +$$

$$+ D_0 + D_{s1}\sin\phi_1 + D_{c1}\cos\phi_1 \tag{46}$$

where the four unknown coefficients L_{11}, L_{12}, L_{13} and L_{14} must be determined with the help of the initial conditions of Regime No.2.

For the convenience of later analysis, all harmonic terms with identical frequencies in the above solutions are now transformed into sine functions, together with their associated phase angles. Thus,

$$q = e^{-\alpha_1\phi_1/\dot{\phi}_1}\sqrt{(L_{11}^2 + L_{12}^2)}\sin\left(\frac{\omega_1}{\dot{\phi}_1}\phi_1 + \gamma_1\right) + e^{-\alpha_2\phi_1/\dot{\phi}_1}\sqrt{(L_{13}^2 + L_{14}^2)}\sin\left(\frac{\omega_2}{\dot{\phi}_1}\phi_1 + \gamma_2\right) +$$

$$+ C_0 + C_1\sin(\phi_1 + \alpha_c) \tag{47}$$

$$\phi_5 = e^{-\alpha_1\phi_1/\dot{\phi}_1}\sqrt{(L_{11}^2 + L_{12}^2)(n_1^2 + m_1^2)}\sin\left(\frac{\omega_1}{\dot{\phi}_1}\phi_1 + \gamma_1 + \theta_1\right) +$$

$$+ e^{-\alpha_2\phi_1/\dot{\phi}_1}\sqrt{(L_{13}^2 + L_{14}^2)(n_2^2 + m_2^2)}\sin\left(\frac{\omega_2}{\dot{\phi}_1}\phi_1 + \gamma_2 + \theta_2\right) +$$

$$+ D_0 + D_1\sin(\phi_1 + \alpha_d) \tag{48}$$

where the amplitudes and the phase angles are determined by

$$\gamma_1 = \tan^{-1}(L_{11}/L_{12}) \tag{49}$$

$$\gamma_2 = \tan^{-1}(L_{13}/L_{14}) \tag{50}$$

$$C_1 = \sqrt{(C_{s1}^2 + C_{c1}^2)}$$
$$D_1 = \sqrt{(D_{s1}^2 + D_{c1}^2)} \tag{51}$$

$$\theta_1 = \tan^{-1}(m_1/n_1)$$
$$\theta_2 = \tan^{-1}(m_2/n_2) \tag{52}$$

$$\alpha_c = \tan^{-1}(C_{c1}/C_{s1})$$
$$\alpha_d = \tan^{-1}(D_{c1}/D_{s1}) \tag{53}$$

e. Clutch Windup Angle $\phi_{5/4}$

The dynamic behavior of the sprag clutch is best described by the relative rotation between its inner and its outer race, i.e. the windup angle $\phi_{5/4} = \phi_5 - \phi_{4e}$. To this end, substitution of equations (14), (47) and (48) into the latter expression furnishes:

$$\phi_{5/4} = \phi_5 - \phi_{4e} = \phi_5 - (F_2 q + \phi_{4r})$$
$$= e^{-\alpha_1 \phi_1/\dot{\phi}_1} X_1 \cdot \sin\left(\frac{\omega_1}{\dot{\phi}_1}\phi_1 + \gamma_1 + \psi_1\right) + e^{-\alpha_2 \phi_1/\dot{\phi}_1} X_2 \cdot \sin\left(\frac{\omega_2}{\dot{\phi}_1}\phi_1 + \gamma_2 + \psi_2\right) +$$
$$+X_3 \cdot \sin(\phi_1 + \psi_3) + (T_b/K_{sp})^{2/3} \tag{54}$$

where the amplitudes are given by:

$$X_1 = \sqrt{L_{11}^2 + L_{12}^2} \cdot \sqrt{n_1^2 + m_1^2 + F_2^2 - 2F_2\sqrt{n_1^2 + m_1^2}\cos\theta_1} \tag{55}$$

$$X_2 = \sqrt{L_{13}^2 + L_{14}^2} \cdot \sqrt{n_2^2 + m_2^2 + F_2^2 - 2F_2\sqrt{n_2^2 + m_2^2}\cos\theta_2} \tag{56}$$

$$X_3 = [(D_1^2 + a_{31}^2 + b_{31}^2 + F_2^2 C_1^2) - 2D_1\sqrt{a_{31}^2 + b_{31}^2}\cos(\alpha_d - \alpha_{31}) -$$
$$-2D_1 C_1 F_2 \cos(\alpha_d - \alpha_c) + 2F_2 C_1\sqrt{a_{31}^2 + b_{31}^2}\cos(\alpha_{31} - \alpha_c)]^{1/2} \tag{57}$$

and the phase angles by:

$$\psi_1 = \tan^{-1}\left(\frac{\sqrt{n_1^2+m_1^2}\cdot\sin\theta_1}{\sqrt{n_1^2+m_1^2}\cdot\cos\theta_1 - F_2}\right) \tag{58}$$

$$\psi_2 = \tan^{-1}\left(\frac{\sqrt{n_2^2+m_2^2}\cdot\sin\theta_2}{\sqrt{n_2^2+m_2^2}\cdot\cos\theta_2 - F_2}\right) \tag{59}$$

$$\psi_3 = \tan^{-1}\left(\frac{D_1\sin\alpha_d - \sqrt{a_{31}^2+b_{31}^2}\sin\alpha_{31} - F_2C_1\sin\alpha_c}{D_1\cos\alpha_d - \sqrt{a_{31}^2+b_{31}^2}\cos\alpha_{31} - F_2C_1\cos\alpha_c}\right) \tag{60}$$

$$\alpha_{31} = \tan^{-1}\left(\frac{b_{31}}{a_{31}}\right) \tag{61}$$

This regime terminates when the rocker angle reaches its upper most extreme position and the velocity of the rocker must be zero, i.e.:

$$\phi'_{4c}(\phi_1) = \phi'_{4r}(\phi_1) + F_2 q'(\phi_1) \geq 0 \tag{62}$$

7. COMPARISON BETWEEN COMPUTED AND EXPERIMENTAL RESULTS

In order to verify the mathematical solutions obtained from the linearized and simplified system equations for the feed mechanism, it is necessary that they are compared with experimental results. To this end, as in the non-linear numerical solution by Chassapis and Lowen (1991), the coupler strain and the clutch windup angle are used as comparison criteria.

a. Method of Computation

To start with, $q(\phi_1)$ and $\phi_{5/4}(\phi_1)$ are obtained for a complete cycle of the feed mechanism operation with the help of equations (47), (55), (D.8), (E.8) and (F.6). The computation begins with Regime No.1 and continues with Regimes 2, 3 and 4. The end values for each regime serve as the initial conditions for the following one.

Since the true initial conditions for Regime No.1 are impossible to know before the end conditions for Regime No.4 are obtained, one assumes, for a start-up cycle, that both $q(\phi_1)$ and $q'(\phi_1)$ are equal to zero, and that the angles ϕ_1 and ϕ_5, associated with the initial extreme position of ϕ_4, are found from rigid body kinematics. Once the start-up cycle is completed, the initial conditions for Regime No.1 are changed to the end conditions of Regime No.4.

An example of a complete computation for Run No.1 (as defined below) is given in Appendix H. It shows the computations for two complete mechanism cycles, starting from stand-still. Experience has indicated that the second cycle sets the standard for all variables in subsequent cycles.

b. Determination of coupler strain

The deflections of individual points on the two coupler sections may be obtained with the help of equations (3), (4) and (47). Since strain at the outer fibers of the coupler sections is given by,

$$\varepsilon = \frac{D_o}{2} \cdot \frac{d^2 v_i}{dx_i^2} \qquad (i = 1,2) \tag{63}$$

one finds

$$\varepsilon = q(t) \cdot \frac{D_o}{2} \left(\frac{\pi}{2L} \right)^2 \sin\left(\frac{\pi}{2L} x_i \right) \tag{64}$$

c. Experimental Setup

Figure 4 shows the experimental setup, which is essentially that described earlier by Chassapis and Lowen (1990).

A schematic of the instrumentation is presented in Figure 5. The dynamic behavior of the bent coupler is monitored with the help of a strain gage located in the coupler bending plane ABC and at $x_1 = 11$ in.

The angular motions of the crank (input) shaft, the rocker shaft and the feed roller (output) shaft are obtained by way of three angular encoders, which are able to furnish pulses for every 0.036 degree of angular motion. A data acquisition system is used to store and subsequently transmit to a PC the following data for a complete mechanism cycle:

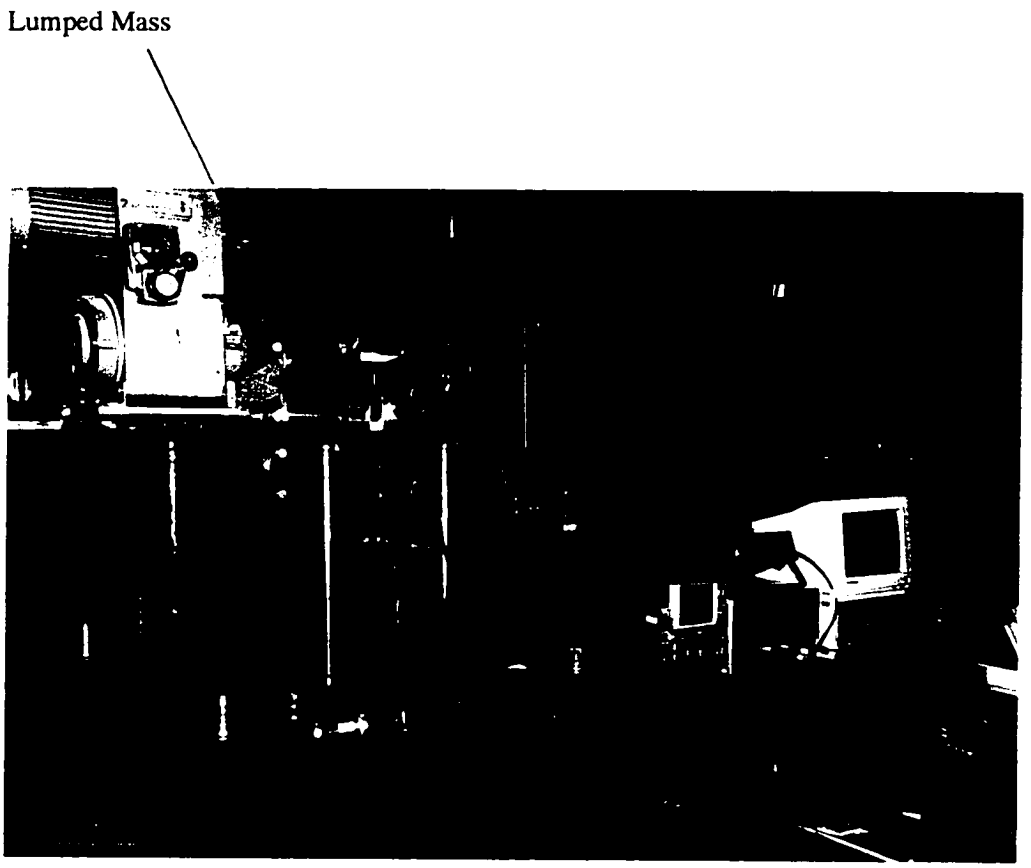

Figure 4 Experimental Setup of the Feed Mechanism with Lumped Mass Attached to Coupler

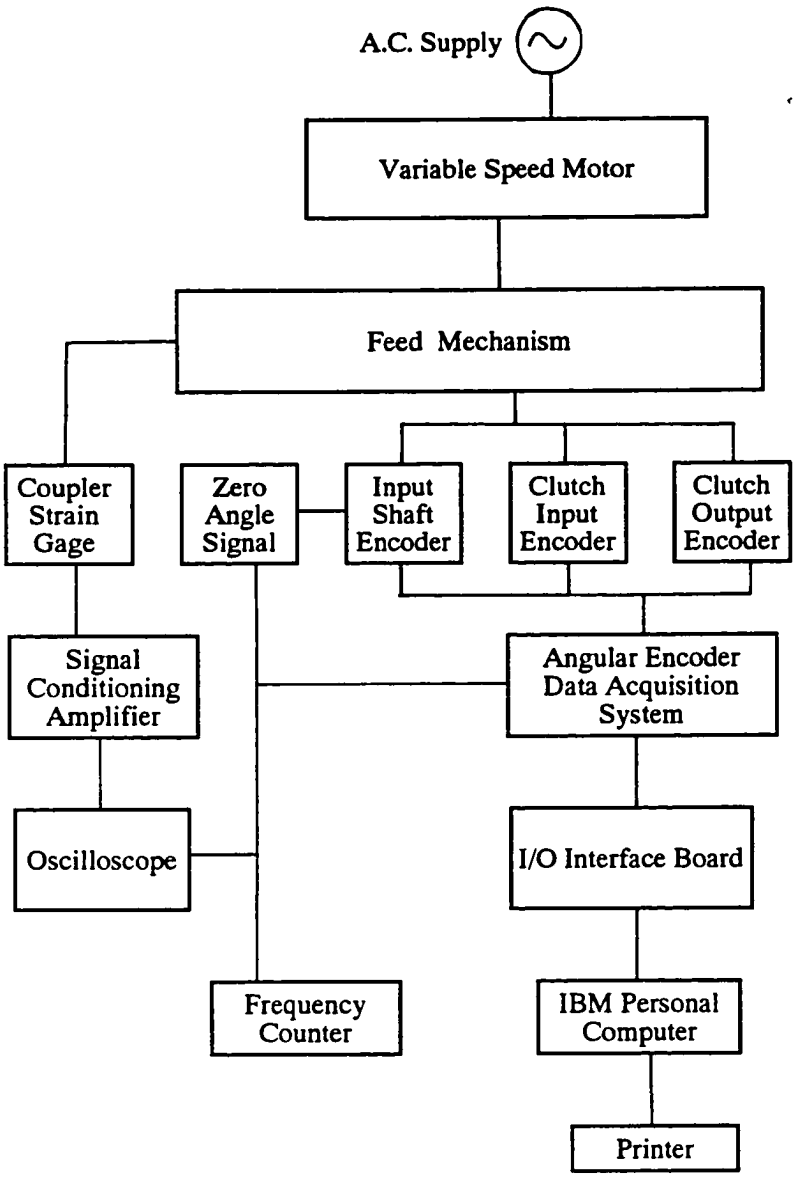

Figure 5 Schematic of Instrumentation

(1) The time associated with each 0.036 degree rotation of the mechanism input angle ϕ_1, with zero time corresponding to $\phi_1 = 0°$.

(2) The time associated with each 0.036 degree of forward rotation of the rocker link (clutch input) angle ϕ_4.

(3) The time associated with each 0.036 degree of forward rotation of the feed roller (clutch output) angle ϕ_5.

A newly written algorithm, given in Appendix I, makes it possible for the aforementioned PC to establish the windup angle $\phi_{5/4}$ as a function of the mechanism input angle ϕ_1 for the forward stroke with the help of the angles ϕ_1, ϕ_4 and ϕ_5, which correspond to a given time in the cycle.

d. Physical Parameters

Unless otherwise defined, the physical parameters used in the computations are those of the standard experimental setup and are listed in Table 1. Note that the density ρ of the coupler, which used in connection with the kinetic energy of the coupler in Appendix B, represents a uniform link approximation of the actual coupler.

The values of the damping constants C_{co} and C_{sp}, which account for the energy dissipation of the coupler and the clutch, respectively, were selected such that the best fit with the experimental results for Run No.1 was obtained. (It must be remembered that there are a number of not readily quantifiable causes of energy dissipation, such as material damping, viscous and Coulomb damping in the bearings, as well as bearing impacts, in this type of machinery.)

Linkage Dimensions
$a_1 = 0.965$(in) $a_3 = 32.523$(in) $a_4 = 4.500$(in)
$s_1 = 1.156$(in) $s_2 = 8.260$(in) $s_3 = 31.410$(in)
Coupler Parameters
$L = 16.625$(in) $\alpha = 12.0$(degree) $D_o = 1.00$(in)
$D_i = 0.75$(in) $I = 3.35 \times 10^{-2}$(in^4) $E = 30 \times 10^6$(lb/in^2)
$\rho = 7.3 \times 10^{-4}$(lb-in^{-4}-sec^2) $C_{co} = 0.06$(lb-in^{-1}-sec)
Clutch Parameters
$K_{sp} = 2 \times 10^5$(lb-in-rad$^{-3/2}$) $C_{sp} = 11.0$(lb-in-sec)
Other Parameters
Rocker and clutch input shaft assembly moment of inertia:
$J_{o4} = 0.1286$(lb-in-sec^2)
Clutch output shaft assembly and strip moment of inertia:
$J_{o5} = 0.114$ + referred strip inertia(lb-in-sec^2)
Total resisting torque on clutch output shaft:
T_b = variable(lb-in)

Table 1 Parameters of the Standard Feed Mechanism

e. Model Verification

For purposes of model verification by comparison of computed and experimental results, three runs with different operating conditions were made. While Figure 6 gives an oscilloscope trace of the coupler strain for Run No.1, the associated figures 7, 8 and 9 show both computed and experimental coupler strains in part (a) and clutch windup angles[6] in part (b), respectively. (R.1, etc. refers to regimes)

Although only the responses of the coupler and the clutch during regime No.2 are of real importance for this work, the coupler strain histories are shown for all regimes, while the clutch windup angle traces are only given for the first two regimes (Since they vanish after that.)

The coupler parameters of runs No.1 and No.2 are the standard ones given in Table 1. In order to show the influence of a lower than standard coupler natural frequency, a lumped mass has been added to the coupler at point B for run No.3. Appendix G shows how this reflects itself both in the experiment as well as in the model.

(1) The parameters associated with Run No.1 are:

Input speed $\dot{\phi}_1$ = 200 (RPM)

Resisting Torque T_b = 160 (lb-in)

Steel feed strip = 4.0 x 0.125 x 130.0 (in)

(Referred moment of inertia = 0.298)

Coupler = Standard

---

6 To follow the experimentally influenced convention of Chassapis and Lowen, where $\phi_{5/4} = -(\phi_5 - \phi_4)$, the various plots of equation (55) will have reversed signs in this work.

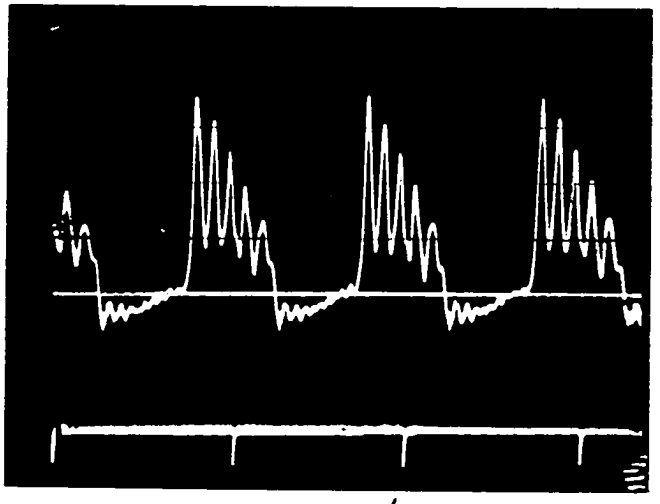

Figure 6 Run No.1: Oscillogram of Coupler Strain

Horizontal Scale: .1 sec/div

Vertical Scale: 40 microstrain/div

Input Speed: 200 RPM

Strip Size: 4.0x.125x130.0 in

Brake Torque: 160 lb-in

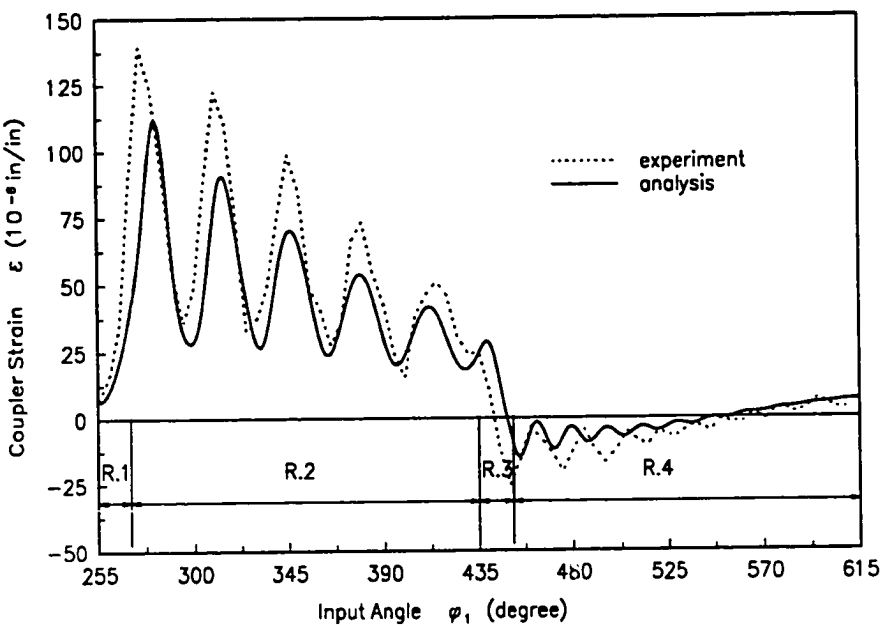

a. Coupler Strain vs. Input Angle

Figure 7 Comparison between Computed and Experimental Results for Run No.1

Input Speed: 200 RPM, Strip Size: 4.0x.125x130.0 in

Brake Torque: 160 lb-in, Coupler: Standard (without lumped mass)

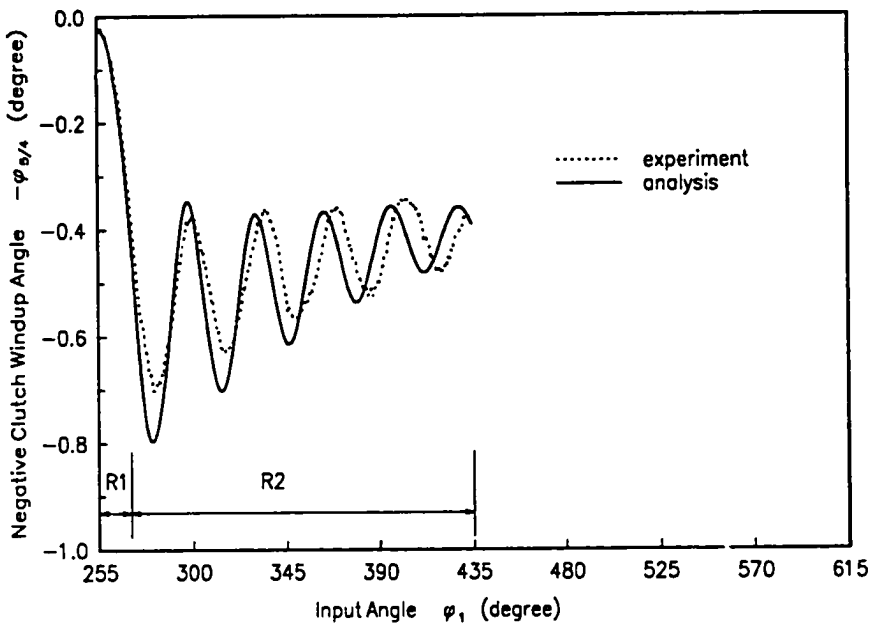

b. Clutch Windup Angle vs. Input Angle

Figure 7 Comparison between Computed and Experimental Results for Run No.1

Input Speed: 200 RPM, Strip Size: 4.0x.125x130.0 in

Brake Torque: 160 lb-in, Coupler: Standard (without lumped mass)

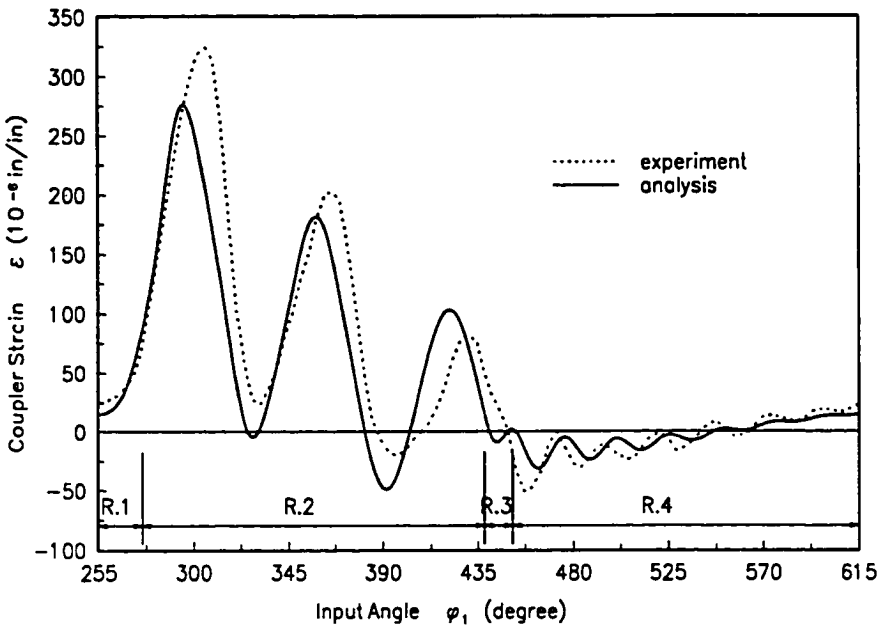

a. Coupler Strain vs. Input Angle

Figure 8 Comparison between Computed and Experimental Results for Run No.2

Input Speed: 300 RPM, Strip Size: 4.0x.25x153.5 in

Brake Torque: 300 lb-in, Coupler: Standard (without lumped mass)

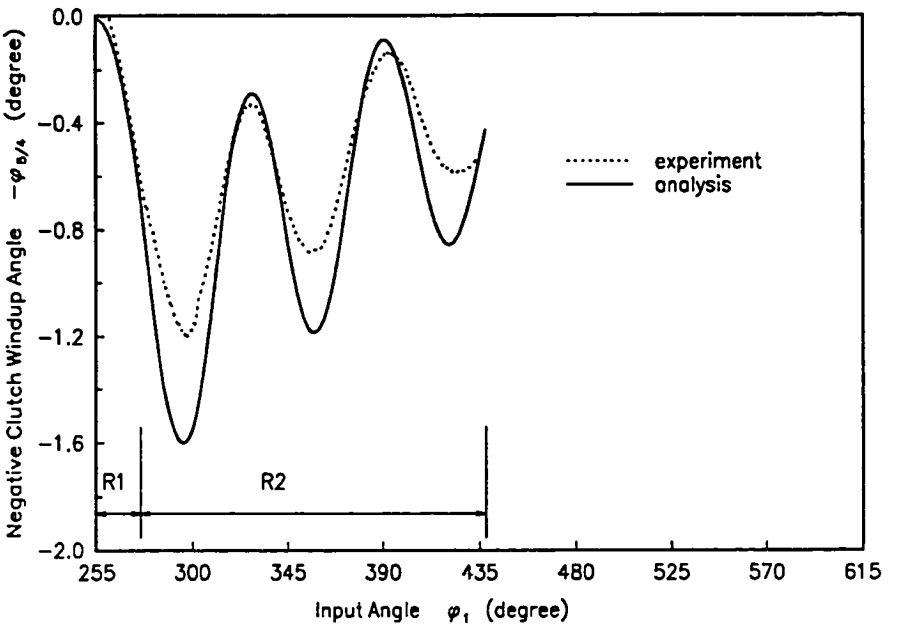

b. Clutch Windup Angle vs. Input Angle

Figure 8 Comparison between Computed and Experimental Results for Run No.2

Input Speed: 300 RPM, Strip Size: 4.0x.25x153.5 in

Brake Torque: 300 lb-in, Coupler: Standard (without lumped mass)

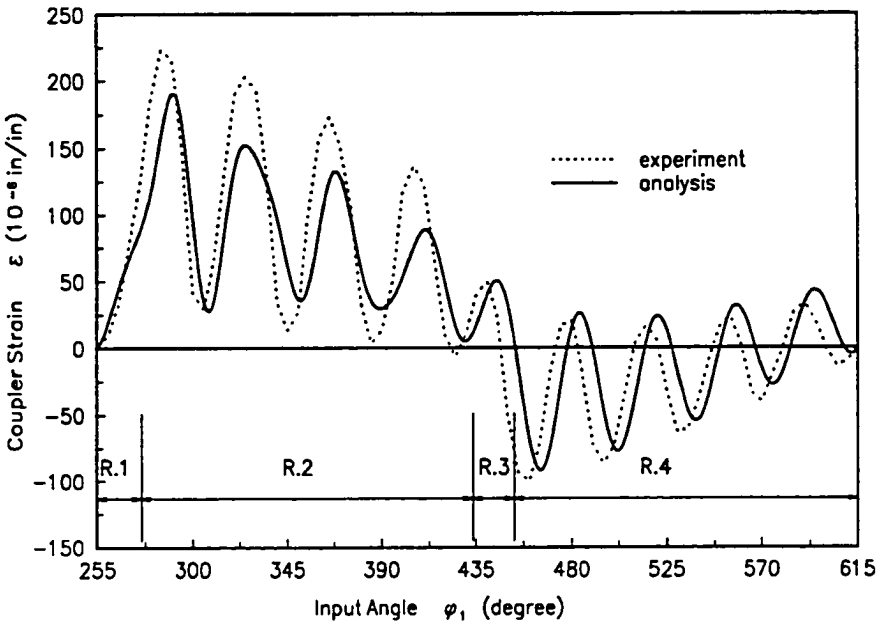

a. Coupler Strain vs. Input Angle

Figure 9 Comparison between Computed and Experimental Results for Run No.3

Input Speed: 200 RPM, Strip Size: 4.0x.125x130.0 in

Brake Torque: 260 lb-in, Coupler: Modified (with lumped mass)

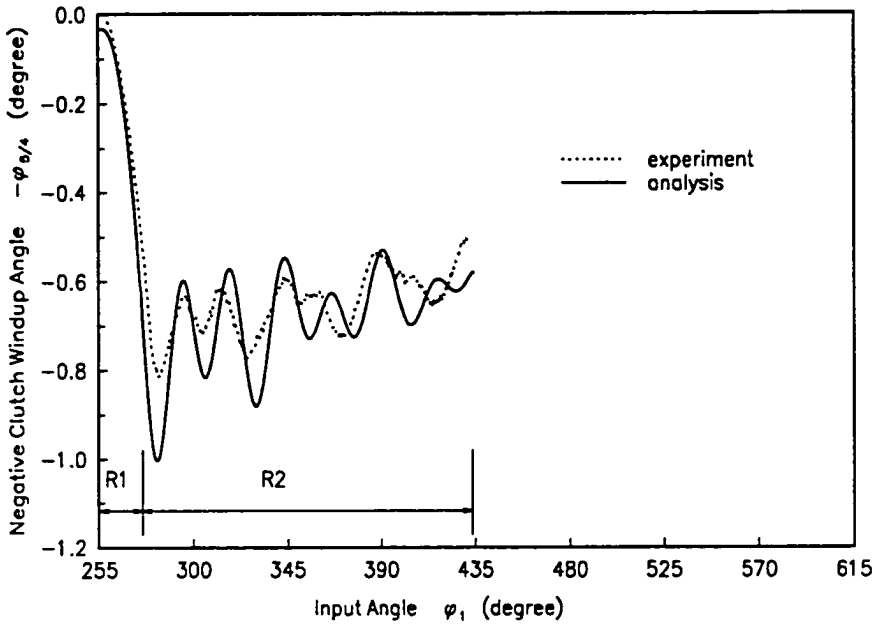

b. Clutch Windup Angle vs. Input Angle

Figure 9 Comparison between Computed and Experimental Results for Run No.3

Input Speed: 200 RPM, Strip Size: 4.0x.125x130.0 in

Brake Torque: 260 lb-in, Coupler: Modified (with lumped mass)

Coupler natural frequency $\omega_{co} = (\sqrt{K_c/M_c})/(2\pi) = 73.1$ (Hz)

(evaluated according to equations (19) and (20))

Clutch natural frequency $\omega_{sp} = (\sqrt{K_{12}/J_{o5}})/(2\pi) = 41.5$ (Hz)

(evaluated according to equation (C.3))

(2) The parameters associated with Run No.2 are:

Input speed $\dot{\phi}_1 = 300$ (RPM)

Resisting Torque $T_b = 300$ (lb-in)

Steel feed strip = 4.0 x 0.25 x 153.5 (in)

(Referred moment of inertia = 0.703)

Coupler = Standard

Coupler natural frequency $\omega_{co} = (\sqrt{K_c/M_c})/(2\pi) = 73.1$ (Hz)

(evaluated according to equations (19) and (20))

Clutch natural frequency $\omega_{sp} = (\sqrt{K_{12}/J_{o5}})/(2\pi) = 36.7$ (Hz)

(evaluated according to equation (C.3))

(3) The parameters associated with Run No.3 are:

Input speed $\dot{\phi}_1 = 200$ (RPM)

Resisting Torque $T_b = 260$ (lb-in)

Steel feed strip = 4.0 x 0.125 x 130.0 (in)

(Referred moment of inertia = 0.298)

Coupler = Modified (See Appendix G)

Coupler natural frequency $\omega_{co} = (\sqrt{K_c/M_c})/(2\pi) = 32.5$ (Hz)

(evaluated according to equations (19) and (20))

Clutch natural frequency $\omega_{sp} = (\sqrt{K_{12}/J_{o5}})/(2\pi) = 45.0$ (Hz)

(evaluated according to equation (C.3))

Considering the many simplifications in this linearized model of the mechanism, there is generally reasonable agreement in terms of amplitude and phase angle for the coupler strain. This also holds true for the clutch windup angle for Runs No.1 and No.2. For Run No.3, the clutch windup angle trace is lacking in agreement, but makes it amply clear that the second system frequency plays a considerable part in addition to the first one. This point will be discussed in detail in the next section.

Thus, one may conclude that the new linearized mathematical model with its closed solution can be used to obtain a better qualitative understanding of the interrelationship between the various parameters and system frequencies of the mechanism. Further, the strain histories of the coupler justify the assumed approximation of the coupler shape function.

8. INSIGHTS TO BE GAINED FROM NEW ANALYTICAL SOLUTION

a. Responses During Forward Motion

Figures 10, 11 and 12 show plots of each of the four components of the coupler strain and the clutch windup angle (see footnote 6) during forward motion for runs 1, 2 and 3, respectively, with the help of equations (47) and (54). In each case, there are two transient oscillations of the first and second system (natural) frequencies, respectively, as well as two forced responses. One of the latter is constant and due to the resisting torque. The other is caused by the input speed dependent inertia of the system. It is important to note the large role played by the transient responses in this type of multi-regime per cycle machinery.

Further, with the exception of the clutch windup angle in Run 3, the amplitudes of the first system frequencies are generally much larger than those of the second for the given set of parameters. This explains the essentially identical frequency characteristics of the strain and the clutch windup angle shown for regime No.2 in Figures 7 and 8. The fact that the clutch windup angle response in Figure 9 shows a different frequency characteristic than that of the strain is due to the more pronounced amplitude of the higher frequency oscillation. In all cases, the forced responses only influence the mean position of the transient oscillations.

b. Relationship between Component Frequencies and System Frequencies

Chassapis and Lowen (1990) observed that the frequency responses of the coupler strain and the clutch windup angle in regime No.2 of the standard mechanism, were not only

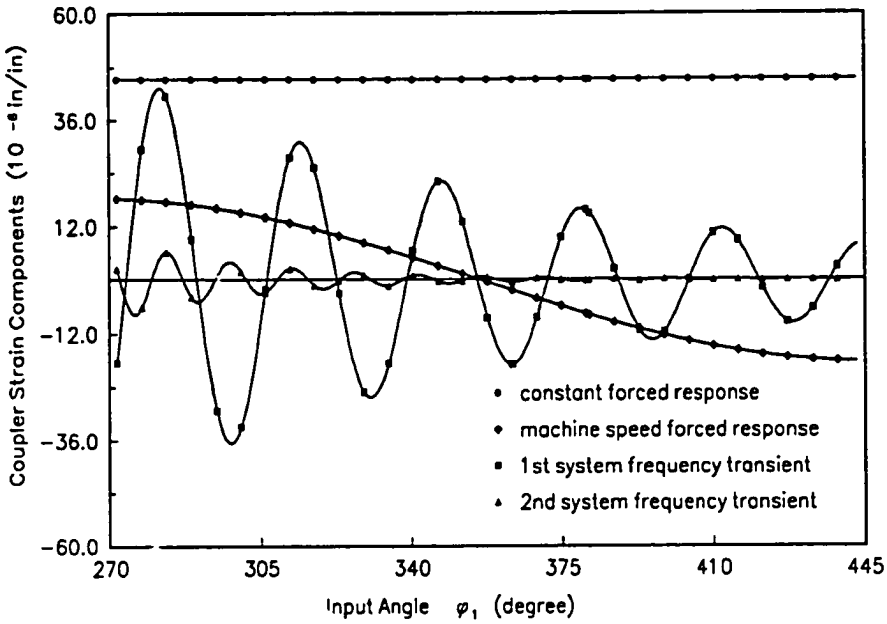

a) Coupler Strain

Figure 10 Components of Coupler and Clutch Responses for Run No.1

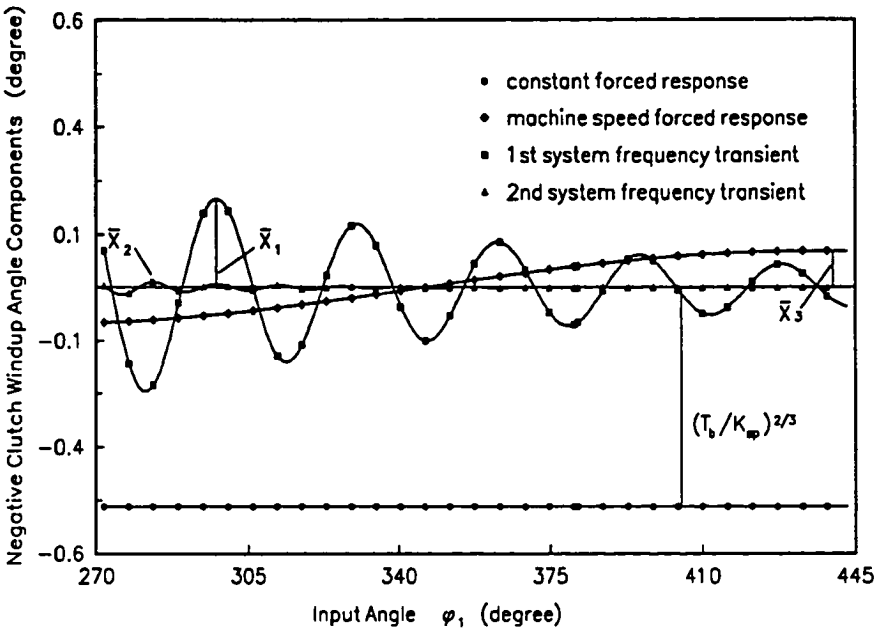

b) Clutch Windup Angle

Figure 10 Components of Coupler and Clutch Responses for Run No.1

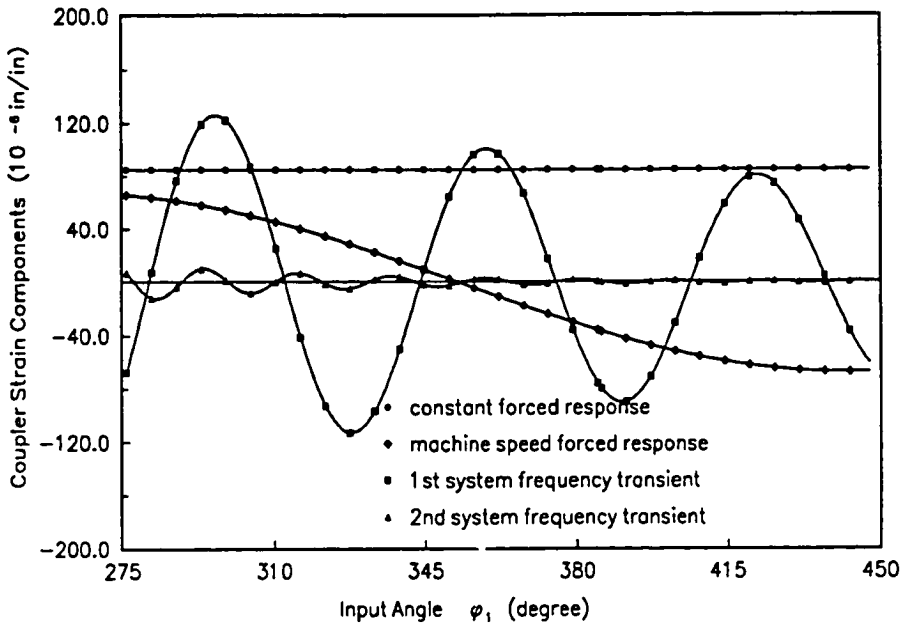

a) Coupler Strain

Figure 11 Components of Coupler and Clutch Responses for Run No.2

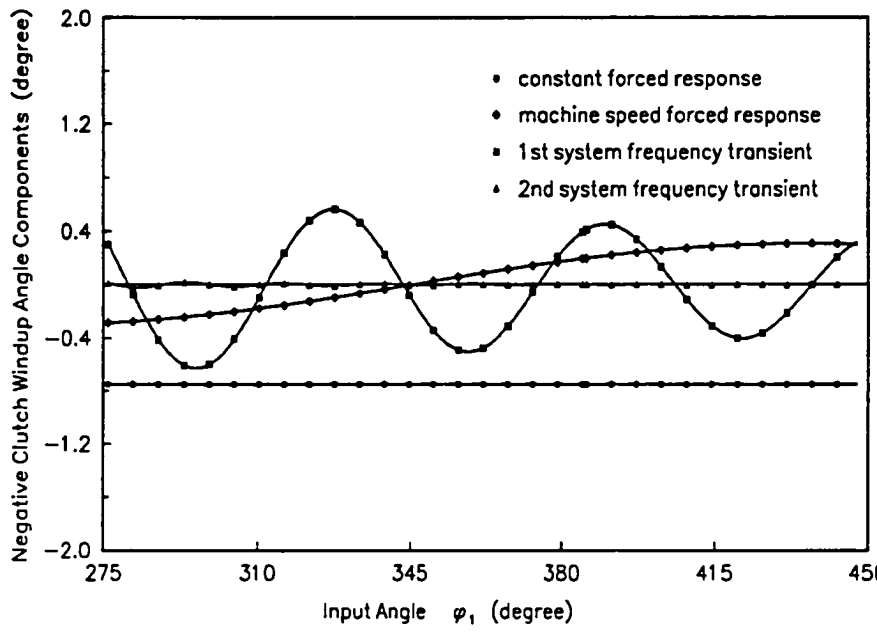

b) Clutch Windup Angle

Figure 11 Components of Coupler and Clutch Responses for Run No.2

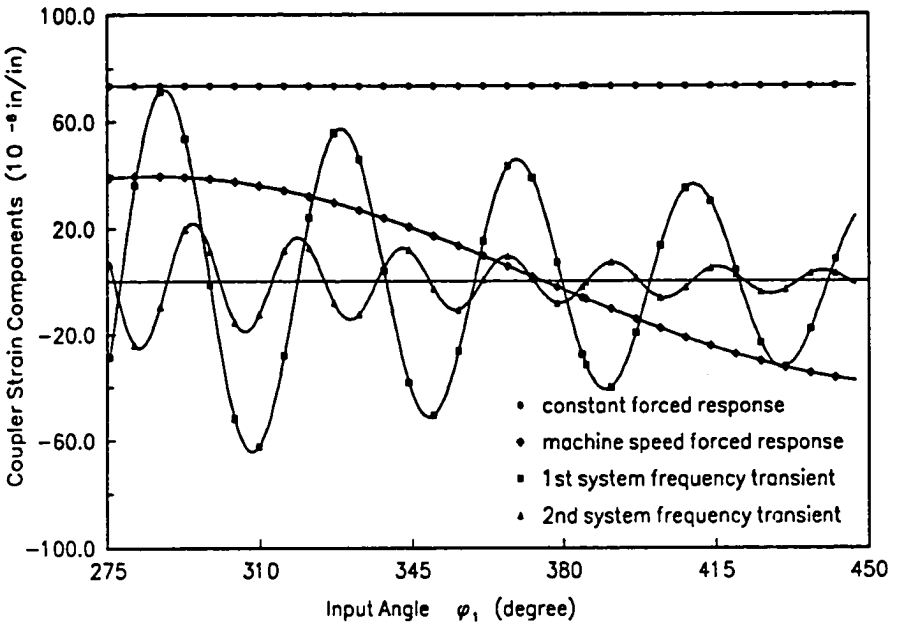

a) Coupler Strain

Figure 12 Components of Coupler and Clutch Responses for Run No.3

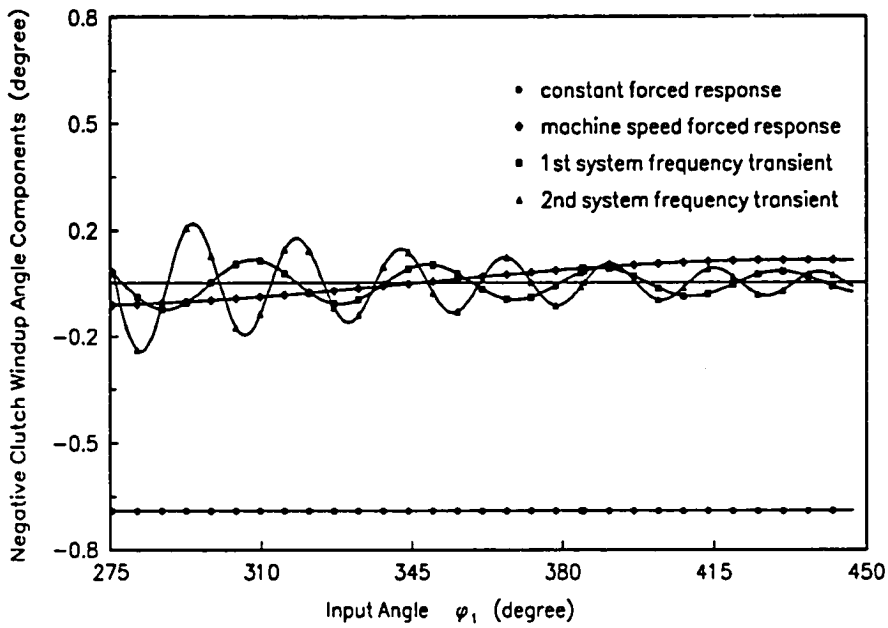

b) Clutch Windup Angle

Figure 12 Components of Coupler and Clutch Responses for Run No.3

identical, as discussed above, but also were very close to the linearized clutch natural frequency of a particular run. Figures 13 and 14 shed light on the relationship between the two transient system frequencies and the component frequencies of the clutch system and the coupler as functions of the coupler diameter and its density (by use of equations (27) and (28)).

Figure 13 shows that for D_o = 1.000 inch, i.e. the standard configuration, the system frequencies ω_1 and ω_2 are close to the component frequencies ω_{sp} and ω_{co}, respectively. This phenomenon becomes more pronounced as D_o increases, i.e. the coupler becomes stiffer.

As D_o is decreased, however, the system and component frequencies deviate more and more from their original association until it is reversed. Thus, one may state that the lower system frequency is always near to and smaller than the lower component frequency, while the higher system frequency is always near to and larger than the higher component frequency.

Figure 14 shows the identical frequency association reversal as the coupler frequency is lowered by increasing the coupler density. Note that again for Run No.1 the first system frequency is close to that of the clutch, while it is close to that of the coupler for Run No.3, where the equivalent density has been increased.

Presently, there is no information on what exactly influences the relative size of the amplitudes associated with each of the system frequencies, other than the observation that the lower system frequency usually has the larger amplitude.

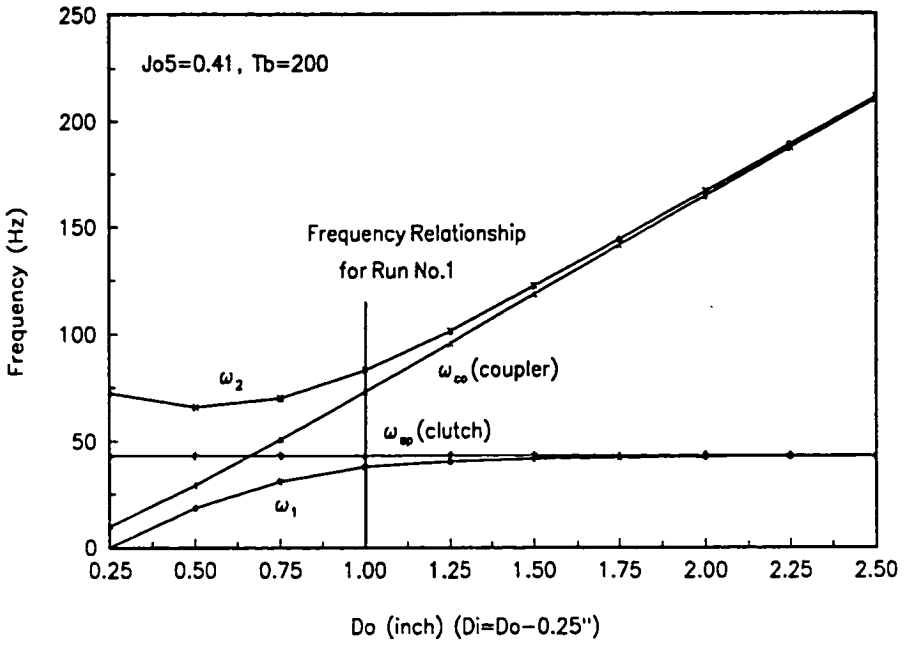

Figure 13 Relationship between System and Component Frequencies as function of Coupler Diameter

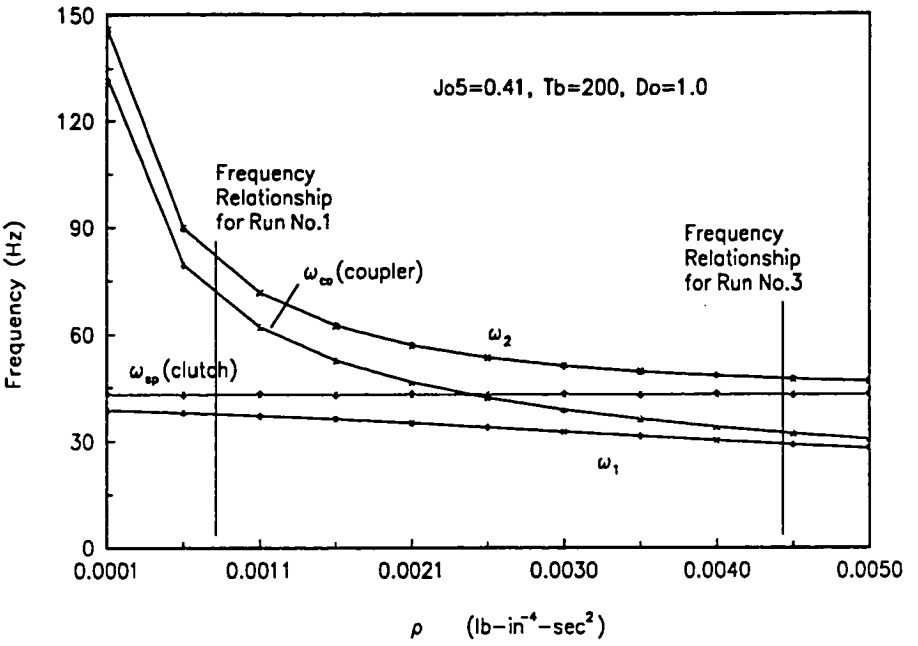

Figure 14 Relationship between System and Component Frequencies as function of Coupler Density

c. Maximum Coupler and Clutch Deflections

Figure 15 shows plots of the maximum computed deflections of the coupler, which occurs at point B, as functions of the coupler stiffness, i.e. D_o, for four combinations of clutch output moment of inertia J_{o5}, coupler density ρ and clutch stiffness K_{sp}. Clearly, the smaller D_o, the greater the deflection. This is especially pronounced for the larger strip size as well as for a coupler with increased density. As might be expected, the spring constant of the clutch has no influence on the coupler deflection at the low speeds considered.

Figure 16 deals with the influence of the clutch stiffness on the maximum value of the clutch windup angle for four combinations of coupler stiffness, coupler density and strip size. Naturally, the softer the clutch spring the larger the windup angle for any of the combinations. Since J_{o5} represents the principal load, the deflection increases with an increase of this value. It is of interest to note that the influence of the coupler density is minimal. For a very soft coupler, i.e. with a small D_o, the clutch windup angle is shown to be somewhat smaller that for a stiffer one. This might be explained by the fact that in the dynamic situation the coupler stretches and causes a slight increase in rocker angle ϕ_4.

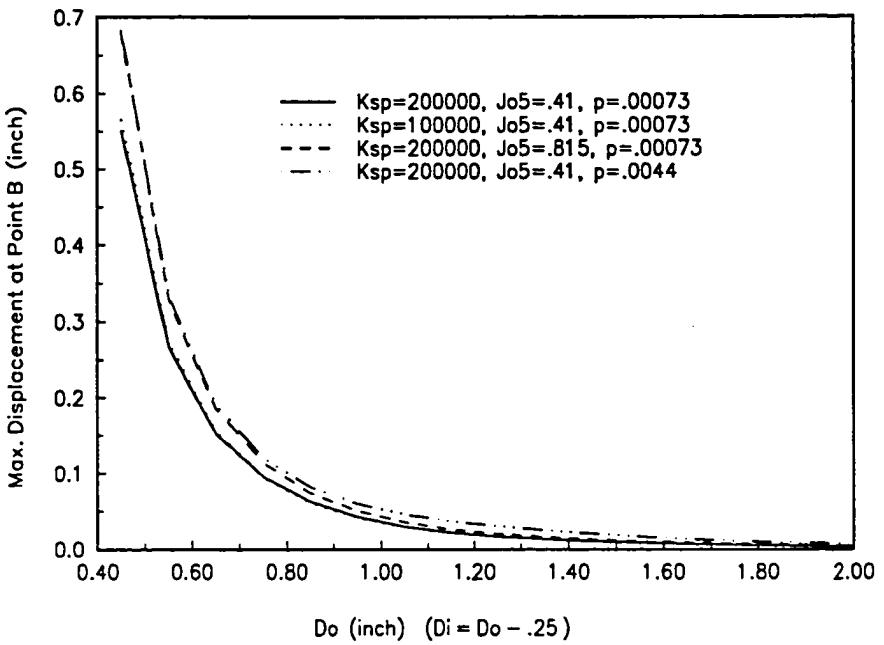

Figure 15 Maximum Coupler Deflection as Function of Coupler Diameter for Various Parameter Combinations and 200 RPM

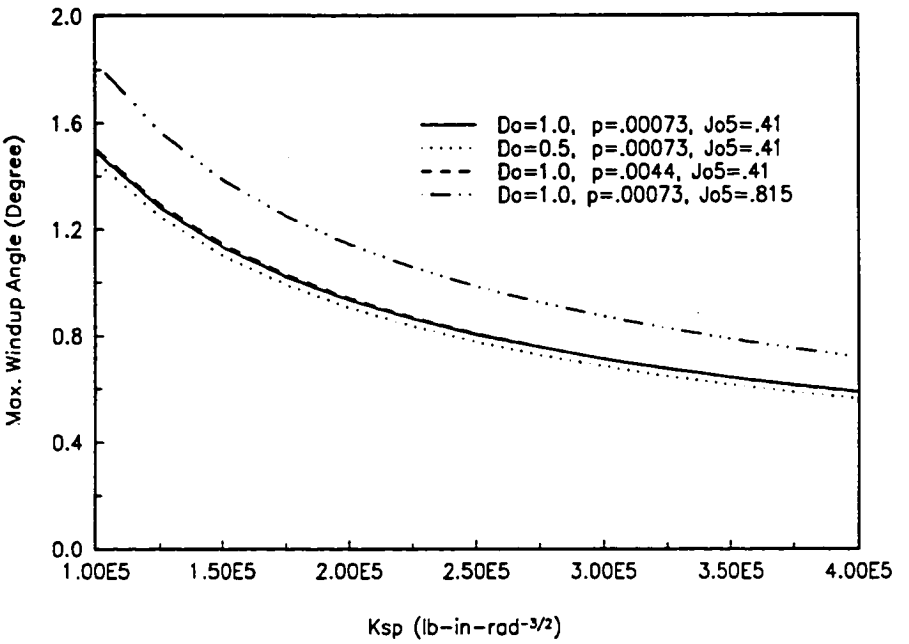

Figure 16 Maximum Clutch Windup Angle as Function of Clutch Stiffness for Various Parameter Combinations and 200 RPM

9. ESTIMATE OF MINIMUM BRAKE TORQUE

Chassapis and Lowen (1990) have shown that in order to have normal operation of the clutch during the forward stroke and to avoid overshooting of the stock at the end of the forward stroke, the clutch must never disengage. This means that the negative clutch windup angle must never become positive (see footnote 2), i.e.:

$$-(\phi_5 - \phi_4)_{min} < 0 \tag{65}$$

during regimes No.1 and No.2.

To attain this goal conservatively, one assumes a worst condition in which the three maximum oscillatory amplitudes $\overline{X}_i$ in the direction of unwinding of the clutch, as shown in Figure 10b, are added. This modification of equation (55) takes the form:

$$\phi_{5/4(min)} = (T_b/K_{sp})^{2/3} - (\overline{X}_1 + \overline{X}_2 + \overline{X}_3) > 0 \tag{66}$$

The estimated minimum brake torque then becomes:

$$T_{(min)} = K_{sp}(\overline{X}_1 + \overline{X}_2 + \overline{X}_3)^{3/2} \tag{67}$$

It is to be noted that table friction has also been conservatively disregarded.

Figure 17 represents a graph of $T_{(min)}$ vs machine speed for various strip sizes and the standard configuration according to equation (67). It shows that the necessary minimum brake torque increases as the machine speed increases and the feeding stock becomes heavier.

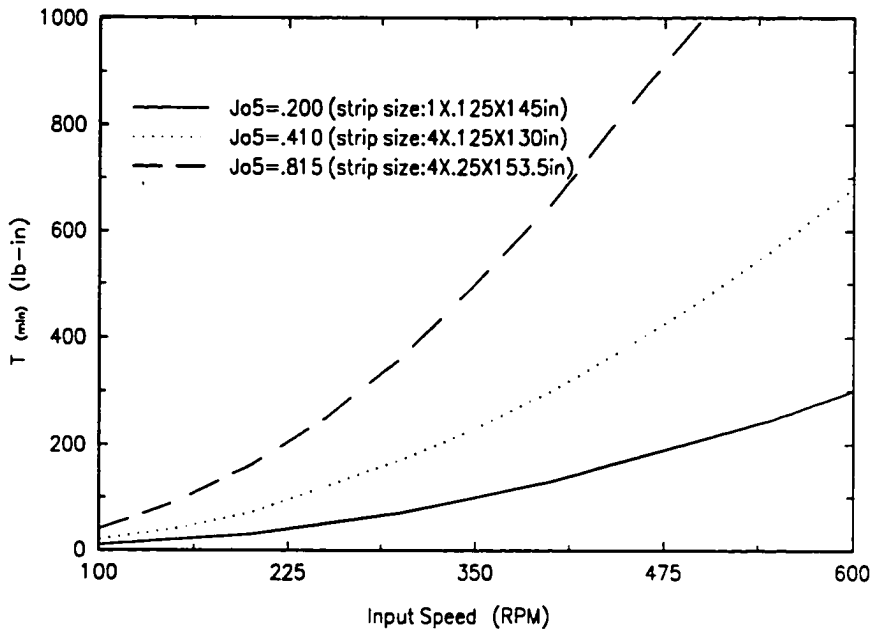

Figure 17 Estimated Minimum Brake Torque Requirement as a Function of Input Speed for Various Strip Sizes

10. CONCLUSIONS

(1) A new linearized, constant coefficient, two degree of freedom model of the feed mechanism has been developed. It uses a predetermined "inverted cantilever" type space function for the coupler and a lumped spring representation for the sprag clutch.

(2) This simplified model allows a closed solution which approximates the dynamic behavior of the clutch as well as the coupler during all four regimes of the mechanism cycle.

(3) The computed results of coupler strain and clutch windup angle for a number of runs with different parameters agreed reasonably well with experimentation. The experimental work associated with the clutch windup angle was greatly facilitated by the development of PC-based algorithms for the processing of the angular encoder data.

(4) The analytical solution for the all-important regime No.2 of the forward stroke of the mechanism clearly showed that the principal parts of the coupler strain and the clutch windup angle responses are transient in nature and contain the two system frequencies.

(5) It was found that the lower system frequency of the transient response is always near to and smaller than the lower of the two component frequencies, while the higher system frequency is always near to and larger than the higher component frequency. Specifically, for the standard configuration, where the component frequency of the clutch is considerably lower than the component frequency of the coupler, the lower system frequency is near that of the clutch, while higher system frequency is near that of the coupler. When the coupler component frequency was made lower than that of the clutch, the lower system frequency was nearer to that of the coupler.

(6) While no general rule concerning the amplitudes associated with the two transient system frequencies could be discerned, it was found in the analysis of the standard configuration, that the amplitude associated with the lower system frequency was always

considerably greater, both for the coupler strain and the clutch windup angle, than that associated with the higher system frequency. Since all the cases considered by Chassapis and Lowen (1990) dealt with the standard configuration, their observation of the predominance of the component frequency of the clutch in the coupler strain and the clutch windup angle is not surprising.

When the coupler component frequency was made lower than the clutch component frequency, the amplitude associated with the lower system frequency (i.e. near that of the coupler component frequency) lost some of its importance. While for the strain response the higher frequency amplitude was approximately one third of the that of the lower frequency one, it became larger than the latter for the windup angle response.

(7) It was found that the maximum deflections of the coupler and the clutch windup angle are essentially independent of each other over a wide range of parameters at speed of 200 RPM. Thus, each of these deflections may be minimized without much consideration for the other. The coupler deflection may be reduced dramatically by a modest increase of the coupler stiffness. As might be expected, the windup angle becomes smaller with a higher spring constant of the clutch.

PART II

A NEW DAMPING MODEL FOR NON-LINEAR STIFFNESS SYSTEMS WITH VARIABLE PRELOAD DISPLACEMENTS AND CONSTANT AMPLITUDE DECAY RATIO

1. INTRODUCTION

This part of the investigation was stimulated by the observation of the special nature of the vibrations of an overrunning sprag clutch which has non-linear spring characteristics and is part of a press feed mechanism (Chassapis and Lowen, 1990). These oscillations between the output and input sides of the clutch, during the forward stroke, are always about an already attained preload displacement and never in the direction of unloading because of the presence of a constant brake torque. In addition, it was found experimentally that the amplitude decay ratio is essentially constant, regardless of the level of the preload. This led to the question of the influence of such preloads on the energy dissipation in non-linear stiffness systems and with that to the question of what represents the best damping model for such systems, including the sprag clutch.

A thorough literature search showed no previous investigations in this direction. The work of Hunt and Crossley (1975), which postulates a non-linear damping model in the analysis of impact energy dissipation and which was later used by Yang and Lin (1987) in connection with the dynamics of spur gears, deals with a different phenomenon.

The aforementioned experimental observation of the constant amplitude decay ratio, which forms the pre-condition of this paper, may be explained to some degree by the work of Lazan and Goodman (1961). These investigators determined that, in any cycle of vibrations of a steel specimen without a preload, the ratio of the energy loss with respect to the maximum strain energy, is constant as long as the pattern of stress distribution is not changed. They further indicated that under this condition the amplitude decay ratio also stays constant. Similar results were found in the experimental work of Johnson (1985) with respect to the contact vibrations of two steel spheres, where the preload displacement was not zero.

In order to clarify the approach taken by the author in the determination of an appropriate damping model for a non-linear stiffness system with a preload, a linear mass-spring system is first considered. By introducing the concept of interchangeable potential energy, it could be shown that the energy loss per cycle of such system and with that the damping coefficient of a linear damping model is independent of the preload displacement.

The extension of these ideas to a non-linear stiffness system showed that the damping coefficient associated with a linear damping model depends very much on the momentary preload displacement and therefore such a model cannot satisfy all preloading conditions.

Subsequently, a new non-linear damping model, which takes displacement in addition to velocity into account, is introduced. Such a model has the desired generality, since the influence of the preload displacement on the associated damping coefficient can be minimized.

Finally, this new damping model is incorporated into the mathematical description of the sprag clutch. Very good agreement between computed and experimental results was found when the experimentally obtained damping ratio was used.

2. LINEAR DAMPING MODEL FOR SYSTEMS WITH LINEAR SPRINGS

As stated in the introduction, the following will demonstrate the approach taken in this paper and show that in a linear stiffness system, with a linear (viscous) damping force, the damping coefficient is independent of the preload displacement.

If the mass spring system shown in Figure 18 has a constant force F applied on the mass, any possible oscillations of the mass will be about the preload displacement (static equilibrium position) $x = \delta = F/K$, where K is the spring constant.

The potential energy, which is added to the system during the travel of the mass from the preload displacement $x = \delta$ to the maximum position $x = \delta + X$ is given by:

$$E_X = \int_{\delta}^{\delta+X} Kx dx = \frac{1}{2}K(\delta+X)^2 - \frac{1}{2}K\delta^2 \tag{68}$$

or

$$E_X = \frac{1}{2}KX^2 + K\delta X = \frac{1}{2}KX^2 + FX \tag{69}$$

Since the potential energy component FX will always be removed from the system as negative work done by the force F when the mass moves from $x = \delta + X$ back to $x = \delta$, it cannot make any contribution to the kinetic energy and any possible energy dissipation. Thus, only

$$E = E_X - FX = \frac{1}{2}KX^2 \tag{70}$$

is available for this purpose.

The above potential energy E, which causes the subsequent free vibration will be called "interchangeable potential energy". The value of this energy is reduced a certain

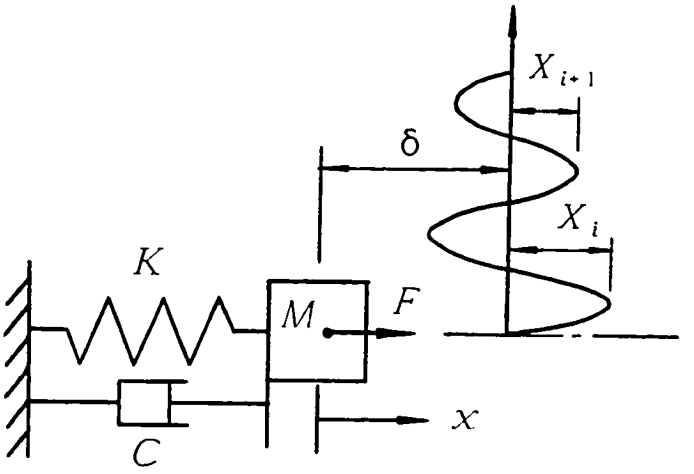

Figure 18 Damped Spring-Mass System Oscillating about Non-Zero Preload Displacement δ

amount after each cycle in the presence of damping. This energy loss per cycle ΔE may be found from:

$$\Delta E = E(X_i) - E(X_{i+1}) = \frac{1}{2}KX_i^2 - \frac{1}{2}KX_{i+1}^2 = \frac{1}{2}KX_i^2(1-R^2) \tag{71}$$

where

$$R = \frac{X_{i+1}}{X_i} \tag{72}$$

is defined as the amplitude decay ratio, which is constant in the present investigation. X_i and X_{i+1} represent two successive oscillation peak amplitudes. Equation (71) shows that the energy loss per cycle of a system with a linear spring is independent of the preload displacement δ of the mass.

The following demonstrates the same independence of δ for the damping coefficient C, when linear damping is assumed. The usual way (Thomson, 1981) of expressing the work W_d done by a viscous damping force in one cycle of a system, oscillating near its natural frequency, also holds in the presence of a preload, i.e.:

$$W_d = C\pi X_{av}^2\sqrt{K/M} \tag{73}$$

where, $X_{av} = (X_i + X_{i+1})/2$, the average amplitude of two successive oscillations.

The damping coefficient C is then obtained after setting equations (71) and (73) equal to each other:

$$C = \frac{2}{\pi}\sqrt{KM}\frac{(1-R)}{(1+R)} \tag{74}$$

With R known, equation (74) may be used in place of the logarithmic decrement for the determination of the damping ratio.

3. POSSIBLE DAMPING MODELS FOR SYSTEMS WITH NON-LINEAR SPRINGS

It will now be shown that in the presence of a non-linear spring, the energy loss per cycle depends on the preload displacement δ of the oscillating mass. Further, it will be explored to what extent the damping coefficients in possible linear and non-linear damping models are functions of δ.

Assuming that the spring force F_s of such a system is given by

$$F_s = Kx^{\beta} \quad (\beta \neq 1) \tag{75}$$

Then, the expression comparable to equation (68) becomes

$$E_X = \int_{\delta}^{\delta+X} Kx^{\beta}dx = \frac{K}{\beta+1}[(\delta+X)^{\beta+1} - \delta^{\beta+1}] \tag{76}$$

To find the associated "interchangeable potential energy", the work of the constant force F must again be subtracted. Then,

$$E = E_X - FX \tag{77}$$

If one now expresses

$$F = K\delta^{\beta} \tag{78}$$

and substitutes it together with equation (76) into equation (77), one obtains

$$E = \frac{K}{\beta+1}[(\delta+X)^{\beta+1} - \delta^{\beta+1}] - K\delta^{\beta}X \tag{79}$$

Finally, the energy loss per cycle, parallel to equation (71), becomes:

$$\Delta E = E(X_i) - E(X_{i+1}) = KA(\delta) \tag{80}$$

where,

$$A(\delta) = \frac{1}{\beta+1}[(\delta+X_i)^{\beta+1} - (\delta+RX_i)^{\beta+1}] - \delta^{\beta}(X_i - RX_i) \tag{81}$$

Clearly, ΔE is influenced by the preload displacement δ.

It remains now to see how the damping coefficients are related to the displacement δ when either a linear or a non-linear damping model is postulated. In either case, it is assumed that the systems are lightly damped and not highly non-linear, so that near-harmonic oscillations result and the motion may be approximated by: (see also figure 18)

$$x = \delta + X_{av}\sin\omega t \tag{82}$$

where, $\omega = \sqrt{[d(F_s)_\delta/dx]/M} = \sqrt{\beta K\delta^{\beta-1}/M}$ is the local linearized natural frequency evaluated at the preload displacement δ.

a. Linear (Viscous) Damping Model

The damping force F_d for a linear (viscous) damping model is described by:

$$F_d = C_l\dot{x} \tag{83}$$

where, C_l serves as the damping coefficient.

The work done by this damping force during a cycle of vibrations is expressed with the help of equation (82), i.e.:

$$W_d = \oint F_d dx = \int_0^{2\pi/\omega} C_l(X_{av}\omega)^2\cos^2(\omega t)dt$$

$$= C_l\pi X_{av}^2\delta^{(\beta-1)/2}\sqrt{(\beta K)/M} \tag{84}$$

Since the energy loss per cycle ΔE of equation (80) must be equal to the above W_d, the damping coefficient C_l becomes:

$$C_l = \frac{4\sqrt{MK/\beta}}{\pi X_i^2 (1+R)^2}\,\delta^{(1-\beta)/2} A(\delta) \tag{85}$$

The above expression indicates that the linear damping coefficient is very much dependent on δ when the spring is non-linear. (Note that for $\beta = 1$, the expression reduces to equation (74).) Therefore, it is desirable to develop a damping model which produces a damping coefficient that is either not at all, or only minimally, influenced by the preload displacement δ.

b. Non-linear Damping Model

Equation (80), for the energy loss per cycle ΔE, is some exponential function of δ. In order to make the damping coefficient independent of δ, it is necessary that the work of the damping force is also an exponential function of δ, so that a certain proportionality between ΔE and W_d can be obtained.

To achieve this, the following non-linear damping force, which depends on the displacement in addition to the velocity, is assumed:

$$F_d = C_{nl} x^n \dot{x} \tag{86}$$

where, the unknown exponent n of the displacement is introduced for the manipulative opportunity of maximizing the proportionality between ΔE and W_d and with that of minimizing the influence of the preload displacement δ on the damping coefficient C_{nl}. With this damping force and equation (82), the work done per cycle becomes:

$$W_d = \oint F_d dx = \int_0^{2\pi/\omega} C_{nl}(X_{av}\sin\omega t + \delta)^n (X_{av}\omega)^2 \cos^2(\omega t)dt$$

$$= C_{nl}X_{av}^2\delta^{n+(\beta-1)/2}\sqrt{(\beta K)/M}\int_0^{2\pi}\left(\frac{X_{av}}{\delta}\sin\tau + 1\right)^n \cos^2\tau d\tau \qquad (87)$$

After equating the energy loss per cycle of equation (80) with this new W_d, the damping coefficient takes the form:

$$C_{nl} = \frac{(4\sqrt{MK/\beta})/[X_i^2(1+R)^2]}{\int_0^{2\pi}\left(\frac{X_{av}}{\delta}\sin\tau + 1\right)^n \cos^2\tau d\tau}\ \delta^{-n+(1-\beta)/2}A(\delta) \qquad (88)$$

It will now be shown that, since $X_i/\delta < 1$[7] in the general case of free vibrations of preloaded systems, it is always possible, regardless of the value of β, to make C_{nl} essentially independent of δ, if n is chosen appropriately.

As a first step $A(\delta)$ is approximated by a single exponential function of δ with the help of a power series expansion in X_i/δ, where terms of order higher than 2 are eventually neglected. Appendix J proves that such an approximation furnishes with only small errors:

$$A(\delta) = \frac{\beta}{2}X_i^2(1-R^2)\delta^{\beta-1} \qquad (89)$$

If the above is substituted into equation (88), one obtains

$$C_{nl} = \frac{2\sqrt{MK\beta}}{\int_0^{2\pi}[(X_{av}/\delta)\sin\tau + 1]^n \cos^2\tau d\tau}\ \frac{1-R}{1+R}\ \delta^{-n+(\beta-1)/2} \qquad (90)$$

---

7 See experimentation below for typical values of X_i/δ

With small values of X_i/δ and n, the integral in the above denominator has a value close to π (see footnote 4). Finally, one notes that C_{nl} becomes a constant if the exponent of δ is made zero, i.e.

$$n = (\beta - 1)/2 \tag{91}$$

The next section applies this new damping model to a sprag clutch.

4. APPLICATION OF THE NON-LINEAR DAMPING MODEL TO A SPRAG CLUTCH

a. System Description

To facilitate the understanding of the following analytical and experimental aspects of this investigation of the energy dissipation in a sprag clutch, the construction and function of the associated modified press feed mechanism is first briefly described. (For a description of the original mechanism, see Chassapis and Lowen, 1990.)

Figure 19 shows that the input side of the sprag clutch is driven by a spatial RSSR linkage with a straight coupler, while its output side drives the feed rollers which advance the strip stock into a power press. The action of the clutch must be such that it advances the stock during the forward stroke of the mechanism and that it stands still, i.e. over-runs, during the return stroke. In order to prevent the overshooting of the stock during the forward stroke, the feed roller shaft rotation is opposed at all times by the indicated constant torque brake. The mathematical model of the clutch makes use of the following nomenclature:

(1) The input side, as represented by the outer race, experiences the known angular displacement ϕ_4, which is a function of the input angle ϕ_1 of the rigid body RSSR linkage. $\phi_{4\,max}$ represents the rocker/outer race angle at the beginning of the forward stroke.

(2) The angle ϕ_5 is associated with the output side, which is represented by the inner race and the feed roller shaft.

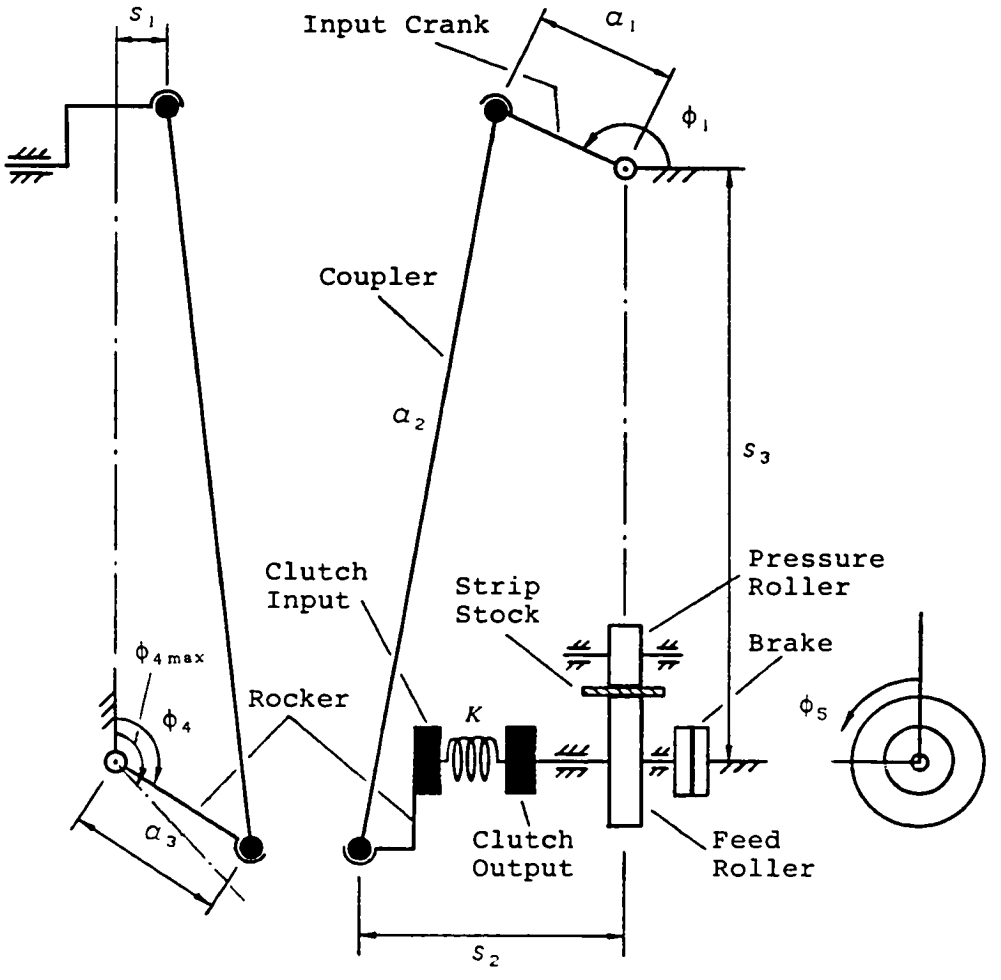

Figure 19 Schematic Diagram of Feed Mechanism with Sprag Clutch

(3) The clutch elasticity, which is due to the sprags, is expressed with the help of the spring torque (as shown by Chassapis and Lowen, 1990) as:

$$T = K(\phi_5 - \phi_4)^{3/2}$$

Note that this expression represents the torsional form of equation (75), adapted to the relative motion of the clutch, with $\beta = 3/2$.

(4) T_b represents the combined brake and referred table friction torques. The latter is due to the sliding of the stock over the feed table in the experiment.

b. Mathematical Model of Sprag Clutch with Non-linear Damping

Considering the clutch-brake system of Figure 19 with the assumption of non-linear damping between the driving outer and the driven inner race and neglecting the small bearing friction, one obtains the following differential equation for the motion of the feed roller shaft during the forward stroke:

$$J\ddot{\phi}_5 + C_{nl}(\phi_5 - \phi_4)^n(\dot{\phi}_5 - \dot{\phi}_4) + K(\phi_5 - \phi_4)^{3/2} = T_b \qquad (92)$$

where J is the combined moment of inertia of all components on the clutch output side. It includes the inner race of the clutch, the feed and pressure rollers and their associated shafts, the moving parts of the brake as well as the referred moment of inertia of the strip stock.

The time t_0 of the start of motion of the output side occurs when the damping and the spring torques have overcome the retarding action of the combined resisting torque. This condition is represented by the following modification of equation (92), with $\phi_5 = \phi_{4\max}$ and its derivatives set equal to zero:

$$C_{nl}(\phi_{4\max} - \phi_4(t_0))^n\dot{\phi}_4(t_0) - K(\phi_{4\max} - \phi_4(t_0))^{3/2} + T_b = 0 \qquad (93)$$

The dynamic behavior of the clutch is best described as a function of the wind-up angle $\phi_{5/4}$, which represents the relative motion between the two unidirectional rotations ϕ_5 and ϕ_4, i.e.:

$$\phi_{5/4} = \phi_5 - \phi_4 \tag{94}$$

To this end, one now subtracts $J\ddot{\phi}_4$ from both sides of equation (92). This leads to:

$$J\ddot{\phi}_{5/4} + C_{nl}\phi_{5/4}^{n}\dot{\phi}_{5/4} + K\phi_{5/4}^{3/2} = -J\ddot{\phi}_4 + T_b \tag{95}$$

The associated initial conditions become:

$$\phi_{5/4}(t_0) = \phi_{4\max} - \phi_4(t_0) \tag{96}$$

and

$$\dot{\phi}_{5/4}(t_0) = -\dot{\phi}_4(t_0) \tag{97}$$

c. Determination of Damping Parameters

To determine the damping parameters C_{nl} and n for the clutch, equation (90) must be first changed to reflect the nomenclature of the clutch. Thus, M becomes the moment of inertia J, and X_i and X_{av} become $\Phi_{5/4(i)}$ and $\Phi_{5/4(av)}$, respectively, where $\Phi_{5/4(i)}$ represents the oscillation amplitude of the windup angle about its local preload displacement δ. In addition,

$$R = \frac{\Phi_{5/4(i+1)}}{\Phi_{5/4(i)}} .$$

Then,

$$C_{nl} = \frac{2\sqrt{JK\beta}}{\int_0^{2\pi}[(\Phi_{5/4(av)}/\delta)\sin\tau + 1]^n \cos^2\tau d\tau} \frac{1-R}{1+R} \delta^{-n+(\beta-1)/2} \tag{98}$$

With $\beta = 3/2$, as indicated earlier in section 4(a), equation (91) gives:

$$n = \frac{1}{4}$$

Further[8],

$$\int_0^{2\pi} \left(\frac{\Phi_{5/4(av)}}{\delta} \sin\tau + 1 \right)^{1/4} \cos^2\tau d\tau = \pi \tag{99}$$

Finally, equation (98) for the damping coefficient becomes:

$$C_{nl} = \frac{1}{\pi} \sqrt{6JK} \, \frac{(1-R)}{(1+R)} \tag{100}$$

The value of the amplitude decay ratio R must now be determined by experiment.

d. Experimental Setup

The experimental setup is essentially that described earlier in section 7c of Part I. For present purposes, only the angular encoders and the data evaluation system are of importance.

Each of the three angular encoders, which are attached to the mechanisms input shaft, the rocker shaft and the feed roller shaft, respectively, are able to furnish pulses for every 0.036 degree of angular motion. In addition the input shaft encoder provides a signal when $\phi_1 = 0°$.

The angular encoder data acquisition system has a sampling rate of one micro-second for each of the channels. It is capable of storing and subsequently transmitting to a PC the following data for a complete mechanism cycle:

(1) The time associated with each 0.036 degree rotation of the mechanism input angle ϕ_1,

---

8 For $0 \le \Phi_{5/4}/\delta \le 1$, the integral has values between π and 3.04.

with zero time corresponding to $\phi_1 = 0°$.

(2) The time associated with each 0.036 degree of forward rotation of the rocker link (clutch input) angle ϕ_4.

(3) The time associated with each 0.036 degree of forward rotation of the feed roller (clutch output) angle ϕ_5.

An appropriate algorithm (see Appendix I) makes it possible for the PC to establish the windup angle $\phi_{5/4}$ as a function of the mechanism input angle ϕ_1 for the forward stroke of the machine by way of obtaining the angles ϕ_1, ϕ_4 and ϕ_5 which correspond to a given time in the cycle.

e. Experimental Determination of Amplitude Decay Ratio

Figure 20 shows three typical experimentally obtained plots of the windup angle $\phi_{5/4}$ vs. the input angle ϕ_1 during the forward stroke of the mechanism. In order to highlight the physical lag of ϕ_5 with respect to ϕ_4, the sign of the windup angle is changed in all figures. Note the typical local preload displacement δ of the uppermost curve and that the ratio $\Phi_{5/4(i)}/\delta$ is smaller than unity.

In each of these runs a 0.635 cm×10.15 cm (0.25 in×4.00 in) steel strip of 3.9 m (12.8 ft) length was used at a speed of 72 RPM. The approximate resisting torque was varied from $T_b = 9.0$ N-m (80 lb-in), to 28.2 N-m (250 lb-in) and 41.8 N-m (370 lb-in) (see below). This was done to show that the amplitude decay ratio is essentially constant and not influenced by the value of the preload displacement δ, which is mainly a function of the combined resisting torque.

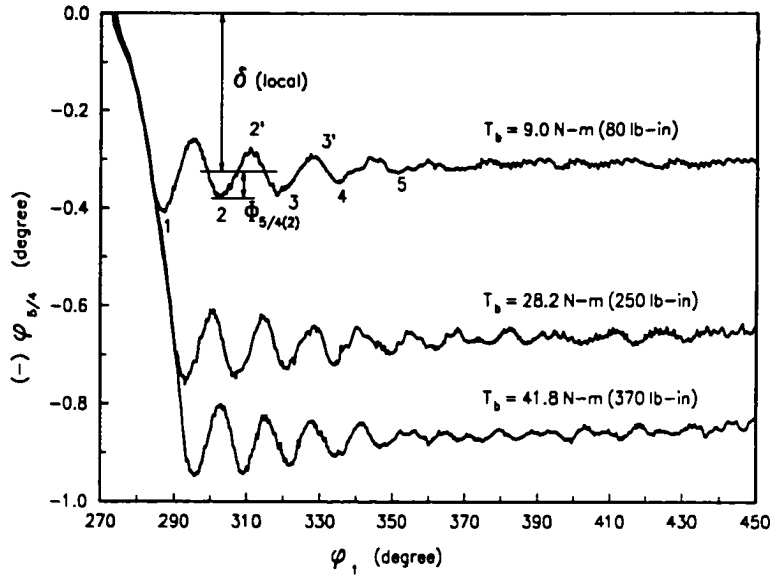

Figure 20 Typical Experimental Curves of Windup Angle vs. Input Crank Angle

In order to determine the overall average amplitude decay ratio, five separate runs were made for each of the brake settings and the average amplitude decay ratios $\Phi_{5/4(3)}/\Phi_{5/4(2)}$, $\Phi_{5/4(4)}/\Phi_{5/4(3)}$ and $\Phi_{5/4(5)}/\Phi_{5/4(4)}$ were obtained by the procedure described in Appendix K. The first amplitude $\Phi_{5/4(1)}$ was not used, since it was found to be too much influenced by the overall elastic deflection of the mechanism. Table 2 shows the results of three tests.

Decay Ratio	T_b = 9.0 N-m (80 lb-in)	T_b = 28.2 N-m (250 lb-in)	T_b = 41.8 N-m (370 lb-in)
$(\Phi_{5/4(3)}/\Phi_{5/4(2)})_{avg}$	0.681	0.657	0.701
$(\Phi_{5/4(4)}/\Phi_{5/4(3)})_{avg}$	0.661	0.672	0.671
$(\Phi_{5/4(5)}/\Phi_{5/4(4)})_{avg}$	0.656	0.667	0.647
Overall Average Amplitude Decay Ratio R= 0.669			

Table 2 Determination of Amplitude Decay Ratio

Clearly, the amplitude decay ratios are fairly constant within the test range and one may use the overall average value for

$R = \Phi_{5/4(i+1)}/\Phi_{5/4(i)} = 0.669$.

f. Determination of Damping Constant

According to equation (100), the value of the damping constant becomes, with $R = 0.669$:

$$C_{nl} = 0.155\sqrt{KJ} \tag{101}$$

The moment of inertia of the clutch output side, including the referred inertia of the strip has been calculated to be:

$J = 0.092$ N-m-sec^2-rad^{-1} (0.815 lb-in-sec^2-rad^{-1})

Further, according to previous experimentation on the torque curve of the clutch (Chassapis and Lowen, 1990) and recent dynamical refinements involving the local linearized natural frequencies, the approximate value of the stiffness constant is found to be:

$K = 22580$ N-m-rad$^{-3/2}$ (200,000 lb-in-rad$^{-3/2}$)

Then, equation (101) gives:

$C_{nl} = 7.065$ N-m-sec-rad$^{-5/4}$ (62.6 lb-in-sec-rad$^{-5/4}$)

g. Comparison between Computed and Experimental Results

In order to obtain the numerical results of equation (95) as functions of the input crank angle ϕ_1 for comparison with experimental results, the following modifications of this expression must be made:

$$J\dot{\phi}_1^2\frac{d^2\phi_{5/4}}{d\phi_1^2} + C_{nl}\dot{\phi}_1\dot{\phi}_{5/4}^n\frac{d\phi_{5/4}}{d\phi_1} + K\phi_{5/4}^{3/2} = -J\ddot{\phi}_4 + T_b \tag{102}$$

Similarly, the initial conditions given by equations (96) and (97) are modified:

$$\phi_{5/4}[\phi_1(t_0)] = \phi_{4\max} - \phi_4[\phi_1(t_0)] \tag{103}$$

and

$$\dot{\phi}_{5/4}[\phi_1(t_0)] = -\dot{\phi}_4[\phi_1(t_0)] \tag{104}$$

Because of the previously noted mechanism deflections at the beginning of motion the above initial conditions are taken from the experimental data. Once the motion of ϕ_5 starts, the rocker angular acceleration $\ddot{\phi}_4$ is determined as a function of the crank input angle according to the work of R.S. Hartenberg and J. Denavit (1964), using the dimensions of the RSSR mechanism given in Table 3.

a_1	a_2	a_3	s_1	s_2	s_3
2.477 cm (0.975 in)	81.478 cm (32.078 in)	11.43 cm (4.5 in)	5.715 cm (2.25 in)	0.00 cm (0.0 in)	79.566 cm (31.325 in)

Table 3 RSSR Linkage Dimensions

Due to the difficulty of experimentally measuring the resisting torque accurately for a given run, it was decided to determine this quantity by varying it in the computations until the computed preload windup angles matched with the experimental ones.

Figure 21 shows four comparisons between experimental and computed results. In each case the mechanism speed was 72 RPM and the matching values of the resisting torques, used in the computations, were found to be 5.9, 28.2, 41.8 and 53.1 $N-m$ (52, 250, 370 and 470 lb-in).

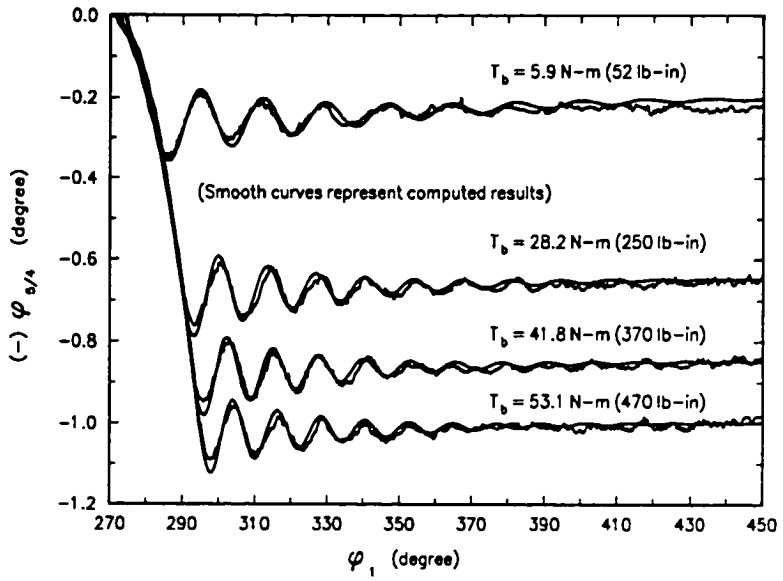

Figure 21 Comparison between Experimental and Computed Results of Windup Angle vs. Input Crank Angle at 72 RPM

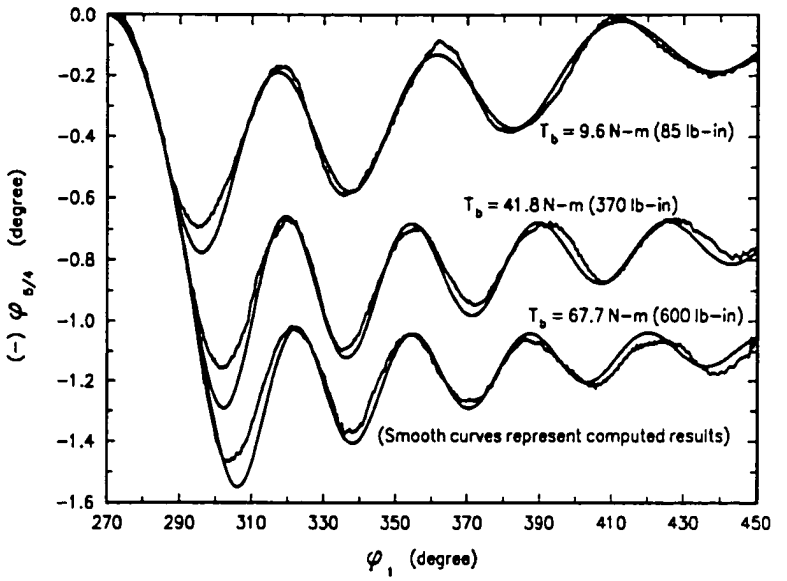

Figure 22 Comparison between Experimental and Computed Results of Windup Angle vs. Input Crank Angle at 197 RPM

Figure 22 shows similar comparisons at 197 RPM and matching resisting torques at 9.6, 41.8 and 67.7 $N-m$ (85, 370 and 600 lb-in).

It is interesting to note that in Figure 21, where the speed is low and with that the inertia contribution to the resisting torque stays small, the associated preload displacement δ is fairly constant in the individual runs. This is not the case in Figure 22, where the upward slope of the preload displacement is due to the substantial, but diminishing inertia torque as the forward stroke proceeds.

Clearly, the graphs in both figures show very good agreement in amplitude and frequency after the first half cycle. This lack of agreement during the first half cycle is again due to the previously discussed mechanism deflections.

5. LACK OF GENERALITY OF LINEAR DAMPING MODEL FOR SPRAG CLUTCH

The following demonstrates, by way of a relationship between C_l and C_{nl}, that the linear damping model is less general since it requires the knowledge of the preload displacement δ.

As the energy dissipation must be the same, one can find the above relationship, for the present non-linear system, by equating the work W_d done by the linear damping force of equation (84) with that done by the non-linear one, according to equation (87). Thus,

$$C_l = \frac{1}{\pi}\left[\int_0^{2\pi}\left(\frac{X_{av}}{\delta}\sin\tau + 1\right)^n \cos^2\tau d\tau\right]\delta^n C_{nl} \tag{105}$$

With $n = 1/4$, the integral can be approximated by π, as stated earlier, and one obtains

$$C_l = \delta^{1/4} C_{nl} \tag{106}$$

Clearly, C_l is not a "damping constant", but depends on δ, while C_{nl} has been shown to be constant. If one still wishes to use the linear damping model, one must be aware of the fact that C_l changes with δ.

6. CONCLUSIONS

This investigation, which concerned itself with the influence of preloads on the energy dissipation in non-linear stiffness systems and with that the determination of the best damping model for such systems, allows the following conclusions:

(1) Based on the concept of interchangeable potential energy it has been shown that for non-linear stiffness system the energy dissipation per cycle is not independent of the preload displacement. This dependence on preload was not found for linear stiffness systems and therefore a viscous damping model is adequate for them.

(2) If such a viscous damping model is applied to a non-linear stiffness system, the work of the damping force per cycle depends on the preload displacement in a different manner than the corresponding energy dissipation. This leads to an undesirable variable damping coefficient, which is a function of the preload displacement.

(3) To minimize this dependence of the damping coefficient on the preload displacement, a new damping model, which is a function of displacement and velocity, has been introduced. Its work per cycle is related to the preload displacement in approximately the same manner as the corresponding energy dissipation. This approach may be used regardless of the value of the exponent β as long as $X/\delta < 1$.

(4) When this new damping force, with its constant damping coefficient, was incorporated into a sprag clutch model, it was found that the resulting computational results for the windup angle agreed well with experimentally obtained ones.

(5) In conjunction with this sprag clutch investigation, the pre-condition of a constant amplitude decay ratio for different preload displacements could also be experimentally verified.

PART III

A MATHEMATICAL MODEL OF AN OVER-RUNNING SPRAG CLUTCH

1. INTRODUCTION

a. Background and Outline of Present Work

The work by Chassapis and Lowen (1990) used a "lumped" spring-mass model of a over-running sprag clutch[9], in which the presence of the sprags is disregarded, in their mathematical simulation of a press-feed mechanism. The torque of the clutch was experimentally found to be proportional to the 3/2 power of the windup angle (the difference between input and output rotations) and its energy dissipation was described by a linear damping model. A subsequent effort by Xu and Lowen (1992) showed that a non-linear damping model, together with the "lumped" spring-mass description of the clutch gave better agreement with experimental results.

The present paper represents, to the best knowledge of the authors, the first attempt at a complete mathematical model for an over-running sprag clutch. It considers the inertias of the sprags and the output race, the Hertzian contact forces between the sprags and the races and the previously developed non-linear damping model.

In order to express the Hertzian contact forces in terms of the windup angle, the work of Stoelzle and Hart (1961) is adapted. It assumes that the motion of all clutch components can be expressed by way of an epicyclic train model in which an imaginary arm rolls the planet wheel (sprag) between a sun wheel (inner race) and a ring wheel (outer race), as the local deformations due to the contact forces between sprags and races provide the needed "clearance" for motion.

---

9 Throughout this work a Formsprag Indexing Clutch, Model HPI-500, is involved.

The resulting differential equations allow both the determination of the clutch output rotation and of the windup angle histories for a given input motion.

b. Previous Work

Previous work has dealt essentially with geometric and static properties of these mechanisms, which are used in the transmissions of automobiles, aircraft, helicopters and pump power trains, as well as in power press feed mechanisms. The only known dynamic analysis deals with the critical driving acceleration of the clutch at the start of the forward motion (Williams et al, 1973).

Along these lines, R.L. Daniels (1957), in his first paper, discussed the basic geometry of the sprags and defined locking and over-running conditions. He pointed out that, in order to get safe locking the strut angles (see angles α and β in Figure 24) should be small, while for maximum torque transmission they should be as large as possible. In addition, this author showed that for the circular arc type sprag the strut angle increases as locking proceeds. Finally, he reported that experimentation has shown the need for a sprag cage to assure simultaneous engagement of all sprags. In a later paper (1967), the same author describes various applications of sprag clutches.

F.A. Ferris (1973) gave much useful information on sprag geometry, material selection and clutch lubrication, as well as the design of energizing springs. He also stressed the need for a sprag cage.

V.A. Novikov (1973) showed how to determine sprag radii as well as the associated eccentricities which will keep the increase in the strut angle at a minimum as the sprags rotate into locking. In a later paper (1977), together with A.K. Radzhapov, the same author extended the above optimization to sprags with logarithmic spiral and involute type profiles.

The book by K. Stoelzle and S. Hart (1961) deals in general with all types of over-running clutches and provides a good deal of information on their design and operation. As stated earlier, the present investigation uses their work concerning the dependence of the windup angle on the contact deformations at the sprag-race interfaces.

In the first of the only set of papers which deal with the dynamics of the sprag clutch, F.C. Williams, D. Tipping and T.A. Henry (1973) showed, with a simplified model, that whenever the acceleration of the driving race, just after motion reversal of the clutch, is greater than that which the friction driven sprag contact point can reach, the clutch may become unstable. In a second paper (1975), the same authors demonstrated that the occurrence of this instability, may be avoided by the introduction of a sprag retainer cage which rotates with the velocity of the driving race.

2. CLUTCH DESCRIPTION

Figure 23 shows a manufacturers cut-out view of a complete sprag clutch, while Figure 24a gives a simplified schematic of its basic components. Such a clutch allows motion to be transmitted in the "forward" direction, while it over-runs in the other. It consists of an outer race of contact radius R_o, a full complement of sprags, as well as an inner race of radius R_i. Its one-way action ideally occurs as the outer race causes the variable diameter sprags to roll into a wedging position between it and the inner race and when the driving torque on the outer race is sufficient to overcome the resisting torque T on the inner one. When the clutch is in the overrunning mode, the outer race reverses motion and rolls the sprags out of engagement. Subsequently the sprags slide over the inner race without transmitting any motion.

The angular displacements of the outer and inner races are described by the angles ϕ_4 and ϕ_5, respectively. As Figure 24b indicates, at the beginning of the forward motion both angles coincide at the arbitrary position ϕ_{40}. Because of the resisting torque T on the inner race, ϕ_4 will be "ahead" of ϕ_5 at all times during normal forward operation. This makes the windup angle $\phi_{5/4} = \phi_5 - \phi_4$ a positive quantity at all times.

The centers of sprag curvature C_o and C_i are offset from each other to assure the needed variable sprag diameter. The associated strut angles α and β are expressed with respect to a line connecting the inner and outer contact points I and O, respectively. It is assumed that the center of mass C_s of the sprag lies at the center of this line.

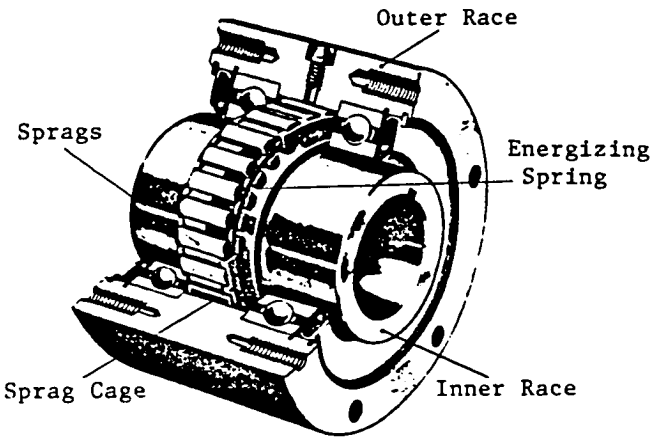

Figure 23 Formsprag Indexing Clutch Model HPI-500

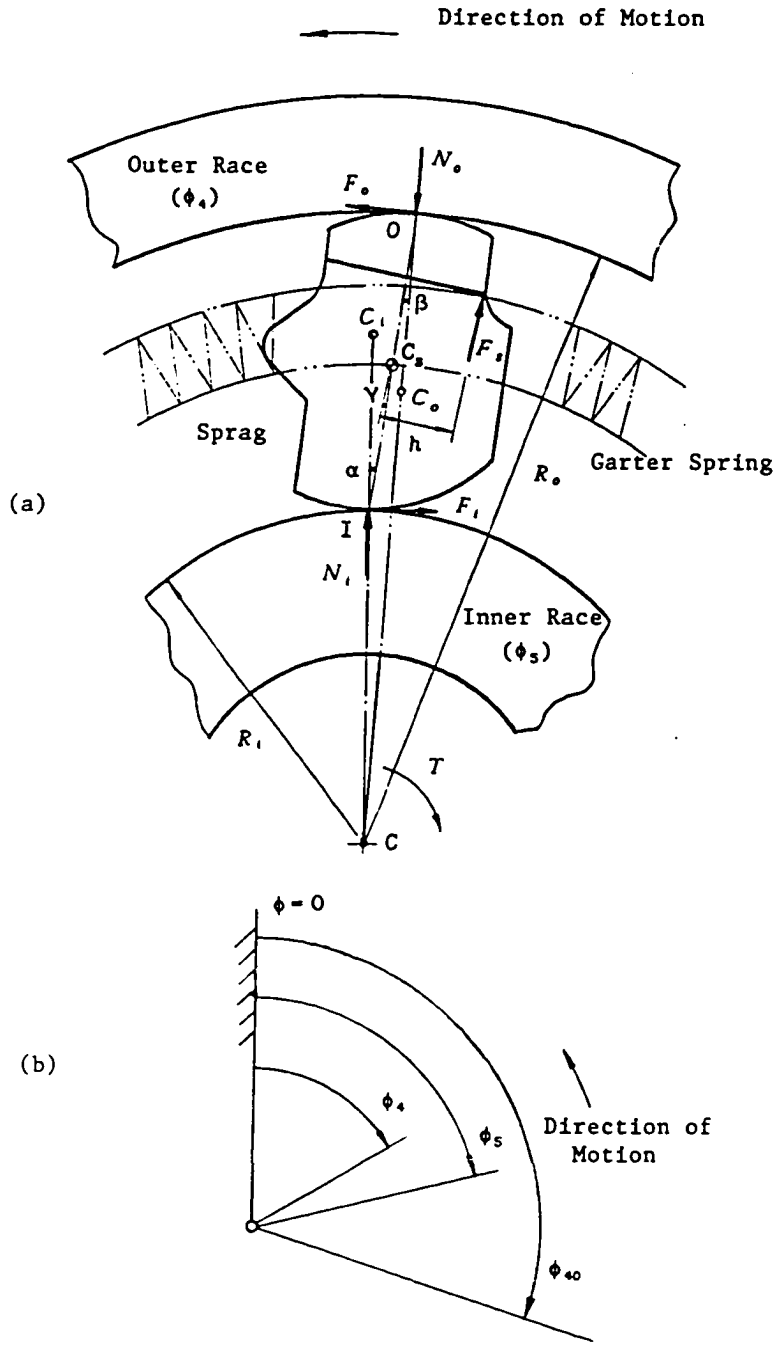

Figure 24 Schematic of Sprag Clutch (All Forces Shown to Act on Sprag)

In the assembled clutch, a retainer cage spaces the sprags and a garter spring pushes them outward. Because of the eccentricity h of the spring force F_s, the individual sprag is rotated such that it makes contact with both races and is in the appropriate position when the "forward" motion starts.

3. DETERMINATION OF NORMAL CONTACT FORCES

Before the differential equation of motion of the mechanism can be derived, it is necessary to determine the normal contact forces N_i and N_o, shown in figures 24 and 25.

The contribution of the spring force F_s to the normal contact forces is disregarded, since it is very small when compared to the Hertzian forces, which are a consequence of the winding up of the clutch.

Each of the contact forces has the following two components:

(1) N_{ih} and N_{oh}, which are due to the Hertzian contact deformations after the clutch engages. Both of these forces may be assumed to be equal since the contribution of the sprag related radial D'Alembert force is small when compared to that causing the local deformation. Thus, $N_{ih} = N_{oh} = N_h$.

(2) N_{id} and N_{od} are contact damping forces which account for the energy dissipation during the Hertzian deformations.

Each of these component forces will now be discussed in some detail.

a. Hertzian Contact Force N_h

In order to express the contact force N_h in terms of the windup angle $\phi_{5/4}$, the work of Stoelzle and Hart (1961) is adapted. It assumes that the motions of all clutch components can be expressed by way of an epicyclic train model in which an imaginary arm rolls the planet (sprag) between a sun (inner race) and a ring (outer race), as the local deformations δ_i and δ_o at the inner and outer interfaces, respectively, provide the "clearance" for motion.

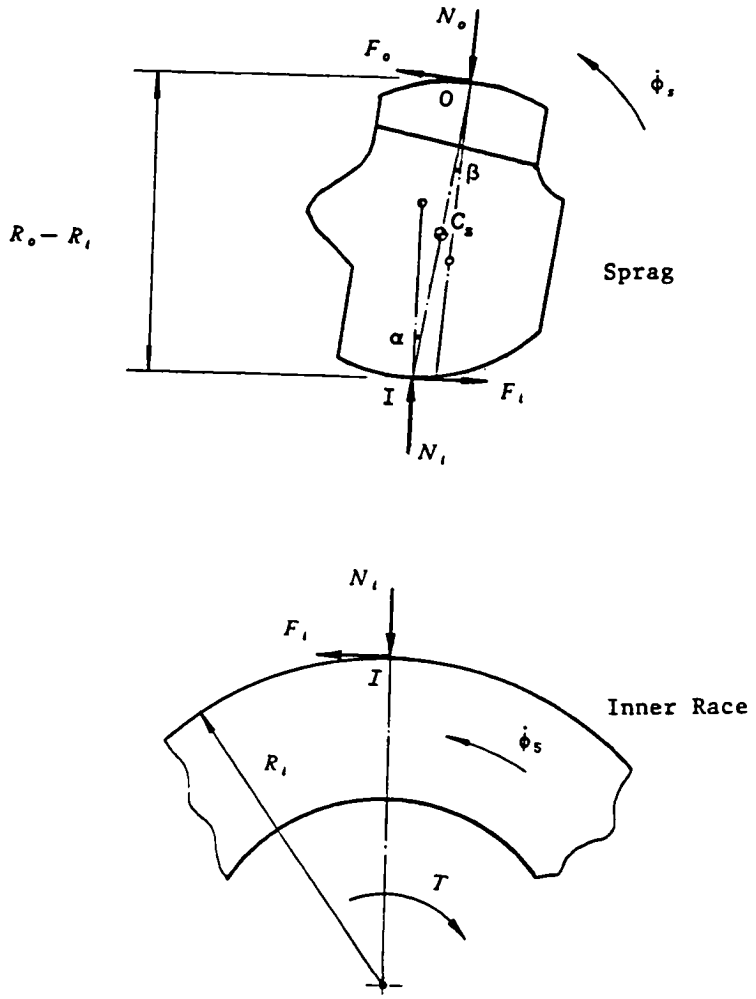

Figure 25 Free Body Diagrams of Sprag and Inner Race in Locking Mode

Appendix L shows that in this way the windup angle becomes proportional to these deformations, i.e.

$$\phi_5 - \phi_4 = \frac{R_o + R_i}{R_o R_i} R_s (D_o \delta_o + D_i \delta_i) \tag{107}$$

where D_o and D_i are clutch geometry dependent constants.

Since the extruded steel sprags are not further machined after heat treating and since one cannot assume perfect assembly of the clutch, it is impossible to state with certainty what the real nature of the contact mode between the sprags and the races is.

Fortunately, the results of previous clutch experimentation (Chassapis and Lowen, 1990), which shows that the torque transmitted is nearly proportional to the 3/2 power of the windup angle, suggest an approach for overcoming this difficulty. Appendix M compares torque curves based on assumptions of line, single point and two point contact between sprags and races with the experimental torque curve. It could be shown that while neither line nor single point contact assumptions agree with experimental results, a two point contact postulation, which furnishes a 3/2 power relationship, is most desirable for this purpose. (The torque curves for line and single point contacts are either much stiffer or softer, respectively, than the experimental one.)

Appendix M shows that, for the two point contact assumption, the Hertzian contact force may be expressed in the following form:

$$N_h = G(\phi_5 - \phi_4)^{3/2} \tag{108}$$

where G is a stiffness related constant, given by equation (M.14) in Appendix M.

b. Contact Damping Forces N_{id} and N_{od}

As indicated earlier, the present author and G. Lowen (1992) have shown that, when dealing with non-linear spring-mass systems which oscillate about variable preload positions, as occurs in the clutch due to load changes, the energy dissipation per cycle depends on these preload displacements. It was further found that if a linear damping model is used in such cases, the damping coefficient becomes a function of the preload displacement. To eliminate this dependency, it was demonstrated that the damping force F_d is best expressed as a function of the displacement x as well as the velocity $\dot{x}$ of the mass, i.e.:

$$F_d = C_{nl} x^n \dot{x} \tag{109}$$

where C_{nl} is the damping constant for this non-linear model and n an exponent which depends on the exponent of the non-linear spring force of the form Kx^β.

When this formulation was applied (Xu and Lowen, 1992) to the "lumped" sprag clutch model with $\beta = 3/2$, n was found to be 1/4 and the damping torque T_d could be expressed as:

$$T_d = C_{nl}(\phi_5 - \phi_4)^{1/4}(\dot{\phi}_5 - \dot{\phi}_4) \tag{110}$$

The energy dissipation due to damping in the present "distributed" system, where it is assumed to take place at the contact interfaces between the sprags and the races, must be the same as that in the earlier "lumped" one. Therefore an expression for the contact damping forces N_{id} and N_{od} at each sprag may be obtained by dividing equation (110) by the number of sprags Z and one of the race radii, together with its associated strut angle, i.e.:

$$N_{id} = N_{od} = \frac{T_d}{ZR_i\alpha} = \frac{T_d}{ZR_o\beta} = \frac{C_{nl}}{ZR_i\alpha}(\phi_5 - \phi_4)^{1/4}(\dot{\phi}_5 - \dot{\phi}_4) \tag{111}$$

4. EQUATION OF MOTION

a. Derivation of Equation of Motion

This section gives a derivation of the equation of motion of the inner race of the clutch when the input motion of the outer race is a known angular displacement in the direction of locking and the inner race motion is opposed by a resisting torque T. It is assumed that the sprags roll on both races from the inception of motion and that the rolling resistance is small and may be neglected.

The torque equation for the inner race, according to the free body diagrams of Figure 25, is given as follows:

$$T - ZR_iF_i = J_i\ddot{\phi}_5 \tag{112}$$

In order to obtain an expression for the friction force F_i, it is best to write a torque equation for the forces acting on the sprag with respect to the accelerated point O on the sprag. Since there is rolling at this point its absolute tangential acceleration equals $R_o\ddot{\phi}_4$. Then, according to Becker (1954), one obtains:

$$-F_i(R_o - R_i) + N_i(R_o - R_i)\alpha = \left[J_s + m_s\frac{(R_o - R_i)^2}{4}\right]\ddot{\phi}_s - \frac{1}{2}m_s(R_o - R_i)R_o\ddot{\phi}_4 \tag{113}$$

where $\ddot{\phi}_s$, the absolute angular acceleration of the sprag, is defined with the help of the epicyclic train model as:

$$\ddot{\phi}_s = \frac{1}{R_o - R_i}[R_o\ddot{\phi}_4 - R_i\ddot{\phi}_5] \tag{114}$$

Equation (113), together with equation (114), furnishes the desired expression for F_i:

$$F_i = -\frac{J_s}{(R_o - R_i)^2}(R_o\ddot{\phi}_4 - R_i\ddot{\phi}_5) - \frac{m_s}{4}(R_o\ddot{\phi}_4 - R_i\ddot{\phi}_5) + \frac{m_s}{2}R_o\ddot{\phi}_4 + \alpha N_i \tag{115}$$

The above is now substituted into equation (112), i.e.:

$$J_i\ddot{\phi}_5 = T - ZR_i\left[-\frac{J_s}{(R_o - R_i)^2}(R_o\ddot{\phi}_4 - R_i\ddot{\phi}_5) + \frac{m_s}{4}(R_o\ddot{\phi}_4 + R_i\ddot{\phi}_5) + \alpha N_i\right] \tag{116}$$

According to equations (108) and (111), the resultant normal force N_i is given by:

$$N_i = N_{ih} + N_{id} = G(\phi_5 - \phi_4)^{3/2} + \frac{C_{nl}}{ZR_i\alpha}(\phi_5 - \phi_4)^{1/4}(\dot{\phi}_5 - \dot{\phi}_4) \tag{117}$$

Substitution of this expression into equation (116) leads to the final differential equation for the inner race motion:

$$A_1\ddot{\phi}_5 + C_{nl}(\phi_5 - \phi_4)^{1/4}(\dot{\phi}_5 - \dot{\phi}_4) + \alpha R_i ZG(\phi_5 - \phi_4)^{3/2} = T + A_2\ddot{\phi}_4 \tag{118}$$

where

$$A_1 = J_i + \frac{ZR_i^2}{(R_o - R_i)^2}J_s + \frac{ZR_i^2}{4}m_s \tag{119}$$

and

$$A_2 = \frac{ZR_i^2}{(R_o - R_i)^2}J_s - \frac{ZR_iR_o}{4}m_s \tag{120}$$

This differential equation becomes active only after the driving torque has overcome the resisting torque, acting on the output shaft. The associated starting time t_s can be obtained from equation (118) by setting ϕ_5 equal to ϕ_{40}, the angle of ϕ_4 at $t = 0$ (see Figure 24b), and letting $\dot{\phi}_5$ and $\ddot{\phi}_5$ be equal to zero. This furnishes:

$$-C_{nl}[\phi_{40} - \phi_4(t_s)]^{1/4}\dot{\phi}_4(t_s) + \alpha R_i ZD[\phi_{40} - \phi_4(t_s)]^{3/2} - T - A_2\ddot{\phi}_4(t_s) = 0 \tag{121}$$

Then the initial conditions for equation (118) become:

$$\phi_5(t_s) = \phi_{40} \tag{122}$$

and

$$\dot{\phi}_5(t_s) = 0 \tag{123}$$

To obtain the differential equation for the windup angle $\phi_{5/4} = (\phi_5 - \phi_4)$, whose time history has been found to be most useful for comparison with experimental results, the term $A_1\ddot{\phi}_4$ is subtracted from both sides of equation (118). This leads to:

$$A_1\ddot{\phi}_{5/4} + C_{nl}\phi_{5/4}^{1/4}\dot{\phi}_{5/4} + \alpha R_i Z D \phi_{5/4}^{3/2} = T + (A_2 - A_1)\ddot{\phi}_4 \tag{124}$$

The starting time t_s is again found with the help of equation (121) and the now applicable initial conditions are given by:

$$\phi_{5/4}(t_s) = \phi_{40} - \phi_4(t_s) \tag{125}$$

and

$$\dot{\phi}_{5/4}(t_s) = -\dot{\phi}_4(t_s) \tag{126}$$

b. Influence of Sprags in Differential Equations

To obtain insight concerning the importance of the sprag parameters contained in the coefficients A_1 and A_2, it is best to consider the magnitudes of the various parameters in equation (124). Table 4 makes this possible.

Table 5 lists the component magnitudes of the coefficients A_1 and A_2 as well as the resulting magnitude of $(A_2 - A_1)$. It is to be noted that the value of J_i only represents the moment of inertia of the inner race assembly of the clutch (see below).

Clutch Parameters	Sprag parameters	Material Properties
$R_o = 1.349\,\text{in}$	$R_s = 0.1878\,\text{in}$	$E_i = E_o = E_s = 30 \times 10^6$ psi
$R_i = 0.9735\,\text{in}$	$a = 0.0224\,\text{in}$	$\nu_i = \nu_o = \nu_s = 0.3$
$Z = 24$	$L_i = 0.864\,\text{in}$	
$\alpha = 0.07\,\text{rad}$	$L_o = 1.087\,\text{in}$	
$\beta = 0.05\,\text{rad}$	$m_s = 5.67 \times 10^{-5}\,\text{lb-sec}^2/\text{in}$	
	$J_s = 8.71 \times 10^{-7}\,\text{lb-sec}^2/\text{in}$	

Table 4 Clutch Data for Formsprag Indexing Clutch Model HPI-500

$A_1 =$	J_i	$+\frac{ZR_i^2}{(R_o - R_i)^2} J_s$	$+\frac{ZR_i^2}{4} m_s$
	34.7×10^{-4}	1.405×10^{-4}	3.224×10^{-4}
$A_2 =$		$+\frac{ZR_iR_o}{(R_o - R_i)^2} J_s$	$-\frac{ZR_iR_o}{4} m_s$
		1.947×10^{-4}	-4.4677×10^{-4}
$A_2 - A_1$	$-J_i - 7.15 \times 10^{-4}$		

Table 5 Component Magnitudes of Coefficients

Accordingly, the sprag contribution to A_1 is 13 percent, while $(A_2 - A_1)$ is 20 percent larger in absolute value than the given value of J_i. Normally, the value of J_i is considerably larger due to the referred moment of inertia of the parts driven by the clutch output. For example, when then clutch was used in a press feed mechanism to advance a 12 foot long steel strip of 0.125 by 1.000 inch cross-section, the total value of J_i was equal to 1907×10^{-4} lb-sec^2/in. Clearly, under those circumstances the influence of the sprag mass can be neglected and one may use the "lumped" form of the windup angle equation, given in Xu and Lowen (1992) i.e.:

$$J_i\ddot{\phi}_{5/4} + C_{nl}\phi_{5/4}^{1/4}\dot{\phi}_{5/4} + K\phi_{5/4}^{3/2} = T - J_i\ddot{\phi}_4 \qquad (127)$$

The above spring constant K is obtained with the help of the expression

$$K = \alpha R_i ZG = \beta R_o ZG$$

of equation (124) and equation (M.14) of Appendix M.

5. CONCLUSIONS

(1) A complete mathematical model for a sprag clutch has been developed. It includes the sprag and inner race inertias, the Hertzian contact forces and the previously determined non-linear damping model.

(2) Comparison with experiment has shown that a line contact model between the races and the sprags, which one would normally assume, is not valid and that a two point contact assumption gives a better description of the existing Hertzian contact mode.

(3) Whenever the total referred moment of inertia of the inner race is much larger than that of the sprags, the earlier developed "lumped" model of the clutch yields satisfactory results.

(4) The two point contact model makes it possible to rationally estimate the spring constant K for the "lumped" model. The associated analytical expression indicates the influence of the various clutch parameters on the clutch stiffness.

PART IV

A PRACTICAL ANALYTICAL APPROACH FOR THE DETERMINATION OF THE TRANSIENT RESPONSE IN ELASTIC MECHANISMS

1. INTRODUCTION

Work on multi-regime per cycle machinery containing elastic links has made it clear that in this type of systems the contribution of the transient response of the link deflections cannot be neglected (Chassapis and Lowen, 1990).

This represents a new departure in machine science, since most previously considered elastic mechanisms (Erdman and Sandor, 1972, Lowen and Jandrasits, 1972, Lowen and Chassapis, 1986, Thompson and Sung, 1986) were assumed to run without any sudden changes in the loading conditions or mechanism configuration. Transient responses occurred only during the starting of the machine and since they disappeared after a few rotations of the input link, they were not considered to be of great importance.

Based on mathematical work by Whittaker (1944), this paper shows a practical analytic approach for obtaining such transient responses by way of the determination of the characteristic exponent in the stable regions[10] of the Floquet solution to Hill's equation, which arises from elastic mechanism problems.

This technique, together with the known analytical solution of the steady state response, due to Kotowski (1943) and applied to mechanism by Jandrasits and Lowen (1979), makes it possible to get a complete analytical solution for forced Hill-type differential equation. It further allows the separation of the response components after the constants of integration have been evaluated and with that one may investigate the influence of the various mechanism parameters on the shape of the transient response alone. This separation is not possible by strictly numerical integration of the differential equation.

---

10 Industrial machinery is confined to operate in stable regions.

To start with, this paper gives a brief review of the results of Floquet theory, pertaining to Hill's equation. This includes the form of the general solution, the various possibilities for the characteristic exponent, as well as the determination of the 2π and 4π periodic instability boundaries by way of Hill's determinant.

Subsequently, the new technique of obtaining the characteristic exponent in the stable regions is presented.

Finally, an application to a specific mechanism problem, introduced by Badlani and Midha (1983), is given. In it the time portion of the product solution for the deflection of an elastic connecting rod takes the form of a Mathieu equation. Using dimensions similar to those used by Thompson and Sung (1984), complete calculations for a number of sample responses are carried out.

2. BACKGROUND

The solution to the partial differential equations for the lateral deflections of elastic mechanism links is usually obtained by way of a product solution method, such as that of Kantorovich (Jandrasits and Lowen, 1979). By assuming shape functions, the resulting expressions for the time functions are governed by a set of damped, forced and coupled Hill-type differential equations.

When only the fundamental mode of the shape functions needs to be considered and damping is neglected[11], the homogeneous portion of the resulting equation becomes a standard Hill's equation:

$$\frac{d^2y}{d\phi^2} + [\lambda + p(\phi)]y = 0 \tag{128}$$

In the above, the unknown y is a time function associated with the link deflection and the independent variable ϕ represents the mechanism input angle. The coefficient λ is usually expressed by the ratio $\omega^2/\dot{\phi}^2$, with ω the first natural frequency of the link and $\dot{\phi}$ the input speed of the mechanism. The time dependent coefficient $p(\phi)$, which is a function of the loading conditions, the mechanism geometry and the shape function associated with the link deflection, is 2π periodic.

---

11 A damped Hill's equation can be easily transformed into a standard one (Magnus and Winkler, 1966).

Floquet theory (Strutt, 1932, Klotter, 1941, Whittaker and Watson, 1944, Bolotin, 1964, Magnus and Winkler, 1966) shows that for stable as well as unstable regions the general solution of Hill's differential equation has the form:

$$y(\phi) = Be^{\mu\phi}p_1(\phi) + Ce^{-\mu\phi}p_2(\phi) , \tag{129}$$

where B and C are constants of integration and $p_1(\phi)$ and $p_2(\phi)$ are 2π periodic functions.

The exponent μ is known as the characteristic exponent, which is generally of the form $a + ib$. This gives rise to the following well known possibilities:

(1) If a is not equal to zero and b has the value $k/2$, where $k = 0, 1, 2, 3, \ldots$, the solution lies in an unstable region.

(2) If a is equal to zero and b has the value $k/2$, where $k = 0, 2, 4, 6, \ldots$ even, the solution lies on the 2π periodic boundaries of an associated 2π periodic region of instability. (Recall that for large values of λ, the two boundaries may be interpreted as coincident.)

(3) If a is equal to zero and b has the value $k/2$, where $k = 1, 3, 5, \ldots$ odd, the solution lies on the 4π periodic boundaries of an associated 4π periodic instability region. (Again if λ is large, the two boundaries coincide.)

(4) If a is equal to zero and b has values other than $k/2$, where $k = 0, 1, 2, 3, \ldots$, the solution lies within one of the stable regions.

In order to obtain the complete solution to Hill's equation as well as the above stability boundaries, the function $p(\phi)$ is first expanded into a complex Fourier series:

$$p(\phi) = \sum_{m=-\infty}^{+\infty} a_m e^{im\phi} , \tag{130}$$

where

$$a_m = \frac{1}{2\pi}\int_0^{2\pi} p(\phi)e^{-im\phi}d\phi \quad (m = 0, \pm1, \pm2, \pm3, \ldots) \tag{131}$$

Note that the a_m are equal to the conjugates of the a_{-m}.

If one now expresses the solution functions $p_1(\phi)$ and $p_2(\phi)$ as complex Fourier series, i.e.:

$$p_1(\phi) = \sum_{n=-\infty}^{+\infty} c_n e^{in\phi} \tag{132}$$

and

$$p_2(\phi) = \sum_{n=-\infty}^{+\infty} b_n e^{in\phi}\,, \tag{133}$$

the general solution of Hill's equation (128), together with equation (129), will have the following form:

$$y(\phi) = Be^{\mu\phi} \sum_{n=-\infty}^{+\infty} c_n e^{in\phi} + Ce^{-\mu\phi} \sum_{n=-\infty}^{+\infty} b_n e^{in\phi} \tag{134}$$

Substitution of equation (134), together with equation (130), into Hill's equation (128) leads to the following two systems of simultaneous equations in terms of the c_n and b_n, respectively:

$$[(\mu + in)^2 + \lambda]c_n + \sum_{m=-\infty}^{+\infty} a_m c_{n-m} = 0 \qquad (n = \ldots, -3, -2, -1, 0, 1, 2, 3, \ldots) \tag{135}$$

and

$$[(\mu - in)^2 + \lambda]b_n + \sum_{m=-\infty}^{+\infty} a_m b_{n-m} = 0 \qquad (n = \ldots, -3, -2, -1, 0, 1, 2, 3, \ldots) \tag{136}$$

Since only the stable solution, for which μ must be imaginary, is considered here, one can show that equation (136) is equivalent to:

$$[(\mu + in)^2 + \lambda]\overline{b}_{-n} + \sum_{m=-\infty}^{+\infty} a_m \overline{b}_{-(n-m)} = 0 \qquad (n = \ldots, -3, -2, -1, 0, 1, 2, 3, \ldots) \tag{137}$$

where $\overline{b}_{-n}$ is the conjugate of b_{-n}.

Comparison of equations (135) and (137) indicates that only one of these equations needs to be solved, if one defines the relationship of the solution coefficients as:

$$c_n = \overline{b}_{-n} \quad \text{or} \quad b_{-n} = \overline{c}_n \tag{138}$$

Equation (135) is now written in matrix form:

$$\begin{bmatrix} \cdot & \cdot & \cdot & \cdot & \cdot & \cdot & \cdot & \cdot \\ \cdot & (\mu-3i)^2+a_0+\lambda & a_{-1} & a_{-2} & a_{-3} & a_{-4} & a_{-5} & a_{-6} & \cdot \\ \cdot & a_1 & (\mu-2i)^2+a_0+\lambda & a_{-1} & a_{-2} & a_{-3} & a_{-4} & a_{-5} & \cdot \\ \cdot & a_2 & a_1 & (\mu-i)^2+a_0+\lambda & a_{-1} & a_{-2} & a_{-3} & a_{-4} & \cdot \\ \cdot & a_3 & a_2 & a_1 & \mu^2+a_0+\lambda & a_{-1} & a_{-2} & a_{-3} & \cdot \\ \cdot & a_4 & a_3 & a_2 & a_1 & (\mu+i)^2+a_0+\lambda & a_{-1} & a_{-2} & \cdot \\ \cdot & a_5 & a_4 & a_3 & a_2 & a_1 & (\mu+2i)^2+a_0+\lambda & a_{-1} & \cdot \\ \cdot & a_6 & a_5 & a_4 & a_3 & a_2 & a_1 & (\mu+3i)^2+a_0+\lambda & \cdot \\ \cdot & \cdot & \cdot & \cdot & \cdot & \cdot & \cdot & \cdot & \cdot \end{bmatrix} \begin{bmatrix} \cdot \\ c_{-3} \\ c_{-2} \\ c_{-1} \\ c_0 \\ c_1 \\ c_2 \\ c_3 \\ \cdot \end{bmatrix} = 0$$

(139)

Recall that the above infinite coefficient determinant is known as Hill's determinant and that its value must be equal to zero for the non-trivial solution of the c_n. Further, if the value of μ is known, the coefficients c_n of the series solution may be readily determined in terms of c_0 as well as the cofactor of the determinant.

The stability boundaries for a given system result from the eigenvalue solution of the coefficient determinant for λ with $\mu = i(k/2)$ $(k = 0, 1, 2, 3, \ldots)$. Since the use of various values of odd or even k's only implies a shift of the center of the infinite determinant, it is practical to solve for the 2π periodic boundaries by letting $\mu = i0$. Similarly the 4π periodic boundaries are obtained with $\mu = i/2$ (Jandrasits and Lowen, 1979).

Figure 26 shows a typical "stability line" which relates the stability boundaries as well as stable and unstable regions, associated with ascending numbers of k, to the value of λ, i.e. the mechanism speed.

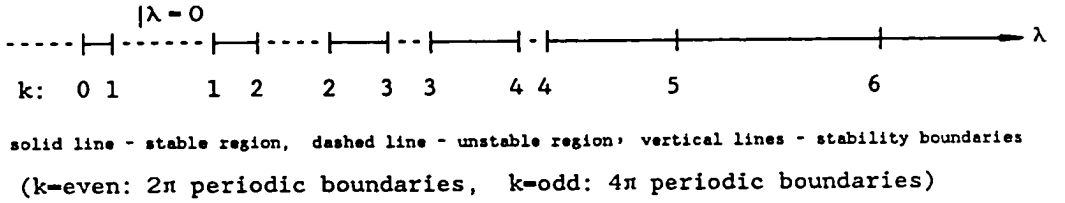

Figure 26 Typical Stability Line

3. DETERMINATION OF CHARACTERISTIC EXPONENT IN STABLE REGIONS

After dividing the typical row of the zero valued Hill's determinant of equation (139) by $(a_0+\lambda-n^2)$ to secure convergence, one obtains the following Hill's determinantal equation, which allows the computation of μ when λ and a_m are known from the physical problem:

$$\Delta(\mu)=\begin{bmatrix}
\vdots & \vdots & \vdots & \vdots & \vdots & \vdots & \vdots \\
\frac{(\mu-3i)^2+a_0+\lambda}{a_0+\lambda-3^2} & \frac{a_{-1}}{a_0+\lambda-3^2} & \frac{a_{-2}}{a_0+\lambda-3^2} & \frac{a_{-3}}{a_0+\lambda-3^2} & \frac{a_{-4}}{a_0+\lambda-3^2} & \frac{a_{-5}}{a_0+\lambda-3^2} & \frac{a_{-6}}{a_0+\lambda-3^2} \\
\frac{a_1}{a_0+\lambda-2^2} & \frac{(\mu-2i)^2+a_0+\lambda}{a_0+\lambda-2^2} & \frac{a_{-1}}{a_0+\lambda-2^2} & \frac{a_{-2}}{a_0+\lambda-2^2} & \frac{a_{-3}}{a_0+\lambda-2^2} & \frac{a_{-4}}{a_0+\lambda-2^2} & \frac{a_{-5}}{a_0+\lambda-2^2} \\
\frac{a_2}{a_0+\lambda-1^2} & \frac{a_1}{a_0+\lambda-1^2} & \frac{(\mu-i)^2+a_0+\lambda}{a_0+\lambda-1^2} & \frac{a_{-1}}{a_0+\lambda-1^2} & \frac{a_{-2}}{a_0+\lambda-1^2} & \frac{a_{-3}}{a_0+\lambda-1^2} & \frac{a_{-4}}{a_0+\lambda-1^2} \\
\frac{a_3}{a_0+\lambda} & \frac{a_2}{a_0+\lambda} & \frac{a_1}{a_0+\lambda} & \frac{\mu^2+a_0+\lambda}{a_0+\lambda} & \frac{a_{-1}}{a_0+\lambda} & \frac{a_{-2}}{a_0+\lambda} & \frac{a_{-3}}{a_0+\lambda} \\
\frac{a_4}{a_0+\lambda-1^2} & \frac{a_3}{a_0+\lambda-1^2} & \frac{a_2}{a_0+\lambda-1^2} & \frac{a_1}{a_0+\lambda-1^2} & \frac{(\mu+i)^2+a_0+\lambda}{a_0+\lambda-1^2} & \frac{a_{-1}}{a_0+\lambda-1^2} & \frac{a_{-2}}{a_0+\lambda-1^2} \\
\frac{a_5}{a_0+\lambda-2^2} & \frac{a_4}{a_0+\lambda-2^2} & \frac{a_3}{a_0+\lambda-2^2} & \frac{a_2}{a_0+\lambda-2^2} & \frac{a_1}{a_0+\lambda-2^2} & \frac{(\mu+2i)^2+a_0+\lambda}{a_0+\lambda-2^2} & \frac{a_{-1}}{a_0+\lambda-2^2} \\
\frac{a_6}{a_0+\lambda-3^2} & \frac{a_5}{a_0+\lambda-3^2} & \frac{a_4}{a_0+\lambda-3^2} & \frac{a_3}{a_0+\lambda-3^2} & \frac{a_2}{a_0+\lambda-3^2} & \frac{a_1}{a_0+\lambda-3^2} & \frac{(\mu+3i)^2+a_0+\lambda}{a_0+\lambda-3^2} \\
\vdots & \vdots & \vdots & \vdots & \vdots & \vdots & \vdots
\end{bmatrix}=0 \tag{140}$$

Whittaker (1944) has shown mathematically that the above determinant $\Delta(\mu)$, regardless of the value of μ, can be expressed by way of the following formulation:

$$\Delta(\mu)=\Delta(0)-\sin^2(\pi i\mu)\operatorname{cosec}^2(\pi\sqrt{\lambda+a_0}) \tag{141}$$

where $\Delta(0)$ is the value of this determinant for $\mu=0$ and known values for λ and a_m. This determinant $\Delta(0)$ will yield a real value since its conjugate $\overline{\Delta(0)}$ is identical to $\Delta(0)$. For equation (141) to hold, the coefficient sum $\sum a_m$ associated with function $p(\phi)$ must be absolutely convergent, which is always the case in elastic linkages.

The present work shows for the first time, to the best knowledge of the author, how this relationship may be applied for the determination of the characteristic exponent μ in the stable regions.

Since $\Delta(\mu)$ must vanish according to (140), equation (141) becomes:

$$\sin(\pi i\mu) = \pm\sqrt{\Delta(0)}\sin(\pi\sqrt{\lambda + a_0}) \tag{142}$$

This furnishes sets of positive and negative μ's of the same absolute value. Since the use of either of these μ's yields the same solution from equation (134), only the positive μ will be considered in the following.

It is further to be noted that the value of μ changes in all stable regions from $i(k/2)$ at the left boundary to $i(k + 1)/2$ at the right one. Therefore, for a practical application, it is useful to define

$$\mu = bi = \left(\frac{k}{2} + A\right)i \quad \text{(see case 4 of section 2 in Part IV)}, \tag{143}$$

where A is considered positive and represents the change of the value of μ from that at the left boundary to that at any point in the given stable region.

When expression (143) is substituted into equation (142) with the intention of obtaining a positive A, one finds that:

$$\sin(\pi A) = \sqrt{\Delta(0)}\,|\sin(\pi\sqrt{\lambda + a_0})| \quad \text{(k=even)} \tag{144}$$

and

$$\cos(\pi A) = \sqrt{\Delta(0)}\,|\sin(\pi\sqrt{\lambda + a_0})| \quad \text{(k=odd)} \tag{145}$$

As the restoring force during the elastic bending deformation of a link is always opposite to the displacement, the value of λ must be positive and larger than $|a_0|$. In addition, to obtain a real non-zero value of A, which assures a stable solution of Hill's equation, the

value of $\Delta(0)$ must be greater than zero and the absolute value of $[\sqrt{\Delta(0)}\sin(\pi\sqrt{\lambda + a_0})]$ must be smaller than unity. With the above, equation (144) furnishes for A:

$$A = \frac{1}{\pi}\sin^{-1}[\sqrt{\Delta(0)} \mid \sin(\pi\sqrt{\lambda + a_0}) \mid] \qquad \text{(k=even)} \tag{146}$$

while equation (145) leads to

$$A = \frac{1}{\pi}\cos^{-1}[\sqrt{\Delta(0)} \mid \sin(\pi\sqrt{\lambda + a_0}) \mid] \qquad \text{(k=odd)} \tag{147}$$

Thus, for the determination of μ within any of the stable regions, the following steps should be taken:

(1) After finding both the 2π and the 4π periodic instability boundaries in terms of λ, draw a "stability line" of the type shown in Figure 23.

(2) Determine the value of k of the left instability boundary of the stable region under investigation with the help of the "stability line".

(3) If $k = 0, 2, 4, \ldots$ even, use equation (146) with the given value of λ to determine A.

(4) If $k = 1, 3, 5, \ldots$ odd, use equation (147) with the given value of λ to determine A.

(5) The value of μ can then be obtained by substituting the values of k and A, of parts (3) or (4) above, respectively, into equation (143).

Finally, since only the solution in the stable region is considered, where μ is always imaginary, the complex series solution form (134) is best converted, according to Euler's identity, into the real form:

$$y(\phi) = D_1 \sum_{n=-\infty}^{+\infty} [\alpha_n \cos(|\mu| + n)\phi - \beta_n \sin(|\mu| + n)\phi] +$$

$$+ D_2 \sum_{n=-\infty}^{+\infty} [\alpha_n \sin(|\mu| + n)\phi + \beta_n \cos(|\mu| + n)\phi] \tag{148}$$

where α_n and β_n are the real and imaginary parts of the complex solution coefficients c_n,

respectively.

4. APPLICATION TO MECHANISM EXAMPLE

The method of the previous section is now applied to the determination of the transient part of the deflection of the elastic connecting rod of the slider-crank mechanism shown in Figure 27. It must be understood that by omitting the forced part of the response and with that the true constants of integration, one can only determine the general shape of the transient contribution.

Badlani and Midha (1983) derived the first mode governing equation for the time portion of the product solution for the connecting rod. When their damping and forcing terms are omitted for present purposes, and the expression is put into the notation of this paper, one obtains the following Mathieu equation, which is the simplest form of the homogeneous Hill's equation:

$$\frac{d^2y}{d\phi^2} + (\lambda + \gamma\cos\phi)y = 0 \tag{149}$$

Again,

$\lambda = \omega^2/\dot{\phi}^2$,

with

$\omega = \sqrt{(\pi^4 EI)/(\rho SL^4)}$,

the first natural frequency of the coupler.

Further,

$$\gamma = \frac{\pi^2 RM}{\rho SL^2} ,$$

where, R and L are crank and connecting rod lengths, respectively. ρ stands for the mass density of the connecting rod, S the cross-sectional area of the connecting rod and M the

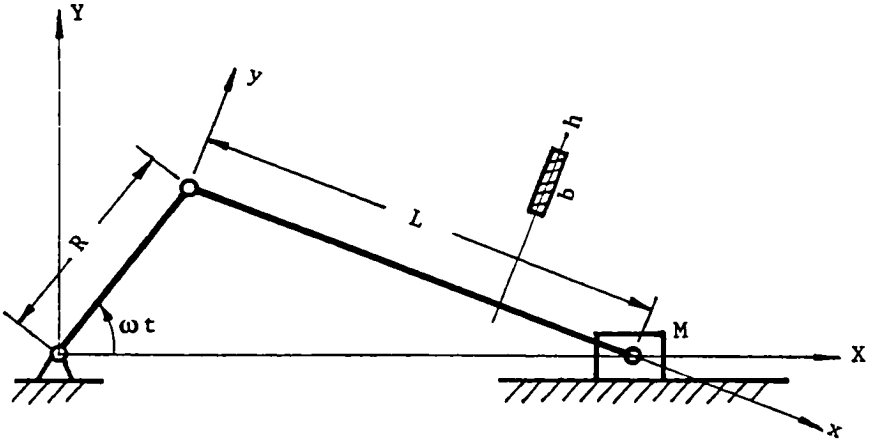

Figure 27 Slider-Crank Mechanism

mass of piston.

Note that in terms of equation (128):

$$p(\phi) = \gamma \cos\phi \tag{150}$$

With the exception of

$$a_1 = a_{-1} = \gamma/2\ , \tag{151}$$

all the coefficients of equation (130) vanish and the system of equations (139) reduces to the following form:

$$\begin{bmatrix} \cdot & \cdot & \cdot & \cdot & \cdot & \cdot & \cdot & \cdot & \cdot \\ \cdot & (\mu-3i)^2+\lambda & \gamma/2 & 0 & 0 & 0 & 0 & 0 & \cdot \\ \cdot & \gamma/2 & (\mu-2i)^2+\lambda & \gamma/2 & 0 & 0 & 0 & 0 & \cdot \\ \cdot & 0 & \gamma/2 & (\mu-i)^2+\lambda & \gamma/2 & 0 & 0 & 0 & \cdot \\ \cdot & 0 & 0 & \gamma/2 & \mu^2+\lambda & \gamma/2 & 0 & 0 & \cdot \\ \cdot & 0 & 0 & 0 & \gamma/2 & (\mu+i)^2+\lambda & \gamma/2 & 0 & \cdot \\ \cdot & 0 & 0 & 0 & 0 & \gamma/2 & (\mu+2i)^2+\lambda & \gamma/2 & \cdot \\ \cdot & 0 & 0 & 0 & 0 & 0 & \gamma/2 & (\mu+3i)^2+\lambda & \cdot \\ \cdot & \cdot & \cdot & \cdot & \cdot & \cdot & \cdot & \cdot & \cdot \end{bmatrix} \begin{bmatrix} \cdot \\ c_{-3} \\ c_{-2} \\ c_{-1} \\ c_0 \\ c_1 \\ c_2 \\ c_3 \\ \cdot \end{bmatrix} = 0 \tag{152}$$

The specific example computations for the slider-crank mechanism are based on dimensions similar to those used by Thompson and Sung (1984), i.e.

R = 50.8 mm (2.000 in), L = 304.8 mm (12.000 in), h = 1.4 mm (0.055 in),

b = 19.05 mm (0.750 in), ρ = 7867 kg/m^3 (7.3243×10^{-4} lb-sec^2/in^4),

M = 0.45 kg (0.002588 lb-sec^2/in), E = 206.8 Mpa (30×10^6 psi).

With the above,

$\omega = 220.24$ rad/sec and $\gamma = 11.742$.

This value of γ is now substituted into the coefficient matrix of equation (152), first together with $\mu = 0i$ and then with $\mu = 0.5i$, in order to obtain the 2π and 4π periodic instability boundaries, respectively, by way of the associated eigenvalue problems.

Table 6 lists a part of the results of these computations, indicating the values of λ at both types of boundaries, together with the corresponding mechanism speeds. (A 71×71 matrix was used.)

Note that the operation of the mechanism is essentially stable up to 507 RPM, with only coinciding boundaries below that speed. Further stable regions are located between 508-561, 570-610, 653-672 and 791-796 RPM. There is a small stable region between 1131 and 1132 RPM.

Figure 28 gives the associated "stability line", which now represents a horizontal line in a Strutt Chart (Strutt, 1932).

As the first case, let it be required to find the value of μ corresponding to 590 RPM at $\lambda = 12.7066$ in the stable region between 570 RPM and 610 RPM, (i.e. $13.60742 > \lambda > 11.87115$), according to the previously given procedure:

(1) From the "stability line" of Figure 28, one notes that $k = 6$ at the left boundary of the region involved.

k (even)	2π Boundary (λ)	speeds (RPM)	k (odd)	4π Boundary (λ)	speeds (RPM)
0	-9.3832*		1	-9.3832*	
2	-4.8023*		1	-4.8023*	
2	-0.5103*		3	-0.5098*	
4	3.4583	1131	3	3.4496	1132
4	6.9764	796	5	7.0701	791
6	10.3737	653	5	9.8015	672
6	11.8711	610	7	13.6074	570
8	17.1193	508	7	14.0697	561
8	17.1945	507	9	21.1353	457
10	25.7098	415	9	21.1432	457
10	25.7104	415	11	30.8319	379
12	36.4864	348	11	30.8320	379
12	36.4864	348	13	42.6630	322
14	49.3552	299	13	42.6630	322
14	49.3552	299	15	56.5589	279
16	64.2711	262	15	56.5589	279
16	64.2711	262	17	72.4899	247
18	81.2138	233	17	72.4899	247
18	81.2138	233	19	90.4418	221
20	100.1730	210	19	90.4418	221
20	100.1730	210	21	110.4068	200
22	121.1428	191	21	110.4068	200

Table 6 Instability Boundaries of Mechanism Example

(*These six boundaries have no physical meaning for the present example, but are needed for the counting of the k's.)

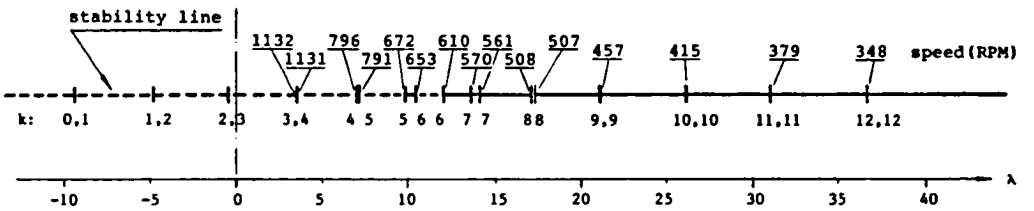

solid line - stable region, dashed line - unstable region; vertical lines - stability boundaries

(k=even: 2π periodic boundaries, k=odd: 4π periodic boundaries)

Figure 28 Stability Line of Mechanism Example

(2) Since k is even, equation (146) becomes applicable for the determination of A. With $\Delta(0) = 0.65251$, as obtained with the help of a 71×71 determinant in the evaluation of equation (140), one obtains $A = 0.29054$ (Appendix N shows the program for the determination of $\Delta(0)$).

(3) Finally, according to equation (143):

$\mu = (0.29054 + 3)i = 3.29054i$

To determine the general shape of the transient solution with the above parameters, one needs also to find the series coefficients c_n according to the simultaneous equation (152).

Table 7 gives the first sixteen coefficients of this solution series in terms of c_0 equal to unity. (Again, a 71×71 matrix is utilized.)

n	1	2	3	4	5	6	7	8
c_n	1.81620	0.76396	0.17252	0.02543	0.00269	0.00022	0.00001	0.00000
c_{-n}	-2.13750	1.71603	-1.08969	0.62671	-0.21297	-0.27179	0.46135	0.35458
n	9	10	11	12	13	14	15	16
c_n	0.00000	0.00000	0.00000	0.00000	0.00000	0.00000	0.00000	0.00000
c_{-n}	0.11073	0.02060	0.00262	0.00025	0.00002	0.00000	0.00000	0.00000

Table 7 Coefficients of Solution Series

After substitution of these coefficients which are all real in this example into equation (148), and assuming the initial conditions as $y(0) = 1.0$ and $\dot{y}(0) = 1.0$, the constants of integration are found to be: (see discussion at the beginning of this section)

$D_1 = 0.29745$ and $D_2 = 0.10097$

With the above, the expression for the solution series (148) becomes:

$$\begin{aligned} y(\phi) = & 0.3[\cos(3.3\phi) + 1.82\cos(4.3\phi) - 2.14\cos(2.3\phi) + \\ & + 0.76\cos(5.3\phi) + 1.72\cos(1.3\phi) + \ldots] + \\ & + 0.1[\sin(3.3\phi) + 1.82\sin(4.3\phi) - 2.14\sin(2.3\phi) + \\ & + 0.76\sin(5.3\phi) + 1.72\sin(1.3\phi) + \ldots] \end{aligned} \tag{153}$$

Figure 29 shows a plot of this transient response at a machine speed of 590 RPM for two machine cycles. (For multi-regime per cycle machinery only a portion of a cycle would be involved.) Clearly, this response is non-periodic with varying amplitudes.

Figure 30 gives such a response for the same initial conditions, when the mechanism speed is decreased to 430 RPM, corresponding to $\lambda = 23.9219$ in the stable region, where $k = 9$ on the left boundary. It is less non-periodic than before, with smaller changes in the amplitude. Its oscillation frequency is close to the fundamental one of 220.24 rad/sec.

Finally, Figure 31 represents a similarly obtained response at 205 RPM, corresponding to $\lambda = 105.25$ in the stable region, with $k = 20$ at the left boundary. Here the oscillation is close to harmonic motion at the fundamental frequency.

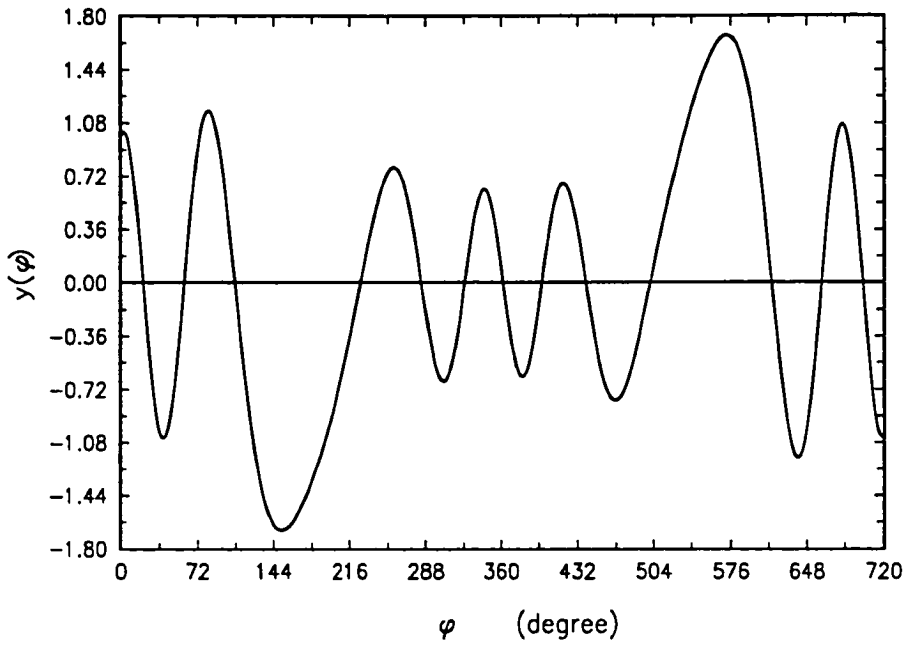

Figure 29 Homogeneous Solution with λ = 12.7066 (590 RPM) and γ = 11.742

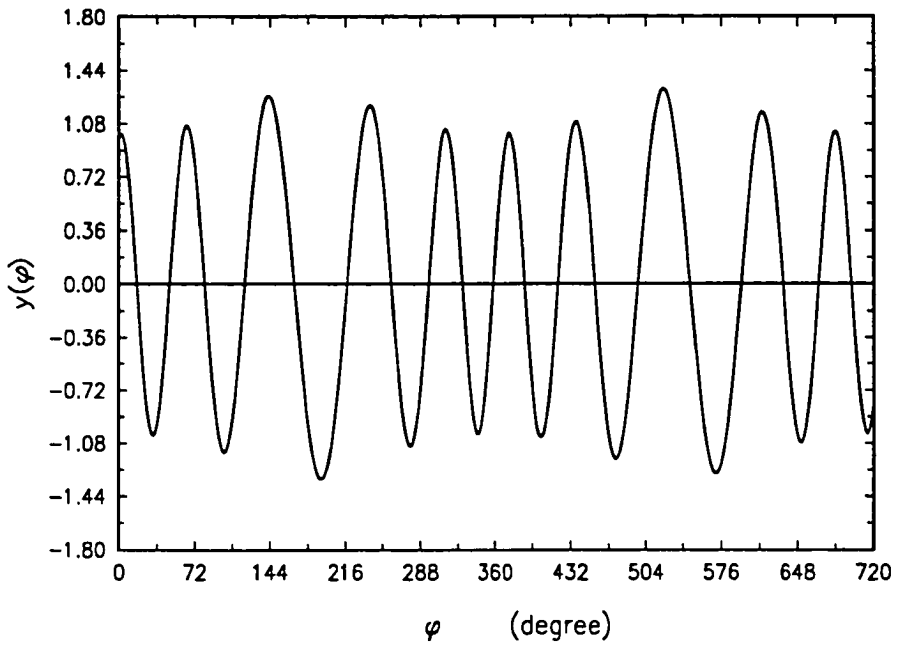

Figure 30 Homogeneous Solution with $\lambda = 23.9219$ (430 RPM) and $\gamma = 11.742$

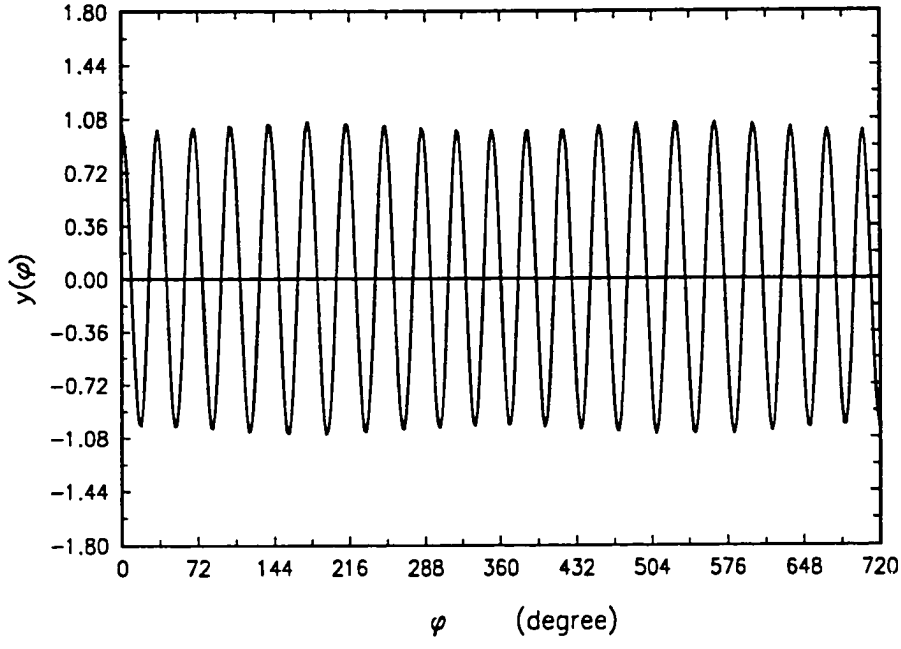

Figure 31 Homogeneous Solution with $\lambda = 105.2507$ (205 RPM) and $\gamma = 11.742$

5. DISCUSSION AND CONCLUSIONS

(1) Based on E.T. Whittaker's mathematical work, a practical approach for the determination of the value of the characteristic exponent in the stable regions of the Floquet solution of Hill's equation has been developed. This allows for the first time to obtain an analytical expression for the transient response of the lateral deflection of links in an elastic mechanism. It is of special importance for multi-regime per cycle machinery, where such transient responses have been found to occur and never disappear.

(2) An application of this solution approach to a mechanism problem, where the first mode transient time response is governed by a Mathieu equation, has shown that the nature of the responses depends on the location of the stable region, which is a function of the mechanism speed, the mechanism parameters and the loading conditions. It may vary from being almost periodic, with a frequency near the first natural one of the lateral deflection, to fully non-periodic with vastly changing amplitudes.

(3) Figure 32 indicates the manner in which the numerical value of the characteristic exponent changes between the boundaries of the stable region of the first case. It is noted that the increase of the value of μ between the boundaries, which in each case equals $0.5i$, is very smooth. Thus a straight line approximation might be used, whenever the region is not too narrow (i.e. when the machine speed is relatively low).

(4) While all computations employed 71×71 matrices, to allow an accurate comparison with a parallel numerical integration of the example differential equation, much smaller matrices will furnish reasonable results.

(5) Fast convergence of the series solution, i.e. equation (148), is assured when the value of μ is relatively large. This is the case in the regions where most industrial machinery operates.

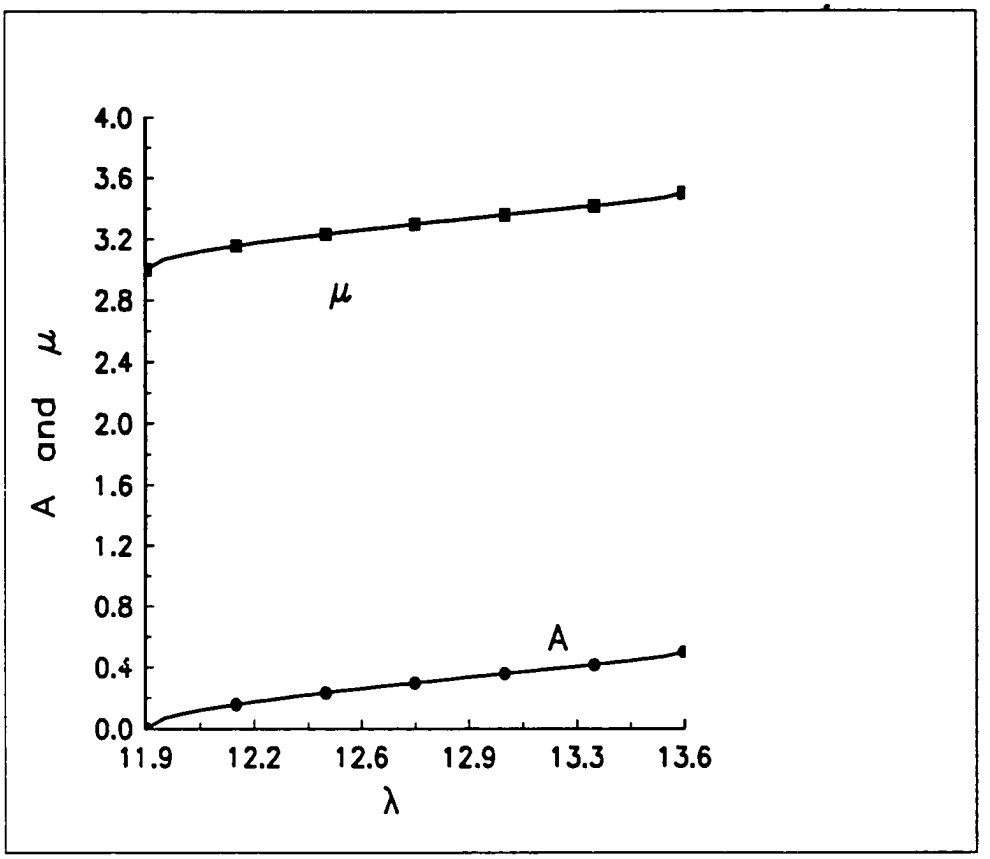

Figure 32 Values of the Parameter A and the Characteristic Exponent μ in Stable Region where $11.7811 \leq \lambda \leq 13.6074$

APPENDIX A. KINEMATICS OF THE LINKAGE

a. Elastic Constraint Equations and Various Angles

In order to obtain the elastic kinematics of the feed mechanism, one first writes the elastic loop equation of the replacement RRRSR mechanism as follows (see Figure 1):

$$\overline{O_1A} + \overline{AC'} + \overline{CO_2} + \overline{O_2O_1} = 0 \tag{A.1}$$

The substitution of the appropriate expressions of the vectors $\overline{O_1A}, \overline{AC'}, \overline{CO_2}$ and $\overline{O_2O_1}$, in terms of $\bar{i}_0, \bar{j}_0$ and $\bar{k}_0$, leads to the following three elastic constraint equations:

$$s_1 + AC'\cos\alpha\cos\phi_{32e} - a_4\sin\phi_{4e} = 0 \tag{A.2}$$

$$a_1\cos\phi_1 + AC'(\sin\alpha\sin\phi_{2e} - \cos\alpha\cos\phi_{2e}\sin\phi_{32e}) + s_2 = 0 \tag{A.3}$$

$$a_1\sin\phi_1 - AC'(\sin\alpha\cos\phi_{2e} + \cos\alpha\sin\phi_{2e}\sin\phi_{32e}) - a_4\cos\phi_{4e} + s_3 = 0 \tag{A.4}$$

where each of the elastic angles ϕ_{ie} is composed of the rigid body component ϕ_{ir} and the additional rotational component $\Delta\phi_i$. The latter is due solely to the elastic change of length ΔAC of the coupler. Then,

$$\phi_{2e} = \phi_{2r} + \Delta\phi_2 \quad \text{(rotations about an axis parallel to } \bar{i}_0) \tag{A.5}$$

$$\phi_{32e} = \phi_{32r} + \Delta\phi_{32} \quad \text{(rotations parallel to axis } \bar{j}_1) \tag{A.6}$$

$$\phi_{4e} = \phi_{4r} + \Delta\phi_4 \quad \text{(rotations about an axis parallel to } \bar{j}_0) \tag{A.7}$$

In the above, the rigid body angles as functions of input angle ϕ_1 can be found according to Hartenberg and Denavit (1964) as:

$$\phi_{4r} = 2\tan^{-1}\left[\frac{A + \sqrt{A^2 + B^2 - C^2}}{B + C}\right] \tag{A.8}$$

where

$$A = 2s_1 a_4 \tag{A.9a}$$

$$B = 2a_4(s_3 + a_1 \sin\phi_1) \tag{A.9b}$$

$$C = a_4^2 + s_1^2 + s_2^2 + s_3^2 + a_1^2 - a_3^2 + 2a_1 s_2 \cos\phi_1 + 2s_3 a_1 \sin\phi_1 \tag{A.9c}$$

$$\phi_{32r} = \cos^{-1}\left(\frac{a_4 \sin\phi_{4r} - s_1}{a_3 \cos\alpha}\right) \tag{A.10}$$

$$\phi_{2r} = 2\tan^{-1}\left[\frac{A^* - \sqrt{A^{*2} + B^{*2} - C^{*2}}}{B^* + C^*}\right] \tag{A.11}$$

and where

$$A^* = s_2 + a_1 \cos\phi_1 \tag{A.12a}$$

$$B^* = -s_3 - a_1 \sin\phi_1 + a_4 \cos\phi_{4r} \tag{A.12b}$$

$$C^* = -a_3 \sin\alpha \tag{A.12c}$$

The velocities and the accelerations of these rigid body angles can be readily obtained by taking the derivatives of equations (A.8), (A.10) and (A.11) with respect to time, respectively.

b. Additional Component of Rotation and Virtual Rotation of the Elastic Angles

The elastic components $\Delta\phi_4$, $\Delta\phi_2$ and $\Delta\phi_{32}$ of the elastic angles, which are due to the change of the length ΔAC of the coupler, are solved for by substituting equations (A.5) to (A.7) as well as $AC' = a_3 + 2q(t)\sin\alpha$ (see equation (9)), into equations (A.2) to (A.4). Since these elastic components and ΔAC are small, one finds after simultaneous solution:

$$\Delta\phi_4 = [2\eta_4(\phi_1)\sin\alpha]q \tag{A.13}$$

$$\Delta\phi_{32} = [2\eta_{32}(\phi_1)\sin\alpha]q \tag{A.14}$$

and

$$\Delta\phi_2 = [2\eta_2(\phi_1)\sin\alpha]q \tag{A.15}$$

where

$$\eta_4(\phi_1) = \frac{-2a_3}{(A\cos\phi_{4r} - B\sin\phi_{4r})} \tag{A.16}$$

$$\eta_{32}(\phi_1) = \frac{(\cos\alpha\cos\phi_{32r} - a_4\cos\phi_{4r}\eta_4)}{a_3\cos\alpha\sin\phi_{32r}} \tag{A.17}$$

and

$$\eta_2(\phi_1) = \frac{[\cos\alpha\cos\phi_{2r}(a_3\cos\phi_{32r}\eta_{32} + \sin\phi_{32r}) - \sin\alpha\sin\phi_{2r}]}{a_3(\sin\alpha\cos\phi_{2r} + \cos\alpha\sin\phi_{2r}\sin\phi_{32r})} \tag{A.18}$$

To obtain the virtual rotations $\delta\phi_{3e}$ and $\delta\phi_{4e}$, one needs to take variations of the angles $\Delta\phi_{3e}$ and $\Delta\phi_{4e}$ only, since there are no variations of the rigid body components:

$$\delta\bar{\phi}_{3e} = \delta\bar{\phi}_{2e} + \delta\bar{\phi}_{32e} = \delta(\Delta\phi_2)\bar{i}_0 + \delta(\Delta\phi_{32})\bar{j}_1 = 2\sin\alpha(\eta_2\bar{i}_0 + \eta_{32}\bar{j}_1)\delta q \tag{A.19}$$

After appropriate transformation of the coordinates, one finds $\delta\bar{\phi}_{3e}$ in the body fixed system:

$$\delta\bar{\phi}_{3e} = 2\sin\alpha[\eta_2(\phi_1)\cos\phi_{32r}\bar{i}_1 + \eta_{32}(\phi_1)\bar{j}_1 + \eta_2(\phi_1)\sin\phi_{32r}\bar{k}_1]\delta q \tag{A.20}$$

Similarly,

$$\delta\bar{\phi}_{4e} = \delta(\Delta\phi_4)\bar{j}_0 = [\eta_4(\phi_1)2\sin\alpha\bar{j}_0]\delta q \qquad (A.21)$$

The development of the expression for the angular velocity associated with $\Delta\phi_3$, the additional component of the rotation of the coupler, is parallel to equations (A.19) and (A.20):

$$\dot{\overline{\Delta\phi}}_3 = \frac{d}{dt}(\Delta\phi_2)\bar{i}_0 + \frac{d}{dt}(\Delta\phi_{32})\bar{j}_1$$

$$= 2\sin\alpha[\eta_2(\phi_1)\cos\phi_{32}\bar{i}_1 + \eta_{32}(\phi_1)\bar{j}_1 + \eta_2(\phi_1)\sin\phi_{32}\bar{k}_1]\dot{q} \qquad (A.22)$$

The angular acceleration of this elastic component, with ϕ_1 fixed, can be obtained by further differentiation:

$$\ddot{\overline{\Delta\phi}}_3 = \frac{d}{dt}(\dot{\overline{\Delta\phi}}_3) = 2\sin\alpha[\eta_2(\phi_1)\cos\phi_{32}\bar{i}_1 + \eta_{32}(\phi_1)\bar{j}_1 + \eta_2(\phi_1)\sin\phi_{32}\bar{k}_1]\ddot{q} \qquad (A.23)$$

c. Elastic Angular Velocity and Acceleration of the Coupler

The total elastic angular velocity and acceleration of the coupler are represented by the respective sums of the rigid and elastic body components involved. Thus,

$$\dot{\bar{\phi}}_{3e} = \dot{\bar{\phi}}_{3r} + \dot{\overline{\Delta\phi}}_3 \qquad (A.24)$$

where $\dot{\overline{\Delta\phi}}_3$ is given by equation (A.22) and the rigid body angular velocity may be expressed in either of the two body fixed coordinate systems:

$$\dot{\bar{\phi}}_{3r} = (\dot{\phi}_{2r}\bar{i}_0 + \dot{\phi}_{32r}\bar{j}_1) = G_1\bar{i}_1 + G_2\bar{j}_1 + G_3\bar{k}_1 = H_1\bar{i}_2 + H_2\bar{j}_2 + H_3\bar{k}_2 \qquad (A.25)$$

where

$$\begin{aligned} G_1(\phi_1) &= \dot{\phi}_{2r}\cos\phi_{32r} & H_1(\phi_1) &= \dot{\phi}_{2r}\cos 2\alpha\cos\phi_{32r} + \dot{\phi}_{32r}\sin 2\alpha \\ G_2(\phi_1) &= \dot{\phi}_{32r} & H_2(\phi_1) &= -\dot{\phi}_{2r}\sin 2\alpha\cos\phi_{32r} + \dot{\phi}_{32r}\cos 2\alpha \\ G_3(\phi_1) &= \dot{\phi}_{2r}\sin\phi_{32r} & H_3(\phi_1) &= \dot{\phi}_{2r}\sin\phi_{32r} \end{aligned} \qquad (A.26)$$

The derivative of equation (A.24) gives the elastic angular acceleration of the coupler, i.e.

$$\bar{\ddot{\phi}}_{3e} = \bar{\ddot{\phi}}_{3r} + \overline{\Delta\ddot{\phi}}_3 \qquad (A.27)$$

with $\overline{\Delta\ddot{\phi}}_3$ given by equation (A.23). The rigid body angular acceleration of the coupler may again be expressed in two ways:

$$\bar{\ddot{\phi}}_{3r} = \frac{d}{dt}(\bar{\dot{\phi}}_{3r}) = \dot{G}_1\bar{i}_1 + \dot{G}_2\bar{j}_1 + \dot{G}_3\bar{k}_1 = \dot{H}_1\bar{i}_2 + \dot{H}_2\bar{j}_2 + \dot{H}_3\bar{k}_2 \qquad (A.28)$$

where

$$\begin{aligned} \dot{G}_1(\phi_1) &= \ddot{\phi}_{2r}\cos\phi_{32r} - \dot{\phi}_{2r}\dot{\phi}_{32r}\sin\phi_{32r} & \dot{H}_1(\phi_1) &= \dot{G}_1(\phi_1)\cos 2\alpha + \dot{G}_2(\phi_1)\sin 2\alpha \\ \dot{G}_2(\phi_1) &= \ddot{\phi}_{32r} & \dot{H}_2(\phi_1) &= -\dot{G}_1(\phi_1)\sin 2\alpha + \dot{G}_2(\phi_1)\cos 2\alpha \\ \dot{G}_3(\phi_1) &= \ddot{\phi}_{2r}\sin\phi_{32r} + \dot{\phi}_{2r}\dot{\phi}_{32r}\cos\phi_{32r} & \dot{H}_3(\phi_1) &= \dot{G}_3(\phi_1) \end{aligned} \qquad (A.29)$$

d. Kinematics of Points on Elastic Coupler

The following furnishes expressions for the position, the velocity and the acceleration vectors of arbitrary points P_1 and P_2 on sections 1 and 2 of the coupler, respectively. These vectors are composed of both rigid body and elastic components and are given in inertial terms.

(1) Position vectors

The position vector of point P_1 with respect to origin O_1 is given by:

$$\bar{r}_{P_1} = \bar{r}_A + x_1\bar{i}_1 + \bar{d}_1 \qquad (A.30)$$

For $\bar{d}_1$ see equation (6), while

$$\bar{r}_A = a_1(\cos\phi_1\bar{j}_o + \sin\phi_1\bar{k}_o) \qquad (A.31)$$

Similarly, the position vector of point P_2 with respect to O_1 is given by:

$$\bar{r}_{P_2} = \bar{r}_A + L\bar{i}_1 + x_2\bar{i}_2 + \bar{d}_2 \qquad (A.32)$$

For $\bar{d}_2$ see equation (7).

(2) Velocity vectors

The derivatives of the position vectors $\bar{r}_{p1}$ and $\bar{r}_{p2}$ with respect to time furnish the following velocity vectors:

$$\dot{\bar{r}}_{P_1} = \dot{\bar{r}}_A + \dot{\bar{d}}_1 + \dot{\bar{\phi}}_{3\epsilon} \times (x_1\bar{i}_1 + \bar{d}_1) \qquad (A.33)$$

and

$$\dot{\bar{r}}_{P_2} = \dot{\bar{r}}_A + \dot{\bar{d}}_2 + \dot{\bar{\phi}}_{3\epsilon} \times (L\bar{i}_1 + x_2\bar{i}_2 + \bar{d}_2) \qquad (A.34)$$

(3) Acceleration vectors

The differentiation of the velocity vectors $\dot{\bar{r}}_{p1}$ and $\dot{\bar{r}}_{p2}$ with respect to time furnishes the following acceleration vectors:

$$\ddot{\bar{r}}_{P_1} = \ddot{\bar{r}}_A + \ddot{\bar{d}}_1 + \ddot{\bar{\phi}}_{3\epsilon} \times (x_1\bar{i}_1 + \bar{d}_1) + \dot{\bar{\phi}}_{3\epsilon} \times [\dot{\bar{\phi}}_{3\epsilon} \times (x_1\bar{i}_1 + \bar{d}_1)] + 2\dot{\bar{\phi}}_{3\epsilon} \times \dot{\bar{d}}_1 \qquad (A.35)$$

and

$$\ddot{\bar{r}}_{P_2} = \ddot{\bar{r}}_A + \ddot{\bar{d}}_2 + \ddot{\bar{\phi}}_{3\epsilon} \times (L\bar{i}_1 + x_2\bar{i}_2 + \bar{d}_2) + \dot{\bar{\phi}}_{3\epsilon} \times [\dot{\bar{\phi}}_{3\epsilon} \times (L\bar{i}_1 + x_2\bar{i}_2 + \bar{d}_2)] + 2\dot{\bar{\phi}}_{3\epsilon} \times \dot{\bar{d}}_2 \qquad (A.36)$$

After substituting the various terms, expressed in appropriate body fixed coordinate systems, into the above two equations, computing the cross products and neglecting the

non-linear terms involving various product combinations of q and its derivatives, one obtains the following expressions for the acceleration vectors:

$$\begin{aligned}\ddot{\bar{r}}_{P_1} = &\{[a_1\dot{\phi}_1^2\cos(\phi_1-\phi_{2r})\sin\phi_{32r} - x_1(G_2^2+G_3^2)] + [V_1(G_1G_2-\dot{G}_3)]q - [2x_1\dot{\sin}\alpha(G_2\eta_{32} + \\ &+ G_3\eta_2\sin\phi_{32r}) + 2V_1G_3]\dot{q}\}\bar{i}_1 + \{[a_1\dot{\phi}_1^2\sin(\phi_1-\phi_{2r}) + x_1(G_1G_2+\dot{G}_3)] - [V_1(G_1^2 + \\ &+G_3^2)]q + 2x_1\sin\alpha(G_1\eta_{32} + G_2\eta_2\cos\phi_{32r})]\dot{q} + [V_1 + 2x_1\eta_2\sin\alpha\sin\phi_{32r}]\ddot{q}\}\bar{j}_1 + \\ &+ \{[-a_1\dot{\phi}_1^2\cos(\phi_1-\phi_{2r})\cos\phi_{32r} + x_1(G_1G_3-\dot{G}_2)] + [V_1(G_2G_3+\dot{G}_1)]q + [2V_1G_1 + \\ &+ 2x_1\sin\alpha(G_1\eta_2\sin\phi_{32r} + G_3\eta_2\cos\phi_{32r})]\dot{q} - [2x_1\eta_{32}\sin\alpha]\ddot{q}\}\bar{k}_1 \qquad (A.37)\end{aligned}$$

and

$$\begin{aligned}\ddot{\bar{r}}_{P_2} = &\{[a_1\dot{\phi}_1^2\sin 2\alpha\sin(\phi_1-\phi_{2r}) + a_1\dot{\phi}_1^2\cos 2\alpha\sin\phi_{32r}\cos(\phi_1-\phi_{2r}) + (\dot{H}_3 - H_1H_2)L\sin 2\alpha - \\ &- (H_2^2+H_3^2)(L\cos 2\alpha + x_2)] + [(H_1H_2 - \dot{H}_3)V_2 - (H_2^2+H_3^2)\sin 2\alpha]q - [2V_2H_3 - \\ &- 4x_2H_2\eta_2\sin\alpha\sin 2\alpha\cos\phi_{32r} + 2H_2\eta_{32}\sin\alpha(L + 2x_2\cos 2\alpha) + 4H_3\eta_2\sin\alpha\sin\phi_{32r}\cdot \\ &\cdot(L\cos 2\alpha + x_2) + 2\sin\alpha(LH_1\sin 2\alpha + LH_2\cos 2\alpha)(\eta_{32}\cos 2\alpha - \eta_2\sin 2\alpha\cos\phi_{32r})]\dot{q} + \\ &+ [\sin 2\alpha(1 + 2L\eta_2\sin\alpha\sin\phi_{32r}]\ddot{q}\}\bar{i}_2 + \{[a_1\dot{\phi}_1^2\cos 2\alpha\sin(\phi_1-\phi_{2r}) - a_1\dot{\phi}_1^2\sin 2\alpha\cdot \\ &\cdot\sin\phi_{32r}\cos(\phi_1-\phi_{2r}) + (\dot{H}_3 + H_1H_2)(L\cos 2\alpha + x_2) + (H_1^2+H_3^2)L\sin 2\alpha] + [(\dot{H}_3 + \\ &+ H_1H_2)\sin 2\alpha - (H_1^2+H_3^2)V_2]q + [2H_3\sin 2\alpha + 2H_1\eta_{32}\sin\alpha(L + x_2\cos 2\alpha) - 2H_1\eta_2\cdot \\ &\cdot x_2\sin\alpha\sin 2\alpha\cos\phi_{32r} + 4LH_3\eta_2\sin\alpha\sin 2\alpha\sin\phi_{32r} + 2\sin\alpha(\eta_2\cos 2\alpha\cos\phi_{32r} + \\ &+ \eta_{32}\sin 2\alpha)(LH_1\sin 2\alpha + LH_2\cos 2\alpha + x_2H_2)]\dot{q} + [V_2 + 2\eta_2\sin\alpha\sin\phi_{32r}(L\cos 2\alpha + \\ &+ x_2)]\ddot{q}\}\bar{j}_2 + \{[-a_1\dot{\phi}_1^2\cos\phi_{32r}\cos(\phi_1-\phi_{2r}) - (H_2H_3 + \dot{H}_1)L\sin 2\alpha + (H_1H_3 - \dot{H}_2)\cdot \\ &\cdot(L\cos 2\alpha + x_2)] + [(H_1H_3 - \dot{H}_2)\sin 2\alpha + (H_2H_3 + \dot{H}_1)V_2]q + [2H_1V_2 - 2H_2\sin 2\alpha + \\ &+ 2\eta_2\sin\alpha\sin\phi_{32r}(LH_1\cos 2\alpha + H_1x_2 - LH_2\sin 2\alpha) + 2H_3\sin\alpha(\eta_2\cos 2\alpha\cos\phi_{32r} + \\ &+ \eta_{32}\sin 2\alpha)(L\cos 2\alpha + x_2) + 2LH_3\sin\alpha\sin 2\alpha(\eta_2\sin 2\alpha\cos\phi_{32r} - \eta_{32}\cos 2\alpha)]\dot{q} - \\ &- [2\sin\alpha(L\eta_{32} + x_2\eta_{32}\cos 2\alpha - x_2\eta_2\sin 2\alpha\cos\phi_{32r})]\ddot{q}\}\bar{k}_2 \qquad (A.38)\end{aligned}$$

e. Virtual Displacement of Points on Elastic Coupler

The virtual displacements of points P_1 and P_2 can be obtained by taking the variations of position vectors $\bar{r}_{P_1}$ and $\bar{r}_{P_2}$ of equations (A.30) and (A.31):

$$\delta\bar{r}_{P_1} = \delta\bar{d}_1 + \delta\bar{\phi}_{3e} \times (x_1\bar{i}_1 + \bar{d}_1) \tag{A.39}$$

and

$$\delta\bar{r}_{P_2} = \delta\bar{d}_2 + \delta\bar{\phi}_{3e} \times (L\bar{i}_1 + x_2\bar{i}_2 + \bar{d}_2) \tag{A.40}$$

The substitution of equation (5) for $\bar{d}_1$, equation (7) for $\bar{d}_2$ and equation (A.20) for $\delta\bar{\phi}_{3e}$ into equations (A.39) and (A.40) as needed, together with the appropriate coordinate transformations, leads to the following expressions:

$$\begin{aligned}\delta\bar{r}_{P_1} = &[-(2q\eta_2 V_1 \sin\alpha \sin\phi_{32r})\bar{i}_1 + (2x_1\eta_2 \sin\alpha \sin\phi_{32r} + V_1)\bar{j}_1 + \\ &+ (2q\eta_2 V_1 \sin\alpha \cos\phi_{32r} - 2x_1\eta_{32} \sin\alpha)\bar{k}_1]\delta q\end{aligned} \tag{A.41}$$

and

$$\begin{aligned}\delta\bar{r}_{P_2} = &\{[\sin 2\alpha(1 + 2L\eta_2 \sin\alpha \sin\phi_{32r}) - 2q\eta_2 V_2 \sin\alpha \sin\phi_{32r}]\bar{i}_2 + [V_2 + \\ &+ 2\eta_2 \sin\alpha \sin\phi_{32r}(L\cos 2\alpha + x_2) + 2q\eta_2 \sin\alpha \sin 2\alpha \sin\phi_{32r}]\bar{j}_2 + \\ &+ [2x_2 \sin\alpha(\eta_2 \sin 2\alpha \cos\phi_{32r} - \eta_{32}\cos 2\alpha) - 2L\eta_{32}\sin\alpha + 2q\sin\alpha \cdot \\ &\cdot (\eta_2 V_2 \cos 2\alpha \cos\phi_{32r} + \eta_{32} V_2 \sin 2\alpha + \eta_2 \sin^2 2\alpha \cos\phi_{32r} - \\ &- \eta_{32} \sin 2\alpha \cos 2\alpha)]\bar{k}_2\}\delta q\end{aligned} \tag{A.42}$$

APPENDIX B. DERIVATION OF EQUATIONS OF MOTION FOR REGIME NO.2

a. Kinetic Energy of System and Its Variation

The kinetic energy T of the system is the sum of all the kinetic energies of the rigid and elastic links, the clutch assembly and the material being fed. Since motion of the input link is prescribed, its kinetic energy has zero variation. Thus, the kinetic energy of the remaining system has the form:

$$T = \frac{1}{2}\left[J_{o4}(\dot{\bar{\phi}}_{4c})^2 + J_{o5}(\dot{\bar{\phi}}_5)^2\right] + \frac{1}{2}\rho A\left[\int_0^L (\dot{\bar{r}}_{P_1}\cdot\dot{\bar{r}}_{P_1})dx_1 + \int_0^L (\dot{\bar{r}}_{P_2}\cdot\dot{\bar{r}}_{P_2})dx_2\right] \qquad (B.1)$$

where

J_{o4} = the combined moment of inertia of the rocker and the outer race of the clutch with respect to their axis of rotation.

J_{o5} = the combined moment of inertia of the inner race of the clutch, the output shaft assembly and the referred moment of inertia of the material strip with respect to axis of rotation of the output shaft.

The variation of the integral of this kinetic energy gives the following:

$$\delta\int_{t_0}^{t_1} T dt = -\int_{t_0}^{t_1}\left[J_{o4}\dot{\bar{\phi}}_{4c}\cdot\delta\bar{\phi}_{4c} + J_{o5}\dot{\bar{\phi}}_5\cdot\delta\bar{\phi}_5 + \int_0^L \rho A\,\dot{\bar{r}}_{P_1}\cdot\delta\bar{r}_{P_1}dx_1 + \int_0^L \rho A\,\dot{\bar{r}}_{P_2}\cdot\delta\bar{r}_{P_2}dx_2\right]dt \qquad (B.2)$$

b. Potential Energy of System and Its Variation

The potential energy V of the system consists of the strain energy of the elastic coupler and the potential energy associated with the spring of the sprag clutch (see equation (1)). Thus,

$$V = \frac{1}{2}EI\left[\int_0^L \left(\frac{\partial^2 v_1}{\partial x_1^2}\right)^2 dx_1 + \int_0^L \left(\frac{\partial^2 v_2}{\partial x_2^2}\right)^2 dx_2\right] + \int_0^{\phi_5-\phi_{4e}} K_{sp}(\phi_5-\phi_{4e})^{3/2} d(\phi_5-\phi_{4e}) \qquad (B.3)$$

where EI is the product of the modulus of elasticity of the coupler and the area moment of inertia with respect to any centroidal axis of the tubular cross section of the coupler. K_{sp} is the stiffness constant of the non-linear spring of the sprag clutch.

After substituting the deflections v_1 and v_2, according equations (3) and (4), into the above equation, the potential energy becomes:

$$V = \frac{EI}{2L^3}\left(\frac{\pi}{2}\right)^4 q^2 + \frac{2}{5}K_{sp}(\phi_5-\phi_{4e})^{5/2} \qquad (B.4)$$

Taking variation of the integral of this potential energy, one obtains:

$$\delta\int_{t_0}^{t_1} V dt = \int_{t_0}^{t_1}\left[\frac{EI}{L^3}\left(\frac{\pi}{2}\right)^4 q\delta q + K_{sp}(\phi_5-\phi_{4e})^{3/2}\delta\phi_5 - K_{sp}(\phi_5-\phi_{4e})^{3/2}\delta\phi_{4e}\right]dt \qquad (B.5)$$

c. Virtual Work Done by Non-Conservative Forces

The non-conservative forces in the system are the assumed viscous damping forces in both the coupler and the sprag clutch as well as the combined resisting friction force due to the brake and feeding table. The integral of the virtual work of these forces is found as:

$$\delta\int_{t_0}^{t_1} W dt = \int_{t_0}^{t_1}\left[-\int_0^L C_{co}\frac{\partial v_1}{\partial t}\delta v_1 dx_1 - \int_0^L C_{co}\frac{\partial v_2}{\partial t}\delta v_2 dx_2 + T_b\delta\phi_5 - C_{sp}(\dot{\phi}_5-\dot{\phi}_{4e})\delta(\phi_5-\phi_{4e})\right]dt \qquad (B.6)$$

where C_{co} and C_{sp} are the coefficients of damping for the coupler and the sprag clutch, respectively. T_b is the total resisting torque exerted on the clutch output shaft. With the expressions of coupler deflections v_1 and v_2, the above expression becomes:

$$\delta\int_{t_0}^{t_1} W dt = \int_{t_0}^{t_1}[-(3-8/\pi)LC_{co}\dot{q}\delta q + T_b\delta\phi_5 - C_{sp}(\dot{\phi}_5 - \dot{\phi}_{4c})\delta(\phi_5 - \phi_{4c})]dt \qquad (B.7)$$

d. Working Form of Hamilton's Integral

The working form of Hamilton's integral is obtained by the substitution of the accelerations $\ddot{\bar{r}}_{p_1}$ and $\ddot{\bar{r}}_{p_2}$ of points on the coupler, given by equations (A.36) and (A.37), and the virtual displacements $\delta\bar{r}_{p_1}$ and $\delta\bar{r}_{p_2}$ of points on the coupler, given by equations (A.40) and (A.41), together with $\delta\bar{\phi}_{4c}$ of equation (A.21), into Hamilton's integral of equation (11). After the dot products are computed, one obtains:

$$\int_{t_0}^{t_1} \Big\{ [J_{o5}\ddot{\phi}_5 + C_{sp}(\dot{\phi}_5 - \dot{\phi}_{4c}) + K_{sp}(\phi_5 - \phi_{4c})^{3/2} - T_b]\delta\phi_5 + \{[0.45LC_{co}]\dot{q} + [\frac{EI\pi^4}{L^3 2^4}]q -$$

$$-2\eta_4\sin\alpha[K_{sp}(\phi_5 - \phi_{4c})^{3/2} + C_{sp}(\dot{\phi}_5 - \dot{\phi}_{4c}) - J_{4o}\ddot{\phi}_{4c}]\}\delta q + \rho A\int_0^L \Big[\{[a_1\dot{\phi}_1^2\cos(\phi_1 - \phi_{2r})\cdot$$

$$\cdot\sin\phi_{32r} - x_1(G_2^2 + G_3^2)] + [V_1(G_1G_2 - \dot{G}_3)]q - [4x_1\sin\alpha(G_2\eta_{32} + G_3\eta_2\sin\phi_{32r}) + 2V_1G_3]\dot{q}\}\cdot$$

$$\cdot(-2q\eta_2V_1\sin\alpha\sin\phi_{32r}) + \{[a_1\dot{\phi}_1^2\sin(\phi_1 - \phi_{2r}) + x_1(G_1G_2 + \dot{G}_3)] - [V_1(G_1^2 + G_3^2)]q +$$

$$+[2x_1\sin\alpha(G_1\eta_{32} + G_2\eta_2\cos\phi_{32r})]\dot{q} + [V_1 + 2x_1\eta_2\sin\alpha\sin\phi_{32r}]\ddot{q}\}(2x_1\eta_2\sin\alpha\sin\phi_{32r} +$$

$$+V_1) + \{[-a_1\dot{\phi}_1^2\cos(\phi_1 - \phi_{2r})\cos\phi_{32r} + x_1(G_1G_3 - \dot{G}_2)] + [V_1(G_2G_3 + \dot{G}_1)]q + [2V_1G_1 +$$

$$+2x_1\sin\alpha(G_1\eta_2\sin\phi_{32r} + G_3\eta_2\cos\phi_{32r})]\dot{q} - [2x_1\eta_{32}\sin\alpha]\ddot{q}\}(2q\eta_2V_1\sin\alpha\cos\phi_{32r} -$$

$$-2x_1\eta_{32}\sin\alpha\Big]\delta q dx_1 + \rho A\int_0^L \Big[\{[a_1\dot{\phi}_1^2\sin\alpha\sin(\phi_1 - \phi_{2r}) + a_1\dot{\phi}_1^2\cos\alpha\sin\phi_{32r}\cdot$$

(continue)

$$\cdot\cos(\phi_1-\phi_{2'})+(\dot{H}_3-H_1H_2)Lsin2\alpha-(H_2^2+H_3^2)(L\cos2\alpha+x_2)]+[(H_1H_2-\dot{H}_3)V_2-(H_2^2+$$

$$+H_3^2)\sin2\alpha]q-[2V_2H_3+4x_2H_2\eta_2\sin\alpha\sin2\alpha\cos\phi_{32'}+2H_2\eta_{32}\sin\alpha(L+2x_2\cos2\alpha)+$$

$$+4H_3\eta_2\sin\alpha\sin\phi_{32'}(Lcos2\alpha+x_2)+2\sin\alpha(LH_1\sin2\alpha+LH_2\cos2\alpha)(\eta_{32}\cos2\alpha-$$

$$-\eta_2\sin2\alpha\cos\phi_{32'})]\dot{q}+[\sin2\alpha(1+2L\eta_2\sin\alpha\sin\phi_{32'}]\ddot{q}\}\ [\sin2\alpha(1+2L\eta_2\sin\alpha\sin\phi_{32'})-$$

$$-2q\eta_2V_2\sin\alpha\sin\phi_{32'}]\quad+\quad\{[a_1\dot{\phi}_1^2\cos2\alpha\sin(\phi_1-\phi_{2'})-a_1\dot{\phi}_1^2\sin2\alpha\sin\phi_{32'}\cos(\phi_1-\phi_{2'})+$$

$$+(\dot{H}_3+H_1H_2)(L\cos2\alpha+x_2)+(H_1^2+H_3^2)L\sin2\alpha]+[(\dot{H}_3+H_1H_2)\sin2\alpha-(H_1^2+H_3^2)V_2]q+$$

$$+[2H_3\sin2\alpha+2H_1\eta_{32}\sin\alpha(L+x_2\cos2\alpha)-2H_1\eta_2x_2\sin\alpha\sin2\alpha\cos\phi_{32'}+4LH_3\cdot$$

$$\cdot\eta_2\sin\alpha\sin2\alpha\sin\phi_{32'}+2\sin\alpha(\eta_2\cos2\alpha\cos\phi_{32'}+\eta_{32}\sin2\alpha)(LH_1\sin2\alpha+LH_2\cos2\alpha+$$

$$+x_2H_2)]\dot{q}+[V_2+2\eta_2\sin\alpha\sin\phi_{32'}(Lcos2\alpha+x_2)]\ddot{q}\}\ [V_2+2\eta_2\sin\alpha\sin\phi_{32'}(L\cos2\alpha+x_2)+$$

$$+2q\eta_2\sin\alpha\sin2\alpha\sin\phi_{32'}]\quad+\quad\{[-a_1\dot{\phi}_1^2\cos\phi_{32'}\cos(\phi_1-\phi_{2'})-(H_2H_3+\dot{H}_1)L\sin2\alpha+$$

$$+(H_1H_3-\dot{H}_2)(L\cos2\alpha+x_2)]+[(H_1H_3-\dot{H}_2)\sin2\alpha+(H_2H_3+\dot{H}_1)V_2]q+[2H_1V_2-$$

$$-2H_2\sin2\alpha+2\eta_2\sin\alpha+2\eta_2\sin\alpha\sin\phi_{32'}(LH_1\cos2\alpha+H_1x_2-LH_2\sin2\alpha)+2H_3\sin\alpha\cdot$$

$$\cdot(\eta_2\cos2\alpha\cos\phi_{32'}+\eta_{32}\sin2\alpha)(L\cos2\alpha+x_2)+2LH_3\sin\alpha\sin2\alpha(\eta_2\sin2\alpha\cos\phi_{32'}-$$

$$-\eta_{32}\cos2\alpha)]\dot{q}-[2\sin\alpha(L\eta_{32}+x_2\eta_{32}\cos2\alpha-x_2\eta_2\sin2\alpha\cos\phi_{32'})]\ddot{q}\}\ [2x_2\sin\alpha(\eta_2\sin2\alpha\cdot$$

$$\cdot\cos\phi_{32'}-\eta_{32}\cos2\alpha)-2L\eta_{32}\sin\alpha+2q\sin\alpha(\eta_2V_2\cos2\alpha\cos\phi_{32'}+\eta_{32}V_2\sin2\alpha+$$

$$+\eta_2\sin^2 2\alpha\cos\phi_{32'}-\eta_{32}\sin2\alpha\cos2\alpha)]\ \Big]\ \delta qdx_2\ \Big\}\ dt\ =\ 0 \qquad (B.8)$$

In order for the above integral to vanish, the coefficients of $\delta\phi_5$ and δq must be equal to zero, respectively. This furnishes two equations, one of which contains integrals in terms of x_1 and x_2.

e. Final Form of Equations of Motion for Regime No.2

In order to obtain the final form of the equations of motion of Regime No.2, the following integrations of the functions V_1 and V_2, associated with the deflected coupler shape and given by equations (6) and (8), must be performed:

$$V_{s1} = \frac{1}{L}\int_0^L V_1 dx_1 = 2/\pi \qquad (B.9)$$

$$V_{s2} = \frac{1}{L}\int_0^L V_2 dx_2 = \cos 2\alpha - 1 + 2/\pi \qquad (B.10)$$

$$V_{2s1} = \frac{1}{L}\int_0^L V_1^2 dx_1 = 1/2 \qquad (B.11)$$

$$V_{2s2} = \frac{1}{L}\int_0^L V_2^2 dx_2 = \cos^2 2\alpha - (2 - 4/\pi)\cos 2\alpha + (3/2 - 4/\pi) \qquad (B.12)$$

$$V_{s1x} = \frac{1}{L^2}\int_0^L x_1 V_1 dx_1 = (2/\pi)^2 \qquad (B.13)$$

$$V_{s2x} = \frac{1}{L^2}\int_0^L x_2 V_2 dx_2 = 1/2(\cos 2\alpha - 1) - 4/\pi^2 + 2/\pi \qquad (B.14)$$

Only keeping the linear terms in q and its derivatives because of the assumption of small deflections, one obtains the following two equations of motion for the feed mechanism:

$$\rho A[(V_{2s1} + V_{2s2} + \sin^2 2\alpha)L + P_1(\phi_1)]\ \ddot{q} + [0.45LC_{co} + \rho A P_2(\phi_1)]\ \dot{q} + [(\pi^4 EI)/(2^4 L^3) +$$
$$+ \rho A P_3(\phi_1)]\ q = \rho A F_1(\phi_1) + [K_{sp}(\phi_5 - \phi_{4c})^{3/2} + C_{sp}(\dot{\phi}_5 - \dot{\phi}_{4c}) - J_{o4}\ddot{\phi}_{4c}]F_2(\phi_1) \qquad (B.15)$$

and

$$J_{o5}\ddot{\phi}_5 + C_{sp}(\dot{\phi}_5 - \dot{\phi}_{4c}) + K_{sp}(\phi_5 - \phi_{4c})^{3/2} = T_b \qquad (B.16)$$

where the input angle dependent functions are defined by:

$$P_1(\phi_1) = [4L^2 \sin\alpha \sin\phi_{32r}(V_{s1x} + V_{s2x} + \sin^2 2\alpha + V_{s2}\cos 2\alpha)]\eta_2(\phi_1) + [L^3(2\sin\alpha\sin\phi_{32r})^2$$
$$(5/3 + \cos 2\alpha)]\eta_2^2(\phi_1) + [(2\sin\alpha)^2 L^3(4/3 + \cos 2\alpha + 1/3\cos^2 2\alpha)]\eta_{32}^2(\phi_1) +$$
$$+ [-\sin\alpha \sin 2\alpha \cos\phi_{32r} L^3(1 + 2/3\cos 2\alpha)]\eta_2(\phi_1)\eta_{32}(\phi_1) \qquad (B.17)$$

$$P_2(\phi_1) = L^2[2\sin\alpha\cos\phi_{32r}V_{s1x}G_2 + 2\sin\alpha\sin 2\alpha(H_1V_{s2x} - 1/2H_2\sin 2\alpha)\cos\phi_{32r} +$$
$$+ 2\sin\alpha[H_1\sin 2\alpha\cos\phi_{32r}(\sin^2 2\alpha + V_{s2}\cos 2\alpha) + H_2\cos\phi_{32r}(\sin^2 2\alpha\cos 2\alpha +$$
$$+ 1/2\sin^2 2\alpha + V_{s2}\cos^2 2\alpha + V_{s2x}\cos 2\alpha)]]\eta_2(\phi_1) + L^2 2\sin\alpha[H_2\sin 2\alpha(1 +$$
$$+ 1/2\cos 2\alpha) - H_1(V_{s2} + V_{s2x}\cos 2\alpha) - G_1V_{s1x} + H_1\sin^2 2\alpha(V_{s2} - \cos 2\alpha) +$$
$$+ H_2\sin 2\alpha(V_{s2x} + V_{s2}\cos 2\alpha - \cos^2 2\alpha - 1/2\cos 2\alpha)]\eta_{32}(\phi_1) + 4L^3\sin^2\alpha\cos\phi_{32r} \cdot$$
$$\cdot[1/3G_2\sin\phi_{32r} + H_1\sin 2\alpha\sin\phi_{32r} + H_2\sin\phi_{32}(1/2\cos^2 2\alpha + 4/3\cos 2\alpha +$$
$$+ 1/2) + H_3\sin 2\alpha\cos\phi_{32r}(1/2 + 1/3\cos 2\alpha)]\eta_2^2(\phi_1) + L^3[-4/3G_3\sin^2\alpha\cos\phi_{32r} +$$
$$+ 2\sin\alpha[H_1\sin\alpha\sin\phi_{32r}\sin^2 2\alpha + H_2\sin\alpha\sin 2\alpha\sin\phi_{32r}(\cos 2\alpha + 2/3) -$$
$$- 2H_3\sin\alpha\cos\phi_{32r}(2/3 + 2/3\cos^2 2\alpha + \cos 2\alpha)]]\eta_2(\phi_1)\eta_{32}(\phi_1) + L^3[-4\sin^2\alpha \cdot$$
$$\cdot\sin 2\alpha H_3(1/2 + 1/3\cos 2\alpha)]\eta_{32}^2(\phi_1) \qquad (B.18)$$

$$P_3(\phi_1) = -L[-(G_1^2+G_3^2)V_{2s1}+2H_1H_2V_{s2}\sin 2\alpha - H_1^2V_{2s2} - H_2^2\sin^2 2\alpha - H_3^2(\sin^2 2\alpha + V_{2s2})] +$$

$$+L[-2a_1\dot{\phi}_1^2V_{s1}\sin\alpha\cos(\phi_1-\phi_{2r}) + 2LV_{s1x}(G_2^2-G_1^2)\sin\alpha\sin\phi_{32r} + 2LV_{s1x}(G_1G_3 -$$

$$-\dot{G}_2)\sin\alpha\cos\phi_{32r} + 2a_1\dot{\phi}_1^2\sin(\phi_1-\phi_{2r})\sin\alpha\sin 2\alpha\sin\phi_{32r}(\cos 2\alpha - V_{s2}) - 2a_1\dot{\phi}_1^2\cdot$$

$$\cdot\sin\alpha\cos(\phi_1-\phi_{2r})(V_{s2}\cos 2\alpha + \sin^2 2\alpha) + 2L(H_1H_2+\dot{H}_3)\sin\alpha\sin 2\alpha\sin_{32r}\cdot$$

$$\cdot(2\cos 2\alpha + 1) + 4LV_{s2}(H_1H_2-\dot{H}_3)\sin\alpha\sin 2\alpha\sin\phi_{32r} + 2L(H_1^2-H_2^2)(\sin^2\alpha -$$

$$-V_{s2}\cos 2\alpha - V_{s2x})\sin\alpha\sin\phi_{32r} + 2L(H_2H_3+\dot{H}_1)(V_{s2x}-V_{s2}\cos 2\alpha - \sin^2 2\alpha)\sin\alpha\cdot$$

$$\cdot\sin 2\alpha\cos\phi_{32r} + 2L(H_1H_3-\dot{H}_2)(V_{s2}\cos^2 2\alpha + V_{s2x}\cos 2\alpha + \sin^2\alpha + \cos\alpha\sin^2 2\alpha)\cdot$$

$$\cdot\sin\alpha\cos\phi_{32r}]\eta_2(\phi_1) + L[-2LV_{s1x}(\dot{G}_1+G_2G_3)\sin\alpha + 2a_1\dot{\phi}_1^2\cos(\phi_1-\phi_{2r})\sin\alpha\cdot$$

$$\cdot\sin 2\alpha\cos\phi_{32r}(\cos 2\alpha - V_{s2}) + 2L\sin\alpha(H_2H_3+\dot{H}_1)(\cos 2\alpha\sin^2 2\alpha - V_{s2}\sin^2 2\alpha -$$

$$-V_{s2} - V_{s2x}\cos 2\alpha) + 2L\sin\alpha\sin 2\alpha(H_1H_3-\dot{H}_2)(V_{s2}\cos 2\alpha + V_{s2x} - \cos^2 2\alpha -$$

$$-\cos 2\alpha - 1)]\eta_{32}(\phi_1) \qquad (B.19)$$

$$F_1(\phi_1) = -\{L[a_1\dot{\phi}_1^2 V_{s1}\sin(\phi_1-\phi_{2r}) + LV_{s1x}(\dot{G}_3+G_1G_2) + a_1\dot{\phi}_1^2\sin(\phi_1-\phi_{2r})\cdot$$

$$\cdot(\sin^2 2\alpha + V_{s2}\cos 2\alpha) + a_1\dot{\phi}_1^2\cos(\phi_1-\phi_{2r})(\cos 2\alpha - V_{s2})\sin 2\alpha\sin\phi_{32r} +$$

$$+ L\sin^2 2\alpha(\dot{H}_3 - H_1H_2) + L(\dot{H}_3 + H_1H_2)(V_{s2}\cos 2\alpha + V_{s2x}) + L\sin 2\alpha(H_1^2+H_3^2)\cdot$$

$$\cdot(V_{s2} - \cos 2\alpha - 1/2)] + L^2[a_1\dot{\phi}_1^2\sin(\phi_1-\phi_{2r})\sin\alpha\sin\phi_{32r} + 2/3L(\dot{G}_3 +$$

$$+ G_1G_2)\sin\alpha\sin\phi_{32r} + 2a_1\dot{\phi}_1^2\sin(\phi_1-\phi_{2r})(1+1/2\cos\alpha)\sin\alpha\sin\phi_{32r} -$$

$$- a_1\dot{\phi}_1^2\cos(\phi_1-\phi_{2r})\sin\alpha\sin 2\alpha + 2L\sin\alpha\sin^2 2\alpha\sin\phi_{32r}(\dot{H}_3 - H_1H_2) +$$

$$+ 2L\sin\alpha\sin\phi_{32r}(\dot{H}_3 + H_1H_2)(\cos^2 2\alpha + \cos 2\alpha + 1/3) +$$

$$+ 2L\sin\alpha\sin 2\alpha\sin\phi_{32r}(\cos 2\alpha + 1/2)(H_1^2 - H_2^2) - L\sin\alpha\sin^2 2\alpha\cos\phi_{32r}\cdot$$

$$\cdot(H_2H_3 + \dot{H}_1) + L\sin\alpha\sin 2\alpha\cos\phi_{32r}(H_1H_3 - \dot{H}_2)(\cos 2\alpha + 2/3)]\eta_2(\phi_1) +$$

$$+ L^2[a_1\dot{\phi}_1^2\cos(\phi_1-\phi_{2r})\sin\alpha\cos\phi_{32r} + 2/3L\sin\alpha(\dot{G}_2 - G_1G_3) +$$

$$+ a_1\dot{\phi}_1^2\cos(\phi_1-\phi_{2r})(2+\cos 2\alpha)\sin\alpha\cos\phi_{32r} + L\sin\alpha\sin 2\alpha\cdot$$

$$\cdot(H_2H_3 + \dot{H}_1)(2+\cos 2\alpha) - L\sin\alpha(H_1H_3 - \dot{H}_2)(\cos^2 2\alpha +$$

$$+ 8/3\cos 2\alpha + 1)]\eta_{32}(\phi_1)\} \qquad (B.20)$$

$$F_2(\phi_1) = (2\sin\alpha)\eta_4(\phi_1) \qquad (B.21)$$

APPENDIX C. SIMPLIFICATION OF EQUATIONS OF MOTION

a. Linearization of the Clutch Spring For Various Regimes

(1) Operation in Regime No.2

In order to linearize the non-linear (3/2 power) torque-windup angle relationship of the clutch, when it operates in Regime No.2, i.e. "well up the curve", a tangential straight line approximation is assumed. To this end, a tangent is drawn to the curve at a given load point $T = T_b$, as shown in Figure C-1. Its slope, which represents the linearized stiffness of the clutch, can be found from:

$$K_{l2} = \left[\frac{d}{d\phi_{5/4}}(K_{sp}\phi_{5/4}^{3/2})\right]_{\phi_{5/4(b)}} = \frac{3}{2}K_{sp}\phi_{5/4(b)}^{1/2} \qquad (C.1)$$

Since the windup angle corresponding to T_b has the form:

$$\phi_{5/4(b)} = (T_b/K_{sp})^{2/3} \qquad (C.2)$$

the linearized stiffness K_{l2} of equation (C.1) becomes:

$$K_{l2} = \frac{3}{2}K_{sp}^{2/3}T_b^{1/3} \qquad (C.3)$$

With the above, any transmitted torque T near T_b is approximated by (see Figure C-1):

$$T = T_b + K_{l2}(\phi_{5/4} - \phi_{5/4(b)}) \qquad (C.4)$$

Substitution of equations (C.2) and (C.3) into equation (C.4) furnishes the following linear torque-windup angle relationship:

$$T = K_{l2}\phi_{5/4} - T_b/2 \qquad (C.5)$$

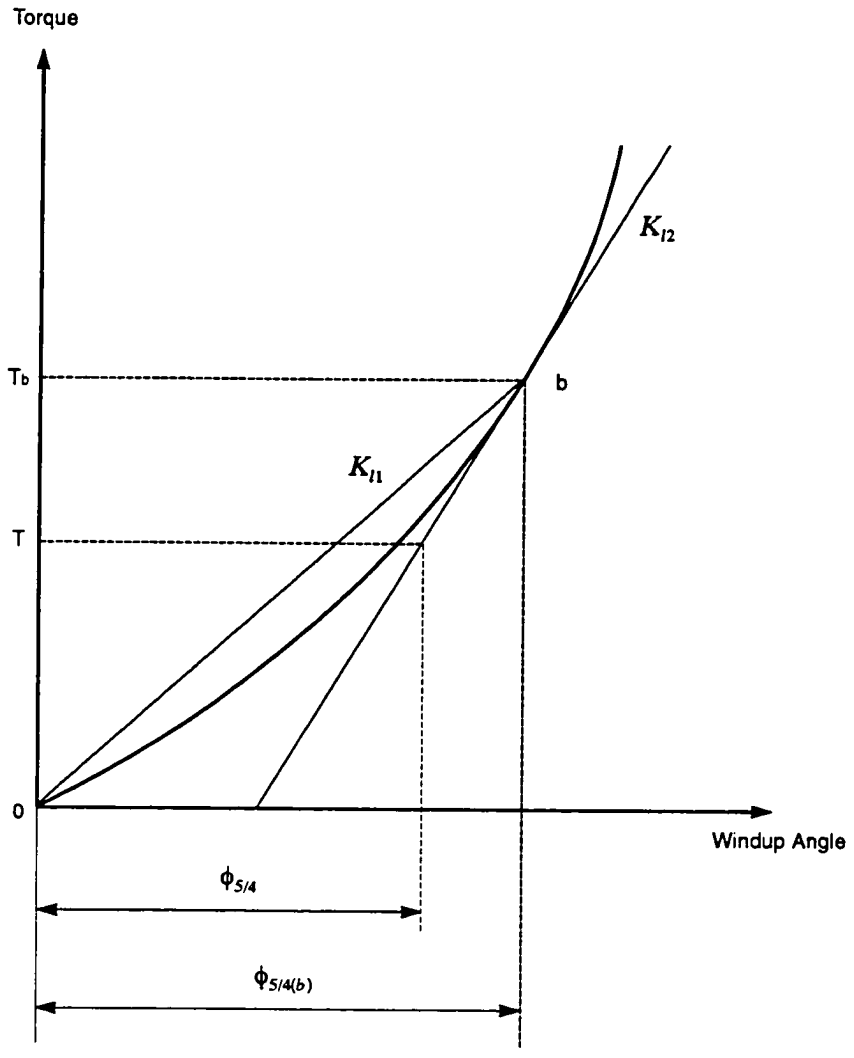

Figure C-1 Linearization of the Clutch Spring for Regimes No.1 and No.2

(2) Operation in Regime No.1

In order to linearize the clutch spring during the windup of Regime No.1, when the torque transmitted by the clutch increases from zero to the load point $T = T_b$, the straight line OB is assumed to replace the original curve (See Figure C-1). Then the torque transmitted at any angle in this regime becomes:

$$T = K_{l1}\phi_{5/4} \qquad (C.6)$$

where the stiffness is given by

$$K_{l1} = T_b/\phi_{5/4(b)} \qquad (C.7)$$

or with the help of equation (C.2):

$$K_{l1} = K_{sp}^{2/3}T_b^{1/3} \qquad (C.8)$$

(3) Operation in Regime No.3

In order to linearize the clutch spring for Regime No.3, when the transmitted torque goes to zero from its final value T_{f2} on the torque line of Regime No.2, one assumes the new straight line relationship

$$T = K_{l3}\phi_{5/4} \qquad (C.9)$$

where

$$K_{l3} = T_{f2}/\phi_{5/4(f2)} = K_{sp}\phi_{5/4(f2)}^{1/2} \qquad (C.10)$$

To this end, it is necessary to know $\phi_{5/4(f2)}$ from the computations of Regime No.2.

b. Simplification of Functions P_1, P_2, P_3 and F_2 (See equations (B.18), (19), (20) and (22))

The simplifications of the subject functions are based on the physical parameters of the standard mechanism as given in table 1.

Figure C-2 shows the magnitudes of these functions, with P_2 and P_3 normalized by way of $\dot{\phi}_1$ and $\dot{\phi}_1^2$, respectively, during the forward stroke, i.e. for $250 \leq \phi_1 \leq 450$.

(1) Function $P_1(\phi_1)$

The function $P_1(\phi_1)$, which is independent of input speed, varies little when compared to its average value of 2.65. Therefore, it will be assumed to have this constant value throughout the forward stroke.

(2) Function $P_2(\phi_1)$

Since every term of $P_2(\phi_1)$ is proportional to the input speed, the comparison with its associated term in equation (12) is made by way of $P_2(\phi_1)/\dot{\phi}_1$. The resulting maximum value of $P_2(\phi_1)/\dot{\phi}_1$ is very small (0.0055) when compared with the term $(0.45LC_{co})/(\dot{\phi}_1 \rho A)$, which has a magnitude greater than 10 for input speeds below 1000 RPM. Thus, $P_2(\phi_1)$ may be neglected.

(3) Function $P_3(\phi_1)$

Since every term of $P_3(\phi_1)$ is proportional to $\dot{\phi}_1^2$, the comparison with its associated term in equation (12) is made by way of $P_3(\phi_1)/\dot{\phi}_1^2$. $P_3(\phi_1)/\dot{\phi}_1^2$ has a maximum absolute value of 0.078. This is very small when compared to the term $(EI\pi^4)/(2^4\dot{\phi}_1^2 L^3 \rho A)$, which has a magnitude greater than 400 for input speeds below 1000 RPM. Therefore, $P_3(\phi_1)$ may also be disregarded.

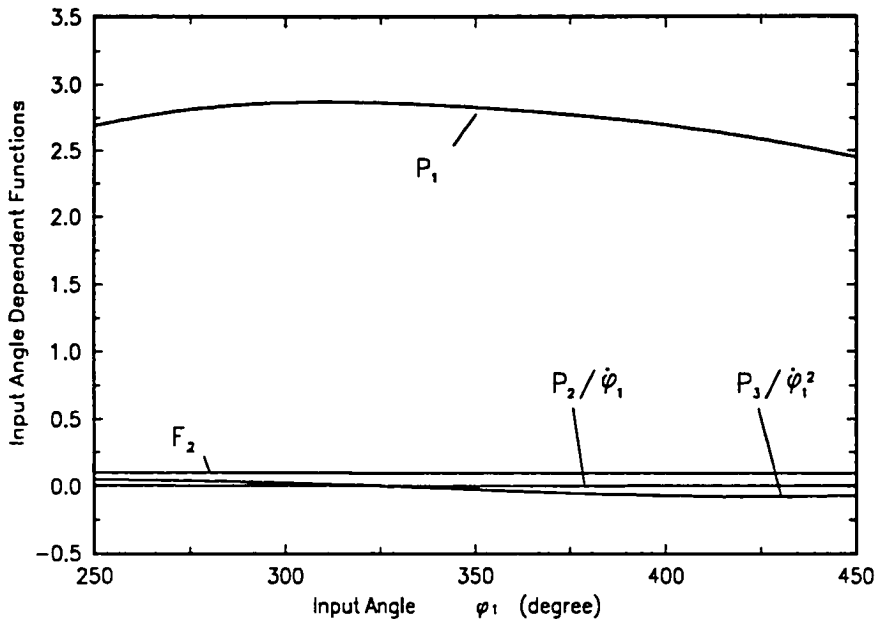

Figure C-2 Magnitudes of Functions P_1, P_2, P_3 and F_2 vs. Input Angle ϕ_1

(4) Function $F_2(\phi_1)$

The coupling function $F_2(\phi_1)$ changes very little during Regime No.2 and therefore may be treated as a constant with a value of 0.098.

c. Fourier Series Representation of Forcing terms R_1 and R_2

The following gives the Fourier series expressions for the forcing terms R_1 and R_2 in equation (19):

(1) Forcing term $R_1(\phi_1, \dot{\phi}_1)$

According to equation (21), the term $R_1(\phi_1, \dot{\phi}_1)$ has the form:

$$R_1(\phi_1,\dot{\phi}_1) = \frac{\rho A}{M_e}\frac{F_1(\phi_1)}{\dot{\phi}_1^2} - F_2\frac{J_{o4}}{M_e}\frac{d^2\phi_{4r}(\phi_1)}{d\phi_1^2} - F_2K_r\lambda_{co}^2\phi_{4r}(\phi_1) - \frac{F_2T_b}{2\dot{\phi}_1^2M_e} \qquad (C.11)$$

Using a Fourier series expansion to represent all the input angle dependent functions, one obtains

$$\begin{aligned} R_1(\phi_1,\dot{\phi}_1) = &-\frac{F_2T_b}{2\dot{\phi}_1^2M_e} + \frac{\rho A}{M_e}\left[a_{10} + \sum_{n=1}^{\infty}(a_{1n}\cos n\phi_1 + b_{1n}\sin n\phi_1)\right] - \\ &-\frac{J_{o4}}{M_e}\left[a_{20} + \sum_{n=1}^{\infty}(a_{2n}\cos n\phi_1 + b_{2n}\sin n\phi_1)\right] - \\ &-F_2K_r\lambda_{co}^2\left[a_{30} + \sum_{n=1}^{\infty}(a_{3n}\cos n\phi_1 + b_{3n}\sin n\phi_1)\right] \end{aligned} \qquad (C.12)$$

where the coefficients of the series are found from:

$$
\begin{aligned}
a_{10} &= \frac{1}{2\pi}\int_0^{2\pi}\frac{F_1(\phi_1)}{\dot{\phi}_1^2}d\phi_1 \\
a_{1n} &= \frac{1}{\pi}\int_0^{2\pi}\frac{F_1(\phi_1)}{\dot{\phi}_1^2}\cos n\phi_1 d\phi_1 \\
b_{1n} &= \frac{1}{\pi}\int_0^{2\pi}\frac{F_1(\phi_1)}{\dot{\phi}_1^2}\sin n\phi_1 d\phi_1
\end{aligned}
\qquad (C.13)
$$

$$
\begin{aligned}
a_{20} &= \frac{1}{2\pi}\int_0^{2\pi}F_2\frac{d^2\phi_{4r}(\phi_1)}{d\phi_1^2}d\phi_1 \\
a_{2n} &= \frac{1}{\pi}\int_0^{2\pi}F_2\frac{d^2\phi_{4r}(\phi_1)}{d\phi_1^2}\cos n\phi_1 d\phi_1 \\
b_{2n} &= \frac{1}{\pi}\int_0^{2\pi}F_2\frac{d^2\phi_{4r}(\phi_1)}{d\phi_1^2}\sin n\phi_1 d\phi_1
\end{aligned}
\qquad (C.14)
$$

and

$$
\begin{aligned}
a_{30} &= \frac{1}{2\pi}\int_0^{2\pi}\phi_{4r}(\phi_1)d\phi_1 \\
a_{3n} &= \frac{1}{\pi}\int_0^{2\pi}\phi_{4r}(\phi_1)\cos n\phi_1 d\phi_1 \\
b_{3n} &= \frac{1}{\pi}\int_0^{2\pi}\phi_{4r}(\phi_1)\sin n\phi_1 d\phi_1
\end{aligned}
\qquad (C.15)
$$

If one combines like terms in equation (C.12), the forcing term $R_1(\phi_1, \dot{\phi}_1)$ becomes

$$
R_1(\phi_1, \dot{\phi}_1) = A_{10} + \sum_{n=1}^{\infty}(A_{1n}\cos n\phi_1 + B_{1n}\sin n\phi_1) \qquad (C.16)
$$

The new resulting coefficients then become:

$$
\begin{aligned}
A_{10} &= \frac{\rho A}{M_e}a_{10} - \frac{J_{o4}}{M_e}a_{20} - F_2K_r\lambda_{co}^2 a_{30} - \frac{F_2T_b}{2\dot{\phi}_1^2M_e} \\
A_{1n} &= \frac{\rho A}{M_e}a_{1n} - \frac{J_{o4}}{M_e}a_{2n} - F_2K_r\lambda_{co}^2 a_{3n} \\
B_{1n} &= \frac{\rho A}{M_e}b_{1n} - \frac{J_{o4}}{M_e}b_{2n} - F_2K_r\lambda_{co}^2 b_{3n}
\end{aligned}
\qquad (C.17)
$$

(2) Forcing term $R_2(\phi_1, \dot{\phi}_1)$

According to equation (22), $R_2(\phi_1, \dot{\phi}_1)$ has the form:

$$R_2(\phi_1, \dot{\phi}_1) = \frac{1.5T_b}{J_{o5}\dot{\phi}_1^2} + 2\zeta_{sp}\lambda_{sp}\frac{d\phi_{4r}(\phi_1)}{d\phi_1} + \lambda_{sp}^2\phi_{4r}(\phi_1) \qquad (C.18)$$

With a Fourier series replacement of the functions $d\phi_{4r}/d\phi_1$ and ϕ_{4r} in the above, one obtains:

$$R_2(\phi_1, \dot{\phi}_1) = \frac{1.5T_b}{J_{o5}\dot{\phi}_1^2} + 2\zeta_{sp}\lambda_{sp}\left[a_{40} + \sum_{n=1}^{\infty}(a_{4n}\cos n\phi_1 + b_{4n}\sin n\phi_1)\right] +$$

$$+ \lambda_{sp}^2\left[a_{30} + \sum_{n=1}^{\infty}(a_{3n}\cos n\phi_1 + b_{3n}\sin n\phi_1)\right] \qquad (C.19)$$

where

$$a_{40} = \frac{1}{2\pi}\int_0^{2\pi}\frac{d\phi_{4r}(\phi_1)}{d\phi_1}d\phi_1$$
$$a_{4n} = \frac{1}{\pi}\int_0^{2\pi}\frac{d\phi_{4r}(\phi_1)}{d\phi_1}\cos n\phi_1 d\phi_1 \qquad (C.20)$$
$$b_{4n} = \frac{1}{\pi}\int_0^{2\pi}\frac{d\phi_{4r}(\phi_1)}{d\phi_1}\sin n\phi_1 d\phi_1$$

When one combines the like terms, equation (C.19) may be rewritten as:

$$R_2(\phi_1, \dot{\phi}_1) = A_{20} + \sum_{n=1}^{\infty}(A_{2n}\cos n\phi_1 + B_{2n}\sin n\phi_1) \qquad (C.21)$$

The above coefficients are defined as:

$$A_{20} = \frac{1.5T_b}{J_{o5}\dot{\phi}_1^2} + 2\zeta_{sp}\lambda_{sp}a_{40} + \lambda_{sp}^2 a_{30}$$
$$A_{2n} = 2\zeta_{sp}\lambda_{sp}a_{4n} + \lambda_{sp}^2 a_{3n} \qquad (C.22)$$
$$B_{2n} = 2\zeta_{sp}\lambda_{sp}b_{4n} + \lambda_{sp}^2 b_{3n}$$

APPENDIX D. SOLUTION FOR REGIME NO.1

a. Equation of Motion

During this initial forward motion of the rocker, the outer race of the clutch winds up against its inner race, which is held stationary by the resisting torque T_b until the latter is overcome. The linearized clutch spring constant K_{l1} of equation (C.8) becomes applicable in equations (18b), (18d) and (18e).

With the clutch output shaft stationary and with that the angle ϕ_5 constant at $\phi_{4e\ max}$, the first expression of equation (17) for $q(\phi_1)$ becomes:

$$q'' + 2\zeta_{co}\lambda_{co}q' + (1 + K_r F_2^2)\lambda_{co}^2 q = R_{1(1)}(\phi_1, \dot{\phi}_1) \qquad (D.1)$$

where the forcing function is given by:

$$R_{1(1)}(\phi_1, \dot{\phi}_1) = K_r F_2 \lambda_{co}^2 \phi_{4e\ max} + \frac{\rho A}{M_e} F_1(\phi_1) - F_2 \frac{J_{o4}}{M_e} \phi_{4r}''(\phi_1) - F_2 K_r \lambda_{co}^2 \phi_{4r}(\phi_1) \qquad (D.2)$$

The second expression of equation (17), with the derivatives of ϕ_5 set equal to zero, furnishes the condition for the end of the regime:

$$K_{l1}(\phi_5 - \phi_{4r} - F_2 q) - C_{sp}(F_2 q' + \phi_{4r}')\dot{\phi}_1 \geq T_b \qquad (D.3)$$

The above indicates that the spring torque has overcome the resisting torque on the clutch output shaft.

b. Complete Solution of Equation of Motion

According to equations (C.13), (C.14) and (C.15), the input angle dependent forcing function of equation (D.2) is expressed in terms of a Fourier series, i.e.:

$$R_{1(1)}(\phi_1, \dot{\phi}_1) = A_{10(1)} + \sum_{n=1}^{\infty} (A_{1n(1)} \cos n\phi_1 + B_{1n(1)} \sin n\phi_1) \qquad (D.4)$$

where

$$\begin{aligned} A_{10(1)} &= K_r F_2 \lambda_{co}^2 \phi_{4e\ max} + \frac{\rho A}{M_e} a_{10} - \frac{J_{o4}}{M_e} a_{20} - F_2 K_r \lambda_{co}^2 a_{30} \\ A_{1n(1)} &= \frac{\rho A}{M_e} a_{1n} - \frac{J_{o4}}{M_e} a_{2n} - F_2 K_r \lambda_{co}^2 a_{3n} \\ B_{1n(1)} &= \frac{\rho A}{M_e} b_{1n} - \frac{J_{o4}}{M_e} b_{2n} - F_2 K_r \lambda_{co}^2 b_{3n} \end{aligned} \qquad (D.5)$$

When only the constant and the first harmonic terms of the series are kept, the complete solution of differential equation (D.1) has the following form:

$$\begin{aligned} q(\phi_1) = e^{-\zeta_{co}\lambda_{co}\phi_1} & [E_1 \sin(\sqrt{1 + K_r F_2 - \zeta_{co}^2}\,\lambda_{co}\phi_1) + E_2 \cos(\sqrt{1 + K_r F_2 - \zeta_{co}^2}\,\lambda_{co}\phi_1)] + \\ & + \frac{A_{10(1)}}{(1 + K_r F_2)\lambda_{co}^2} + \frac{[(1 + K_r F_2)\lambda_{co}^2 - 1]B_{11(1)} + 2\zeta_{co}\lambda_{co}A_{11(1)}}{[(1 + K_r F_2)\lambda_{co}^2 - 1]^2 + (2\zeta_{co}\lambda_{co})^2} \sin\phi_1 + \\ & + \frac{[(1 + K_r F_2)\lambda_{co}^2 - 1]A_{11(1)} - 2\zeta_{co}\lambda_{co}B_{11(1)}}{[(1 + K_r F_2)\lambda_{co}^2 - 1]^2 + (2\zeta_{co}\lambda_{co})^2} \cos\phi_1 \end{aligned} \qquad (D.6)$$

where the constants E_1 and E_2 are to be determined by the initial conditions of q and q', which are equal to their end values of Regime No.4.

APPENDIX E. SOLUTION FOR REGIME NO.3

a. Equation of Motion

During this initial return motion of the rocker, the outer race of the clutch unwinds the sprags out of engagement while the inner race of the clutch is held stationary by the resisting torque. The linearized clutch spring constant K_{l3} given by equation (C.10), is now used in equations (18b), (18d) and (18e).

With the clutch output angle ϕ_5 remaining constant at its end value $\phi_{5(e2)}$ of Regime No.2, the first expression of equation (17) for $q(\phi_1)$ becomes:

$$q'' + 2\zeta_{co}\lambda_{co}q' + (1 + K_r F_2^2)\lambda_{co}^2 q = R_{1(3)}(\phi_1, \dot{\phi}_1) \qquad (E.1)$$

where the forcing function is given by:

$$R_{1(3)}(\phi_1, \dot{\phi}_1) = K_r F_2 \lambda_{co}^2 \phi_{5(e2)} + \frac{\rho A}{M_e} F_1(\phi_1) - F_2 \frac{J_{o4}}{M_e} \phi_{4r}''(\phi_1) - F_2 K_r \lambda_{co}^2 \phi_{4r}(\phi_1) \qquad (E.2)$$

The regime will end when the clutch is completely disengaged, i.e.:

$$\phi_{5/4}(\phi_1) = \phi_{5(e2)} - [\phi_{4r}(\phi_1) + F_2 q(\phi_1)] \le 0 \qquad (E.3)$$

b. Complete Solution of Equation of Motion

Similar to Appendix D, the input angle dependent forcing function in equation (E.2) is now expressed in terms of a Fourier series, i.e.:

$$R_{1(3)}(\phi_1, \dot{\phi}_1) = A_{10(3)} + \sum_{n=1}^{\infty} (A_{1n(3)} \cos n\phi_1 + B_{1n(3)} \sin n\phi_1) \qquad (E.4)$$

where

$$A_{10(3)} = K_r F_2 \lambda_{co}^2 \phi_{5(e2)} + \frac{\rho A}{M_e} a_{10} - \frac{J_{o4}}{M_e} a_{20} - F_2 K_r \lambda_{co}^2 a_{30}$$
$$A_{1n(3)} = A_{1n(1)} \qquad (E.5)$$
$$B_{1n(3)} = B_{1n(1)}$$

If one only considers the constant and the first harmonic terms of the series, the complete solution of differential equation (E.1) has the following form:

$$q(\phi_1) = e^{-\zeta_{co}\lambda_{co}\phi_1}\left[E_3 \sin\left(\sqrt{1 + K_r F_2 - \zeta_{co}^2}\,\lambda_{co}\phi_1\right) + E_4 \cos\left(\sqrt{1 + K_r F_2 - \zeta_{co}^2}\,\lambda_{co}\phi_1\right) + \right.$$
$$+ \frac{A_{10(3)}}{(1 + K_r F_2)\lambda_{co}^2} + \frac{[(1 + K_r F_2)\lambda_{co}^2 - 1]B_{11(3)} + 2\zeta_{co}\lambda_{co}A_{11(3)}}{[(1 + K_r F_2)\lambda_{co}^2 - 1]^2 + (2\zeta_{co}\lambda_{co})^2} \sin\phi_1 +$$
$$\left. + \frac{[(1 + K_r F_2)\lambda_{co}^2 - 1]A_{11(3)} - 2\zeta_{co}\lambda_{co}B_{11(3)}}{[(1 + K_r F_2)\lambda_{co}^2 - 1]^2 + (2\zeta_{co}\lambda_{co})^2} \cos\phi_1 \right] \qquad (E.6)$$

where the constants E_3 and E_4 are to be determined with the initial conditions of q and q', which are equal to their end values of Regime No.2.

APPENDIX F. SOLUTION FOR REGIME NO.4

a. Equation of Motion

During the continued return motion of the rocker, the outer race of the clutch overruns the inner one. Thus, there is no clutch action on the coupler and any terms associated with K_{li} in the first expression of equation (17) vanish. This leads to the following equation of motion:

$$q'' + 2\zeta_{co}\lambda_{co}q' + \lambda_{co}^2 q = R_{1(4)}(\phi_1, \dot{\phi}_1) \tag{F.1}$$

where the forcing function is given by:

$$R_{1(4)}(\phi_1, \dot{\phi}_1) = \frac{\rho A}{M_e}F_1(\phi_1) - F_2\frac{J_{o4}}{M_e}\phi_{4r}''(\phi_1) \tag{F.2}$$

The regime will end when the rocker reaches its maximum angular position $\phi_{4c\ max}$ and its angular velocity becomes negative, i.e.:

$$\phi'_{4c}(\phi_1) = \phi'_4(\phi_1) + F_2 q'(\phi_1) \le 0 \tag{F.3}$$

b. Complete Solution of Equation of Motion

To obtain an analytical solution, the input angle dependent forcing function in equation (F.2) must be first expressed in terms of a Fourier series, i.e.:

$$R_{1(4)}(\phi_1, \dot{\phi}_1) = A_{10(4)} + \sum_{n=1}^{\infty}(A_{1n(4)}\cos n\phi_1 + B_{1n(4)}\sin n\phi_1) \tag{F.4}$$

where

$$A_{10(4)} = \frac{\rho A}{M_e} a_{10} - \frac{J_{o4}}{M_e} a_{20}$$
$$A_{1n(4)} = \frac{\rho A}{M_e} a_{1n} - \frac{J_{o4}}{M_e} a_{2n} \qquad (F.5)$$
$$B_{1n(4)} = \frac{\rho A}{M_e} b_{1n} - \frac{J_{o4}}{M_e} b_{2n}$$

If one only considers the constant and the first harmonic terms of the series, the complete solution of differential equation (F.1) can be found to be:

$$q(\phi_1) = e^{-\zeta_{co}\lambda_{co}\phi_1}\left[E_5 \sin\left(\sqrt{1-\zeta_{co}^2}\,\lambda_{co}\phi_1\right) + E_6 \cos\left(\sqrt{1-\zeta_{co}^2}\,\lambda_{co}\phi_1\right) + \frac{A_{10(4)}}{\lambda_{co}^2} + \right.$$
$$\left. + \frac{(\lambda_{co}^2-1)B_{11(4)} + 2\zeta_{co}\lambda_{co}A_{11(4)}}{(\lambda_{co}^2-1)^2 + (2\zeta_{co}\lambda_{co})^2}\sin\phi_1 + \frac{(\lambda_{co}^2-1)A_{11(4)} - 2\zeta_{co}\lambda_{co}B_{11(4)}}{(\lambda_{co}^2-1)^2 + (2\zeta_{co}\lambda_{co})^2}\cos\phi_1 \right] \qquad (F.6)$$

where the constants E_5 and E_6 are to be determined with the initial conditions of q and q', which are equal to their end values of Regime No.3.

APPENDIX G. EFFECT OF ADDITION OF MASS TO COUPLER AT POINT B

In order to be able to study the influence on the strain and the windup angle responses in the presence of a coupler with a lower than standard component natural frequency, a mass was added to the standard coupler at point B.

a. Experimental Setup

Figure G-1 shows how this addition was accomplished in the experimental setup, by clamping two equal cylindrical masses, weighing a total of approximately 9.1 lbs (together with bolts, washers and nuts) to the coupler.

b. Derivation of Equation of Motion

For purposes of analysis one must assume that a concentrated mass M is located at point B. This means that the shape function for the coupler is the same as before and that this mass only influences the kinetic energy of the link.

The additional kinetic energy term which is to be added to Hamiltons integral, i.e. equation (10) has the form:

$$T_M = \frac{1}{2} M(\vec{r}_B \cdot \vec{r}_B) \qquad (G.1)$$

where the velocity

$$\vec{r}_B = \vec{r}_1(x_1 = L) \qquad (G.2)$$

is evaluated according to equation (A.33)

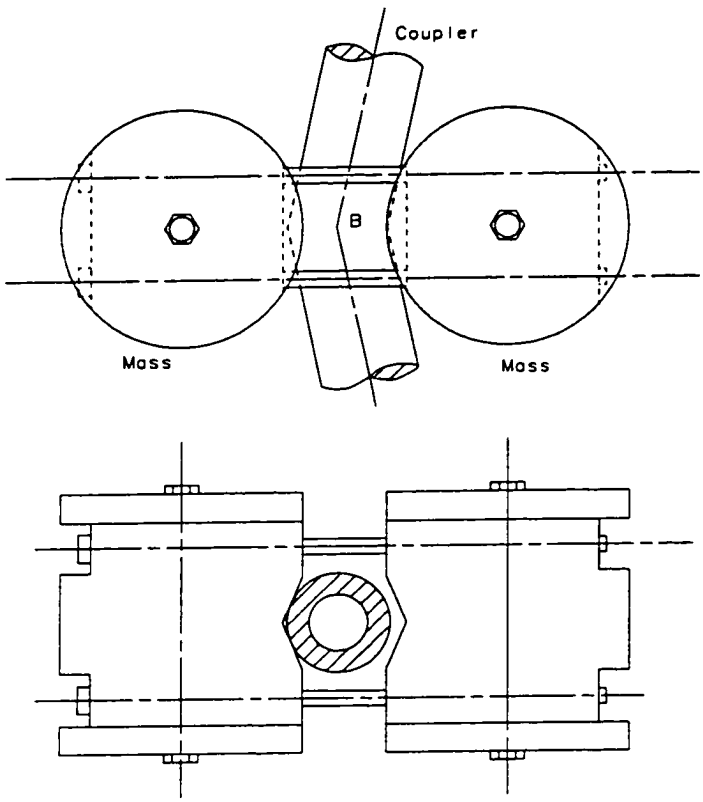

Figure G-1 Addition of Masses to the Coupler at Point B

After the substitution of equation (G.1), as an additional term, into equation (10) and proceeding in the same manner as for equation (11), equation (12) is modified in the following manner:

$$[\rho A(V_{2s1}+V_{2s2}+\sin^2 2\alpha)L+\rho AP_1(\phi_1)+M+MQ_1(\phi_1)]\frac{d^2q}{d\phi_1^2}+\frac{1}{\dot{\phi}_1}[0.45LC_{co}+$$

$$+\rho AP_2(\phi_1)+MQ_2(\phi_1)]\frac{dq}{d\phi_1}+\frac{1}{\dot{\phi}_1^2}[\left(\frac{\pi}{2}\right)^4\frac{EI}{L^3}+\rho AP_3(\phi_1)+MQ_3(\phi_1)]q$$

$$=[\frac{1}{\dot{\phi}_1^2}K_{sp}(\phi_5-\phi_{4e})^{3/2}+\frac{1}{\dot{\phi}_1}C_{sp}(\frac{d\phi_5}{d\phi_1}-\frac{d\phi_{4e}}{d\phi_1})-J_{o4}\frac{d^2\phi_{4e}}{d\phi_1^2}]F_2(\phi_1)+\rho A\frac{F_1(\phi_1)}{\dot{\phi}_1^2}+MF_3(\phi_1) \qquad (G.3)$$

where the newly added input angle dependent functions are given by:

$$Q_1(\phi_1)=(4L\sin\alpha\sin\phi_{32r})\eta_2(\phi_1)+4L^2(\sin\alpha\sin\phi_{32r})^2\eta_2^2(\phi_1)+$$

$$4L^2(\sin\alpha)^2\eta_{32}^2 \qquad (G.4)$$

$$Q_2(\phi_1)=2L\sin\alpha\cos\phi_{32r}G_2\eta_2(\phi_1)-2L\sin\alpha G_1\eta_{32}(\phi_1)+$$

$$+4L^2\sin^2\alpha\cos\phi_{32r}\sin\phi_{32r}G_2\eta_2^2(\phi_1)-$$

$$-4L^2\sin^2\alpha\cos\phi_{32r}G_3\eta_2(\phi_1)\eta_{32}(\phi_1) \qquad (G.5)$$

$$Q_3(\phi_1)=-(G_1^2+G_3^2)-[2a_1\dot{\phi}_1^2\sin\alpha\cos(\phi_1-\phi_{2r})+2L(G_1^2-G_2^2)\sin\alpha\sin\phi_{32r}+$$

$$+2L(\dot{G}_2-G_1G_3)\sin\alpha\cos\phi_{32r}]\eta_2(\phi_1)-2L(\dot{G}_1+G_2G_3)\sin\alpha\eta_{32}(\phi_1) \qquad (G.6)$$

$$F_3(\phi_1)=-\{a_1\dot{\phi}_1^2\sin(\phi_1-\phi_{2r})+L(\dot{G}_3+G_1G_2)+[2La_1\dot{\phi}_1^2\sin(\phi_1-\phi_{2r})\sin\alpha\sin\phi_{32r}+$$

$$+2L^2(\dot{G}_3+G_1G_2)\sin\alpha\sin\phi_{32r}]\eta_2(\phi_1)+[2La_1\dot{\phi}_1^2\cos(\phi_1-\phi_{2r})\sin\alpha\cos\phi_{32r}+$$

$$+2L^2(\dot{G}_2-G_1G_3)\sin\alpha]\eta_{32}(\phi_1)\} \qquad (G.7)$$

It is to be noted that the form of equation (13) is not influenced by the addition of mass M.

The evaluation of the new functions shows that the maximum values of $MQ_2(\phi_1)$ and $MQ_3(\phi_1)$ are very small (4.7×10^{-6} and 9.4×10^{-5}, respectively) when compared to terms $(.45LC_{co})/\dot{\phi}_1$ and $(EI\pi^4)/(2^4\dot{\phi}_1^2L^3)$ (see Appendix C). Therefore, they are neglected.

Further, it is found that the values of the ratio of $1/(V_{2s1}+V_{2s2}+\sin^2 2\alpha)L$, $Q_1(\phi_1)/P_1(\phi_1)$ and $F_3(\phi_1)/F_1(\phi_1)$ are fairly constant near 0.005. Thus, a new equivalent "density" of the coupler, which accounts for the addition of the mass M, can be introduced:

$$\rho_e = \rho + \rho_M \qquad (G.8)$$

where the density increment is defined by

$$\rho_M = 0.05\cdot M/A \qquad (G.9)$$

With the above, equation (G.3) can be rewritten as

$$[\rho_e A(V_{2s1}+V_{2s2}+\sin^2 2\alpha)L+\rho_e AP_1(\phi_1)]\frac{d^2q}{d\phi_1^2}+\frac{1}{\dot{\phi}_1}[0.45LC_{co}+\rho AP_2(\phi_1)]\frac{dq}{d\phi_1}+$$

$$+\frac{1}{\dot{\phi}_1^2}[\left(\frac{\pi}{2}\right)^4\frac{EI}{L^3}+\rho AP_3(\phi_1)+]\,q = [\frac{1}{\dot{\phi}_1^2}K_{sp}(\phi_5-\phi_{4c})^{3/2}+\frac{1}{\dot{\phi}_1}C_{sp}(\frac{d\phi_5}{d\phi_1}-\frac{d\phi_{4c}}{d\phi_1})-J_{o4}\frac{d^2\phi_{4c}}{d\phi_1^2}]F_2(\phi_1)+$$

$$+\rho_e A\frac{F_1(\phi_1)}{\dot{\phi}_1^2} \qquad (G.10)$$

Note that the coefficients of $P_2(\phi_1)$ and $P_3(\phi_1)$ contain the original density ρ of the coupler. With the reasoning of section 5c $P_2(\phi_1)$ and $P_3(\phi_1)$ are now also set equal to zero and the linearized form of equation (17) becomes applicable, with the replacement of ρ by ρ_e in equations (19) and (21).

APPENDIX H. SAMPLE COMPUTATIONS FOR RUN NO.1

The following describes the computations for two complete mechanism cycles (start-up and normal), where each contains the four operating regimes. The start-up cycle begins with Regime No.1. Here, certain assumptions concerning the initial mechanism angles and the initial conditions for the coupler deflection are made (See Part I, section 7a). Subsequently, the final conditions for the mechanism angles and the coupler deflection of any regime become the initial conditions for the following one. Experience has shown that the various values obtained in the second or normal cycle repeat reliably in all further ones.

a. Constants Common to All Regimes

Based on the mechanism parameters listed in Table 1 and the operating parameters of Run No.1 (See section 7e of Part I), Table H-1 lists the values of the commonly used constants of all regimes, according to equations (18), (19) and (20).

Further, according to equations (C.13) to (C.15) and (C.20), the first three coefficients of the Fourier expansions in equations (C.12) and (C.19), which are functions of mechanism geometry, are found to be:

$a_{10} = -0.03798$, $a_{11} = 7.2439$, $b_{11} = -12.2350$

$a_{20} = -0.0002$, $a_{21} = 0.0055$, $b_{21} = -0.0208$

$a_{30} = 1.5431$, $a_{31} = -0.0563$, $b_{31} = -0.2132$

$a_{40} = 0.0000$, $a_{41} = -0.2132$, $b_{41} = 0.0563$

Run No.1: $\dot{\phi}_1$ = 200 (RPM), T_b = 160 (lb-in), Steel Strip Size =4.0x.125x130.0 (in)		
J_{o5}	Clutch Output Shaft and Strip Moment of Inertia	0.41 (lb-in-sec^2)
M_e	Equivalent Mass of Coupler	0.00632 (lb-sec^2/in)
K_e	Equivalent Stiffness of Coupler	1333.78 (lb/in)
ω_{co}	Component Frequency of Coupler	73.1 (Hz)
λ_{co}	Frequency Ratio for Coupler	21.934
ζ_{co}	Damping Ratio for Coupler	0.0773
$F_2 = 0.098$, $P_1 = 2.65$		

Table H-1. Constants Common to All Regimes

b. Computations for Cycle No.1 (Start-up)

(1) Computations for Regime No.1 of Start-up Cycle

According to equations (C.8) and (18.g), the linearized clutch stiffness K_{l1} and the associated stiffness ratio K_r are found to be:

$K_{l1} = 18566.36$, $K_r = 1.364$

The values of the first three coefficients of equation (D.4) are obtained by way of equation (D.5):

$A_{10(1)} = -1012.746$, $A_{11(1)} = 37.126$, $B_{11(1)} = 139.016$

Table H-2 shows the assumed initial values, for the start-up computation, of the angles ϕ_1, ϕ_4 and ϕ_5, as well as the coupler deflection variables q and q'. The angles are obtained from rigid body kinematics.

$\phi_1 = 255.645°$	$\phi_4 = \phi_5 = 101.07°$	$q = 0$	$q' = 0$

Table H-2. Initial Conditions for Regime No.1 of Start-up Cycle

After solving for the constants E_1 and E_2 with the above initial conditions, equation (D.6) takes the following form:

$$q(\phi_1) = e^{-1.695\phi_1}[1.206\sin(23.292\phi_1) + 3.258\cos(23.292\phi_1)] +$$
$$+ 0.266 + 0.256\sin(\phi_1) + 0.067\cos(\phi_1)$$

The regime ends when the inequality (D.3) is no longer satisfied. This furnishes the end values for the input angle and the coupler deflection as given in Table H-3.

$\phi_1 = 271.114°$	$\phi_5 = 101.07°$	$q = 0.0105$	$q' = 0.710$

Table H-3. End Values of Regime No.1 of Start-up Cycle

(2) Computations for Regime No.2 of Start-up Cycle

Table H-4 lists the remaining basic constants for Regime No.2 with the help of equation (18). According to equations (16) the linearized clutch stiffness is:

$K_{l2} = 27849.5$ (lb-in/rad)

The two natural frequencies of the system as well as the damping related constants are found by solving the roots of equation (27):

$\omega_1 = 36.765\,\text{Hz}$, $\omega_2 = 82.166\,\text{Hz}$ and $\alpha_1 = 12.245$, $\alpha_2 = 36.681$

Subsequently, the values of the coefficients of equations (38) and (39), which represent the forcing functions, are obtained by means of equations (C.17) and (C.22):

$A_{10} = -1521.948$, $A_{11} = 55.600$, $B_{11} = 208.978$

$A_{20} = 240.287$, $A_{21} = -8.991$, $B_{21} = -32.942$

With the above, the constants involved in the solution equations (47) and (48) are now calculated according to equations (34)-(37), (42)-(44) and (51)-(53). They are listed in Table H-5.

Using the end values of Regime No.1 as given in Table H-3 as the initial conditions for Regime No.2, the four constants of equation (45) and (46) are found to be:

$L_{11} = -0.130$, $L_{12} = -0.152$, $L_{13} = -3.967$, $L_{14} = 7.590$

Substitution of the above into equations (47) and (54) furnishes:

$$q(\phi_1) = e^{-0.585\phi_1}0.200\sin(11.030\phi_1 + 3.848) + e^{-1.751\phi_1}8.565\sin(24.650\phi_1 - 0.482) + \\ + 0.012 + 0.005\sin(\phi_1 + 3.211)$$

and

K_r	Ratio of the Stiffness	2.046
ω_{sp}	Component Frequency of Clutch-Strip System	41.5 (Hz)
λ_{sp}	Frequency Ratio for Clutch-Strip System	12.444
ζ_{sp}	Damping Ratio for Clutch-Strip System	0.0515

Table H-4. Basic Constants for Regime No.2 of Start-up and Normal Cycles

$n_1 = 0.461$	$D_0 = 1.553$
$m_1 = 0.025$	$D_{s1} = -0.215$
$n_2 = -0.033$	$D_{c1} = -0.057$
$m_2 = -0.003$	$\theta_1 = 0.054$
$C_0 = 0.012$	$\theta_2 = 3.225$
$C_{s1} = -0.005$	$\alpha_c = 3.211$
$C_{c1} = -0.000$	$\alpha_d = 3.399$

Table H-5. Solution Related Constants for Regime No.2 of Start-up and Normal Cycles

$$\phi_{5/4}(\phi_1) = e^{-0.585\phi_1}0.073\sin(11.030\phi_1 + 3.916) + e^{-1.751\phi_1}1.126\sin(24.650\phi_1 - 0.461) +$$
$$+ 0.382\sin(\phi_1 + 0.783) + 0.0086$$

The regime ends when equation (62) is no longer satisfied. Table H-6 gives the end values of Regime No.2 of the start-up cycle.

$\phi_1 = 434.694°$	$\phi_5 = 76.203°$	$q = 0.00608$	$q' = 0.02323$	$\phi_{5/4} = 0.0069$

Table H-6. End Values of Regime No.2 for Start-up Cycle

(3) Computations for Regime No.3 of Start-up Cycle

With $\phi_{5/4(f2)} = 0.0069$ (see Table H-6), the linearized clutch stiffness K_{l3} and the associated stiffness ratio K_r become, according to equations (C.10) and (18.g):

$K_{l3} = 16579.91$, $K_r = 1.218$

The values of the first three coefficients of equation (E.4) are obtained with the help of equation (E.5):

$A_{10(3)} = -904.390$, $A_{11(3)} = 33.172$, $B_{11(3)} = 124.045$

With the end values of Table H-6 as the initial conditions, the constants E_3 and E_4 of equation (E.6) may be obtained and the resulting solution has the form:

$$q(\phi_1) = e^{-1.695\phi_1}[414.531\sin(23.144\phi_1) - 238.928\cos(23.144\phi_1)] -$$
$$- 0.232 + 0.231\sin(\phi_1) + 0.060\cos(\phi_1)$$

The regime ends when the inequality (E.3) is no longer satisfied. Table H-7 gives the end values of Regime No.3

$\phi_1 = 90.450° + 360°$	$q = -0.00172$	$q' = -0.0483$

Table H-7. End Values of Regime No.3 for Start-up Cycle

(4) Computations for Regime No.4 of Start-up Cycle

The values of the first three coefficients of equation (F.4) are obtained by using equation (F.5):

$A_{10(4)} = 0.003$, $A_{11(4)} = 0.176$, $B_{11(4)} = -0.909$

Using the end values of Table H-7 for Regime No.3 as the initial conditions for this regime, one can solve for the constants E_5 and E_6 of equation (F.6). The resulting solution has the form:

$$q(\phi_1) = e^{-1.695\phi_1}[907.443\sin(21.868\phi_1) + 996.400\cos(21.868\phi_1)] +$$
$$+ 0.000 - 0.002\sin(\phi_1) + 0.000\cos(\phi_1)$$

The regime ends when the inequality (F.3) is no longer satisfied. Table H-8 gives the end values for Regime No.4.

$\phi_1 = 255.642° + 360°$	$\phi_4 = \phi_5 = 101.057°$	$q = 0.00174$	$q' = 0.00048$

Table H-8. End Values of Regime No.4 for Start-up Cycle

c. Computations for Cycle No.2 (Normal)

All the constants of the start-up cycle, which do not depend on initial conditions, are also applicable for the normal cycle.

(1) Computations for Regime No.1 of Normal Cycle

The end values of Regime No.4 of the start-up cycle, which are listed in Table H-8, are now used as the initial values for this regime. This furnishes the constants E_1 and E_2 of equation (D.6). The resulting solution of equation (D.6) then has the form:

$$q(\phi_1) = e^{-0.248\phi_1}[1.206\sin(23.292\phi_1) - 0.889\cos(23.292\phi_1)] +$$
$$+ 0.266 + 0.256\sin(\phi_1) + 0.067\cos(\phi_1)$$

As before, the inequality (D.3) gives the end value for this regime, as listed in Table H-9.

$\phi_1 = 271.687°$	$\phi_5 = 101.062°$	$q = 0.0122$	$q' = 0.721$

Table H-9. End Values of Regime No.1 of Normal Cycle

(2) Computations for Regime No.2 of Normal Cycle

The various basic constants given for Regime No.2 of the start-up cycle are still applicable. Using the end values for Regime No.1 of Table H-9 as the present initial conditions, the constants of equations (45) and (46) become:

$L_{11} = -0.122$, $L_{12} = -0.163$, $L_{13} = -9.727$, $L_{14} = 3.808$

Substitution of the above into equations (47) and (54) furnishes:

$$q(\phi_1) = e^{-0.585\phi_1}0.204\sin(11.030\phi_1 + 3.785) + e^{-1.751\phi_1}10.446\sin(24.650\phi_1 - 1.198) +$$
$$+ 0.012 + 0.005\sin(\phi_1 + 3.211)$$

and

$$\phi_{5/4}(\phi_1) = e^{-0.585\phi_1}0.074\sin(11.030\phi_1 + 3.853) + e^{-1.751\phi_1}1.373\sin(24.650\phi_1 - 1.177) +$$
$$+ 0.382\sin(\phi_1 + 0.783) + 0.0086$$

This regime ends when equation (62) is no longer satisfied. Table H-10 gives the associated end values.

$\phi_1 = 434.694°$	$\phi_5 = 76.203°$	$q = 0.00593$	$q' = 0.02276$	$\phi_{5/4} = 0.0068$

Table H-10. End Values of Regime No.2 for Normal Cycle

(3) Computations for Regime No.3 of Normal Cycle

With $\phi_{5/4(f2)} = 0.0068$ (see Table H-10), the linearized clutch stiffness K_{l3} and the associated stiffness ratio K_r become, according to equation (C.10):

$K_{l3} = 16510.01$, $K_r = 1.213$

The values of the first three coefficients of equation (E.4) are obtained with the help of equation (E.5):

$A_{10(3)} = -900.577$, $A_{11(3)} = 33.033$, $B_{11(3)} = 123.518$

With the end values of Table H-10 as the initial conditions, the constants E_3 and E_4 of equation (E.6) may be obtained and the resulting solution has the form:

$$q(\phi_1) = e^{-1.695\phi_1}[421.117\sin(23.140\phi_1) - 239.282\cos(23.140\phi_1)] -$$
$$- 0.231 + 0.230\sin(\phi_1) + 0.060\cos(\phi_1)$$

The regime ends when the inequality (E.3) is no longer satisfied. Table H-11 gives the associated end values.

$\phi_1 = 90.450° + 360°$	$q = -0.00172$	$q' = -0.0483$

Table H-11. End Values of Regime No.3 for Normal Cycle

(4) Computations for Regime No.4 of Normal Cycle

Using the end values of Table H-11 for Regime No.3 as the initial conditions for the present regime, one can solve the constants E_5 and E_6 of equation (F.6). The solution form of the regime then becomes:

$$q(\phi_1) = e^{-1.695\phi_1}[9953.646\sin(21.868\phi_1) + 949.178\cos(21.868\phi_1)] +$$
$$+ 0.000 - 0.002\sin(\phi_1) + 0.000\cos(\phi_1)$$

The regime ends when the inequality (F.3) is no longer satisfied. Table H-12 gives the associated end values. Note that the end values of Tables H-8 and H-12 are the same and one may safely assume that equilibrium of operation has been reached after two cycles.

$\phi_1 = 255.642° + 360°$	$\phi_4 = \phi_5 = 101.057°$	$q = 0.00174$	$q' = 0.00048$

Table H-12. End Values of Regime No.4 for Start-up Cycle

APPENDIX I. COMPUTER ALGORITHMS FOR THE DETERMINATION OF THE WINDUP ANGLE AND SAMPLE OUTPUT

a. Data Transfer from the Data Acquisition System to the Computer

The angular motion data of the mechanism input shaft, the rocker shaft and the feed roller shaft are obtained by way of three angular encoders, which are able to furnish pulses for every 0.036 degree of angular rotation. The times associated with these pulses are stored by the data acquisition system. A typical print-out was shown by Chassapis (1988).

In order to automate the analysis of the vast number of associated data, they needed to be first transferred to the computer. This was achieved with the help of a PIO-12 24-bit Parallel Digital I/O Interface Board. The BASIC programs, which were written for this purpose, are now listed in the following:

```
**********************************************************
(1) PROGRAM FOR TRANSFER OF INPUT SHAFT ENCODER
    DATA (CH7) FROM DATA ACQUISITION SYSTEM TO PC
**********************************************************
X--READ IN DATA FROM DATA ACQUISITION
A--WRITE OUT DATA TO PC
I--COUNTER
**********************************************************
20  DIM A(10010)
40  OPEN "O", #1, "A:CH7.TIM"
60  OUT 771, 180
100 FOR I = 1 TO 10010
120 A(I) = 0: C = 0
140 X = INP(768)
160 IF (X = 32 OR X = 13) GOTO 220
170 IF (X > 57 OR X < 48) GOTO 340
180 X = X - 48
200 A(I) = 10 * A(I) + X: GOTO 140
220 C = C + 1
240 IF C = 2 GOTO 420
260 GOTO 140
300 X = INP(768)
320 IF (X = 32 OR X = 13) GOTO 360
340 A(I) = 0: GOTO 300
360 C = C + 1
380 IF C = 2 GOTO 480
400 GOTO 300
420 IF (I = 1 OR I = 2) GOTO 480
440 IF (A(I) = 0) THEN A(I) = A(I - 1): A(I) = 0
480 NEXT I
600 FOR J = 1 TO 1001
610 I = 2 + (J - 1) * 10
620 PRINT #1, A(I)
640 NEXT J
660 CLOSE #1
680 END
```

```
*****************************************************
(2) PROGRAM FOR TRANSFER OF ROCKER SHAFT ENCODER
    DATA DURING FORWARD MOTION (CH2) FROM DATA
    ACQUISITION SYSTEM TO PC
*****************************************************
X--READ IN DATA FROM DATA ACQUISITION
A--WRITE OUT DATA TO PC
I--COUNTER
*****************************************************
20  DIM A(2500)
40  OPEN "O", #1, "A:CH2.TIM"
60  OUT 771, 180
100 FOR I = 1 TO 2500
120 A(I) = 0: C = 0
140 X = INP(768)
160 IF (X = 32 OR X = 13) GOTO 220
170 IF (X > 57 OR X < 48) GOTO 300
180 X = X - 48
200 A(I) = 10 * A(I) + X: GOTO 140
220 C = C + 1
240 IF C = 2 GOTO 420
260 GOTO 140
300 X = INP(768)
320 IF (X = 32 OR X = 13) THEN C = C + 1
380 IF C = 2 GOTO 410
400 GOTO 300
410 A(I) = 0: GOTO 480
420 IF (I = 1 OR I = 2) GOTO 480
440 IF (A(I) = 0) THEN A(I) = A(I - 1): A(I - 1) = 0
480 NEXT
600 FOR I = 1 TO 2500
620 PRINT #1, A(I)
640 NEXT
660 CLOSE #1
680 END
```

```
**********************************************************
(3) PROGRAM FOR TRANSFER OF ROCKER SHAFT ENCODER
    DATA DURING RETURN MOTION (CH3) FROM DATA
    ACQUISITION SYSTEM TO PC
**********************************************************
X--READ IN DATA FROM DATA ACQUISITION
A--WRITE OUT DATA TO PC
I--COUNTER
**********************************************************
20  DIM A(2500)
40  OPEN "O", #1, "A:CH3.TIM"
60  OUT 771, 180
100  FOR I = 1 TO 2500
120  A(I) = 0: C = 0
140  X = INP(768)
160  IF (X = 32 OR X = 13) GOTO 220
170  IF (X > 57 OR X < 48) GOTO 300
180  X = X - 48
200  A(I) = 10 * A(I) + X: GOTO 140
220  C = C + 1
240  IF C = 2 GOTO 420
260  GOTO 140
300  X = INP(768)
320  IF (X = 32 OR X = 13) THEN C = C + 1
380  IF C = 2 GOTO 410
400  GOTO 300
410  A(I) = 0: GOTO 480
420  IF (I = 1 OR I = 2) GOTO 480
440  IF (A(I) = 0) THEN A(I) = A(I - 1): A(I - 1) = 0
480  NEXT
600  FOR I = 1 TO 2500
620  PRINT #1, A(I)
640  NEXT
660  CLOSE #1
680  END
```

```
**********************************************************
(4) PROGRAM FOR TRANSFER OF FEED ROLLER SHAFT ENCODER
    DATA DURING FORWARD MOTION (CH4) FROM DATA
    ACQUISITION SYSTEM TO PC[12]
**********************************************************
X--READ IN DATA FROM DATA ACQUISITION
A--WRITE OUT DATA TO PC
I--COUNTER
**********************************************************
20  DIM A(2500)
40  OPEN "O", #1, "A:CH4.TIM"
60  OUT 771, 180
100 FOR I = 1 TO 2500
120 A(I) = 0: C = 0
140 X = INP(768)
160 IF (X = 32 OR X = 13) GOTO 220
170 IF (X > 57 OR X < 48) GOTO 300
180 X = X - 48
200 A(I) = 10 * A(I) + X: GOTO 140
220 C = C + 1
240 IF C = 2 GOTO 420
260 GOTO 140
300 X = INP(768)
320 IF (X = 32 OR X = 13) THEN C = C + 1
340 IF C = 2 GOTO 410
400 GOTO 300
410 A(I) = 0: GOTO 480
420 IF (I = 1 OR I = 2) GOTO 480
440 IF (A(I) = 0) THEN A(I) = A(I - 1): A(I - 1) = 0
480 NEXT
600 FOR I = 1 TO 2500
620 PRINT #1, A(I)
640 NEXT
660 CLOSE #1
680 END
```

12 The return motion channel of the feed roller shaft encoder never indicated any such motion

The following gives printouts of various angular encoder data of a normal cycle of Run No.1, which were transferred from the data acquisition system to the hard disc of the computer. They will subsequently be used for the determination of the clutch windup angle as a function of the mechanism input angle.

All time counts are in microsecond and are relative to zero time which corresponds to the zero degree position of the input crank. Note that all zeros, but the first of CH7.TIM, represent bad data which are eventually replaced by interpolation and that data are to be read column by column.

(a) Times (μsec) associated with the angular position of the input crank

CH7.TIM (Only one of every ten data are recorded here.)

0	12674	25133	37696	50434	63171	75752	88397	101134	113974
303	12971	25431	37996	50738	63474	76054	88701	101472	114283
606	13270	25726	38296	51048	63775	76353	89002	101743	114592
913	13568	26022	38599	51357	64072	76652	89303	102048	0
1219	13864	26321	38902	51656	64368	76952	89605	102353	115202
1521	14163	26620	39203	51958	64672	77253	89910	102658	115511
1823	14461	26917	39503	52266	64975	77553	90212	102963	115819
0	14759	27214	39806	52575	65272	77852	90513	103268	116125
2434	15054	27513	40109	52876	65568	78152	90815	103573	116429
2737	15351	27812	40411	0	65871	78454	91119	103879	116737
0	15649	28107	40712	53485	66175	78755	91422	104185	117045
3344	15947	28403	41015	53793	66474	79055	91724	104491	117350
3648	16243	28703	41319	54094	66771	79354	92026	104795	117653
3953	16540	29002	41622	54396	67070	79657	92330	105101	117961
4254	16838	29298	41923	54703	67369	79959	92633	105406	118269
4558	17136	29595	42226	55013	67668	80259	92935	0	118574
0	17430	29895	42530	55315	67966	80558	93237	106017	118910
5165	17726	30195	42833	55615	68267	80860	93541	106322	119188
5466	18021	0	43135	55919	68567	81162	93844	106627	119497
5769	18317	30790	43438	56227	68865	81462	94147	106934	119801
6072	18612	31090	43778	56530	69163	81761	94451	107239	120106
6373	18908	31391	44046	56829	69463	82062	94756	107545	120416
6673	19206	31689	44348	57131	69764	82364	95058	107851	120725
6976	0	31986	44652	57437	70064	82665	95360	108158	121029
7278	19799	32286	44957	57740	70361	82964	95664	108464	121331
7579	20095	32588	45262	58041	70661	83266	95969	108769	121639
7878	20393	32888	45564	58346	70961	83569	96271	109076	121947
8180	20689	33185	45868	58654	71260	83871	96573	109383	122251
8482	20983	33485	46173	0	71557	84171	96876	109688	122554
8784	21279	33788	46478	59254	71857	84473	97181	109994	122861
0	21575	34088	46780	59555	72157	84775	0	110300	123170
9386	21872	0	47083	59860	72457	85078	97788	110607	123475
9686	22167	34686	47389	60162	72755	0	98091	110913	123779
9984	22463	34988	47696	60460	73055	85679	98396	111219	124087
10281	22760	35289	47997	60760	73355	85982	98700	111525	124395
10580	23057	35588	48300	61066	73656	86285	99004	111833	124700
10881	23352	35888	48608	61368	73954	86585	99307	112138	125001
11180	0	36190	48915	0	74253	86887	99612	112444	125306
11478	23946	36492	49216	61968	74553	87189	99917	112749	125612
11778	24243	36791	49519	62273	74854	87493	100222	0	125916
12078	24538	37091	49827	62575	75153	87793	100525	113364	126221
12377	24834	37394	0	62873	0	88095	100830	113670	126528

126834	140472	154019	167597	0	194947	208724	222339	235861	249515
127139	140774	154323	167899	181533	195254	209026	222643	236162	249819
127441	141076	154623	168199	181838	195561	209330	222942	236464	250123
127747	141376	154922	168500	0	195866	209637	223238	236767	250428
128054	141678	155224	168805	182446	196171	209940	223573	237069	250735
128358	141981	155529	169108	182749	196479	210242	223844	237371	251038
128659	142282	155828	169408	183053	196787	210549	0	237674	251339
0	142580	156127	169709	183358	197091	210857	224438	237976	0
129269	142882	156429	170014	183662	197395	211160	224739	238279	251947
129573	143186	156734	170316	183964	197702	211496	225043	238582	252250
129875	143489	157035	170616	184269	198011	211772	225341	238885	252552
130180	143788	157333	170919	184575	198315	212080	225637	239188	252858
130487	144088	157635	171225	184879	198620	212379	225939	239490	253164
130792	144391	157940	171527	185182	0	212678	226243	239793	253468
131093	144692	158240	171828	185487	199234	212983	226542	240096	253772
131396	144989	158538	172131	185792	199540	213288	226838	240399	0
131701	145289	158841	172437	186096	199846	213588	227140	240702	254385
132005	145593	159146	172738	186400	200153	213890	227442	0	254685
132337	145896	159448	173039	186704	200461	214197	227741	241309	254986
132608	146193	159748	173343	187010	0	214503	228037	241612	255291
132912	146494	160048	173648	187345	201072	214804	228338	241915	255596
133217	146799	160353	173950	187619	201378	215106	228641	242220	255897
133519	147103	160654	174250	187924	201684	215412	0	242524	256200
133821	147400	160953	174554	188230	201990	215715	229237	242825	256506
134125	147699	161254	174858	188534	202297	216013	229540	243128	256809
134429	148002	161559	175160	188838	202603	216313	229843	243433	0
134731	148305	0	175462	189143	202908	216618	230142	243738	257414
135034	148601	162159	175766	189449	203214	216920	230441	244040	257721
135337	148899	162460	176070	189753	203521	217218	230743	244342	258025
135641	149203	162766	176373	190058	203829	217522	231045	244649	258326
135942	149507	163069	176675	190363	204134	217828	231343	244953	258627
136244	149805	163368	176980	190669	204440	218130	231641	245254	258930
136546	150105	163669	177284	190974	204779	218428	231944	245558	259233
136851	150409	163974	177586	191279	205053	218731	232245	245866	259533
137153	150713	164276	177889	191585	205358	219036	232544	246171	259836
137454	151012	164575	178193	191891	205665	219336	232845	246473	260141
137755	151310	164876	178497	192196	205972	219633	233149	246777	260444
138059	151612	165180	178800	192501	206276	219935	233450	247082	260746
138362	151917	165482	179102	0	206580	220240	233749	247386	261050
138663	152215	165782	179407	193114	206886	220538	234049	247689	261355
138963	152513	166084	179712	193419	207194	220834	234353	247993	261658
0	152815	166389	180015	193725	207499	0	234655	248299	261959
139568	153120	166691	180317	194031	207804	221442	234955	248603	262261
139869	153420	166991	180622	194337	208110	0	235256	248905	262565
140169	153717	167292	180927	194642	208419	222037	235559	249209	262866

263166	276817	290414
263469	277121	290714
263773	277422	291017
264075	277724	291322
264377	278028	291623
264680	278332	291923
264984	278634	292227
265288	278937	292531
265590	279242	292831
265893	279546	293132
266195	279846	293435
0	280149	293739
266798	280454	294040
267101	280757	294341
267405	281058	294681
267708	281361	294950
268010	281666	295250
268315	281967	295551
268619	282267	295856
268922	282605	296160
269225	282874	296460
269529	283174	296762
269833	283473	297067
270136	283776	0
270437	284082	297670
270740	284383	297972
271045	284683	298278
271349	284985	298582
271651	0	298883
271955	285589	299185
272260	285888	299491
0	286191	299797
272868	286495	300098
273207	286796	300400
273476	287096	300704
273779	287398	301007
274082	287702	301307
274386	288002	301609
274690	288301	301913
274994	288604	302216
275297	288908	
275602	289208	
0	289507	
276209	289809	
276512	290113	

(b) Times (μsec) associated with the angular position of the rocker during forward motion

CH2.TIM

6	5821	12215	19539	27227	36521	55444	239541	247908	255445
166	6003	12411	19764	27457	36876	56324	239742	248026	255596
279	6102	12551	19888	27623	37078	57012	240062	248248	255841
449	6275	12761	20100	27870	37425	58119	240219	248391	255964
542	6396	12876	20252	28007	37680	58816	240507	248625	256192
703	6580	13076	20477	28241	38065	60229	240692	248741	256343
817	6679	13217	20602	28410	38286	***61777***	240989	248958	256588
989	6854	13431	20815	28661	38664	***219330***	241135	249100	256711
1081	6976	13548	20967	28801	38941	221197	241404	249331	256941
1245	7162	13750	21194	29040	39362	221939	241577	249447	257093
1358	7263	13894	21319	29212	39603	223137	241858	249665	257339
1531	7439	14111	0	29467	40016	223834	241996	0	257462
1625	7563	14229	21684	29609	40321	0	242252	250041	257691
1789	7751	14434	21911	29853	40782	0	242418	250158	257842
1904	7853	14580	22036	30028	41046	226250	242687	250377	258086
2078	8031	14799	22250	30288	0	226799	242820	250520	258209
2172	0	14920	0	30434	41834	227683	243066	250752	258436
2338	8347	15127	22631	30682	42336	0	243226	250868	258586
2453	8451	15275	22757	30861	42622	228919	243485	251086	258829
2629	8632	15498	22972	31127	43109	229442	243613	251229	258952
0	8759	15620	23126	31276	43471	230298	243851	251464	259178
2890	8952	15830	23356	31530	44015	230720	244006	251581	259328
3006	9057	15980	23483	31713	44327	231501	244257	251801	259568
3183	9241	16203	23699	31987	44856	232004	244382	251946	259689
3278	9370	16326	23854	32141	0	232804	244613	252182	259912
3445	9565	16538	24085	32402	45826	233186	244764	252300	260060
3562	9672	16688	24213	32592	46157	233867	245009	252520	260297
0	9857	16913	24432	32874	46718	234290	245131	252665	260416
3836	9988	17037	24589	33033	47132	234933	245355	252901	260637
4004	10186	17250	24823	33303	47751	235234	245505	253019	260782
4122	10294	17401	24953	33500	48106	235762	245745	253239	0
4300	10481	17627	25174	33794	48714	236089	245864	253386	261134
4397	10614	17751	25333	33959	0	236591	246088	253624	261351
4566	10814	17964	0	34243	49854	236828	246233	253744	261495
4685	10923	18115	25701	34449	50253	237248	246470	253968	261725
4864	11114	18340	25925	34758	50943	237510	246588	254115	261841
4962	11249	18464	26086	34933	51464	237920	246809	254356	262056
5132	11452	18677	26326	35232	52252	238116	246953	254476	262197
5251	11563	18828	26459	35450	52708	238472	247189	254702	262424
5432	11757	19052	26686	35779	53485	238697	247306	254851	262539
5529	11894	19176	26849	35965	54063	239054	247527	255095	262750
5701	0	19388	27092	36286	54937	239226	247671	255217	262889

263113	270109	276099	282082	288491	295008	301091	
263226	270282	276205	282261	288589	295178	301202	
263434	270396	276373	282353	288765	295296	301369	
263571	270579	276460	282521	288886	295476	301460	
263791	270672	276618	282635	289073	295571	301618	
263902	270842	276725	282814	289172	295740	301729	
264108	270955	276894	282907	289349	295857	0	
264243	271134	276981	283076	289471	296035	301989	
264460	271225	0	283191	289658	296129	0	
264569	271392	277141	283370	0	296296	302260	
264771	271503	277418	283464	289935	296412	302430	
264905	271679	277506	283634	290057	296587		
265118	271769	277666	283749	290246	296681		
265226	271933	277774	283929	290346	296846		90°position
265424	272042	277945	284024	290523	296961		during forward
265556	272216	278033	284194	0	297135		motion
265766	272304	278195	284310	290835	297228		
265872	272466	278303	284491	290935	297391		
266068	272574	278475	284586	291113	297504		
266197	272745	278564	284756	291235	297677		
0	272832	278725	284873	291424	297768		
266509	272993	278834	285055	291524	297930		
266701	273099	279007	285150	291701	298043		
266829	273269	279096	285322	291824	298213		
267033	273355	279258	285439	292013	298304		
267136	273514	279368	285621	292112	298464		
267326	273620	279541	285717	292290	298575		
267451	273788	279631	285890	292412	298744		
267651	273874	279794	286008	292600	298835		
267753	274032	279905	286191	292699	298993		
267939	274138	280079	286287	292876	299104		
268062	274306	280169	286459	292998	299272		
268258	0	280333	286578	293184	299361		
268358	274549	280444	286761	293283	299519		
268541	274654	280619	286858	293459	299629		
268662	274822	280710	287031	293580	299796		
268854	274908	280876	287150	293765	0		
268952	275065	280987	287334	293863	300043		
269131	275170	281163	287432	294037	300153		
269250	275338	281255	287606	294157	300320		
269439	275424	281421	287726	294340	300409		
269535	275581	281533	287911	294438	300567		
269712	275687	281710	288009	294610	300677		
269828	275854	281802	288184	294729	300844		
270014	275941	281969	288305	294911	300934		

(c) Times (μsec) associated with the angular position of the rocker during return motion

CH3.TIM

65882	87321	97641	105809	113149	119806	131886	128899	137702	143455
67408	87563	97870	105968	113327	119938	132011	129042	137844	143576
68579	87849	98084	106157	113494	120095	132162	129169	137982	143725
69546	88129	98277	106342	113645	120249	132309	129323	138102	143867
70637	88393	98504	106518	113823	120396	132450	129472	138250	144005
71625	88631	98726	106676	113998	120526	132574	129615	138392	144126
72500	88913	98935	106864	114163	120683	132725	129742	138529	144275
73255	89189	99122	107048	114312	120836	132870	129895	138650	144418
74097	89449	99343	107223	114489	120981	133010	130043	138798	144556
74870	89682	99559	107380	114663	121111	133134	130186	138940	144678
75551	89959	99762	107568	114825	121267	133284	130312	139077*	144827
76131	90229	99945	107752	114972	121419	133429	130464	139198	144971
76774	90484	100161	107926	115147	121564	133569	130612	139347	145110
77357	90713	100372	108083	115318	121693	133692	130754	139487	145232
77869	90985	100570	108270	115479	121848	133841	130880	139624	145382
78305	91250	100749	108454	115624	122000	133986	131032	139745	145526
78795	91500	100960	108628	115797	122143	134125	131180	139892	145666
79251	91725	101167	108785	115965	122272	0	131321	140034	145788
79663	91992	101361	108972	116124	122427	134248	131447	140171	145939
80024	92252	101535	109155	116267	122578	134541	131598	140292	146083
80438	92497	101741	109330	116436	122721	134680	131745	140439	146224
80831	92717	101943	109486	116602	122850	125879	134803	140581	146346
81190	92979	102133	109674	116759	123004	126029	134951	140718	146498
81508	93234	102304	109857	116899	123155	126172	135095	140838	146643
81880	93474	102506	110032	117066	123298	126299	135234	140986	146783
82237	93691	102704	110188	117230	123426	126453	135356	141128	146906
82569	93948	102891	110375	117384	123580	126603	135504	141265	147058
82865	94199	103058	110559	117523	123730	126746	135648	141385	147203
83211	94435	103257	110733	117688	123873	126873	135786	141533	147344
83546	94648	103452	110889	117849	124001	127027	135907	141675	147467
83858	94901	103635	111075	118001	124155	127177	136056	141812	147620
84137	95147	103800	111258	118138	124305	127320	136199	141932	147765
84464	95380	103996	0	118300	124448	127448	136337	142080	147906
84780	95589	104188	111586	118460	124576	127602	136458	142222	148029
85074	95836	104369	111771	118610	124729	127752	136606	142359	148182
85337	96078	104532	111953	118745	124879	127895	136748	142479	148327
85645	96305	104725	112125	118905	125022	128022	136886	142627	148469
85943	96509	104915	112280	119063	125150	128176	137007	142769	148593
86221	96751	105093	112464	119211	125304	128325	137154	142907	148746
86471	96987	105254	112644	119345	125454	128469	137297	143020	148891
86765	0	105445	112815	119503	125597	128596	137434	0	0
87051	97406	105633	112968	119659	125725	128750	137555	143317	149033

* 90° position during return motion.

149310	155734	162388	169602	177592	187286	0
149455	155880	162521	169786	177784	187540	202812
149597	156006	162689	169957	177978	187756	203441
149721	156163	162846	170128	178144	188038	204040
149874	156310	163002	170273	178356	188296	204673
150020	156456	163136	170459	178552	188560	205233
150162	156582	163306	170631	178749	188783	206005
150286	156740	163463	170803	178917	189074	206767
150440	156887	163621	170950	179133	189341	207614
150585	157034	163756	171137	179332	189613	208420
150728	157160	163928	171311	179534	189844	209668
150852	157319	164087	171484	179705	190145	211205
151006	157467	164247	171632	179927	190421	
151152	157615	164383	171821	180130	190702	
151295	157741	164556	171996	180336	190941	
151420	157901	164717	172172	180512	191252	
151575	158050	164879	172321	180739	191538	
151721	158199	165017	172513	180947	0	
151865	158326	165192	172690	181158	192076	
151989	158487	165355	172867	181338	192400	
152145	158636	165517	173019	181570	192697	
152291	158786	165656	173213	181784	193002	
152436	158914	165833	173393	182001	193263	
152561	159075	165997	173572	182185	193606	
152717	159226	166161	173726	182423	193924	
152863	159376	166302	173923	182643	194250	
153008	159504	166480	174104	182865	194528	
153133	159667	166646	174286	183054	194894	
0	159818	166811	0	183298	195233	
153437	159970	166953	174640	183523	195584	
153581	160099	167133	174823	183751	195887	
153707	160263	167300	175007	183945	196288	
153864	160415	0	175164	184197	196659	
154011	160568	167610	175365	184427	197042	
154156	160698	167791	175550	184661	197370	
154281	160863	167960	175735	184860	197804	
154438	161017	168128	175894	185118	198207	
154585	161171	168271	176097	185354	198625	
154730	161302	168454	176285	185594	198984	
0	161469	168622	176473	185798	199463	
155012	161623	168791	176633	186062	199907	
155160	161778	168935	176839	186305	200368	
155305	161910	169118	177029	186552	200769	
155430	162077	169288	177220	186762	201308	
155587	162233	169457	177383	187035	201815	

(d) Times (μsec) associated with the angular position of the roller shaft during forward motion

CH4.TIM

6	4946	10781	17895	25047	32027	44469	237900	245701	251914
107	5095	10925	18134	25187	0	44961	238158	245902	0
258	5206	11110	18298	25398	32417	45629	238484	246036	252261
363	5374	11247	18509	25541	32673	46130	238715	246211	252403
498	5490	11457	18664	25731	32850	46910	239056	246340	252592
599	5641	11603	18901	25870	33085	47437	239274	246537	252731
750	5754	11792	19064	26080	33262	48124	239551	246669	0
854	5925	11932	19273	26223	33532	48621	239751	246841	253092
990	6043	0	19427	26413	33720	0	240048	246969	253285
1092	6196	12296	19662	26553	33971	49852	240240	247163	246211
1244	6311	12488	19823	26763	34161	50477	240486	247294	246340
1349	6485	12631	20031	26907	34450	50924	240665	247464	246537
1485	6606	12850	20183	27097	34652	51600	240934	247590	246669
1586	6762	13003	20414	27238	34923	52053	241109	247784	246841
1739	6879	13201	20572	27451	35127	52642	241333	247914	246969
1844	7057	13346	20777	27596	35440	53072	241498	248084	247163
1982	7180	13570	20927	27789	35657	53739	241746	248210	247294
2084	7340	13725	21156	27932	0	54196	241908	248404	247464
2239	7460	13926	21311	28148	36170	54803	242117	248534	247590
2346	7641	14075	21514	28295	36510	55255	242271	248705	247784
2484	7768	14304	21662	28492	36747	55963	242504	248832	247914
2588	7932	14463	21887	28637	37066	56451	242658	249027	248084
2744	8054	14668	22041	28856	37309	57111	242856	249158	248210
2851	8239	14819	22241	29007	37683	57615	243003	249330	248404
2992	8369	15053	22387	29206	37944	58446	243225	249457	248534
3097	8537	15216	22610	29354	38298	59062	0	249653	248705
3256	8662	15425	22761	0	38567	59980	0	249785	248832
3365	8852	15578	22958	29732	38986	60790	243564	249959	249027
3507	8985	15815	23103	29936	39283	***62533***	243921	250088	249158
3613	9157	15979	23322	30087	39689	***232492***	244064	250288	249330
3773	9284	16191	23470	30316	40000	233393	244250	250422	249457
3884	0	16347	23665	30474	40498	234412	244387	250599	249653
4028	9614	16587	23807	30684	40851	234930	244596	250730	249785
4136	9790	16752	24022	0	41340	235532	244736	250933	249959
4299	9922	16965	0	31075	0	235917	244918	251070	250088
4411	10122	17121	24360	31237	42315	236468	245052	251251	250288
4557	10261	17362	24501	31453	42742	236798	245256	251384	250422
4667	10442	17527	24713	31614	43323	237202	245392	251590	250599
4832	10576	17739	24857	31858	43767	237488	245570	251729	250730

250933	259339	267713	273657	279116	285171	292344	298625
251070	259575	267833	273809	279219	285338	292470	298781
251251	259745	268018	273910	279358	285461	292659	298891
251384	260010	268140	274046	279458	285650	292788	299033
251590	260187	268303	274144	279612	285778	292957	299136
251729	260422	268421	274295	279717	285949	293081	299292
251914	260591	268601	274396	279857	286075	293266	299400
0	260854	268720	274531	279958	286267	293393	299541
252261	261029	268878	274628	280114	286398	293560	299644
252403	261263	268993	274778	280220	286572	293681	299798
252592	261430	269168	274878	280363	286700	293863	0
252731	261689	269284	275013	280466	286896	293988	300044
0	261861	269438	275110	0	287029	294152	300146
253092	262091	269550	275259	280731	287206	294271	300299
253285	262255	269721	275360	280876	287336	294450	300406
253427	262507	269834	275494	280980	287534	294572	300545
253648	262675	269985	275591	281140	287669	294733	300646
253797	262898	270094	275740	281250	0	294858	300798
253996	263057	270262	275840	281397	287980	295024	300904
254142	263302	270372	275974	281503	288181	295145	301042
254368	263463	270519	276070	281667	288317	295302	301143
254521	0	270626	276219	281778	288498	295417	301294
254726	263829	270791	276319	281928	288631	295588	301400
254876	264064	270899	276453	282036	288832	295706	301537
255110	264218	271044	276550	282203	288969	295861	301638
255268	264423	271150	276698	282316	289150	295972	301789
255479	264569	271311	276798	282469	289284	296140	301894
255634	264793	271418	276932	282579	289485	296257	302030
255876	264941	271560	277029	282749	289621	296408	302130
256040	265137	271664	277177	282865	289801	296518	302281
256259	265277	271823	277278	283021	289934	296683	302382
256419	265492	271928	277412	283134	290135	296797	
256669	265633	272069	277509	283307	290271	296946	
256838	265821	272171	277658	283424	290450	297054	
257065	265955	272328	277759	283583	290581	297216	
257229	266161	272432	277894	283698	290779	297330	
257485	266296	272571	277991	283875	290912	297477	
257658	266476	272671	278140	283995	291089	297584	
257890	266605	272826	278241	284156	291219	297744	
258058	266802	272929	278378	284274	291414	297856	
258319	266932	273067	278475	284454	291547	298001	
258494	267105	273167	278626	284576	291721	298107	
258729	267229	273320	278728	284741	291849	298265	
258898	267420	273422	278865	284862	292041	298377	
259162	267545	273558	278964	285046	292172	298520	

To compute the clutch windup angle it is necessary to further know the following:

(e) The times associated with the 90° reference positions of the rocker, which are given in the output of CH2.TIM and CH3.TIM (actually obtained by a different channel of the identical encoder).

During return motion: 139077 μsec

During forward motion: 290346 μsec

Both are indicated in applicable printouts

(f) The time interval between the end of the first part of the forward motion of the rocker and the beginning of the second part. (They are interrupted by the return stroke.) According to the bold-italic numbers of CH2.TIM, this interval is given by:

219330-61777=157553 μsec

(g) The time interval between the end of the first part of the forward motion of the feed roller shaft and the beginning of the second part. (They are interrupted by the return stroke.) According to the bold-italic numbers of CH4.TIM, this interval is given by:

232492-62533=169959 μsec

b. Determination of Windup Angle $\phi_{5/4}$

(1) Program

Using the above data, the rocker angle ϕ_4, the roller shaft angle ϕ_5 and the windup angle $\phi_{5/4}$ may be obtained, as a function of the input crank position, with the help of the following FORTRAN program:

```
**************************************************************************
THE FOLLOWING PROGRAM IS WRITTEN FOR DETERMINING THE ROCKER
ANGULAR POSITIONS PHI4 AND ROLLER SHAFT ANGLE PHI5F IN TERMS
OF THE INPUT CRANK ANGLE PHI1.
**************************************************************************
PHI4F-ABS ROCKER ANGLE AS FUNCTION OF TIME (FORWARD STROKE)
PHI4R-ABS ROCKER ANGLE AS FUNCTION OF TIME (RETURN STROKE)
PHI5F-REL ROLLER ANGLE AS FUNCTION OF TIME (FORWARD STROKE)
PHI4A-ABS ROCKER ANGLE AS FUNCTION OF PHI1 (ONE COMPLETE CYCLE)
PHI4RF-REL ROCKER ANGLE AS FUNCTION OF PHI1 (FORWARD STROKE)
PHI5RF-REL ROLLER SHAFT ANGLE AS FUNCTION OF PHI1
**************************************************************************
      REAL PHI1(1000),PHI4F(2300),PHI4R(2300),PHI5F(2300)
      REAL PHI4A(1000),PHI4RF(1000),PHI5RF(1000)
      REAL T4MAX,T4MIN,PHI1MAX,PHI1MIN,PHI4MAX,PHI4MIN
      INTEGER I,J,D4,D5,A,L,N,M,T1(1000),T4F(2300),T4R(2300),T5F(2300)
      INTEGER T42,T44,T45,T46,T47,T48,T52,T56,T58,TR4,TR7
* READ TIME T1 FROM DATA FILE "CH7.TIM" *
      OPEN (UNIT=1,FILE='A:CH7.TIM')
      I=0
 10   READ (1,20,END=30) A
 20   FORMAT (I7)
      I=I+1
      T1(I)=A
      GOTO 10
* FIX ZEROES AND BAD DATA IN THE DATA T1(I) *
 30   DO 40 I=2,1000
      IF (T1(I) .EQ. 0) T1(I)=T1(I-2)+(T1(I-2)-T1(I-4))
      IF ((T1(I-1) .LE. T1(I-2)) .OR. (T1(I-1) .GE. T1(I))) THEN
```

```
      T1(I-1)=(T1(I-2)-T1(I-4))+T1(I-3)
      END IF
 40   CONTINUE
* DETERMINE ANGULAR POSITIONS PHI1 & GIVE ZEROS TO PHI4 & PHI5 *
      DO 60 I=1,1000
      PHI1(I)=(I-1)*0.36
      PHI41F(I)=0.0
      PHI51F(I)=0.0
 60   CONTINUE
* READ 90 DEGREE REFERENCE DATA AND DWELL TIME *
      OPEN (UNIT=2,FILE='A:CH1.TIM')
      READ (2,90) TR7,TR4,D4,D5
 90   FORMAT (I7)
* READ TIME T4F FROM DATA FILE "CH2.TIM"*
      OPEN (UNIT=3,FILE='A:CH2.TIM')
      I=0
 110  READ (3,120,END=100) A
 120  FORMAT (I7)
      I=I+1
      T4F(I)=A
      GOTO 110
 100  T48=I
* FIX ZEROES & BAD DATA IN THE DATA T4F(I) & OBTAIN T42,T46,T47 *
      DO 140 I=2,T48
      IF (T4F(I) .EQ. 0) T4F(I)=T4F(I-2)+(T4F(I-2)-T4F(I-4))
      IF ((T4F(I-1) .LE. T4F(I-2)) .OR. (T4F(I-1) .GE. T4F(I))) THEN
      T4F(I-1)=T4F(I-2)-T4F(I-4)+T4F(I-3)
      END IF
      IF ((T4F(I)-T4F(I-1)) .EQ. D4) THEN
      T42=I-1
      T46=I
      END IF
      IF (T4F(I) .EQ. TR7) T47=I
 140  CONTINUE
* DETERMINATION OF ANGULAR POSITIONS PHI4F *
      DO 150 I=T47,T42
      PHI4F(I)=90+(T47-I)*0.036
 150  CONTINUE
      DO 160 I=T47,1,-1
      PHI4F(I)=90+(T47-I)*0.036
 160  CONTINUE
```

```
      DO 170 I=T48,T46,-1
      PHI4F(I)=PHI4F(1)+(T48+1-I)*0.036
170   CONTINUE
* READ TIME T4R FROM DATA FILE "CH3.TIM" *
      I=0
      OPEN (UNIT=4,FILE='A:CH3.TIM')
510   READ (4,520,END=530) A
520   FORMAT (I7)
      I=I+1
      T4R(I)=A
      GOTO 510
530   T45=I
* FIX ZEROES & BAD DATA IN THE DATA T4R(I) & OBTAIN T44 *
      DO 540 I=1,T45
      IF (T4R(I) .EQ. 0) T4R(I)=T4R(I-2)+(T4R(I-2)-T4R(I-4))
      IF ((T4R(I-1) .LE. T4R(I-2)) .OR. (T4R(I-1) .GE. T4R(I))) THEN
      T4R(I-1)=T4R(I-2)-T4R(I-4)+T4R(I-3)
      END IF
      IF (T4R(I) .EQ. TR4) T44=I
540   CONTINUE
* DETERMINATION OF ANGULAR POSITIONS PHI4R *
      DO 550 I=T44,1,-1
      PHI4R(I)=90-(T44-I)*0.036
550   CONTINUE
      DO 560 I=T44,T45
      PHI4R(I)=90+(I-T44)*0.036
560   CONTINUE
* FIND THE MAX AND MIN PHI4 AS WELL AS ASSOCIATED TIME *
      PHI4MAX=PHI4F(T46)+0.018
      PHI4MIN=PHI4F(T42)-0.018
      T4MAX=(T4R(T45)+T4F(T46))/2
      T4MIN=(T4F(T42)+T4R(1))/2
* READ TIME T5F FROM DATA FILE "CH4.TIM" *
      OPEN (UNIT=6,FILE='A:CH4.TIM')
      I=0
180   READ (6,190,END=200) A
190   FORMAT (I7)
      I=I+1
      T5F(I)=A
      GOTO 180
200   T58=I
* FIX ZEROES IN THE DATA T5F AND OBTAIN T52 AND T56 *
```

```
      DO 240 I=2,T58
      IF (T5F(I) .EQ. 0) T5F(I)=T5F(I-2)+(T5F(I-2)-T5F(I-4))
      IF ((T5F(I-1) .LE. T5F(I-2)) .OR. (T5F(I-1) .GE. T5F(I))) THEN
      T5F(I-1)=T5F(I-2)-T5F(I-4)+T5F(I-3)
      END IF
      IF ((T5F(I)-T5F(I-1)) .EQ. D5) THEN
      T52=I-1
      T56=I
      END IF
240   CONTINUE
* DETERMINATION OF ANGULAR POSITIONS PHI5F *
      DO 250 I=T56,T58
      PHI5F(I)=0.018+(I-T56)*0.036
250   CONTINUE
      DO 260 I=1,T52
      PHI5F(I)=PHI5F(T58)+I*0.036
260   CONTINUE
* DETERMINATION OF ROCKER ANGLES PHI4 IN TERMS OF PHI1 *
      N=1
      M=1
      L=T46
      DO 300 I=2,1000
      IF ((T1(I) .GT. T4F(T42)) .AND. (T1(I) .LT. T4R(1))) GOTO 380
      IF ((T1(I) .GE. T4R(1)) .AND. (T1(I) .LE. T4R(T45))) GOTO 360
      IF ((T1(I) .GT. T4R(T45)) .AND. (T1(I) .LT. T4F(T46))) GOTO 380
      IF (T1(I) .GE. T4F(T46)) GOTO 340
* FIND PHI4A & PHI4RF WHEN T1(I) IS BETWEEN T4F(T41) & T4F(T42) *
      DO 320 J=N,(T42-1)
      IF ((T1(I) .GE. T4F(J)) .AND. (T1(I) .LE. T4F(J+1))) THEN
      PHI4A(I)=(PHI4F(J)+(T1(I)-T4F(J))*(PHI4F(J+1)-PHI4F(J))
     1/(T4F(J+1)-T4F(J)))
      PHI4RF(I)=PHI4MAX-PHI4A(I)
      N=J
      GOTO 300
      END IF
320   CONTINUE
* DETERMINE PHI4A BETWEEN TIME T4R(T43) TO T4R(T45) *
360   DO 370 J=M,(T45-1)
      IF ((T1(I) .GE. T4R(J)) .AND. (T1(I) .LE. T4R(J+1))) THEN
      PHI4A(I)=PHI4R(J)+(T1(I)-T4R(J))*(PHI4R(J+1)-PHI4R(J))
     1/(T4R(J+1)-T4R(J))
      M=J
```

```
      GOTO 300
      END IF
 370  CONTINUE
* FIND PHI4A & PHI4RF WHEN T1(I) IS BETWEEN T4F(T46) AND T4F(T48) *
 340  DO 330 J=L,(T48-1)
      IF ((T1(I) .GE. T4F(J)) .AND. (T1(I) .LE. T4F(J+1))) THEN
      PHI4A(I)=PHI4F(J)+(T1(I)-T4F(J))*(PHI4F(J+1)-PHI4F(J))
     1/(T4F(J+1)-T4F(J))
      PHI4RF(I)=PHI4MAX-PHI4A(I)
      L=J
      GOTO 300
      END IF
 330  CONTINUE
* FIND PHI4A & PHI4RF WHEN T1(I) IS LARGER THAN T4F(T48) *
      PHI4A(I)=2*PHI4A(I-1)-PHI4A(I-2)
      PHI4RF(I)=PHI4MAX-PHI4A(I)
      GOTO 300
* DETERMINE ANGLES OF PHI1 ASSOCIATED WITH PHI4MAX & PHI4MIN *
 380  PHI4A(I)=0
      IF ((T1(I) .LE. T4MIN) .AND. (T1(I+1) .GE. T4MIN)) THEN
      PHI1MIN=PHI1(I)+(T4MIN-T1(I))*(PHI1(I+1)-PHI1(I))/
     1(T1(I+1)-T1(I))
      END IF
      IF ((T1(I) .LE. T4MAX) .AND. (T1(I+1) .GE. T4MAX)) THEN
      PHI1MAX=PHI1(I)+(T4MAX-T1(I))*(PHI1(I+1)-PHI1(I))/
     1(T1(I+1)-T1(I))
      END IF
 300  CONTINUE
* DETERMINE PHI4A & PHI4RF AT TIME T1(1)=0 *
      PHI4A(1)=(PHI4A(2)+PHI4A(1000))/2
      PHI4RF(1)=PHI4MAX-PHI4A(1)
* DETERMINATION RELATIVE ROLLER ANGLES PHI5RF IN TERMS OF PHI1 *
      N=1
      M=T56
      DO 400 I=1,1000
      IF (T1(I) .EQ. 0) GOTO 400
      IF ((T1(I) .GT. T5F(T52)) .AND. (T1(I) .LT. T5F(T56))) GOTO 400
      IF (T1(I) .GE. T5F(T56)) GOTO 440
* FIND PHI5RF WHEN T1(I) IS BETWEEN T5F(T51) AND T5F(T52) *
```

```
      DO 420 J=N,(T52-1)
      IF ((T1(I) .GE. T5F(J)) .AND. (T1(I) .LE. T5F(J+1))) THEN
      PHI5RF(I)=PHI5F(J)+(T1(I)-T5F(J))*(PHI5F(J+1)-PHI5F(J))
     1/(T5F(J+1)-T5F(J))
      N=J
      GOTO 400
      END IF
 420  CONTINUE
* FIND PHI5RF WHEN T1(I) IS BETWEEN T5F(T56) AND T5F(T58) *
 440  DO 430 J=M,(T58-1)
      IF ((T1(I) .GE. T5F(J)) .AND. (T1(I) .LE. T5F(J+1))) THEN
      PHI5RF(I)=PHI5F(J)+(T1(I)-T5F(J))*(PHI5F(J+1)-PHI5F(J))
     1/(T5F(J+1)-T5F(J))
      M=J
      GOTO 400
      END IF
 430  CONTINUE
* FIND THE PHI5RF WHEN T1(I) IS LARGER THAN T5F(T58) *
      PHI5RF(I)=2*PHI5RF(I-1)-PHI5RF(I-2)
 400  CONTINUE
* DETERMINE PHI5RF AT TIME T1(1)=0 *
      PHI5RF(1)=(PHI5RF(2)+PHI5RF(1000))/2
* OUTPUT THE RESULTS TOGETHER WITH THE INPUT DATA *
      OPEN (UNIT=7,FILE='A:PHI541.DAT')
      WRITE (7,460) PHI1MAX,PHI4MAX,PHI1MIN,PHI4MIN
      WRITE (7,470)
      WRITE (7,450) (PHI1(I),PHI4A(I),PHI4RF(I),PHI5RF(I),
     1(PHI4RF(I)-PHI5RF(I)),I=1,1000)
 450  FORMAT (I6,2X,F7.3,2X,F7.3,2X,F7.3,2X,F7.3,F7.3)
 460  FORMAT ('AT PHI1=',F10.3,2X,'PHI4MAX=',F10.3,2X,'AT PHI1=',F10.3,
     12X,'PHI4MIN=',F10.3)
 470  FORMAT (6X,'PHI1',5X,'PHI4A',5X,'PHI4R'4X,'PHI5R',
     13X,'PHI5/4')
      STOP
      END
```

(2) Output of the Angles for Run No.1 (Normal)

The output shown below lists the following angles as functions of the input shaft angle PHI1 (These are the data for Figure 7b):

PHI4A = absolute rocker angle, which extends from its maximum value PHI4MAX=102.76 degree, at the beginning of the forward stroke, to its minimum value PHI4MIN=77.55 degree, at the end of the forward stroke.

PHI4R = relative rocker angle, which is defined as PHI4MAX-PHI4A, during forward stroke.

PHI5R = relative roller shaft angle with respect to PHI4MAX during forward stroke.

PHI5/4 = PHI4R-PHI5R

PHI1	PHI4A	PHI4R	PHI5R	PHI5/4	
.000	86.835	15.927	15.426	.501	<- beginning
.360	86.755	16.007	15.513	.494	of second part
.720	86.674	16.088	15.608	.481	of forward
1.080	86.596	16.166	15.694	.472	motion
1.440	86.514	16.248	15.780	.468	
1.800	86.438	16.324	15.871	.453	
2.160	86.353	16.409	15.959	.450	
2.520	86.272	16.490	16.048	.441	
2.880	86.190	16.572	16.133	.439	
3.240	86.111	16.651	16.216	.434	
3.600	86.032	16.730	16.308	.422	
3.960	85.954	16.808	16.391	.417	
4.320	85.875	16.887	16.478	.409	
4.680	85.799	16.963	16.559	.404	
5.040	85.725	17.037	16.640	.397	
5.400	85.646	17.116	16.722	.394	
5.760	85.573	17.189	16.803	.386	
6.120	85.490	17.272	16.889	.383	
6.480	85.415	17.347	16.967	.380	
6.840	85.336	17.426	17.049	.377	
7.200	85.259	17.503	17.125	.378	
7.560	85.183	17.579	17.203	.376	
7.920	85.106	17.656	17.277	.378	
8.280	85.032	17.730	17.354	.376	
8.640	84.957	17.805	17.428	.377	
9.000	84.885	17.877	17.502	.375	
9.360	84.811	17.951	17.574	.377	
9.720	84.737	18.025	17.647	.378	
10.080	84.666	18.096	17.718	.378	
10.440	84.595	18.167	17.789	.378	
10.800	84.522	18.240	17.859	.381	
11.160	84.453	18.309	17.931	.378	
11.520	84.381	18.381	17.997	.384	

PHI1	PHI4A	PHI4R	PHI5R	PHI5/4
11.880	84.313	18.449	18.065	.384
12.240	84.244	18.518	18.130	.388
12.600	84.177	18.585	18.199	.386
12.960	84.110	18.652	18.259	.393
13.320	84.042	18.720	18.324	.395
13.680	83.980	18.782	18.383	.399
14.040	83.910	18.852	18.447	.404
14.400	83.840	18.922	18.513	.409
14.760	83.778	18.984	18.573	.411
15.120	83.715	19.047	18.637	.410
15.480	83.647	19.115	18.694	.421
15.840	83.583	19.179	18.755	.424
16.200	83.516	19.246	18.810	.436
16.560	83.456	19.307	18.871	.436
16.920	83.396	19.366	18.932	.434
17.280	83.333	19.429	18.990	.439
17.640	83.275	19.487	19.048	.440
18.000	83.209	19.553	19.098	.455
18.360	83.148	19.614	19.157	.457
18.720	83.083	19.679	19.217	.462
19.080	83.024	19.738	19.271	.467
19.440	82.968	19.794	19.326	.468
19.800	82.908	19.854	19.379	.476
20.160	82.848	19.914	19.437	.477
20.520	82.783	19.979	19.496	.482
20.880	82.723	20.039	19.545	.494
21.240	82.663	20.099	19.600	.499
21.600	82.606	20.156	19.657	.499
21.960	82.552	20.210	19.713	.497
22.320	82.487	20.275	19.770	.505
22.680	82.427	20.335	19.820	.515
23.040	82.363	20.399	19.878	.521
23.400	82.306	20.456	19.937	.519
23.760	82.250	20.512	19.993	.520
24.120	82.189	20.573	20.049	.524
24.480	82.129	20.633	20.103	.530
24.840	82.065	20.697	20.163	.534
25.200	82.005	20.757	20.223	.534
25.560	81.948	20.814	20.279	.536
25.920	81.899	20.863	20.337	.526

PHI1	PHI4A	PHI4R	PHI5R	PHI5/4
26.280	81.834	20.928	20.392	.536
26.640	81.770	20.992	20.453	.539
27.000	81.709	21.053	20.514	.539
27.360	81.647	21.115	20.574	.541
27.720	81.592	21.170	20.635	.535
28.080	81.541	21.221	20.689	.532
28.440	81.476	21.286	20.751	.535
28.800	81.418	21.344	20.813	.531
29.160	81.355	21.407	20.878	.528
29.520	81.300	21.462	20.940	.522
29.880	81.249	21.513	21.000	.513
30.240	81.187	21.575	21.064	.511
30.600	81.126	21.636	21.122	.514
30.960	81.068	21.694	21.185	.509
31.320	81.014	21.748	21.248	.500
31.680	80.965	21.797	21.313	.485
32.040	80.902	21.860	21.377	.482
32.400	80.846	21.916	21.440	.476
32.760	80.787	21.975	21.504	.471
33.120	80.736	22.026	21.561	.465
33.480	80.684	22.078	21.624	.454
33.840	80.625	22.137	21.683	.454
34.200	80.569	22.193	21.746	.447
34.560	80.521	22.241	21.809	.432
34.920	80.466	22.296	21.869	.427
35.280	80.412	22.350	21.928	.422
35.640	80.356	22.406	21.986	.420
36.000	80.307	22.455	22.043	.412
36.360	80.257	22.505	22.103	.402
36.720	80.200	22.562	22.161	.401
37.080	80.150	22.612	22.216	.396
37.440	80.105	22.657	22.269	.388
37.800	80.048	22.714	22.328	.387
38.160	79.997	22.765	22.385	.380
38.520	79.956	22.806	22.437	.369
38.880	79.900	22.862	22.487	.375
39.240	79.849	22.913	22.542	.371
39.600	79.809	22.953	22.596	.357
39.960	79.756	23.006	22.646	.360
40.320	79.707	23.055	22.692	.364

PHI1	PHI4A	PHI4R	PHI5R	PHI5/4
40.680	79.669	23.093	22.744	.350
41.040	79.616	23.146	22.792	.354
41.400	79.570	23.192	22.835	.357
41.760	79.532	23.230	22.883	.347
42.120	79.481	23.281	22.925	.355
42.480	79.443	23.319	22.969	.351
42.840	79.401	23.361	23.011	.351
43.200	79.359	23.403	23.050	.353
43.560	79.319	23.443	23.096	.347
43.920	79.276	23.486	23.128	.357
44.280	79.245	23.517	23.171	.346
44.640	79.199	23.563	23.206	.358
45.000	79.167	23.595	23.246	.349
45.360	79.127	23.635	23.276	.360
45.720	79.098	23.664	23.315	.348
46.080	79.055	23.707	23.346	.361
46.440	79.026	23.736	23.385	.351
46.800	78.989	23.773	23.411	.362
47.160	78.962	23.800	23.444	.356
47.520	78.927	23.835	23.474	.362
47.880	78.894	23.868	23.504	.364
48.240	78.865	23.897	23.534	.363
48.600	78.833	23.929	23.556	.373
48.960	78.809	23.953	23.584	.369
49.320	78.772	23.990	23.610	.380
49.680	78.748	24.014	23.632	.381
50.040	78.723	24.039	23.662	.377
50.400	78.690	24.072	23.683	.389
50.760	78.668	24.094	23.701	.393
51.120	78.636	24.126	23.724	.402
51.480	78.608	24.154	23.748	.406
51.840	78.585	24.177	23.766	.410
52.200	78.555	24.207	23.787	.419
52.560	78.532	24.230	23.815	.416
52.920	78.512	24.250	23.828	.421
53.280	78.479	24.283	23.844	.440
53.640	78.458	24.304	23.863	.441
54.000	78.433	24.329	23.886	.443
54.360	78.404	24.358	23.902	.456

PHI1	PHI4A	PHI4R	PHI5R	PHI5/4
54.720	78.387	24.375	23.918	.457
55.080	78.367	24.395	23.939	.455
55.440	78.335	24.427	23.960	.467
55.800	78.315	24.447	23.974	.473
56.160	78.295	24.467	23.988	.479
56.520	78.268	24.494	24.006	.488
56.880	78.249	24.513	24.027	.486
57.240	78.231	24.531	24.044	.487
57.600	78.203	24.559	24.059	.500
57.960	78.181	24.581	24.079	.503
58.320	78.162	24.600	24.101	.499
58.680	78.136	24.626	24.117	.509
59.040	78.114	24.648	24.132	.516
59.400	78.100	24.662	24.151	.512
59.760	78.085	24.677	24.172	.504
60.120	78.060	24.702	24.190	.513
60.480	78.039	24.723	24.208	.516
60.840	78.023	24.739	24.231	.508
61.200	78.005	24.757	24.253	.505
61.560	77.983	24.779	24.269	.510
61.920	77.967	24.795	24.286	.508
62.280	77.953	24.809	24.310	.498
62.640	77.939	24.823	24.331	.492
63.000	77.915	24.848	24.350	.498
63.360	77.896	24.866	24.374	.492
63.720	77.882	24.880	24.396	.484
64.080	77.868	24.894	24.412	.482
64.440	77.849	24.913	24.430	.483
64.800	77.831	24.931	24.454	.477
65.160	77.818	24.944	24.474	.470
65.520	77.806	24.956	24.492	.464
65.880	77.791	24.971	24.515	.457
66.240	77.769	24.993	24.537	.456
66.600	77.753	25.009	24.552	.457
66.960	77.741	25.021	24.568	.454
67.320	77.728	25.034	24.589	.445
67.680	77.713	25.049	24.610	.438
68.040	77.698	25.064	24.627	.438

PHI1	PHI4A	PHI4R	PHI5R	PHI5/4	
68.400	77.684	25.078	24.643	.434	
68.760	77.674	25.088	24.665	.423	
69.120	77.664	25.098	24.683	.414	
69.480	77.655	25.107	24.696	.411	
69.840	77.640	25.122	24.710	.412	
70.200	77.624	25.138	24.726	.411	
70.560	77.613	25.149	24.744	.406	
70.920	77.605	25.157	24.758	.400	
71.280	77.597	25.165	24.769	.396	
71.640	77.589	25.173	24.781	.391	
72.000	77.582	25.180	24.794	.386	
72.360	77.575	25.187	24.807	.380	
72.720	77.568	25.194	24.821	.374	
73.080	77.561	25.201	24.828	.374	
73.440	77.554	25.208	24.834	.375	
73.800	77.546	25.216	24.840	.375	<- end of
74.160	-	-	24.846	-	second part
74.520	-	-	24.853	-	of forward
74.880	-	-	-	-	motion
75.240	-	-	-	-	
75.600	-	-	-	-	
75.960	-	-	-	-	
76.320	-	-	-	-	
76.680	-	-	-	-	
77.040	-	-	-	-	
77.400	-	-	-	-	
77.760	-	-	-	-	
78.120	-	-	-	-	
78.480	-	-	-	-	
78.840	-	-	-	-	
79.200	77.551	-	-	-	<- beginning
79.560	77.558	-	-	-	of return
79.920	77.565	-	-	-	motion
80.280	77.572	-	-	-	
80.640	77.579	-	-	-	
81.000	77.588	-	-	-	
81.360	77.597	-	-	-	
81.720	77.606	-	-	-	

PHI1	PHI4A	PHI4R	PHI5R	PHI5/4
82.080	77.616	-	-	-
82.440	77.627	-	-	-
82.800	77.638	-	-	-
83.160	77.649	-	-	-
83.520	77.659	-	-	-
83.880	77.669	-	-	-
84.240	77.679	-	-	-
84.600	77.689	-	-	-
84.960	77.700	-	-	-
85.320	77.711	-	-	-
85.680	77.722	-	-	-
86.040	77.734	-	-	-
86.400	77.746	-	-	-
86.760	77.758	-	-	-
87.120	77.772	-	-	-
87.480	77.786	-	-	-
87.840	77.800	-	-	-
88.200	77.813	-	-	-
88.560	77.826	-	-	-
88.920	77.839	-	-	-
89.280	77.853	-	-	-
89.640	77.867	-	-	-
90.000	77.883	-	-	-
90.360	77.899	-	-	-
90.720	77.916	-	-	-
91.080	77.935	-	-	-
91.440	77.952	-	-	-
91.800	77.969	-	-	-
92.160	77.987	-	-	-
92.520	78.006	-	-	-
92.880	78.026	-	-	-
93.240	78.047	-	-	-
93.600	78.071	-	-	-
93.960	78.095	-	-	-
94.320	78.117	-	-	-
94.680	78.141	-	-	-
95.040	78.165	-	-	-

PHI1	PHI4A	PHI4R	PHI5R	PHI5/4
95.400	78.191	-	-	-
95.760	78.222	-	-	-
96.120	78.248	-	-	-
96.480	78.275	-	-	-
96.840	78.303	-	-	-
97.200	78.333	-	-	-
97.560	78.367	-	-	-
97.920	78.396	-	-	-
98.280	78.426	-	-	-
98.640	78.458	-	-	-
99.000	78.492	-	-	-
99.360	78.526	-	-	-
99.720	78.558	-	-	-
100.080	78.591	-	-	-
100.440	78.626	-	-	-
100.800	78.664	-	-	-
101.160	78.697	-	-	-
101.520	78.731	-	-	-
101.880	78.769	-	-	-
102.240	78.809	-	-	-
102.600	78.844	-	-	-
102.960	78.881	-	-	-
103.320	78.921	-	-	-
103.680	78.962	-	-	-
104.040	78.999	-	-	-
104.400	79.038	-	-	-
104.760	79.082	-	-	-
105.120	79.121	-	-	-
105.480	79.160	-	-	-
105.840	79.201	-	-	-
106.200	79.245	-	-	-
106.560	79.284	-	-	-
106.920	79.324	-	-	-
107.280	79.368	-	-	-
107.640	79.410	-	-	-
108.000	79.450	-	-	-
108.360	79.493	-	-	-

PHI1	PHI4A	PHI4R	PHI5R	PHI5/4
108.720	79.537	-	-	-
109.080	79.578	-	-	-
109.440	79.621	-	-	-
109.800	79.668	-	-	-
110.160	79.709	-	-	-
110.520	79.751	-	-	-
110.880	79.798	-	-	-
111.240	79.842	-	-	-
111.600	79.884	-	-	-
111.960	79.931	-	-	-
112.320	79.977	-	-	-
112.680	80.021	-	-	-
113.040	80.067	-	-	-
113.400	80.115	-	-	-
113.760	80.159	-	-	-
114.120	80.205	-	-	-
114.480	80.255	-	-	-
114.840	80.300	-	-	-
115.200	80.347	-	-	-
115.560	80.398	-	-	-
115.920	80.443	-	-	-
116.280	80.493	-	-	-
116.640	80.543	-	-	-
117.000	80.591	-	-	-
117.360	80.641	-	-	-
117.720	80.695	-	-	-
118.080	80.744	-	-	-
118.440	80.797	-	-	-
118.800	80.850	-	-	-
119.160	80.901	-	-	-
119.520	80.958	-	-	-
119.880	81.010	-	-	-
120.240	81.064	-	-	-
120.600	81.122	-	-	-
120.960	81.174	-	-	-
121.320	81.239	-	-	-
121.680	81.288	-	-	-
122.040	81.344	-	-	-
122.400	81.405	-	-	-
122.760	81.460	-	-	-

PHI1	PHI4A	PHI4R	PHI5R	PHI5/4
123.120	81.520	-	-	-
123.480	81.578	-	-	-
123.840	81.636	-	-	-
124.200	81.699	-	-	-
124.560	81.755	-	-	-
124.920	81.819	-	-	-
125.280	81.877	-	-	-
125.640	81.938	-	-	-
126.000	82.001	-	-	-
126.360	82.060	-	-	-
126.720	82.125	-	-	-
127.080	82.184	-	-	-
127.440	82.249	-	-	-
127.800	82.310	-	-	-
128.160	82.372	-	-	-
128.520	82.436	-	-	-
128.880	82.496	-	-	-
129.240	82.562	-	-	-
129.600	82.622	-	-	-
129.960	82.688	-	-	-
130.320	82.748	-	-	-
130.680	82.812	-	-	-
131.040	82.875	-	-	-
131.400	82.936	-	-	-
131.760	83.002	-	-	-
132.120	83.062	-	-	-
132.480	83.129	-	-	-
132.840	83.188	-	-	-
133.200	83.255	-	-	-
133.560	83.316	-	-	-
133.920	83.379	-	-	-
134.280	83.444	-	-	-
134.640	83.506	-	-	-
135.000	83.573	-	-	-
135.360	83.636	-	-	-
135.720	83.705	-	-	-
136.080	83.767	-	-	-
136.440	83.837	-	-	-
136.800	83.901	-	-	-

PHI1	PHI4A	PHI4R	PHI5R	PHI5/4
137.160	83.969	-	-	-
137.520	84.036	-	-	-
137.880	84.104	-	-	-
138.240	84.173	-	-	-
138.600	84.240	-	-	-
138.960	84.311	-	-	-
139.320	84.379	-	-	-
139.680	84.451	-	-	-
140.040	84.520	-	-	-
140.400	84.592	-	-	-
140.760	84.663	-	-	-
141.120	84.737	-	-	-
141.480	84.807	-	-	-
141.840	84.889	-	-	-
142.200	84.954	-	-	-
142.560	85.031	-	-	-
142.920	85.103	-	-	-
143.280	85.179	-	-	-
143.640	85.254	-	-	-
144.000	85.330	-	-	-
144.360	85.405	-	-	-
144.720	85.479	-	-	-
145.080	85.557	-	-	-
145.440	85.631	-	-	-
145.800	85.710	-	-	-
146.160	85.782	-	-	-
146.520	85.863	-	-	-
146.880	85.936	-	-	-
147.240	86.015	-	-	-
147.600	86.088	-	-	-
147.960	86.168	-	-	-
148.320	86.243	-	-	-
148.680	86.321	-	-	-
149.040	86.395	-	-	-
149.400	86.472	-	-	-
149.760	86.548	-	-	-
150.120	86.625	-	-	-
150.480	86.702	-	-	-
150.840	86.778	-	-	-

PHI1	PHI4A	PHI4R	PHI5R	PHI5/4
151.200	86.857	-	-	-
151.560	86.931	-	-	-
151.920	87.010	-	-	-
152.280	87.083	-	-	-
152.640	87.163	-	-	-
153.000	87.236	-	-	-
153.360	87.315	-	-	-
153.720	87.390	-	-	-
154.080	87.467	-	-	-
154.440	87.541	-	-	-
154.800	87.619	-	-	-
155.160	87.694	-	-	-
155.520	87.774	-	-	-
155.880	87.851	-	-	-
156.240	87.927	-	-	-
156.600	88.005	-	-	-
156.960	88.081	-	-	-
157.320	88.162	-	-	-
157.680	88.243	-	-	-
158.040	88.316	-	-	-
158.400	88.391	-	-	-
158.760	88.472	-	-	-
159.120	88.547	-	-	-
159.480	88.627	-	-	-
159.840	88.704	-	-	-
160.200	88.781	-	-	-
160.560	88.863	-	-	-
160.920	88.941	-	-	-
161.280	89.022	-	-	-
161.640	89.098	-	-	-
162.000	89.180	-	-	-
162.360	89.256	-	-	-
162.720	89.337	-	-	-
163.080	89.415	-	-	-
163.440	89.496	-	-	-
163.800	89.574	-	-	-
164.160	89.653	-	-	-
164.520	89.735	-	-	-
164.880	89.812	-	-	-
165.240	89.895	-	-	-

PHI1	PHI4A	PHI4R	PHI5R	PHI5/4
165.600	89.970	-	-	-
165.960	90.053	-	-	-
166.320	90.129	-	-	-
166.680	90.210	-	-	-
167.040	90.287	-	-	-
167.400	90.368	-	-	-
167.760	90.449	-	-	-
168.120	90.527	-	-	-
168.480	90.609	-	-	-
168.840	90.685	-	-	-
169.200	90.768	-	-	-
169.560	90.844	-	-	-
169.920	90.925	-	-	-
170.280	91.001	-	-	-
170.640	91.080	-	-	-
171.000	91.162	-	-	-
171.360	91.240	-	-	-
171.720	91.321	-	-	-
172.080	91.397	-	-	-
172.440	91.479	-	-	-
172.800	91.553	-	-	-
173.160	91.634	-	-	-
173.520	91.709	-	-	-
173.880	91.790	-	-	-
174.240	91.864	-	-	-
174.600	91.943	-	-	-
174.960	92.021	-	-	-
175.320	92.099	-	-	-
175.680	92.176	-	-	-
176.040	92.252	-	-	-
176.400	92.332	-	-	-
176.760	92.407	-	-	-
177.120	92.486	-	-	-
177.480	92.558	-	-	-
177.840	92.650	-	-	-
178.200	92.713	-	-	-
178.560	92.792	-	-	-
178.920	92.866	-	-	-
179.280	92.945	-	-	-
179.640	93.020	-	-	-

PHI1	PHI4A	PHI4R	PHI5R	PHI5/4
180.000	93.097	-	-	-
180.360	93.172	-	-	-
180.720	93.249	-	-	-
181.080	93.327	-	-	-
181.440	93.401	-	-	-
181.800	93.478	-	-	-
182.160	93.552	-	-	-
182.520	93.632	-	-	-
182.880	93.704	-	-	-
183.240	93.782	-	-	-
183.600	93.854	-	-	-
183.960	93.934	-	-	-
184.320	94.005	-	-	-
184.680	94.078	-	-	-
185.040	94.156	-	-	-
185.400	94.235	-	-	-
185.760	94.307	-	-	-
186.120	94.384	-	-	-
186.480	94.457	-	-	-
186.840	94.535	-	-	-
187.200	94.608	-	-	-
187.560	94.683	-	-	-
187.920	94.758	-	-	-
188.280	94.833	-	-	-
188.640	94.908	-	-	-
189.000	94.980	-	-	-
189.360	95.055	-	-	-
189.720	95.129	-	-	-
190.080	95.204	-	-	-
190.440	95.275	-	-	-
190.800	95.350	-	-	-
191.160	95.421	-	-	-
191.520	95.496	-	-	-
191.880	95.565	-	-	-
192.240	95.639	-	-	-
192.600	95.709	-	-	-
192.960	95.781	-	-	-
193.320	95.851	-	-	-
193.680	95.923	-	-	-
194.040	95.994	-	-	-

PHI1	PHI4A	PHI4R	PHI5R	PHI5/4
194.400	96.066	-	-	-
194.760	96.134	-	-	-
195.120	96.205	-	-	-
195.480	96.274	-	-	-
195.840	96.344	-	-	-
196.200	96.412	-	-	-
196.560	96.479	-	-	-
196.920	96.550	-	-	-
197.280	96.616	-	-	-
197.640	96.686	-	-	-
198.000	96.751	-	-	-
198.360	96.822	-	-	-
198.720	96.886	-	-	-
199.080	96.956	-	-	-
199.440	97.018	-	-	-
199.800	97.089	-	-	-
200.160	97.151	-	-	-
200.520	97.218	-	-	-
200.880	97.282	-	-	-
201.240	97.348	-	-	-
201.600	97.414	-	-	-
201.960	97.478	-	-	-
202.320	97.545	-	-	-
202.680	97.608	-	-	-
203.040	97.676	-	-	-
203.400	97.737	-	-	-
203.760	97.804	-	-	-
204.120	97.866	-	-	-
204.480	97.930	-	-	-
204.840	97.993	-	-	-
205.200	98.056	-	-	-
205.560	98.122	-	-	-
205.920	98.182	-	-	-
206.280	98.248	-	-	-
206.640	98.306	-	-	-
207.000	98.370	-	-	-
207.360	98.429	-	-	-
207.720	98.489	-	-	-
208.080	98.548	-	-	-
208.440	98.611	-	-	-

PHI1	PHI4A	PHI4R	PHI5R	PHI5/4
208.800	98.675	-	-	-
209.160	98.731	-	-	-
209.520	98.791	-	-	-
209.880	98.851	-	-	-
210.240	98.909	-	-	-
210.600	98.971	-	-	-
210.960	99.027	-	-	-
211.320	99.086	-	-	-
211.680	99.143	-	-	-
212.040	99.199	-	-	-
212.400	99.260	-	-	-
212.760	99.314	-	-	-
213.120	99.371	-	-	-
213.480	99.427	-	-	-
213.840	99.481	-	-	-
214.200	99.541	-	-	-
214.560	99.592	-	-	-
214.920	99.645	-	-	-
215.280	99.701	-	-	-
215.640	99.753	-	-	-
216.000	99.806	-	-	-
216.360	99.858	-	-	-
216.720	99.909	-	-	-
217.080	99.963	-	-	-
217.440	100.012	-	-	-
217.800	100.061	-	-	-
218.160	100.116	-	-	-
218.520	100.162	-	-	-
218.880	100.210	-	-	-
219.240	100.263	-	-	-
219.600	100.307	-	-	-
219.960	100.355	-	-	-
220.320	100.407	-	-	-
220.680	100.450	-	-	-
221.040	100.496	-	-	-
221.400	100.547	-	-	-
221.760	100.589	-	-	-
222.120	100.634	-	-	-
222.480	100.682	-	-	-
222.840	100.725	-	-	-

PHI1	PHI4A	PHI4R	PHI5R	PHI5/4
223.200	100.772	-	-	-
223.560	100.813	-	-	-
223.920	100.857	-	-	-
224.280	100.899	-	-	-
224.640	100.940	-	-	-
225.000	100.987	-	-	-
225.360	101.025	-	-	-
225.720	101.066	-	-	-
226.080	101.110	-	-	-
226.440	101.150	-	-	-
226.800	101.188	-	-	-
227.160	101.228	-	-	-
227.520	101.272	-	-	-
227.880	101.307	-	-	-
228.240	101.346	-	-	-
228.600	101.388	-	-	-
228.960	101.425	-	-	-
229.320	101.460	-	-	-
229.680	101.497	-	-	-
230.040	101.535	-	-	-
230.400	101.572	-	-	-
230.760	101.605	-	-	-
231.120	101.640	-	-	-
231.480	101.675	-	-	-
231.840	101.711	-	-	-
232.200	101.742	-	-	-
232.560	101.774	-	-	-
232.920	101.806	-	-	-
233.280	101.842	-	-	-
233.640	101.869	-	-	-
234.000	101.899	-	-	-
234.360	101.928	-	-	-
234.720	101.957	-	-	-
235.080	101.990	-	-	-
235.440	102.016	-	-	-
235.800	102.042	-	-	-
236.160	102.069	-	-	-
236.520	102.096	-	-	-
236.880	102.126	-	-	-
237.240	102.151	-	-	-

PHI1	PHI4A	PHI4R	PHI5R	PHI5/4	
237.600	102.174	-	-	-	
237.960	102.199	-	-	-	
238.320	102.223	-	-	-	
238.680	102.248	-	-	-	
239.040	102.276	-	-	-	
239.400	102.296	-	-	-	
239.760	102.317	-	-	-	
240.120	102.339	-	-	-	
240.480	102.363	-	-	-	
240.840	102.387	-	-	-	
241.200	102.407	-	-	-	
241.560	102.425	-	-	-	
241.920	102.443	-	-	-	
242.280	102.461	-	-	-	
242.640	102.479	-	-	-	
243.000	102.497	-	-	-	
243.360	102.515	-	-	-	
243.720	102.535	-	-	-	
244.080	102.552	-	-	-	
244.440	102.570	-	-	-	
244.800	102.584	-	-	-	
245.160	102.598	-	-	-	
245.520	102.613	-	-	-	
245.880	102.627	-	-	-	
246.240	102.641	-	-	-	
246.600	102.654	-	-	-	
246.960	102.667	-	-	-	
247.320	102.680	-	-	-	
247.680	102.694	-	-	-	
248.040	102.708	-	-	-	
248.400	102.717	-	-	-	
248.760	102.725	-	-	-	
249.120	102.734	-	-	-	
249.480	102.743	-	-	-	
249.840	102.750	-	-	-	
250.200	102.757	-	-	-	
250.560	102.765	-	-	-	
250.920	102.772	-	-	-	
251.280	102.779	-	-	-	<- end of
251.640	-	-	-	-	return motion

PHI1	PHI4A	PHI4R	PHI5R	PHI5/4	
252.000	-	-	-	-	
252.360	-	-	-	-	
252.720	-	-	-	-	
253.080	-	-	-	-	
253.440	-	-	-	-	
253.800	-	-	-	-	
254.160	-	-	-	-	
254.520	-	-	-	-	
254.880	-	-	-	-	
255.240	-	-	-	-	
255.600	-	-	-	-	
255.960	-	-	-	-	
256.320	-	-	-	-	
256.680	-	-	-	-	
257.040	-	-	-	-	
257.400	-	-	-	-	
257.760	-	-	-	-	
258.120	-	-	-	-	
258.480	-	-	-	-	
258.840	-	-	-	-	
259.200	-	-	-	-	
259.560	-	-	-	-	
259.920	-	-	-	-	
260.280	-	-	-	-	
260.640	-	-	-	-	
261.000	102.744	.018	-	.018	<- beginning
261.360	102.738	.024	-	.024	of first part
261.720	102.732	.030	-	.030	of forward
262.080	102.726	.036	-	.036	motion
262.440	102.721	.041	-	.041	
262.800	102.715	.047	-	.047	
263.160	102.709	.053	-	.053	
263.520	102.696	.066	-	.066	
263.880	102.681	.081	-	.081	
264.240	102.669	.093	-	.093	
264.600	102.660	.102	-	.102	
264.960	102.651	.111	-	.111	
265.320	102.642	.120	-	.120	
265.680	102.631	.131	-	.131	
266.040	102.613	.149	-	.149	

PHI1	PHI4A	PHI4R	PHI5R	PHI5/4	
266.400	102.600	.162	-	.162	
266.760	102.589	.173	-	.173	
267.120	102.583	.179	-	.179	
267.480	102.574	.188	-	.188	
267.840	102.565	.197	-	.197	
268.200	102.549	.213	-	.213	
268.560	102.533	.229	-	.229	
268.920	102.513	.249	-	.249	
269.280	102.492	.270	-	.270	
269.640	102.473	.289	-	.289	
270.000	102.454	.308	-	.308	
270.360	102.442	.320	-	.320	
270.720	102.430	.332	-	.332	
271.080	102.409	.353	-	.353	
271.440	102.378	.384	-	.384	
271.800	102.368	.394	-	.394	
272.160	102.358	.404	-	.404	
272.520	102.347	.415	-	.415	
272.880	102.326	.436	-	.436	
273.240	102.308	.454	-	.454	
273.600	102.295	.467	-	.467	
273.960	102.283	.479	-	.479	
274.320	102.264	.498	-	.498	
274.680	102.239	.523	-	.523	
275.040	102.225	.537	-	.537	
275.400	102.211	.551	-	.551	
275.760	102.194	.568	-	.568	
276.120	102.172	.590	-	.590	
276.480	102.157	.605	-	.605	
276.840	102.144	.618	.020	.598	<- beginning
277.200	102.128	.634	.032	.602	of motion
277.560	102.099	.663	.044	.618	of the roller
277.920	102.082	.680	.056	.624	shaft
278.280	102.066	.696	.067	.629	
278.640	102.045	.717	.077	.640	
279.000	102.020	.742	.088	.654	
279.360	102.004	.758	.107	.652	
279.720	101.985	.777	.127	.649	
280.080	101.950	.812	.145	.666	
280.440	101.930	.832	.165	.668	

PHI1	PHI4A	PHI4R	PHI5R	PHI5/4
280.800	101.905	.857	.193	.664
281.160	101.875	.887	.214	.673
281.520	101.853	.909	.234	.675
281.880	101.817	.945	.267	.678
282.240	101.787	.975	.294	.681
282.600	101.755	1.007	.327	.680
282.960	101.722	1.040	.358	.682
283.320	101.690	1.072	.389	.684
283.680	101.648	1.114	.427	.687
284.040	101.610	1.152	.465	.686
284.400	101.573	1.189	.504	.685
284.760	101.528	1.234	.544	.690
285.120	101.490	1.272	.586	.686
285.480	101.442	1.320	.635	.685
285.840	101.404	1.358	.675	.683
286.200	101.354	1.409	.725	.683
286.560	101.303	1.459	.779	.680
286.920	101.264	1.498	.825	.673
287.280	101.209	1.553	.878	.675
287.640	101.156	1.606	.935	.672
288.000	101.109	1.653	.991	.662
288.360	101.057	1.705	1.050	.655
288.720	101.002	1.760	1.103	.658
289.080	100.943	1.819	1.164	.654
289.440	100.894	1.868	1.226	.642
289.800	100.843	1.919	1.292	.627
290.160	100.781	1.981	1.357	.624
290.520	100.723	2.039	1.416	.623
290.880	100.668	2.094	1.482	.612
291.240	100.611	2.151	1.544	.607
291.600	100.556	2.206	1.611	.594
291.960	100.492	2.270	1.674	.596
292.320	100.432	2.330	1.744	.586
292.680	100.368	2.394	1.812	.583
293.040	100.311	2.451	1.882	.569
293.400	100.259	2.503	1.950	.553
293.760	100.193	2.569	2.021	.548
294.120	100.132	2.630	2.091	.539
294.480	100.067	2.695	2.161	.534
294.840	100.005	2.757	2.232	.524

PHI1	PHI4A	PHI4R	PHI5R	PHI5/4
295.200	99.946	2.816	2.303	.513
295.560	99.887	2.875	2.375	.500
295.920	99.831	2.931	2.445	.486
296.280	99.765	2.997	2.515	.482
296.640	99.703	3.059	2.585	.474
297.000	99.637	3.125	2.657	.469
297.360	99.572	3.190	2.725	.465
297.720	99.515	3.247	2.796	.451
298.080	99.455	3.307	2.863	.444
298.440	99.399	3.363	2.935	.428
298.800	99.332	3.430	2.998	.432
299.160	99.271	3.491	3.066	.425
299.520	99.205	3.557	3.129	.428
299.880	99.144	3.618	3.193	.425
300.240	99.087	3.675	3.256	.419
300.600	99.028	3.734	3.322	.412
300.960	98.971	3.791	3.390	.402
301.320	98.904	3.858	3.451	.406
301.680	98.844	3.918	3.517	.402
302.040	98.779	3.983	3.576	.407
302.400	98.721	4.041	3.638	.403
302.760	98.667	4.095	3.694	.401
303.120	98.607	4.155	3.755	.400
303.480	98.548	4.214	3.815	.399
303.840	98.484	4.278	3.874	.404
304.200	98.424	4.338	3.933	.405
304.560	98.372	4.390	3.983	.408
304.920	98.314	4.448	4.040	.408
305.280	98.256	4.506	4.099	.407
305.640	98.193	4.569	4.152	.418
306.000	98.133	4.629	4.205	.424
306.360	98.078	4.684	4.256	.428
306.720	98.021	4.741	4.312	.429
307.080	97.965	4.797	4.367	.430
307.440	97.901	4.861	4.411	.449
307.800	97.842	4.920	4.466	.454
308.160	97.782	4.980	4.522	.457
308.520	97.727	5.035	4.568	.467
308.880	97.673	5.089	4.620	.469
309.240	97.608	5.154	4.674	.479

PHI1	PHI4A	PHI4R	PHI5R	PHI5/4
309.600	97.548	5.214	4.725	.490
309.960	97.483	5.279	4.775	.504
310.320	97.425	5.337	4.827	.510
310.680	97.363	5.399	4.881	.518
311.040	97.307	5.455	4.934	.521
311.400	97.246	5.516	4.982	.534
311.760	97.180	5.582	5.037	.544
312.120	97.118	5.644	5.095	.549
312.480	97.052	5.710	5.142	.568
312.840	96.990	5.772	5.197	.575
313.200	96.931	5.831	5.254	.577
313.560	96.867	5.895	5.311	.584
313.920	96.807	5.955	5.366	.589
314.280	96.738	6.024	5.421	.604
314.640	96.674	6.088	5.482	.606
315.000	96.604	6.158	5.544	.614
315.360	96.539	6.223	5.606	.617
315.720	96.469	6.293	5.672	.621
316.080	96.402	6.360	5.731	.629
316.440	96.332	6.430	5.797	.633
316.800	96.265	6.497	5.859	.638
317.160	96.195	6.567	5.928	.639
317.520	96.129	6.633	5.993	.640
317.880	96.060	6.702	6.065	.637
318.240	95.989	6.773	6.135	.638
318.600	95.920	6.842	6.209	.633
318.960	95.847	6.915	6.280	.634
319.320	95.775	6.987	6.358	.629
319.680	95.701	7.061	6.431	.630
320.040	95.627	7.135	6.512	.623
320.400	95.552	7.210	6.588	.623
320.760	95.474	7.288	6.671	.617
321.120	95.399	7.363	6.750	.613
321.480	95.322	7.440	6.831	.609
321.840	95.248	7.514	6.910	.604
322.200	95.170	7.592	6.991	.602
322.560	95.094	7.668	7.074	.594
322.920	95.013	7.749	7.159	.590
323.280	94.938	7.824	7.249	.575
323.640	94.853	7.909	7.333	.576

PHI1	PHI4A	PHI4R	PHI5R	PHI5/4
324.000	94.770	7.992	7.418	.574
324.360	94.684	8.078	7.503	.574
324.720	94.600	8.162	7.593	.569
325.080	94.513	8.249	7.695	.553
325.440	94.437	8.325	7.772	.553
325.800	94.358	8.404	7.859	.545
326.160	94.267	8.495	7.951	.544
326.520	94.182	8.580	8.042	.538
326.880	94.096	8.666	8.133	.533
327.240	94.012	8.750	8.221	.529
327.600	93.933	8.829	8.312	.518
327.960	93.845	8.917	8.409	.508
328.320	93.759	9.003	8.495	.507
328.680	93.671	9.091	8.584	.507
329.040	93.588	9.174	8.680	.494
329.400	93.508	9.254	8.771	.482
329.760	93.426	9.336	8.860	.475
330.120	93.346	9.416	8.950	.466
330.480	93.257	9.505	9.042	.464
330.840	93.170	9.592	9.135	.457
331.200	93.090	9.672	9.222	.450
331.560	93.008	9.754	9.309	.445
331.920	92.931	9.831	9.404	.427
332.280	92.848	9.914	9.492	.422
332.640	92.770	9.992	9.579	.413
333.000	92.683	10.079	9.663	.416
333.360	92.600	10.162	9.750	.412
333.720	92.518	10.244	9.842	.402
334.080	92.438	10.324	9.924	.400
334.440	92.361	10.401	10.008	.393
334.800	92.281	10.481	10.089	.392
335.160	92.205	10.557	10.170	.387
335.520	92.124	10.638	10.255	.383
335.880	92.050	10.712	10.334	.378
336.240	91.953	10.809	10.428	.381
336.600	91.885	10.877	10.496	.381
336.960	91.805	10.957	10.574	.382
337.320	91.726	11.036	10.649	.387
337.680	91.651	11.111	10.726	.386
338.040	91.572	11.190	10.801	.389

PHI1	PHI4A	PHI4R	PHI5R	PHI5/4
338.400	91.497	11.265	10.876	.389
338.760	91.419	11.343	10.949	.393
339.120	91.346	11.416	11.022	.394
339.480	91.268	11.494	11.094	.400
339.840	91.194	11.568	11.166	.401
340.200	91.116	11.646	11.237	.408
340.560	91.044	11.718	11.308	.410
340.920	90.961	11.801	11.378	.423
341.280	90.887	11.875	11.448	.427
341.640	90.808	11.954	11.516	.438
342.000	90.732	12.030	11.585	.444
342.360	90.655	12.107	11.652	.455
342.720	90.579	12.183	11.722	.461
343.080	90.505	12.257	11.786	.471
343.440	90.429	12.333	11.855	.478
343.800	90.356	12.406	11.918	.488
344.160	90.281	12.481	11.986	.496
344.520	90.209	12.553	12.048	.505
344.880	90.135	12.627	12.116	.510
345.240	90.061	12.701	12.182	.519
345.600	89.986	12.776	12.251	.525
345.960	89.914	12.848	12.318	.530
346.320	89.839	12.923	12.387	.535
346.680	89.767	12.995	12.457	.538
347.040	89.692	13.070	12.526	.544
347.400	89.621	13.141	12.596	.545
347.760	89.545	13.217	12.666	.552
348.120	89.473	13.289	12.738	.551
348.480	89.397	13.365	12.807	.558
348.840	89.326	13.436	12.880	.556
349.200	89.249	13.513	12.951	.562
349.560	89.177	13.585	13.025	.559
349.920	89.099	13.663	13.097	.565
350.280	89.028	13.734	13.172	.562
350.640	88.935	13.827	13.254	.573
351.000	88.870	13.892	13.322	.571
351.360	88.790	13.972	13.398	.574
351.720	88.712	14.050	13.474	.576
352.080	88.632	14.130	13.553	.577
352.440	88.553	14.209	13.632	.577

PHI1	PHI4A	PHI4R	PHI5R	PHI5/4	
352.800	88.478	14.284	13.715	.569	
353.160	88.398	14.364	13.795	.569	
353.520	88.322	14.440	13.881	.559	
353.880	88.242	14.520	13.958	.562	
354.240	88.165	14.597	14.041	.555	
354.600	88.079	14.683	14.123	.561	
354.960	87.994	14.768	14.206	.562	
355.320	87.911	14.851	14.295	.556	
355.680	87.829	14.933	14.379	.554	
356.040	87.751	15.011	14.465	.546	
356.400	87.666	15.096	14.549	.546	
356.760	87.588	15.174	14.634	.541	
357.120	87.498	15.264	14.725	.539	
357.480	87.412	15.350	14.812	.538	
357.840	87.330	15.432	14.900	.532	
358.200	87.247	15.515	14.985	.530	
358.560	87.169	15.593	15.070	.522	
358.920	87.086	15.676	15.164	.512	
359.280	86.998	15.764	15.251	.513	
359.640	86.915	15.847	15.339	.508	<- end of first part of forward motion

APPENDIX J. APPROXIMATION OF FUNCTION A(δ)

This appendix shows how equation (89), the approximate form of equation (81) is obtained.

Factoring δ from the first term of equation (81) leads to:

$$A(\delta) = \frac{1}{\beta+1}\delta^{\beta+1}\left[\left(1+\frac{X_i}{\delta}\right)^{\beta+1} - \left(1+R\frac{X_i}{\delta}\right)^{\beta+1}\right] - \delta^{\beta}(X_i - RX_i) \qquad (J.1)$$

With a Maclaurin series expansions of the terms $(1+X_i/\delta)^{\beta+1}$ and $(1+RX_i/\delta)^{\beta+1}$, the above becomes:

$$A(\delta) = \frac{1}{\beta+1}\delta^{\beta+1}\left[1+\frac{(\beta+1)}{1!}\left(\frac{X_i}{\delta}\right)+\frac{(\beta+1)\beta}{2!}\left(\frac{X_i}{\delta}\right)^2+\ldots\right] -$$

$$-\frac{1}{\beta+1}\delta^{\beta+1}\left[1+\frac{(\beta+1)}{1!}R\left(\frac{X_i}{\delta}\right)+\frac{(\beta+1)\beta}{2!}R^2\left(\frac{X_i}{\delta}\right)^2+\ldots\right] - \delta^{\beta}(X_i - RX_i) \qquad (J.2)$$

Because the ratio $X/\delta < 1$, the terms of order higher than 2 may be neglected and the function $A(\delta)$ can be approximated by:

$$A(\delta)_{approx} = \frac{\beta}{2}X_i^2(1-R^2)\delta^{\beta-1} \qquad (J.3)$$

This approximation is best for small values of the ratio X_i/δ and always underestimates the value of $A(\delta)$ to some degree.

To get an idea of the relative magnitude of the error with $\beta = 3/2$, for example, one divides equation (J.3) by equation (J.1). Thus:

$$\frac{A_{approx}}{A} = \frac{\frac{3}{4}\left(\frac{X_i}{\delta}\right)^2(1-R^2)}{\frac{2}{5}\left[\left(1+\frac{X_i}{\delta}\right)^{5/2} - \left(1+R\frac{X_i}{\delta}\right)^{5/2}\right] - \left(\frac{X_i}{\delta} - R\frac{X_i}{\delta}\right)} \qquad (J.4)$$

Figure J-1 shows curves for this error ratio for $0 \leq X_i/\delta \leq 1$ when the amplitude decay ratio is between 0.2 and 0.9. They indicate that A_{approx} is very good for realistically small values of X_i/δ over a representative range of amplitude decay ratios (See experimental results in section 4 of Part II).

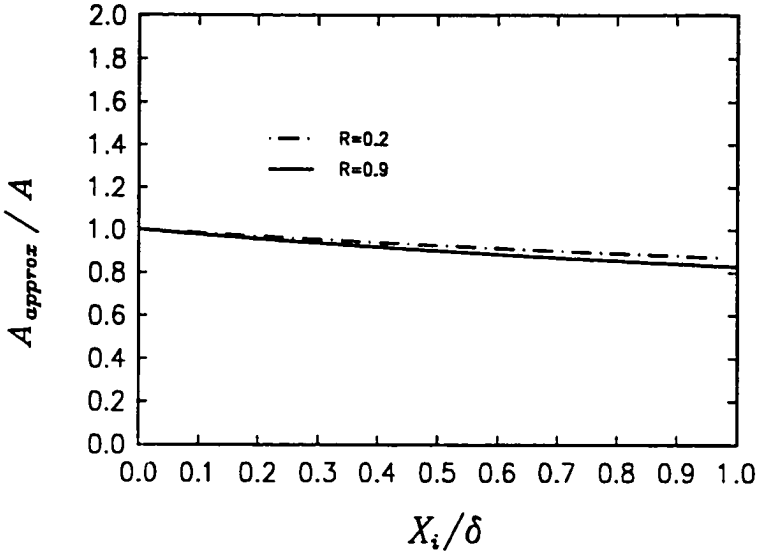

Figure J-1 Error Ratio A_{approx}/A

APPENDIX K. PROCEDURE FOR OBTAINING THE AMPLITUDE DECAY RATIO

Because of the difficulty of determining the exact position of the preload displacement δ during each cycle and with that the accurate value of the individual amplitude $\Phi_{5/4(i)}$, the following procedure for finding the amplitude decay ratio was used. (See the uppermost graph in Figure 20).

The computer output of the experiment easily furnishes the maximum and minimum values $\phi_{5/4(2)}$, $\phi_{5/4(2')}$, $\phi_{5/4(3)}$, etc., respectively. Because of this, rather than evaluate the usual form of the amplitude decay ratio, i.e. for example

$$R = \frac{\Phi_{5/4(3)}}{\Phi_{5/4(2)}}, \tag{K.1}$$

the following type of form has been used:

$$R = \frac{\phi_{5/4(3)} - \phi_{5/4(3')}}{\phi_{5/4(2)} - \phi_{5/4(2')}} \tag{K.2}$$

This is justified by rewriting the above:

$$\frac{\phi_{5/4(3)} - \phi_{5/4(3')}}{\phi_{5/4(2)} - \phi_{5/4(2')}} = \frac{\Phi_{5/4(3)} + \Phi_{5/4(3')}}{\Phi_{5/4(2)} + \Phi_{5/4(2')}} = \frac{\Phi_{5/4(3)}(1 + \Phi_{5/4(3')}/\Phi_{5/4(3)})}{\Phi_{5/4(2)}(1 + \Phi_{5/4(2')}/\Phi_{5/4(2)})} \tag{K.3}$$

Further, with the overall assumption of this work

$$\frac{\Phi_{5/4(3)}}{\Phi_{5/4(2)}} = \frac{\Phi_{5/4(3')}}{\Phi_{5/4(2')}}, \tag{K.4}$$

it is also true that

$$\frac{\Phi_{5/4(3')}}{\Phi_{5/4(3)}} = \frac{\Phi_{5/4(2')}}{\Phi_{5/4(2)}} \tag{K.5}$$

This allows the cancelling of the terms in parenthesis of the last expression in equation (K.3)

and it proves that equation (K.1) may be replaced by equation (K.2).

APPENDIX L. DETERMINATION OF RELATIVE ROTATION $\phi_{5/4}$ DUE TO CONTACT DEFORMATIONS

The following adaptation of the work of Stoelzle and Hart (1961) shows how one may relate the windup angle to the two local contact deformations of the races and the sprag at the inner and outer interfaces, respectively.

To this end, the above authors first assume that the motion of all components may be approximated by an epicyclic train model where the imaginary epicyclic arm has the length of the distance from the center of the assembly to the center of the sprag, i.e. approximately $(R_o - R_s)$.

The simultaneous motions of the outer and inner races as well as the associated rolling of the sprags at the two interfaces are divided into two phases. For the first phase it is assumed that the inner race is stationary and that motion is made possible only by the combined local increase of the radius of the outer race and the associated compression of the sprag at the outer interface. This is the distance δ_o shown in Figure L-1a. For the second phase it is assumed that the outer race is stationary and that motion is due only to the combined local decrease of the radius of the inner race and the associated compression of the sprag at the inner interface. This is the distance δ_i shown in Figure L-1b. In both figures the solid outlines represent the initial positions of the sprag, while the broken ones the final positions. The small circles on these outlines indicate the respective initial and final contact points.

Each of the aforementioned simultaneous motion phases has one part of the total windup angle associated with it, so that

$$\phi_{5/4} = |\phi_{5/4(o)}| + |\phi_{5/4(i)}| \qquad (L.1)$$

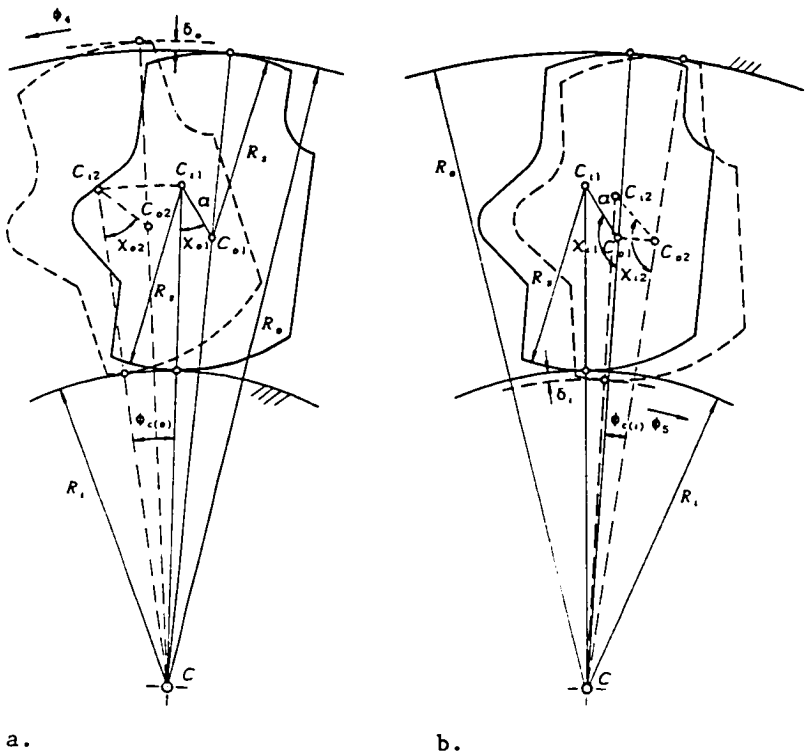

Figure L-1 Determination of Relative Rotation due to Contact Deformation

a. Deformation at Outer Interface with Inner Race Stationary

b. Deformation at Inner Interface with Outer Race Stationary

where

$\phi_{5/4(o)}$ = the windup angle due to δ_o with the inner race stationary,

$\phi_{5/4(i)}$ = the windup angle due to δ_i with the outer race stationary.

a. Windup Angle Due to δ_o

Using the epicyclic train model, the angle $\phi_{5/4(o)}$ becomes:

$$\phi_{5/4(o)} = -(1 + R_i/R_o)\phi_{c(o)} , \qquad (L.2)$$

where $\phi_{c(o)}$ represents the absolute rotation of the imagined epicyclic arm. To obtain an expression for $\phi_{c(o)}$, it is first necessary to define the associated relative rotation $\Delta\chi_o$ of the sprag with respect to the epicyclic arm.

According to Figure L-1a, the initial angle of the sprag $\Delta\chi_{o1}$ with respect to the epicyclic arm is defined by the triangle $C - C_{o1} - C_{i1}$, where the line $C - C_i$ is assumed to represent the epicyclic arm. Thus,

$$\chi_{o1} = \cos^{-1}\left[\frac{a^2 + (R_i + R_s)^2 - (R_o - R_s)^2}{2a(R_i + R_s)}\right] \qquad (L.3)$$

where $a = C_iC_o$.

The final angle of the sprag $\Delta\chi_{o2}$ with respect to the arm indicates the change of position of the line $C_{i2} - C_{o2}$ due to δ_o with respect to line $C - C_i$, which still represents the epicyclic arm. Therefore,

$$\chi_{o2} = \cos^{-1}\left[\frac{a^2 + (R_i + R_s)^2 - (R_o + \delta_o - R_s)^2}{2a(R_i + R_s)}\right] \qquad (L.4)$$

The rotation of the sprag with respect to the arm then becomes:

$$\Delta\chi_o = \chi_{o2} - \chi_{o1} \qquad (L.5)$$

With the epicyclic model, the angle of rotation of the epicyclic arm $\phi_{c(o)}$ is related to the relative rotation $\Delta\chi_o$ by way of:

$$\phi_{c(o)} = \frac{R_s}{R_i}\Delta\chi_o \tag{L.6}$$

Finally, equation (L.2) becomes:

$$\phi_{5/4(o)} = -R_s\frac{R_o + R_i}{R_o R_i}\Delta\chi_o \tag{L.7}$$

b. Windup Angle Due to δ_i

Again, using the epicyclic train model, the angle $\phi_{5/4(i)}$ can be found by:

$$\phi_{5/4(i)} = (1 + R_o/R_i)\phi_{c(i)}\ , \tag{L.8}$$

where $\phi_{c(i)}$ represents the absolute rotation of the imagined epicyclic arm due to the rolling of the sprag on the now fixed outer race. To obtain an expression for $\phi_{c(i)}$, it is first necessary to define the associated relative rotation $\Delta\chi_i$ of the sprag with respect to the epicyclic arm.

According to Figure L-1b, the initial angle of the sprag χ_{i1} with respect to the arm is defined by the triangle $C - C_{o1} - C_{i1}$ and now the line $C - C_o$ represent the epicyclic arm. Then,

$$\chi_{i1} = \cos^{-1}\left[\frac{a^2 + (R_o - R_s)^2 - (R_i + R_s)^2}{2a(R_o - R_s)}\right] \tag{L.9}$$

The final angle χ_{i2} with respect to the arm indicates the change of position of the line $C_{i2} - C_{o2}$, now due to δ_i, with respect to line $C - C_o$. Therefore,

$$\chi_{i2} = \cos^{-1}\left[\frac{a^2 + (R_o - R_s)^2 - (R_i - \delta_i + R_s)^2}{2a(R_o - R_s)}\right] \tag{L.10}$$

So that

$$\Delta\chi_i = \chi_{i2} - \chi_{i1} \qquad (L.11)$$

With the epicyclic model, the angle $\phi_{c(i)}$ is related to the relative rotation $\Delta\chi_i$ by way of:

$$\phi_{c(i)} = \frac{R_s}{R_o}\Delta\chi_i \qquad (L.12)$$

Finally, equation (L.8) becomes:

$$\phi_{5/4(i)} = R_s\frac{R_o + R_i}{R_o R_i}\Delta\chi_i \qquad (L.13)$$

c. Total Windup Angle due to δ_o and δ_i

The total windup angle between the outer and inner race, as given by equation (L.1), becomes with equations (L.7) and (L.13):

$$\phi_{5/4} = R_s\frac{R_o + R_i}{R_o R_i}(|\Delta\chi_o| + |\Delta\chi_i|) \qquad (L.14)$$

With the assumption that δ_o and δ_i are very small, the expressions for $\Delta\chi_o$ and $\Delta\chi_i$, of equations (L.5) and (L.11), respectively, may be simplified by way of a Maclaurin series expansion of the following form:

$$f(\delta) = f(0) + \frac{f'(0)}{1!}\delta + \ldots \qquad (L.15)$$

Then, by neglecting all higher order terms:

$$\Delta\chi_o = D_o\delta_o \qquad (L.16)$$

and

$$\Delta\chi_i = D_i\delta_i\ , \qquad (L.17)$$

where,

$$D_o = \frac{2(R_o - R_s)}{\sqrt{[2a(R_i + R_s)]^2 - [a^2 + (R_i + R_s)^2 - (R_o - R_s)^2]^2}} \qquad (L.18)$$

$$D_i = \frac{2(R_i + R_s)}{\sqrt{[2a(R_o - R_s)]^2 - [a^2 + (R_o - R_s)^2 - (R_i + R_s)^2]^2}} \qquad (L.19)$$

Finally, equation (L.14) becomes:

$$\phi_{5/4} = \phi_5 - \phi_4 = R_s \frac{R_o + R_i}{R_o R_i}(D_o \delta_o + D_i \delta_i) \qquad (L.20)$$

APPENDIX M. DETERMINATION OF REALISTIC CONTACT MODE BETWEEN SPRAGS AND RACES

The following first shows the relationship between the Hertzian contact force N_h and the local deformations δ_i and δ_o for line, single point and two point contact modes between the sprags and the races, with the help of the appropriate formulas given by Roark and Young (1982).

Subsequently, the resulting torque curve associated with each of these cases is compared to the experimentally obtained one. The decision as to the governing contact mode is based on the best fit with the experiment.

a. Line Contact

With the assumption of a line contact mode, as shown in Figure M-1a, one obtains the following relationship between δ_i, δ_o and N_h according to Table 33-2b and 2c of Roark and Young (1982):

$$\delta_i = \frac{1}{\pi E^*}\frac{N_h}{L_i}\left(\frac{2}{3} + \ln\frac{4R_i}{b_i} + \ln\frac{4R_s}{b_i}\right) \qquad (M.1)$$

$$\delta_o = \frac{1}{\pi E^*}\frac{N_h}{L_o}\left(\frac{2}{3} + \ln\frac{4R_o}{b_o} + \ln\frac{4R_s}{b_o}\right) \qquad (M.2)$$

where

$$E^* = \left(\frac{1-\nu_i^2}{E_i} + \frac{1-\nu_s^2}{E_s}\right)^{-1} \qquad (M.3)$$

and the widths of the respective contact areas are given by:

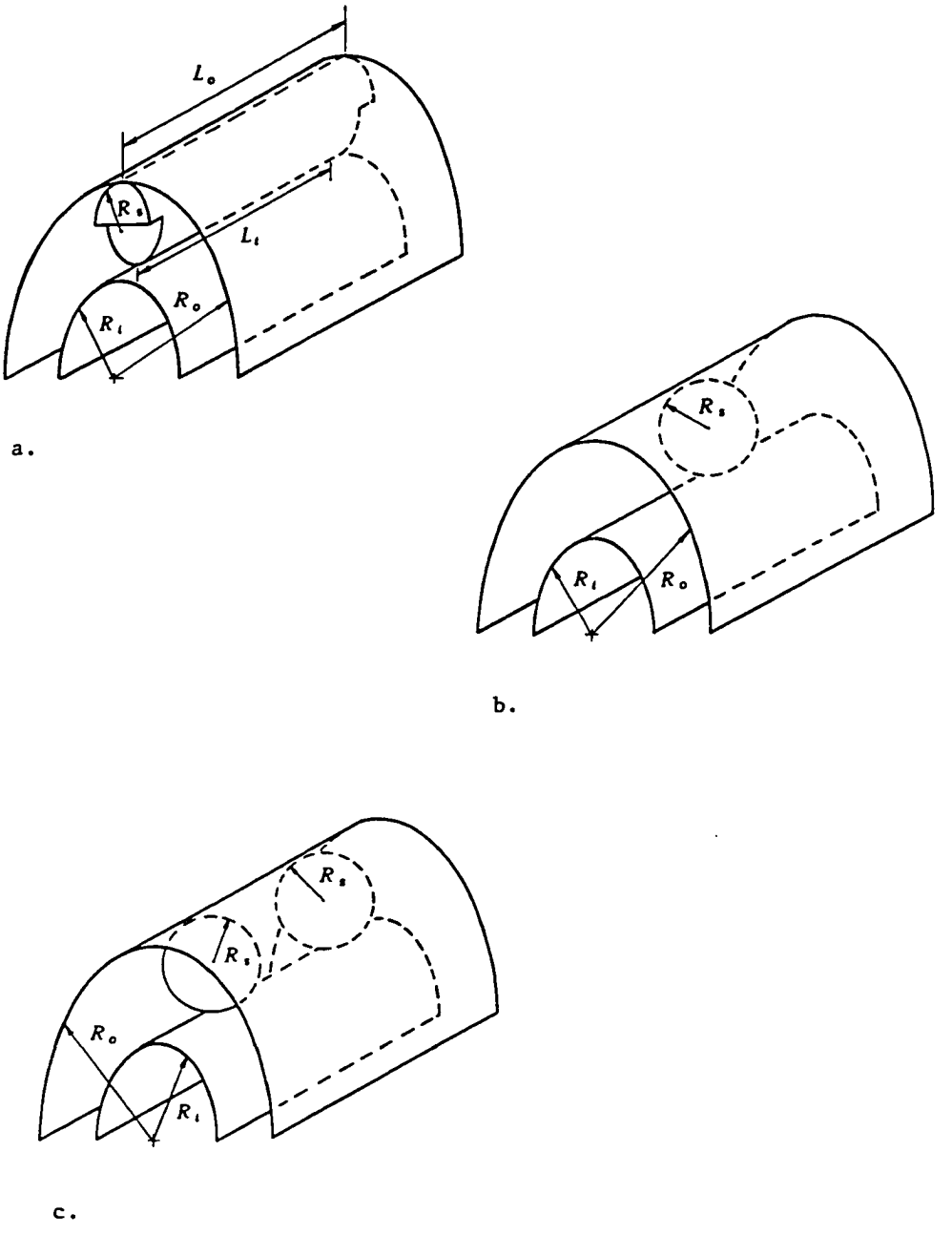

Figure M-1 Examination of Contact Modes at Sprag/Race Interfaces

a. Line Contact b. Single Point Contact c. Two Point Contact

$$b_i = 2.263\left[\frac{N_h}{L_i}\left(\frac{R_i R_s}{R_i + R_s}\right)\frac{1}{E^*}\right]^{1/2} \qquad (M.4)$$

and

$$b_o = 2.263\left[\frac{N_h}{L_o}\left(\frac{R_o R_s}{R_o - R_s}\right)\frac{1}{E^*}\right]^{1/2} \qquad (M.5)$$

b. Single Point Contact

The single point contact mode is based on the assumption that the contact at the two interfaces is equivalent to one where a sphere of radius R_s replaces the sprag while contact with the cylindrical races is made (see Figure M-1b). The associated relationship between δ_i, δ_o and N_h is given in Table 33-4 of Roarke and Young (1982) as:

$$\delta_i = \lambda_i\left(\frac{2R_i + R_s}{1.5R_s R_i}\right)^{1/3}\left(\frac{N_h}{E^*}\right)^{2/3} \qquad (M.6)$$

and

$$\delta_o = \lambda_o\left(\frac{2R_o - R_s}{1.5R_s R_o}\right)^{1/3}\left(\frac{N_h}{E^*}\right)^{2/3} \qquad (M.7)$$

where the constants λ_i and λ_o may be obtained from the same table, with the help of:

$$\cos\theta_i = \left(\frac{R_s R_i}{2R_i + R_s}\right)\frac{1}{R_i} \qquad (M.8)$$

and

$$\cos\theta_o = \left(\frac{R_s R_o}{2R_o - R_s}\right)\frac{1}{R_o} \qquad (M.9)$$

c. Two Point Contact

Figure M-1c shows how in the two point contact mode, the sprag is replaced by 2 spheres of radius R_s. This leads to a halving of the Hertzian contact force at the individual contact point. The substitution of $N_h/2$ for the contact force in equations (M.6) and (M.7) furnishes:

$$\delta_i = \lambda_i \left(\frac{2R_i + R_s}{1.5R_sR_i} \right)^{1/3} \left(\frac{N_h}{2E^*} \right)^{2/3} \qquad (M.10)$$

and

$$\delta_o = \lambda_o \left(\frac{2R_o - R_s}{1.5R_sR_o} \right)^{1/3} \left(\frac{N_h}{2E^*} \right)^{2/3} \qquad (M.11)$$

where λ_i and λ_o are obtained in the same manner as for the single point contact mode above.

d. Comparison of Torque Curves

To be able to obtain the torque vs windup angle curves associated with the three theoretical contact modes for comparison with the experimental one, the following steps are taken:

(1) For a given value of the transmitted torque T, determine the Hertzian contact force $N_h = N_{hi} = N_{ho}$ by way of

$$N_h \alpha R_i Z = N_h \beta R_o Z = T \qquad (M.12)$$

where α and β are the inner and outer strut angles and Z is the number of sprags in the clutch.

(2) With N_h known, one obtains the δ_i and δ_o for the various contact modes.

(3) The windup angle $\phi_{5/4}$, associated with a given torque and contact mode, is then found with the help of equation (L.20).

Figure M-2 gives a comparison of the three theoretical torque curves with the experimentally obtained one, using the data shown in Table 4.

The line contact mode gives a near linear torque curve and has a much higher stiffness than the experimental one. Therefore, it cannot possibly represent the actual contact mode. While both single and two point contact modes yield a 3/2 power torque curve, only the latter fits the experimental data. Thus, the two point contact mode gives the best description.

Finally, the Hertzian contact force of the two point mode can be expressed in terms of the windup angle, by substituting equations (M.10) and (M.11) into equation (L.20), i.e.:

$$N_h = G(\phi_5 - \phi_4)^{3/2} \qquad (M.13)$$

where

$$G = 2.45\frac{E^*}{R_s}\left\{\frac{R_o R_i}{(R_o + R_i)[D_o\lambda_o(2 - R_s/R_o)^{1/3} + D_i\lambda_i(2 + R_s/R_i)^{1/3}]}\right\}^{3/2} \qquad (M.14)$$

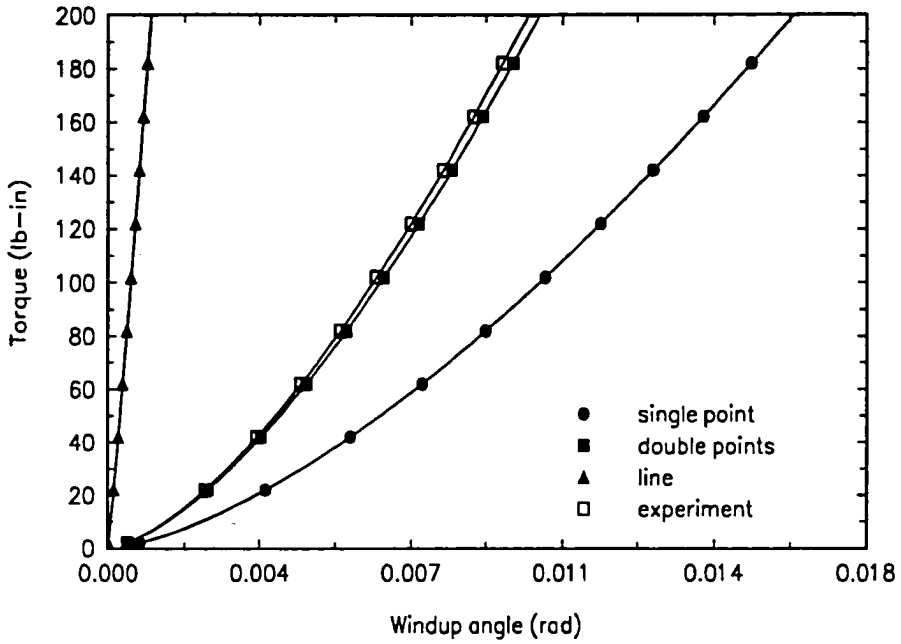

Figure M-2 Comparison of Theoretical Torque Curves with Experimental One

APPENDIX N. FORTRAN PROGRAM FOR THE DETERMINATION OF Δ(0)

```
**************************************************************************
THE FOLLOWING PROGRAM IS USED TO FIND THE CHARACTERISTIC
EXPONENT (U) OF THE SOLUTIONS OF THE MATHIEU EQUATION
WITHIN STABLE OR UNSTABLE REGIONS FOR GIVEN (LA) & (GA)
**************************************************************************
********************* MAIN PROGRAM *******************************
      IMPLICIT  REAL*8(A-Z)
      INTEGER I,II,J,K,N,M,X,Y,MP1,NP1,MPN1,IPVT(71)
      INTEGER KM1,NM1,IP1,STEP
      DIMENSION AP(71), AN(71), MXB(71,71),FAC(71,71)
      COMMON/INTG/N,M
      PI=3.141592654D0
      N=35
      M=35
      MPN1=M+N+1
      LA=12.706577320D0
      GA=11.742D0
-----------------------------------------------------------------
SET ZEROS FOR THE ELEMENTS OF THE DETERMINANT
(FOR MATHIEU'S ONLY)
-----------------------------------------------------------------
      AO=0.0D0
      DO 10 J=1,MPN1
      AP(J)=0.0D0
      AN(J)=0.0D0
 10   CONTINUE
```

```
C-----------------------------------------------------------------
C GIVE THE VALUES TO THE ELEMENTS OF THE DETERMINANT
C (MATHIEU'EQU)
C-----------------------------------------------------------------
      AP(1)=0.5D0
      AN(1)=0.5D0
      CALL MATRIX(LA,GA,AO,AP,AN,MXB)
C-----------------------------------------------------------------
C EVALUATION OF ZERO HILL'S DETERMINANT = DETER(0)
C NOTE THAT "DLFTRG" AND "DLFDRG" ARE THE
C SUBROUTINES FROM MISL.
C-----------------------------------------------------------------
      CALL DLFTRG(MPN1,MXB,MPN1,FAC,MPN1,IPVT)
      CALL DLFDRG(MPN1,FAC,MPN1,IPVT,D1,D2)
      DETER=D1*10.0**D2
      WRITE (6,20) LA,GA, DETER
 20   FORMAT (3X,'LA=',F16.8,1X,'GA=',F5.2,3X,
     1   'DETER(0)=', F20.8)
C-----------------------------------------------------------------
C DETERMINE THE VALUE OF CHARACTERISTIC EXPONENT
C U IN STABLE REGION AS WELL AS IN UNSTABLE REGIONS
C-----------------------------------------------------------------
      IF(LA.LT.0) GO TO 30
      IF(DETER.LT.0) GO TO 50
      RIGHT=DABS(DSQRT(DETER)*DSIN(PI*DSQRT(LA)))
      WRITE(6,40) RIGHT
 40   FORMAT(3X,'RIGHT=',F16.8/)
      IF(RIGHT.GT.1) GO TO 55
      AS=DASIN(RIGHT)/PI
      AC=DACOS(RIGHT)/PI
      WRITE(6,60) AS,AC
 60   FORMAT(3X,'AS=+-',F16.8,2X,'AC=+-',F16.8/)
      GO TO 70
```

```
 50   AE=1.0/PI*DASINH(DSQRT(DABS(DETER))*DSIN(PI*DSQRT(LA)))
      WRITE(6,65) AE
 65   FORMAT(3X,'AE=+-',F16.8,2X,'AE IS A REAL NUMBER.')
      GO TO 70
 55   AO=1.0/PI*DACOSH(DABS(DSQRT(DETER)*DSIN(PI*DSQRT(LA))))
      WRITE(6,75) AO
 75   FORMAT(3X,'AO=+-',F16.8,2X,'AO IS A REAL NUMBER.')
      GO TO 70
 30   IF (DETER.GT.0) GO TO 80
      RIGHT=DABS(DSQRT(DABS(DETER))*DSINH(PI*DSQRT(DABS(LA))))
      IF(RIGHT.GT.1) GO TO 90
      AS=DASIN(RIGHT)/PI
      AC=DACOS(RIGHT)/PI
      WRITE(6,100) AS,AC
100   FORMAT(3X,'AS=',F16.8,2X,'AC=',F16.8)
      GO TO 70
 90   AO=DACOSH(RIGHT)/PI
      WRITE (6,95) AO
 95   FORMAT (2X,'AO=',F16.8,'AO IS A REAL NUMBER, N=ODD')
      GO TO 70
 80   RIGHT=DABS(DSQRT(DETER)*DSINH(PI*DSQRT(DABS(LA))))
      AE=DASINH(RIGHT)/PI
      WRITE (6,85) AE
 85   FORMAT (2X,'AE=',F16.8,'AE IS A REAL NUMBER, N=EVEN')
 70   STOP
      END
```

```
*************** SUBPROGRAM *********************************
THIS SUBROUTINE IS USED TO GIVE THE VALUE TO EACH
ELEMENT OF THE COEFFICIENT DETERMINANT WITH U=0
************************************************************
```

```
      SUBROUTINE MATRIX(LA,GA,AO,AP,AN,MXB)
      IMPLICIT  REAL*8(A-Z)
      INTEGER J,K,N,M,X,Y,MP1,NP1,I,II
      DIMENSION AP(71), AN(71), MXB(71,71)
```

```
      COMMON/INTG/N,M
      MP1=M+1
      DO 701 X=1,MP1
      K=X-1
      NP1=N+1
      DO 601 Y=1,NP1
      J=Y-1
      IF (J.NE.0) GO TO 101
      IF (K.NE.0) GO TO 201
      MXB((M+1),(N+1))=1.0D0
      GO TO 601
201   MXB((M+1-K),(N+1))=GA*AN(K)/(AO+LA-K**2)
      MXB((M+1+K),(N+1))=GA*AP(K)/(AO+LA-K**2)
      GO TO 601
101   IF (K.NE.0) GO TO 301
      MXB((M+1),(N+1-J))=GA*AP(J)/(AO+LA)
      MXB((M+1),(N+1+J))=GA*AN(J)/(AO+LA)
      GO TO 601
301   IF(J.NE.K) GO TO 401
      MXB((M+1-K),(N+1-J))=1.0D0
      MXB((M+1+K),(N+1-J))=GA*AP(J+K)/(AO+LA-K**2)
      MXB((M+1-K),(N+1+J))=GA*AN(J+K)/(AO+LA-K**2)
      MXB((M+1+K),(N+1+J))=1.0D0
      GO TO 601
401   IF(J.LT.K) GO TO 501
      MXB((M+1-K),(N+1-J))=GA*AP(J-K)/(AO+LA-K**2)
      MXB((M+1-K),(N+1+J))=GA*AN(J+K)/(AO+LA-K**2)
      MXB((M+1+K),(N+1-J))=GA*AP(J+K)/(AO+LA-K**2)
      MXB((M+1+K),(N+1+J))=GA*AN(J-K)/(AO+LA-K**2)
      GO TO 601
501   MXB((M+1-K),(N+1-J))=GA*AN(K-J)/(AO+LA-K**2)
      MXB((M+1-K),(N+1+J))=GA*AN(K+J)/(AO+LA-K**2)
      MXB((M+1+K),(N+1-J))=GA*AP(K+J)/(AO+LA-K**2)
      MXB((M+1+K),(N+1+J))=GA*AP(K-J)/(AO+LA-K**2)
```

```
601     CONTINUE
701     CONTINUE
        RETURN
        END
```

APPENDIX O. REVIEW OF REFERENCES ON LINKAGE ELASTICITY

A considerable amount of excellent work has been done in the field of linkage elasticity during the past 30 years by many investigators. Different aspects of this literature, which appeared roughly between 1972 and 1984, have been reviewed by B.S. Thompson and C.K. Sung as well as by G.G. Lowen and C. Chassapis. The period up to approximately 1972 was covered separately by A.G. Erdman and G.N. Sandor and by G.G. Lowen and W.G. Jandrasits. The following briefly describes those publication which appeared since approximately 1984 (hopefully without too many inadvertent omissions). Work on link deflection and stability are grouped separately.

(a) Link deflection

A. Balasubramonian and E. Raghavacharyulu (1987) used Hamilton's principle to derive the equation of motion for the elastic coupler of a four-bar linkage, which was treated as a continuous mass model. The resulting Hill-type equations were solved numerically by a Runge-Kutta-Merson method.

A. Garcia-Reynoso and W.P. Seering (1984) presented a mathematical model of the linearized vibrations of a four-bar linkage with a flexible rocker and torsional spring-type input and output shafts. Both a mode model and a continuous parameter model of the rocker were used in the determination of the system eigenvalues. A non-dimensional analysis of the vibration response forms the basis for their concept of similar dynamic behavior of families of mechanisms

D.R. Flugrad, Jr. (1986) considered the motion of a disk, attached to the crankshaft of a massless slider-crank mechanism whose slider is driven by a cam. The connecting rod is only axially deformable and the crankshaft is considered to be a torsional spring. A procedure

for cam profile synthesis for a desired output motion was presented. The resulting equation of motion of the output link is a forced Hill type one, which was subsequently solved numerically.

F.W. Liou, A.G. Erdman and K.A. Stelson (1988) developed some useful general design rules for high-speed flexible mechanisms, starting from the concept of an instantaneous structure which has equivalent mass and stiffness at associated mechanism positions. The rules were demonstrated by way of a number of examples.

V. Masurekar and K.N. Gupta (1989) used a continuous parameter approach, based on element equilibrium, to find the equation of motion of the coupler of a four-bar linkage. The linearization of this formulation led to a Hill-type equation, which was solved numerically. A spectrum analysis, based on a Fourier series steady state solution, is given. Finally, experimental results compared favorably with the numerical ones.

G.N. Sandor and X. Zhuang (1985) applied the central finite difference method to the solution of a linearized lumped-mass model of an elastic four-bar linkage. The results showed that the error due to linearization is small when compared with the nonlinear model presented earlier by J.P. Sadler and the first author (ref.9 in Sandor 1985). The effects of the rotary inertia of the elements and the end masses of the moving links were found to be considerable.

The following group of papers dealing with the analysis of link deflection employ finite element methods.

D.F. Bartolone and A. Shabana (1989) developed a finite element model, through a Lagrangian formulation, to study the effect of link initial curvature on the dynamics of flexible mechanisms. The mass and stiffness matrices of the governing equations were found to be significantly affected by such initial curvature. Applications to both slider-crank and six-bar mechanisms, with one initially curved link, are shown.

E. Bayo and M.A. Serna (1988) presented a number of penalty methods for the dynamic analysis of flexible mechanisms. Starting with a finite element description of the system, the equations of motion are derived by means of Lagrange's formulation. Subsequently, the penalty constraints, dealing with stiffness, damping and inertia, are inserted into them in the manner of Lagrange Multipliers. The same authors showed an application of their method to the connecting rod of a slider-crank mechanism and a robot arm in Serna (1988).

W.L. Cleghorn, R.G. Fenton and B. Tabarrok (1984) developed a steady state solution procedure for the governing finite element equations of flexible mechanisms by using truncated Fourier series to represent the time dependent components of the equations. The results of the associated system of linear equations showed good agreement with the experimental data of R.M. Alexander (ref.10 in Cleghorn, 1984).

W.L. Cleghorn and K.C. Chao (1988) investigated the steady state response of an undamped flexible four-bar linkage, containing non-uniform cross-section links, by way of a finite element method using tapered elements. The resulting link deflections were compared with ones stemming from an analysis of the same mechanism which used uniform beam elements of the same mass as the tapered ones.

M. Dedo and A.H. Soni (1987) presented a analysis procedure to obtain the link displacements as well as the internal forces of elastic linkages by way of a finite line element method.

S. Dubowsky, J.F. Deck and H. Costello (1987) extended an existing finite element method for modeling flexible spatial mechanisms, developed by W. Sunada and the first author, to include the effects of clearances in the joints. A procedure of replacing the kinematic constraints imposed at the ideal joint connections with force constraints is described. Finally, an impact beam model and a planar slider-crank mechanism with clearances were used as the examples to show the impact response.

Starting with a finite element formulation, X. Gao, Z. King and Q. Zhang (1988) derived a closed-form linear multi-step algorithm to obtain the steady state response of flexible mechanisms. These authors showed that the computational results were more accurate and more efficiently obtained than by way of the Fourier series method, developed by P.K. Nath (ref.3 in Gao, 1988) and W.L. Cleghorn (ref.4 in Gao, 1988).

A.G. Jablokow, S. Nagarajan and D.A. Turcic (1988) developed a finite element solution technique for the matrix equations of motion of elastic mechanism, which include coupling terms and general damping. The application of the method to a four-bar linkage showed the significance of the coupling terms and their effects on the natural frequency variation, as well as on the response of the elastic links at high speeds.

Y.A. Khulief (1988) worked out a finite element formulation with a mixed set of reference and local elastic generalized coordinates. A dynamic simulation of an elastic four-bar linkage was performed. It utilized both physical and modal coordinates and showed how the response varied, depending on types of coordinates used.

J.P. Sadler, Z. Yang and K.E. Rouch (1988) applied the ANSYS general-purpose finite element program to an elastic four-bar linkage. Both transient and steady state bending responses, as well as the variations of the natural frequencies, were obtained.

A. Shabana (1986) showed the effect of temperature on the dynamic response of the connecting rod of a slider-crank mechanism. Assuming a Kelvin-Voight viscoelastic model, the governing equations of motion were derived with the help of a Lagrangian formulation and solved by way of a finite element technique.

A. Shabana and B. Thomas (1987) used a finite element model, which was given earlier by the first author and R.A. Wehage (ref.24 in Shabana, 1987), to investigate the vibrations of the cantilevered toolbit as well as the deflections of the flexible connecting rod of a crank shaper mechanism.

C.K. Sung, B.S. Thompson and J.J. McGrath (1984) utilized a variational principle to develop the equations of motion which govern the response of planar elastic mechanisms subjected to both mechanical and thermal loading. A slider-crank mechanism with a flexible connecting rod was used to illustrate this approach. In another paper (1986), the same authors, extended this method to a hygrothermal loading.

M.A.K. Zobairi, S.S. Rao and B. Sahay (1986) investigated the contribution of kineto-elastodynamic inertia forces to the shaking forces and moments of a mechanism. To this end, a finite element approach, given by Nath and Ghosh (ref.24 in Zobairi, 1986), was adapted for the determination of the acceleration field due to the local deflections of the links. A design optimization, which takes the dimensions and dynamic stresses of the mechanism into account, is extended so that optimum balancing characteristics can be achieved. In a companion paper (1986), the same authors considered the inclusion of counterweights. They concluded that a complete force/moment balance by way of the redistribution of link masses is not possible for flexible mechanisms.

W.S. Yoo and E.J. Haug (1986) presented a finite element based method, which employs both vibration normal modes and static correction modes to define the deformation fields of elastic components, for the simulation of flexible mechanical systems. A spatial four-bar linkage, as well as a windshield wiper mechanism were used as illustrations. The results showed that an appropriate combination of vibration and static correction deformation modes does not only reduce the computing time significantly, when compared with the use of pure vibration modes, but also furnishes accurate deformation information for the elastic links.

The remaining efforts, involving link deflections or their effects, are of an experimental nature.

A. Balasubramonian and E. Raghu (1988) showed the details of an experimental setup for the determination of the ground bearing forces of a four-bar linkage with a flexible coupler. The instrumentation of these bearings, by way of piezoelectric load cells, is of special interest.

F.W. Liou and A.G. Erdman (1989) devised a new experimental approach, which uses a high speed camera and digital imaging techniques, to determine the paths of specific points on the links of a flexible mechanism. This method also allows the sequential image freezing of instantaneous configurations of the total mechanism.

D.X. Liao, C.K. Sung, B.S. Thompson and K. Soong (1986) presented experimentally obtained midspan strain/vibration traces of both the coupler and the rocker of a flexible four-bar linkage at various speeds. The authors associated these responses with quasi static and dynamic regimes, as well as resonance conditions. They state that their results should provide the impetus for further theoretical investigations.

(b) Stability

M.L. Badlani (1988) studied the effects of rotatory inertia and shear deformation on the parametric stability of an undamped elastic connecting rod of a slider-crank mechanism. It was shown that, when the results are compared with those due to Euler-Bernoulli beam theory, there is an increase in the width of parametric instability region as well as a shift to a lower corresponding critical frequency.

D.R. Flugrad, Jr. and H.-T.J. Liu (1988) showed a stability analysis of a Hill's equation by using a novel perturbation technique. The periodic coefficient of the expression is first replaced by a Fourier series. Subsequently, the Fourier coefficients serve for the construction of a small parameter. The method is used to find the stability boundaries of a Mathieu equation as well as a Hill's equation stemming from the mechanism described earlier in Flugrad (1986).

V. Masurekar and K.N. Gupta (1988) showed a stability analysis of the coupler of a four-bar linkage, both with and without damping. The initial partial differential equation is linearized and Galerkin's method, using a half-sine space function, is applied to obtain a Hill type equation. The assumption of a periodic response at the stability boundaries furnished the basis for the determination of their locations. Several examples of numerically obtained responses in stable and unstable regions are presented.

S. Nagarajan and D.A. Turcic (1990) compared two different approaches for the determination of the stability of a four-bar linkage with three elastic members. To this end, they make use of the finite element based set of equations, originally derived by D.A. Turcic and A. Midha (ref.14 in Turcic, 1990). First, they showed a Fourier series approach to obtain the critical speeds for all modes of vibration simultaneously by solving the general eigenvalue problem. The second approach extends the procedure of finding Floquet's multipliers given by Zadoka (1987) to multi-mode systems. In order to accomplish this the system equations must be first decoupled by modal analysis techniques. The practical limitations of both methods were discussed.

I.G. Tadjbakhsh and C.J. Younis (1986) focused on the stability of the flexible connecting rod of a slider-crank mechanism with an external piston load. The equation of motion was derived by way of element equilibrium. The application of Galerkin's product formula led to a system of Hill type equations. Stability boundaries were obtained according to Floquet theory and plotted for the first three modes with speeds and input torques as variables.

R.I. Zadoks and A. Midha (1987) investigated the stability of a two-degree-of-freedom torsional vibration system. While the constant inertia input disc is driven by a constant moment, the output disc, which is connected by a flexible shaft, experiences a position dependent resisting moment and also exhibits position dependent inertia. The equations of motion were derived with Lagrange's formulation and linearized about the steady state

rigid-body response. A procedure for determining Floquet's multipliers, which are used to judge system stability, is developed. In the companion paper, two types of stability charts are presented.

REFERENCES

Badlani, M.L., 1988, "On the Parametric Stability of Elastic Mechanisms", *Trends and Developments in Mechanisms, Machines, and Robotics*, ASME DE-Vol. 15-2, pp.367-372.

Badlani, M. and Midha, A., 1983, "Effect of Internal Material Damping on the Dynamics of a Slider-Crank Mechanism", ASME *Journal of Mechanisms, Transmissions and Automation in Design*, Vol. 105, No. 3, pp. 452-459,

Balasubramonian, A. and Raghavacharyulu, E., 1987, "Vibratory Response of an Elastic Coupler of a Four-Bar Linkage", *Mechanism and Machine Theory*, Vol.22, No.2, pp.153-158.

Balasubramonian, A. and Raghu, E., 1988, "Experimental Study on the Elastodynamic Behavior of the Unbalanced and the Counterweighted Four Bar Mechanisms", *Trends and Developments in Mechanisms, Machines, and Robotics*, ASME DE-Vol. 15-2, pp.373-379.

Bartolone, D.F. and Shabana, A., 1989, "Effect of Beam Initial Curvature on the Dynamics of Deformable Multibody Systems", *Mechanism and Machine Theory*, Vol.24, No.5, pp.411-429.

Bayo, E. and Serna, M.A., 1988, "Penalty Formulations for the Dynamic Analysis of Elastic Mechanisms", *Trends and Developments in Mechanisms, Machines, and Robotics*, ASME DE-Vol. 15-2, pp.381-386.

Becker, R.A., 1954, *Introduction to Theoretical Mechanics*, pp.165-167, McGraw-Hill, New York.

Bolotin, V.V., 1964, *The Dynamic Stability of Elastic Systems*, Holden Day, San Francisco.

Chassapis, C., 1988, "High Speed Dynamics of a Press Feed Mechanism, Mathematical Simulation and Experimental Verification," *Ph.D. Dissertation.*

Chassapis, C. and Lowen, G.G., 1990, "High Speed Dynamics of a Press Feed Mechanism, Part I: Theory, Part II: Application and Experiment," *Proceedings of ASME Mechanisms Conference*, Vol. 24, pp. 415-437. Also accepted for ASME *Journal of Mechanical Design.*

Cleghorn, W.L., Fenton, R.G. and Tabarrok, B., 1984, "Steady-State Vibrational Response of High-Speed Flexible Mechanisms", *Mechanism and Machine Theory*, Vol.19, No.4/5, pp.417-423.

Cleghorn, W.L. and Chao, K.C., 1988, "Kineto-Elastodynamic Modeling of Mechanisms Employing Linearly Tapered Beam Finite Elements", *Mechanism and Machine Theory*, Vol.23, No.5, pp.333-342.

Daniels, R.L., 1957, "The Sprag-Type Over-Running Clutch", ASME *Paper No. 57-A-166.*

Daniels, R.L., 1967, "Design and Performance Characteristics of Over-Running Clutches in Gas Turbine Applications", ASME *Journal of Engineering for Power*, pp.207-216.

Dedo, M. and Soni, A.H., 1987, "Complete Dynamic Analysis of Elastic Linkages", Trans. ASME, *Journal of Mechanisms, Transmissions, and Automation in Design*, Vol.109, No.4, pp.481-486.

Dubowsky, S., Deck, J.F. and Costello, H., 1987, "The Dynamic Modeling of Flexible Spatial Machine Systems with Clearance Connections", Trans. ASME, *Journal of Mechanisms, Transmissions, and Automation in Design*, Vol.109, No.1, pp.87-94.

Erdman, E.G. and Sandor, G.N., 1972, "Kineto-Elastodynamics-A Review of the State of the Art", *Mechanism and Machine Theory*, Vol. 7, No. 1, pp. 19-33.

Ferris, E.A., 1973, "Automotive Sprag Clutches: Design and Application", *Society of Automotive Engineers, Advances in Engineering*, Vol.5, pp.6-16.

Flugrad, Jr. D.R., 1986, "Cam Synthesis and Analysis for an Elastic Follower Linkage", Trans. ASME, *Journal of Mechanisms, Transmissions, and Automation in Design*, Vol.108, No.3, pp.367-372.

Flugrad, Jr. D.R. and Liu, H.-T.J., 1988, "Stability Analysis by a Perturbation Method", *Trends and Developments in Mechanisms, Machines, and Robotics*, ASME DE-Vol. 15-2, pp.397-405.

Gao, X., King, Z. and Zhang, Q., 1988, "A Closed-Form Linear Multi-Step Algorithm for the Steady-State Response of High-Speed Flexible Mechanisms", *Mechanism and Machine Theory*, Vol.23, No.5, pp.361-366.

Garcia-Reynoso, A. and Seering, W.P., 1984, "Vibration Characteristics of an Elastic Linkage with Elastic Input and Output Shafts", Trans. ASME, *Journal of Mechanisms, Transmissions, and Automation in Design*, Vol.106, No.3, pp.272-277.

Hartenberg, R.S. and Denavit, J., 1964, *Kinematic Synthesis of Linkages*, McGraw-Hill Book Company, New York.

Hunt, K.H. and Crossley, F.R.E., 1975, "Coefficient of Restitution Interpreted as Damping in Vibroimpact," ASME *Journal of Applied Mechanics*, pp. 440-445.

Jablokow, A.G., Nagarajan, S. and Turcic, D.A., 1988, "A Modal Analysis Solution Technique to the Equations of Motion for Elastic Mechanism Systems Including the Rigid-Body and Elastic Motion Coupling Terms", *Trends and Developments in Mechanisms, Machines, and Robotics*, ASME DE-Vol. 15-2, pp.407-416.

Jandrasits, W.G. and Lowen, G.G., 1979, "The Elastic-Dynamic Behavior of a Counterweighted Rocker Link with an Overhanging Endmass in a Four-Bar Linkage. Part I: Theory, Part II: Application and Experiment", ASME *Journal of Mechanical Design*, Vol. 101, No. 1, pp. 77-98.

Johnson, K.L., 1985, *Contact Mechanics*, Cambridge University Press, Cambridge, pp. 179-184.

Khulief, Y.A., 1988, "Physical and Modal Coordinates for Dynamic Analysis of Flexible Mechanisms", *Trends and Developments in Mechanisms, Machines, and Robotics*, ASME DE-Vol. 15-2, pp.417-422.

Klotter, K., 1941, "Stabilisierung und Labilisierung durch Schwingungen", *Forschung auf dem Gebiete des Ingenieurwesens*, Band 12 (5), Berlin.

Kotowski, G., 1943, "Loesungen der inhomogenen Mathieuschen Differtialgleichung mit periodischer Stoerfunktion beliebiger Frequenz (mit besonderer Beruecksichtigung der Resonanzloesungen)", *Zeitschrift fur angewandte Mathematik und Mechanik*, Vol. 23, No. 4, pp. 213-229.

Lazan, B.J. and Goodman, L.E., 1961, "Material and Interface Damping", *Shock and Vibration Handbook*, Harris, C.M. and Crede, C.E. edited, McGraw-Hill Book Company, New York, Vol.2, Chap. 36, pp. (36-1)-(36-46).

Liao, D.X., Sung, C.K., Thompson, B.S. and Soong, K., 1986, "A Note on the Quasi-Static Responses, Dynamic Responses, and the Super-Harmonic Resonances of Flexible Linkages: Some Experimental Results", *ASME Paper 86-DET-146*.

Liou, F.W. and Erdman, A.G., 1989, "Experimental Motion Analysis of Flexible Mechanism and Drive System Using High-Speed Camera and Digital Imaging Technique", *Mechanism and Machine Theory*, Vol.24, No.4, pp.257-266.

Liou, F.W., Erdman, A.G. and Stelson, K.A., 1988, "General Design Rules for High-Speed, Flexible Mechanisms", *Trends and Developments in Mechanisms, Machines, and Robotics*, ASME DE-Vol. 15-2, pp.423-431.

Lowen, G.G. and Chassapis, C., 1986, "The Elastic Behavior of Linkages: An Update", *Mechanism and Machine Theory*, Vol. 21, No. 1, pp. 33-42.

Lowen, G.G. and Jandrasits, W.G., 1972, "Survey of Investigations into the Dynamic Behavior of Mechanisms Containing Links with Distributed Mass and Elasticity", *Mechanism and Machine Theory*, Vol. 7, pp. 3-17.

Magnus, W. and Winkler, S., 1966, *Hill's Equation*, Interscience Publishers, New York.

Masurekar, V. and Gupta, K.N., 1988, "Stability Analysis of Four Bar Mechanism. Part I - with the Assumption that Damping is Absent", *Mechanism and Machine Theory*, Vol.23, No.5, pp.367-375.

Masurekar, V. and Gupta, K.N., 1988, "Stability Analysis of Four Bar Mechanism. Part II - Taking Damping into Consideration", *Mechanism and Machine Theory*, Vol.23, No.5, pp.377-382.

Masurekar, V. and Gupta, K.N., 1989, "Theoretical and Experimental Kineto-Elastodynamic Analysis of High Speed Linkage", *Mechanism and Machine Theory*, Vol.24, No.5, pp.325-334.

Nagarajan, S. and Turcic, D.A., 1990, "General Methods of Determining Stability and Critical Speeds for Elastic Mechanism Systems", *Mechanism and Machine Theory*, Vol.25, No.2, pp.209-223.

Novikov, V.A., 1973, "The Design of Free-Wheeling Clutches with Eccentric Rollers", *Russian Engineering Journal*, Vol.48, No.12, pp.33-37.

Novikov, V.A. and Radzhapov, A.K., 1977, "Designing of Geometrical Parameters of a Free-Wheeling Clutch with Eccentric Rollers", *Russian Engineering Journal*, Vol.57, No.9, pp.19-23.

Roark, R.J. and Young, W.C., 1982, *Formulas for Stress and Strain*, 5th. Edition, pp.516-519, McGraw-Hill, New York.

Sadler, J.P., Yang, Z. and Rouch, K.E., 1988, "The Use of ANSYS for the Analysis of Flexible Four-Bar Linkages", *Trends and Developments in Mechanisms, Machines, and Robotics*, ASME DE-Vol. 15-2, pp.441-447.

Sandor, G.N. and Zhuang, X., 1985, "A Linearized Lumped Parameter Approach to Vibration and Stress Analysis of Elastic Linkages", *Mechanism and Machine Theory*, Vol.20, No.5, pp.427-437.

Serna, M.A. and Bayo, E., 1988, "Numerical Implementation of Penalty Methods for the Analysis of Elastic Mechanisms", *Trends and Developments in Mechanisms, Machines, and Robotics*, ASME DE-Vol. 15-2, pp.499-456.

Shabana, A., 1986, "Thermal Analysis of Viscoelastic Multibody Systems", *Mechanism and Machine Theory*, Vol.21, No.3, pp.231-242.

Shabana, A. and Thomas, B., 1987, "Chatter Vibration of Flexible Multibody Machine Tool Mechanisms", *Mechanism and Machine Theory*, Vol.22, No.4, pp.359-369.

Stoelzle, K. and Hart, S., *Freilaufkupplungen*, pp.47-49, Springer Verlag, Berlin (1961).

Strutt, M.J.O., 1932, "Lamesche, Mathieusche und verwandte Funktionen", *Ergebnisse der Mathematik*, I, 3. Berlin, pp.12-51.

Sung, C.K., Thompson, B.S. and McGrath, J.J., 1984, "A Variational Principle for the Linear Coupled Thermoelastodynamic Analysis of Mechanism Systems", Trans. ASME, *Journal of Mechanisms, Transmissions, and Automation in Design*, Vol.106, No.3, pp.291-296.

Sung, C.K. and Thompson, B.S., 1986, "A Variational Principle for the Hygrothermoelastodynamic Analysis of Mechanism Systems", *ASME Paper 86-DET-15*.

Tadjbakhsh, I.G. and Younis, C.J., 1984, "Dynamic Stability of the Flexible Connecting Rod of a Slider Crank Mechanism", *ASME Paper 86-DET-4*.

Thompson, B.S. and Sung, C.K., 1984, "A Variational Formulation for the Nonlinear Finite Element Analysis of Flexible Linkages: Theory, Implementation, and Experimental Results", ASME *Journal of Mechanisms, Transmissions, and Automation in Design*, Vol. 106, pp. 482-488.

Thompson, B.S. and Sung, C.K., 1986, "A Survey of Finite Element Techniques for Mechanism Design", *Mechanism and Machine Theory*, Vol. 21, No. 4, pp. 351-359.

Thomson, W.T., 1981, *Theory of Vibration with Applications*, 2nd Edition, Prentice-Hall, Inc. Englewood Cliffs, N.J., pp. 68-75.

Whittaker, E.T. and Watson, G.N., 1944, *A Course of Modern Analysis*, The Macmillan Co., New York, pp. 412-417.

Williams, F.C., Tipping, D. and Henry, T.A., 1973, "The Dynamics of the Sprag Clutch", *Mechanisms, Instn. Mech. Engrs.*, pp.38-45.

Williams, F.C., Tipping, D. and Henry, T.A., 1975, "An Improved Sprag Clutch", *Fourth World Congress on the Theory of Mach. and Mech.*, pp.593-598. Published by Mechanical Engineering Publ. Ltd., London.

Xu, T. and Lowen, G.G., 1992, "A New Damping Model for Non-Linear Stiffness Systems with Variable Preload Displacements and Constant Amplitude Decay Ratios," *Proceedings of ASME Mechanisms Conference*, DE-Vol.46, pp.27-33. Accepted for publication in *Trans. ASME Journal of Mechanical Design.*

Xu, T. and Lowen, G.G., 1992, "A New Analytical Approach for the Determination of the Transient Response in Elastic Mechanisms," *Proceedings of ASME Mechanisms Conference*, DE-Vol.47, pp.347-352. Accepted for publication in *Trans. ASME Journal of Mechanical Design.*

Xu, T. and Lowen, G.G., 1992, "A Mathematical Model of An Over-Running Sprag Clutch," Accepted for publication in *Mechanism and Machine Theory.*

Yang, D.C.H. and Lin, J.Y., 1987, "Hertzian Damping, Tooth Friction and Bending Elasticity in Gear Impact Dynamics," ASME *Journal of Mechanisms, Transmissions, and Automation in Design*, Vol. 109, pp. 189-196.

Yoo, W.S. and Haug, E.J., 1986, "Dynamics of Flexible Mechanical Systems Using Vibration and Static Correction Modes", Trans. ASME, *Journal of Mechanisms, Transmissions, and Automation in Design*, Vol.108, No.3, pp.315-322.

Zadoks, R.I. and Midha, A., 1987, "Parametric Stability of a Two-Degree-of-Freedom Machine System: Part I - Equations of Motion and Stability", Trans. ASME, *Journal of Mechanisms, Transmissions, and Automation in Design*, Vol.109, pp.210-215.

Zadoks, R.I. and Midha, A., 1987, "Parametric Stability of a Two-Degree-of-Freedom Machine System: Part II - Stability Analysis", *Trans. ASME, Journal of Mechanisms, Transmissions, and Automation in Design*, Vol.109, pp.216-223.

Zobairi, M.A.K., Rao, S.S. and Sahay, B., 1986, "Kineto-Elastodynamic Balancing of 4R-Four Bar Mechanisms Combining Kinematic and Dynamic Stress Considerations", *Mechanism and Machine Theory*, Vol.21, No.4, pp.307-315.

Zobairi, M.A.K., Rao, S.S. and Sahay, B., 1986, "Kineto-Elastodynamic Balancing of 4R-Four Bar Mechanisms by Internal Mass Redistribution", *Mechanism and Machine Theory*, Vol.21, No.4, pp.317-323.